

UC Davis

Research Reports

Title

Development of Performance-Based Specifications for Asphalt Rubber Binder: Interim Report on Phase 1 and Phase 2 Testing

Permalink

<https://escholarship.org/uc/item/4mq5p6sd>

Authors

Jones, David
Rizvi, Hashim Raza
Liang, Yanlong
et al.

Publication Date

2017-09-01

DOI

10.7922/G2T72FQQ

Development of Performance-Based Specifications for Asphalt Rubber Binder: Interim Report on Phase 1 and Phase 2 Testing

Authors:

D. Jones, H. Rizvi, Y. Liang, S. Hung, J. Buscheck, Z. Alavi, and B. Hofko

Partnered Pavement Research Center (PPRC) Contract Strategic Plan Element 4.50/4.63 (DRISI Task 2671/3186)
Performance-Related Specifications for Asphalt Rubber Binder

PREPARED FOR:

California Department of Transportation
Division of Research, Innovation and System Information
Office of Materials and Infrastructure Roadway Research

PREPARED BY:

University of California
Pavement Research Center
UC Davis, UC Berkeley




TECHNICAL REPORT DOCUMENTATION PAGE

1. REPORT NUMBER UCPRC-RR-2017-01	2. GOVERNMENT ASSOCIATION NUMBER	3. RECIPIENT'S CATALOG NUMBER
4. TITLE AND SUBTITLE Development of Performance-Based Specifications for Asphalt Rubber Binder: Interim Report on Phase 1 and Phase 2 Testing		5. REPORT PUBLICATION DATE 09/08/2020
		6. PERFORMING ORGANIZATION CODE
7. AUTHOR(S) D. Jones (ORCID 0000-0002-2938-076X), H. Rizvi (ORCID 0000-0002-2529-0724), Y. Liang (ORCID 0000-0002-7538-9757), S. Hung (ORCID 0000-0002-8879-070X), J. Buscheck (ORCID 0000-0002-0930-6861), Z. Alavi (0000-0002-5217-7305), and B. Hofko (ORCID 0000-0002-8329-8687)		8. PERFORMING ORGANIZATION REPORT NO. UCPRC-RR-2017-01 UCD-ITS-RR-20-83
		10. WORK UNIT NUMBER
9. PERFORMING ORGANIZATION NAME AND ADDRESS University of California Pavement Research Center Department of Civil and Environmental Engineering, UC Davis 1 Shields Avenue Davis, CA 95616		11. CONTRACT OR GRANT NUMBER 65A0542
		13. TYPE OF REPORT AND PERIOD COVERED Research Report
12. SPONSORING AGENCY AND ADDRESS California Department of Transportation Division of Research, Innovation, and System Information P.O. Box 942873 Sacramento, CA 94273-0001		14. SPONSORING AGENCY CODE
		15. SUPPLEMENTAL NOTES https://doi.org/10.7922/G2T72FQQ
16. ABSTRACT In the United States, the Superpave Asphalt Binder Performance Grading (PG) system proposed by the Strategic Highway Research Program (SHRP) is the most common method used to characterize the performance-related properties of unmodified and polymer-modified asphalt binders. Dynamic shear modulus (G^*) and phase angle (δ) are the two main binder properties and they are measured using a dynamic shear rheometer (DSR) with parallel plate geometry and either a 1-mm or 2-mm gap between the plates. Since these Superpave parameters were developed for binders that do not contain additives or particulates, the California Department of Transportation (Caltrans) does not use them for asphalt rubber binder specifications. Instead, penetration and viscosity are used as acceptance of quality control; however, these parameters do not necessarily provide a satisfactory link between the measured binder properties and potential performance in the field over a range of operating temperatures. In California, current specifications require that crumb rubber particles used to produce asphalt rubber binder in the "wet process" must be smaller than 2.36 mm (i.e., 100 percent passing the #8 sieve), and typically these particles vary in size between 1 mm and 2 mm. Consequently, when the parallel plate geometry is used to test this type of binder, the larger incompletely digested rubber particles can contact the plates. If this occurs, the rubber particle rheology can potentially dominate the results, which in turn may not be representative of the modified binder as a whole. To address this problem, a potentially more appropriate DSR testing protocol using concentric cylinder geometry was investigated in Phase 1 of this study to explore an alternative means of determining the performance properties of asphalt rubber binders. Phase 2 of the study, documented in this report, continued the investigation into the use of the concentric cylinder geometry and alternate parallel plate geometry with a 3-mm gap. The use of these geometries for intermediate-temperature testing and multiple stress creep recovery testing was also investigated, along with modified procedures for short- and long-term aging in the rolling thin-film oven and pressurized aging vessel, respectively, and specimen preparation procedures for bending beam rheometer (BBR) testing. Limited mix testing was also conducted to relate high- and low-temperature mix performance to the performance grades determined for the binders used in the mixes. The concentric cylinder testing approach to measuring the rheological properties of asphalt rubber binders is considered feasible, and that with its use, the edge effects and trimming issues associated with parallel plate testing can be eliminated. However, the concentric cylinder method requires a longer testing time and a larger binder sample than the parallel plate test method. Initial findings from performance grading and related mix testing indicate that the incompletely digested rubber particles, which have different sensitivities to temperature and applied stress and strain than the asphalt binder, appear to dominate the test results. This will need to be factored into analyses and interpretation of rheology and mix performance test results. The proposed modifications to the short- and long-term aging procedures and to the BBR specimen preparation procedures are considered to be more aligned with the original intent of the tests and will likely reduce the variability between replicate specimens during testing. The results from Phase 2 support the continuation of testing, which should be in line with the original workplan and objectives of this research effort. The research should continue to refine the testing procedures on additional field binder sources, assess the repeatability and reproducibility of any proposed test methods, and evaluate the applicability of the results to the actual performance properties of mixes produced with asphalt rubber binders.		
17. KEY WORDS Asphalt Rubber, Wet-process Rubberized Binder, Concentric Cylinder, Performance Grade Testing		18. DISTRIBUTION STATEMENT No restrictions. This document is available to the public through the National Technical Information Service, Springfield, VA 22161
19. SECURITY CLASSIFICATION (of this report) Unclassified	20. NUMBER OF PAGES 226	21. PRICE None

Reproduction of completed page authorized

UCPRC ADDITIONAL INFORMATION

1. DRAFT STAGE Final	2. VERSION NUMBER 1				
3. PARTNERED PAVEMENT RESEARCH CENTER STRATEGIC PLAN ELEMENT NUMBER 4.50/4.63	4. DRISI TASK NUMBER 2671/3186				
5. CALTRANS TECHNICAL LEAD AND REVIEWER(S) A. Vasquez and Guadalupe Magana	6. FHWA NUMBER CA212672A				
7. PROPOSALS FOR IMPLEMENTATION Continue with Phase 3 testing					
8. RELATED DOCUMENTS UCPRC-TM-2014-02					
9. LABORATORY ACCREDITATION The UCPRC laboratory is accredited by AASHTO re:source for the tests listed in this report					
10. SIGNATURES					
D. Jones FIRST AUTHOR	J.T. Harvey TECHNICAL REVIEW	D. Spinner EDITOR	J.T. Harvey PRINCIPAL INVESTIGATOR	Guadalupe Magana CALTRANS TECH. LEADS	T.J. Holland CALTRANS CONTRACT MANAGER

Reproduction of completed page authorized

DISCLAIMER STATEMENT

This document is disseminated in the interest of information exchange. The contents of this report reflect the views of the authors who are responsible for the facts and accuracy of the data presented herein. The contents do not necessarily reflect the official views or policies of the State of California or the Federal Highway Administration. This publication does not constitute a standard, specification, or regulation. This report does not constitute an endorsement by the Department of any product described herein.

For individuals with sensory disabilities, this document is available in alternate formats. For information, call (916) 654-8899, TTY 711, or write to California Department of Transportation, Division of Research, Innovation, and System Information, MS-83, P.O. Box 942873, Sacramento, CA 94273-0001.

PROJECT OBJECTIVES

This study is a continuation of PPRC Project 4.45 (performance-based specifications for rubberized binders). The objective of this project is to recommend testing procedures and criteria for performance-based specifications of asphalt rubber binders. This objective will be achieved through completion of the following tasks:

1. Evaluate the rheological properties of laboratory and plant-produced asphalt rubber binders at high and intermediate temperatures using both parallel plate and concentric cylinder geometries.
2. Evaluate and refine short- and long-term aging procedures for asphalt rubber binders.
3. Evaluate low-temperature rheological properties of asphalt rubber binders.
4. Evaluate the relationship between the rheological properties of asphalt rubber binders and mix performance in terms of rutting, fatigue cracking, and low-temperature cracking.
5. Recommend performance-related specification criteria for asphalt rubber binders.

This report provides an update on work completed to date on Tasks 1 through 4.

ACKNOWLEDGEMENTS

The University of California Pavement Research Center acknowledges the following individuals and organizations who contributed to the project:

- Mr. Al Vasquez and Dr. T. Joseph Holland, California Department of Transportation
- Mr. Nate Gauff and Mr. Bob Fuji, California Department of Resources, Recycling, and Recovery
- The staff of Anton Paar testing equipment
- The UCPRC laboratory staff

Blank page

EXECUTIVE SUMMARY

This report documents the first two phases of a three-phase study to investigate test methods for measuring the performance properties of asphalt rubber binders produced according to Caltrans specifications. The current method of rotational viscosity (Haake) testing used by Caltrans is deemed to be an insufficient measure for assessing the expected performance for asphalt rubber binders compared to the more rigorous testing requirements for unmodified, polymer-modified, and tire rubber-modified binders. The first phase of the study consisted of preliminary testing to compare two different dynamic shear rheometer (DSR) geometries, with a goal to make recommendations about whether to adopt similar testing procedures for asphalt rubber binders to supplement those currently used for unmodified and other modified binders. The second phase of the study investigated short- and long-term aging procedures, developed revised specimen preparation procedures for bending beam rheometer (BBR) testing, and conducted preliminary investigations into the use of the two DSR geometries for intermediate-temperature testing and multiple stress creep recovery (MSCR) testing. Three asphalt rubber binders, and loose mixtures produced with them, were sampled from three different field projects to assess the binder testing procedures developed and to relate the tested properties to expected field performance.

Phase 1: DSR Testing Geometries

The high temperature properties of unmodified and other modified asphalt binders are typically measured in tests that use a DSR with parallel plate geometry, with the gap size between the plates dependent on the size of any particulates in the binder. A 2.0 mm gap size is considered to be the maximum appropriate gap for testing asphalt binders (in order to limit variability in results due to specimen trimming and binder flow at higher temperatures), provided that no particulates in the binder exceed the AASHTO/ASTM-recommended maximum particle size of 0.25 mm (or 250 μm [#60]). In addition, DSR-manufacturers recommend that the gap between the plates should be at least four times the maximum particle size to provide reliable results. However, Caltrans specifications allow crumb rubber particles up to 2.36 mm (passing the #8 sieve), which exceeds this maximum recommended size for parallel plate testing (i.e., an 8-mm gap, with correspondingly adjusted plate diameter, would be required for 2.0 mm [#10] particle sizes). Consequently, the appropriateness of the parallel plate geometry for testing asphalt rubber binders is questionable because the rheology of the large incompletely digested rubber particles may dominate the DSR results and give misleading performance parameters for the binder properties. This study therefore assessed the concentric cylinder, an alternative geometry that can accommodate larger particles in the asphalt rubber binder. The two geometries were compared using unmodified, polymer-modified, tire rubber-modified (i.e., binders with no particulates), and wet-process asphalt rubber binders (binder containing incompletely digested rubber particles). Binders with no particles were tested with a 1-mm gap, while the

asphalt rubber binders were tested with a 3-mm parallel plate gap (to better accommodate the incompletely digested rubber particles). Key findings from the work completed to date include the following:

- The results obtained from testing the same unmodified, polymer-modified, and tire rubber-modified binders with concentric cylinder and parallel plate geometries in a DSR showed that the two geometries produced results for the same binder that were statistically similar at a 95 percent confidence interval.
- The results obtained from testing asphalt rubber binders with three different crumb rubber particle size ranges (180 μm to 250 μm , 250 μm to 425 μm , and 425 μm to 850 μm [#40 to #20, #60 to #40, and #80 to #60, respectively]) showed a strong correlation between the two testing geometries for finer particle size ranges but the correlations became weaker with increasing particle size. These weaker correlations in the larger size ranges were attributed in part to the increasing influence of the larger rubber particles in proximity of the plates. Strong correlations between the two geometries were also noted in the test results from assessments of the effects of extender oils and from tire-crushing methods (crushing at ambient versus cryogenic temperatures).

Phase 2a: Short- and Long-Term Aging Procedures

Phase 2a of the study investigated modifications to the AASHTO T 240 rolling thin film oven (RTFO) and AASHTO R 28 pressurized aging vessel (PAV) tests to make them more representative of short- and long-term aging that asphalt rubber binders are subjected to during mix production and during service life. Suggested modifications to the test procedures include the following:

- RTFO testing
 - + Preheating the bottles at 190°C for 10 minutes to improve the uniformity of the coating.
 - + Increasing the sample size from 35 g to 45 g to account for the rubber particles, to ensure that the same amount of the base asphalt binder is tested, and to ensure that sufficient binder is available for rheology testing.
 - + Increasing the RTFO test temperature from 163°C to 190°C to better represent rubberized asphalt concrete mix production temperatures.
- PAV sample preparation
 - + Preheating the pans at 190°C for 10 minutes prior to pouring to facilitate more even spread of the binder to the required thickness.
 - + Increasing the sample size from 50 g to 63 g to account for the rubber particles, to ensure that the same amount of the base asphalt binder is tested, and to ensure that sufficient binder from a single PAV test is available for rheology testing.
 - + Increasing the sample preparation temperature from 163°C to 190°C to be consistent with the temperature of the RTFO-aged binder.
 - + Altering the pouring procedure and agitating the pan during pouring to facilitate even spread of the binder to the required thickness.

Test results revealed the following:

- RTFO testing
 - + Complete coating of the bottle was achieved with the larger sample at the higher temperature. Although coating was satisfactory using the smaller sample at the higher temperature, insufficient material was produced for the desired rheology testing. Film thickness on the bottle was relatively even, but marginally thicker than that measured during aging of conventional unmodified binders, with these results primarily attributed to the presence of incompletely digested rubber particles.
 - + Aging at 190°C increased the shear modulus of the asphalt rubber binder, and reduced the phase angle, as expected. The true high temperature performance grade (PG) typically increased by about 6°C, which equates to a one-grade bump. Sample size and extender oil had limited effect on these parameters.
 - + Rubber particle size had a notable effect on all tests, which is consistent with findings from the literature.
 - + The measured carbonyl and sulfoxide indices for unaged and RTFO-aged binders showed clear trends with respect to the effect of aging temperature and sample size, as expected. Ongoing testing in Phase 3 will attempt to compare laboratory- and plant-produced binders to determine whether the proposed revised aging procedure is representative of aging conditions during plant production, storage, transport to the project, and placement.
 - + The butadiene index appears to increase with increasing rubber content and could be a useful potential indicator of the level of modification in asphalt rubber binders. This index also changed with increasing RTFO-aging temperature and the larger sample size, which implies that some rubber modification may have continued during aging.
- PAV preparation procedures
 - + Complete coating of the pan was achieved with the 63 g sample, and the average film thickness after pouring and after PAV aging met the requirements listed in AASHTO R 28.
 - + Following this method provides an additional 130 g of aged binder per PAV test compared to following the standard method (10 pans of 63 g versus 10 pans of 50 g), which provides sufficient binder for both intermediate-temperature testing (using the concentric cylinder geometry) and low-temperature testing. This is considered to be an important advantage given that one PAV test takes 20 hours, excluding preparation time.
- Preliminary intermediate-temperature testing of PAV-aged binder
 - + No clear trends were observed from the preliminary intermediate-temperature test results on three binders for the different preparation procedures. Only two of the three binders could be tested due to torque limitations of the DSR. The results from one of the binders were consistent with expectations. PAV preparation procedures did not appear to have a significant effect on the test results of the second binder.
- Preliminary BBR testing:
 - + No clear trends were observed from the stiffness testing results, with little variation observed between the different PAV preparation methods across the three binders tested when variation between replicates within each method were considered.
 - + The m-value did not appear to be significantly affected by PAV sample preparation method.

Although only limited DSR and BBR testing was conducted in this phase of the research, the modifications proposed above are considered to be appropriate in reflecting the original intent and mechanisms of the tests. Unfortunately, there is no documented procedure to verify the appropriateness of the procedures given that asphalt rubber binders cannot be effectively extracted and recovered for loose mix or core samples removed from highways.

Phase 2b: Bending Beam Rheometer Specimen Preparation Procedures

Phase 2b investigated modifications to the mold used to prepare BBR specimens. Pouring asphalt rubber binder into a standard BBR mold is very difficult given the mold's small opening and the viscosity and consistency of the binder. Modified molds that allow binder to be poured through a 12.5 mm opening (i.e., the width of the mold) instead of the standard 6.25 mm opening (i.e., the thickness of the specimen) improved the quality of the specimens in terms of dimension uniformity and absence of air bubbles. However, the specimen's wider surface area made trimming more challenging, and the specimen's rougher surface after trimming could influence the dimensions of the beam. Ongoing refinements to the trimming process are being investigated, along with the determination of new variance limits, to accommodate these inconsistencies.

BBR testing indicated that the mold configuration used to prepare beam specimens can affect the measured rheological properties of the binder and that the low-temperature performance grade could change if the modified configuration is used instead of the standard configuration. Results from the modified configuration appeared to be more consistent than those produced with the standard configuration.

Phase 2c: Intermediate-Temperature Testing

Preliminary intermediate-temperature test results indicated that the concentric cylinder geometry is potentially suitable for testing of asphalt rubber binders at intermediate temperatures. However, all testing in this phase of the study was conducted at 25°C, and the test setup will require more testing with a representative set of asphalt rubber binders to determine whether it is appropriate for determining actual intermediate-temperatures, and whether maximum torque ranges of the DSR are likely to be exceeded. Refinements to the testing geometry, such as different bob sizes and testing procedures will also be investigated during planned additional testing.

Phase 2d: Multiple Stress Creep Recovery (MSCR) Testing

Preliminary MSCR test results indicated that the concentric cylinder geometry is also potentially suitable for testing this property of asphalt rubber binders. However, given that only limited testing was undertaken and that the results were somewhat inconsistent, additional testing is required before any conclusions on the appropriateness of using the concentric cylinder geometry for MSCR testing can be drawn. This evaluation will continue in the next phase when field binders are tested.

Phase 2e: Rheology Testing on Plant-Produced Binders

Preliminary rheology testing to determine the high-, intermediate-, and low-temperature performance grades of the three plant-produced asphalt rubber binders using the proposed testing procedures discussed in this report was undertaken to “test” the procedures. The following observations from the high temperature tests were made:

- Concentric cylinder
 - + An increase of four grades over the base binder was recorded for two of the asphalt rubber binders and an increase of five grades was recorded for the third.
 - + Mean true grade results showed that all three binders were relatively close and fell in a range between 91°C and 95°C.
 - + Variation in results of the three replicates in each test was small.
 - + The incompletely digested rubber particles clearly had a significant influence on the results when compared to the base binder.
 - + All results were higher than the maximum grade of 82°C listed in the AASHTO M 320 standard.
- Parallel plates with 3-mm gap
 - + The same grade increases recorded for the tests with the concentric cylinder were observed for the tests with the parallel plate.
 - + Mean true grade results showed that all three binders were relatively close and fell in a range between 92°C and 105°C, a range approximately 7°C higher than the concentric cylinder measurements.
 - + Variation in results of the three replicates for each binder was notably larger than the variation recorded when testing with the concentric cylinder.
- Difference between concentric cylinder and parallel plate
 - + For the unaged binders, $G^*/\sin(\delta)$ values measured with the parallel plate geometry were consistently higher than those determined from concentric cylinder measurements. Similar trends between the different binders were also apparent.
 - + For the RTFO-aged binders, $G^*/\sin(\delta)$ values determined with the parallel plate geometry were again considerably higher than those determined with the concentric cylinder for two of the three binders tested.
- Binder grade
 - + Testing with both geometries provided the same high-temperature grade despite the noted variations in test results discussed above.

The following observations from the low-temperature tests were made:

- Stiffness values were well below the AASHTO M 320 criteria for determining the low-temperature grade ($S \leq 300$) and consequently grades were dictated by the m-value (≥ 0.30). The presence of incompletely digested rubber particles and potential phase separation between these particles and the asphalt binder probably contributed to the low stiffness values.
- Although the acceptable ranges between two test results for the same unmodified binder as listed in AASHTO T 313 (7.2 percent for stiffness and 2.9 percent for m-value) were exceeded in most instances, the low-temperature grade of each tested binder remained the same. These larger differences between results were attributed in part to the rougher beam surfaces after trimming and

to variation in the number, size, and degree of digestion of the rubber particles in each beam. Revised acceptance ranges for asphalt rubber binders will be suggested, if appropriate, after completion of further testing on additional plant-produced binders in Phase 3.

- The AASHTO M 320 procedure contains no recommendations for asphalt rubber binders. The minimum low-temperature grade in the standard table for conventional binders with a high-temperature grade equal to or greater than 76°C is -22°C, which was achieved for two of the tested binders. The low-temperature grade of the third binder did not differ from that of the base binder.
- Questions regarding other factors that may influence results, and specifically the variability between results, and that may require further investigation, include; a) whether changes in the properties of the incompletely digested rubber particles occur at very low temperatures (i.e., in the range of glass transition); b) whether different rubber particles (e.g., synthetic versus natural rubber) have different coefficients of thermal expansion, and c) whether the properties of the rubber particles are in any way effected by the type of temperature control medium used in the BBR (i.e., ethanol for the testing discussed in this report).

A small study was conducted to determine the extent to which incompletely digested particles might affect performance-grading test results. This was achieved by comparing the results from the three plant-produced asphalt rubber binders with the results produced using the same binder but with all particles larger than 300 µm (> #50 sieve) removed. Preliminary testing was limited to the high-temperature grading only. Sieved binders were tested using a 25-mm parallel plate geometry with 2-mm gap according to the standard AASHTO T 315 method. The following observations were made:

- The high temperature performance grades of the sieved binders were consistently two grades lower than those determined for the unsieved binders, indicating that the incompletely digested particles had a significant influence on the test results.
- The percent decrease in $G^*/\sin(\delta)$ when comparing the sieved with the unsieved binders was significant.
- The correlation between the true performance grades of the two types of binders was strong, indicating that testing sieved binders in a standard parallel plate geometry may be an appropriate alternative to testing unsieved binders in the concentric cylinder geometry.

Given that the variability of incompletely digested rubber particles in asphalt rubber binder samples leads to considerable variability in high-, intermediate-, and low-temperature test results, testing sieved binders may be a more appropriate approach to performance grade testing of these binders, or at least for developing a relationship between test results from unsieved and sieved binders as a means to determine a representative PG grading for asphalt rubber binders. Sieved binders will therefore be included as part of the scheduled testing of additional plant-produced binders.

Phase 2f: Performance Testing on Plant-Produced Mixes

Preliminary mix testing was undertaken to assess rutting and cracking performance in relation to performance grading to determine whether the rheology testing approaches provide properties that are

representative of likely field performance. The following observations were made based on the testing of three plant-produced gap-graded asphalt rubber mixes:

- The dynamic and flexural moduli results were similar for all three mixes and were consistent with those measured on other RHMA-G mixes.
- The initial rates of cumulative permanent deformation with increasing loading cycles were similar for the three mixes, but thereafter one mix appeared to be more susceptible to rutting than the other two. Similar trends were recorded in the flow number tests and in tests to determine the number of cycles to three and five percent permanent axial strain. Rankings in these tests were consistent with the true high-temperature grade results of the binders.
- Two of the mixes had similar fatigue life results that were somewhat lower than expected for RHMA-G mixes, when compared with other mixes recently tested at the UCPRC. The remaining mix had a slightly higher fatigue life that was more consistent with other RHMA-G mixes tested.
- The semicircular beam flexibility index results showed the same ranking and trends as the beam fatigue results.

Given that only three plant-produced binders and the mixes produced with them have been tested to date, the database of results is considered to be insufficient for in-depth analysis purposes at this stage of the investigation.

Conclusions

Based on the results obtained to date, the concentric cylinder geometry appears to be a potentially appropriate alternative to the parallel plate geometry for quantifying the properties of asphalt rubber binders produced per Caltrans specifications, and specifically for assessing the performance properties of binders containing crumb rubber particles larger than 250 μm (particles retained on the #60 sieve). Additional testing of a larger number of binders, planned for Phase 3 of this study, is required to confirm these initial findings. The concentric cylinder geometry requires a larger binder sample for testing and it takes longer to complete than testing with the parallel plate geometry. Incompletely digested rubber particles, which have different sensitivities to temperature and applied stress and strain than the base asphalt binder, appear to dominate the test results and this will need to be factored into analyses and interpretation of rheology and mix performance test results. The proposed modifications to the short- and long-term aging procedures and to the BBR specimen preparation procedures are considered to be more aligned with the original intent of the tests and will likely reduce the variability between replicate specimens during testing.

Recommendations

Initial results from this study support the continuation of testing to assess the appropriateness of using the concentric cylinder geometry to measure the performance properties of asphalt rubber binders that are produced according to Caltrans specifications using a wet process with crumb rubber particles larger than 0.25 mm (#60 mesh). This testing should be in line with the original workplan and objectives prepared for

this project, and work should continue to refine the testing procedures on additional plant-produced binders, assess the repeatability and reproducibility of measurements from any proposed test methods, and evaluate the applicability of the results to the actual performance properties of mixes produced with asphalt rubber binders. The potential influence of incompletely digested rubber particles dominating the results will need to be carefully considered in any testing and analysis procedures.

TABLE OF CONTENTS

EXECUTIVE SUMMARY	v
LIST OF TABLES	xvi
LIST OF FIGURES	xvii
LIST OF ABBREVIATIONS	xx
TEST METHODS CITED IN THE TEXT	xxii
CONVERSION FACTORS	xxiii
1. INTRODUCTION	1
1.1 Background	1
1.1.1 Use of Rubberized Asphalt Concrete	1
1.1.2 Production of Rubber-Modified Binders	1
1.1.3 Crumb Rubber Modifier Production	2
1.1.4 Current Caltrans Asphalt Rubber Binder Specifications	2
1.2 Problem Statements	4
1.3 Project Objectives	5
1.4 Measurement Units	8
2. LITERATURE REVIEW	9
2.1 Status Quo on Performance-Related Testing of Asphalt Rubber Binders	9
2.2 Identifying an Alternative to Parallel Plate Testing	9
2.2.1 Concentric Cylinder Geometry (Cup-and-Bob)	10
2.3 Effects of Crumb Rubber Modifier on Asphalt Binder Performance	11
2.3.1 Effect of Crumb Rubber Production Method	11
2.3.2 Effect of Crumb Rubber Particle Size, Shape, and Surface Area	12
2.3.3 Effect of Crumb Rubber Content	12
2.3.4 Effect of Laboratory Aging Method	12
3. Phase 1a: ASSESSMENT OF DSR TESTING GEOMETRIES	15
3.1 Introduction	15
3.1.1 Temperature Calibration and Thermal Equilibrium	15
3.1.2 Calibration of the Conversion Factor (C_{ss})	15
3.2 Testing Plan	16
3.2.1 Testing with Binder-Specific Conversion Factors	16
3.2.2 Testing with a Fixed Conversion Factor	17
3.3 Test Results	17
3.3.1 Testing with Binder-Specific Conversion Factors	17
3.3.2 Testing with Fixed Conversion Factor	22
3.3.3 Testing at Two Different High Temperatures	24
3.4 Phase 1a Findings and Recommendations	24
4. Phase 1b: PRELIMINARY RHEOLOGY TESTING	29
4.1 Introduction	29
4.2 Testing Plan	29
4.3 Binder Preparation	30
4.4 Comparison of Testing Geometries with Three Rubber Particle Size Ranges	30
4.5 Effect of Crumb Rubber Particle Size on Rheological Properties	32
4.6 Effect of Crumb Rubber Particle Surface Area on Rheological Properties	33
4.7 Effect of Crumb Rubber Particle Size on High Temperature Grade	37
4.8 Comparison of Concentric Cylinder and 3-mm Gap Parallel Plate Geometries	38
4.9 Phase 1b Findings and Recommendations	39
5. Phase 2a: SHORT- AND LONG-TERM AGING PROCEDURES	41
5.1 Introduction	41
5.2 Short-Term Aging Procedures	42

5.2.1	Testing Plan	42
5.2.2	Preheating RTFO Bottles Prior to Pouring Binder	44
5.2.3	Visual Inspection of RTFO Bottles after Aging	44
5.2.4	Effects of RTFO Test Parameters on High Temperature Properties	46
5.2.5	Effect of RTFO Test Parameters on Binder Chemistry	47
5.3	Long-Term Aging Procedures	53
5.3.1	Testing Plan	53
5.3.2	Visual Inspection of PAV Pans with 50 g Samples	53
5.3.3	Modified Sample Preparation Procedures	56
5.3.4	Preliminary Intermediate-Temperature Test Results	58
5.3.5	Preliminary Low-Temperature Test Results	60
5.4	Short- and Long-Term Aging Procedure Test Summary	61
6.	Phase 2b: BBR SPECIMEN PREPARATION PROCEDURES	65
6.1	Introduction	65
6.2	Modified Specimen Mold Configuration	66
6.3	Testing Plan	67
6.4	Testing Results	68
7.	Phase 2c: INTERMEDIATE-TEMPERATURE TESTING	71
7.1	Introduction	71
7.2	Testing Geometry	71
7.3	Testing Plan	72
7.4	Testing Results	73
8.	Phase 2d: MULTIPLE STRESS CREEP RECOVERY TESTING	77
8.1	Introduction	77
8.2	Testing Plan	77
8.3	Testing Results	78
9.	Phase 2e: RHEOLOGY TESTING OF PLANT-PRODUCED BINDERS	81
9.1	Introduction	81
9.2	Testing Plan	81
9.3	Crumb Rubber Particle Size Distribution	81
9.4	High-Temperature Testing	82
9.5	Intermediate-Temperature Testing	85
9.6	Low-Temperature Testing	85
9.7	Performance Grade Summary	86
9.8	Effect of Incompletely Digested Rubber Particles on Performance Grading	88
9.8.1	Introduction	88
10.	Phase 2f: TESTING OF PLANT-PRODUCED RHMA-G MIXES	91
10.1	Introduction	91
10.2	Testing Plan	91
10.2.1	Materials	91
10.2.2	Testing Program	91
10.2.3	Specimen Preparation	92
10.3	Specimen Air-Void Contents	92
10.4	Mix Stiffness: AMPT Dynamic Modulus	93
10.4.1	Testing Results	94
10.5	Mix Stiffness: Flexural Modulus	95
10.5.1	Testing Results	95
10.6	Rutting Performance: Unconfined Repeated Load Triaxial	96
10.6.1	Testing Results	97
10.7	Fatigue/Reflective Cracking Performance: Four-Point Beam	99
10.7.1	Testing Results	99
10.8	Fatigue/Reflective Cracking Performance: Semicircular Bend	101
10.8.1	Test Results	101

10.9	Provisional Performance Grading Criteria for Asphalt Rubber Binders	103
11.	CONCLUSIONS AND INTERIM RECOMMENDATIONS.....	105
11.1	Project Summary	105
11.1.1	Phase 1: DSR Testing Geometries.....	105
11.1.2	Phase 2a: Short- and Long-Term Aging Procedures	106
11.1.3	Phase 2b: Bending Beam Rheometer Specimen Preparation Procedures.....	108
11.1.4	Phase 2c: Intermediate-Temperature Testing	108
11.1.5	Phase 2d: Multiple Stress Creep Recovery (MSCR) Testing	108
11.1.6	Phase 2e: Rheology Testing on Plant-Produced Binders	109
11.1.7	Phase 2f: Performance Testing on Plant-Produced Mixes	111
11.2	Conclusions	111
11.3	Recommendations	112
	REFERENCES	113
	APPENDIX A: PROVISIONAL TEST METHODS	117
	APPENDIX B: PHASE 1 TEST RESULTS.....	169
	APPENDIX C: PHASE 2 TEST RESULTS	179

LIST OF TABLES

Table 1.1: Caltrans Specifications for Asphalt Rubber Binder Constituents	3
Table 1.2: Asphalt Rubber Binder Reaction Design Profile	3
Table 1.3: Caltrans Specifications for Asphalt Rubber Binder Quality Control and Acceptance	3
Table 3.1: Specific Conversion Factors for the Evaluated Asphalt Binders	17
Table 3.2: Unmodified Binders: ANOVA Results of $G^*/\sin(\delta)$ with Varied Conversion Factor	18
Table 3.3: Modified Binders: ANOVA Results of $G^*/\sin(\delta)$ with Varied Conversion Factor	20
Table 3.4: RTFO-Aged Binders: ANOVA Results of $G^*/\sin(\delta)$ with Varied Conversion Factor	22
Table 3.5: Unmodified Binders: ANOVA Results of $G^*/\sin(\delta)$ with Fixed Conversion Factor	22
Table 4.1: Experimental Design Factors and Factorial Levels for Phase 1b	29
Table 4.2: Summary of Statistical Comparisons between Testing Geometries	32
Table 4.3: Surface Area of Rubber Particles Produced at Ambient and Cryogenic Temperatures	33
Table 4.4: Round-Robin Study Binder Details	38
Table 4.5: Round-Robin Study Rubber Details	38
Table 5.1: Phase 2a: Experimental Design Factors and Factorial Levels for Short-Term Aging	43
Table 5.2: Phase 2a: Experimental Design Factors and Factorial Levels for Long-Term Aging	53
Table 5.3: Phase 2a: Intermediate-Temperature Test Results	59
Table 5.4: ANOVA Results of $G^* \times \sin(\delta)$ for PAV Preparation Procedures	60
Table 5.4: Phase 2a: Low-Temperature Test Results	60
Table 6.1: Phase 2b: Experimental Design Factors and Factorial Levels	67
Table 7.1: Phase 2c: Experimental Design Factors and Factorial Levels	73
Table 8.1: Phase 2d: Experimental Design Factors and Factorial Levels	77
Table 9.1: Phase 2e: Rubber Particle Gradations used in Plant-Produced Binders	82
Table 9.2: Phase 2e: High-Temperature Grade and True Grade Results	82
Table 9.3: Phase 2e: Low-Temperature Grade Results	86
Table 9.4: Phase 2e: Performance Grade Summary	86
Table 10.1: Phase 2f: Tests Performed on Plant-Produced Mixes	91
Table 10.2: Phase 2f: Dynamic Modulus Master Curve Parameters	94
Table 10.3: Phase 2f: Flexural Modulus Master Curve Parameters	95

LIST OF FIGURES

Figure 1.1: Flowchart of projects tasks/phases.....	6
Figure 2.1: Concentric cylinder geometry.....	10
Figure 3.1: Unmodified binders: G^* with varied conversion factor at 64°C.	19
Figure 3.2: Unmodified binders: δ with varied conversion factor at 64°C.	19
Figure 3.3: Unmodified binders: $G^*/\sin(\delta)$ with varied conversion factor at 64°C.	19
Figure 3.4: Unmodified binders: G^* against δ with varied conversion factor at 64°C.	19
Figure 3.5: Modified binders: G^* with varied conversion factor at 64°C.....	20
Figure 3.6: Modified binders: δ with varied conversion factor at 64°C.....	20
Figure 3.7: Modified binders: $G^*/\sin(\delta)$ with varied conversion factor at 64°C.....	20
Figure 3.8: Modified binders: G^* against δ with varied conversion factor at 64°C.....	20
Figure 3.9: RTFO-aged binders: G^* with varied conversion factor at 64°C.....	21
Figure 3.10: RTFO-aged binders: δ with varied conversion factor at 64°C.....	21
Figure 3.11: RTFO-aged binders: $G^*/\sin(\delta)$ with varied conversion factor at 64°C.	21
Figure 3.12: RTFO-aged binders: G^* against δ with varied conversion factor at 64°C.....	21
Figure 3.13: Unmodified binders, unaged and aged: G^* with fixed conversion factor.....	23
Figure 3.14: Unmodified binders, unaged and aged: δ with fixed conversion factor.....	23
Figure 3.15: Unmodified binders, unaged and aged: $G^*/\sin(\delta)$ with fixed conversion factor.	23
Figure 3.16: Unmodified binders, unaged and aged: G^* against δ with fixed conversion factor.	23
Figure 3.17: Tukey HSD with varied aging condition (95% confidence interval).....	23
Figure 3.18: High temperature (unaged): Shear modulus tested at 64°C.....	25
Figure 3.19: High temperature (unaged): Phase angle tested at 64°C.....	25
Figure 3.20: High temperature (unaged): $G^*/\sin(\delta)$ tested at 64°C.....	25
Figure 3.21: High temperature (unaged): Shear modulus tested at 70°C.....	26
Figure 3.22: High temperature (unaged): Phase angle tested at 70°C.....	26
Figure 3.23: High temperature (unaged): $G^*/\sin(\delta)$ tested at 70°C.....	26
Figure 3.24: High temperature (unaged): Difference between concentric cylinder & parallel plate.	26
Figure 3.25: High temperature (RTFO-aged): Shear modulus tested at 64°C.	27
Figure 3.26: High temperature (RTFO-aged): Phase angle tested at 64°C.	27
Figure 3.27: High temperature (RTFO-aged): $G^*/\sin(\delta)$ tested at 64°C.....	27
Figure 3.28: High temperature (RTFO-aged): Shear modulus tested at 70°C.	28
Figure 3.29: High temperature (RTFO-aged): Phase angle tested at 70°C.	28
Figure 3.30: High temperature (RTFO-aged): $G^*/\sin(\delta)$ tested at 64°C.....	28
Figure 3.31: High temperature (RTFO-aged): Difference between concentric cylinder & parallel plate..	28
Figure 4.1: High shear mixer.....	30
Figure 4.2: Comparison of G^* results for concentric cylinder and parallel plate.....	31
Figure 4.3: Comparison of phase angle results for concentric cylinder and parallel plate.....	31
Figure 4.4: Comparison of $G^*/\sin(\delta)$ results for concentric cylinder and parallel plate.	31
Figure 4.5: $G^*/\sin(\delta)$ versus particle size for Type I ambient rubber binder.	34
Figure 4.6: $G^*/\sin(\delta)$ versus particle size for Type I cryogenic rubber binder.	34
Figure 4.7: $G^*/\sin(\delta)$ versus particle size for Type II ambient rubber binder.	35
Figure 4.8: $G^*/\sin(\delta)$ versus particle size for Type II cryogenic rubber binder.	35
Figure 4.9: $G^*/\sin(\delta)$ versus surface area for Type I ambient rubber binder.	36
Figure 4.10: $G^*/\sin(\delta)$ versus surface area for Type I cryogenic rubber binder.	36
Figure 4.11: $G^*/\sin(\delta)$ versus surface area for Type II ambient rubber binder.	36
Figure 4.12: $G^*/\sin(\delta)$ versus surface area for Type II cryogenic rubber binder.	36
Figure 4.13: Concentric Cylinder: Plot of true temperature grade vs. rubber particle size.	37
Figure 4.14: Parallel Plate: Plot of true temperature grade vs. rubber particle size.	37
Figure 4.15: Comparison of G^* for concentric cylinder and parallel plate with 3-mm gap.....	40
Figure 4.16: Comparison of phase angle for concentric cylinder and parallel plate with 3-mm gap.....	40

Figure 4.17: Comparison of $G^*/\sin(\delta)$ for concentric cylinder and parallel plate with 3-mm gap.	40
Figure 4.18: Difference between $G^*/\sin(\delta)$ for concentric cylinder and parallel plate with 3-mm gap.	40
Figure 5.1: Example normalized FTIR absorbance spectrum with carbonyl and sulfoxide areas.	44
Figure 5.2: Effect of preheating on precoating of RTFO bottles.	44
Figure 5.3: Effect of RTFO test parameters on bottle coating.	45
Figure 5.4: Effect of RTFO test parameters on shear modulus tested at 64°C.	48
Figure 5.5: Effect of RTFO test parameters on phase angle tested at 64°C.	48
Figure 5.6: Effect of RTFO test parameters on $G^*/\sin(\delta)$	48
Figure 5.7: Effect of RTFO test parameters on true high PG limit.	48
Figure 5.8: Effect of RTFO test parameters on binder chemistry.	49
Figure 5.9: Effect of RTFO test parameters on carbonyl index.	52
Figure 5.10: Effect of RTFO test parameters on sulfoxide index.	52
Figure 5.11: Effect of RTFO test parameters on butadiene index.	52
Figure 5.12: Binder coverage of a 50 g sample before and after PAV aging.	54
Figure 5.13: Binder separation at edge of pan after PAV aging.	54
Figure 5.14: Binder coverage and thickness after pouring a 50 g sample.	55
Figure 5.15: Binder coverage and thickness after PAV aging a 50 g sample.	55
Figure 5.16: Binder coverage and thickness after pouring a 50 g sample into preheated pan.	56
Figure 5.17: Binder coverage and thickness after PAV-aging a 50 g sample in preheated pan.	56
Figure 5.18: Binder coverage and thickness after pouring a 63 g sample in preheated pan.	58
Figure 5.19: Binder coverage and thickness after PAV-aging a 63 g sample in preheated pan.	58
Figure 5.20: Intermediate-temperature ($G^*\times\sin(\delta)$) test results for different PAV preparation methods. .	59
Figure 5.21: Low-temperature stiffness test results for different PAV preparation methods.	60
Figure 5.22: Low-temperature m-value test results for different PAV preparation methods.	61
Figure 6.1: Asphalt rubber specimen prepared with conventional BBR mold and method.	65
Figure 6.2: Standard (top) and modified (bottom) BBR specimen mold configurations.	66
Figure 6.3: Modified mold configuration and beam specimen.	66
Figure 6.4: Air pockets noted on third replicate specimen.	66
Figure 6.5: Modified mold configuration to produce three beam specimens in a single pour.	67
Figure 6.6: Uneven surface of asphalt rubber beam specimen after trimming.	68
Figure 6.7: BBR specimen preparation mold comparison: Creep stiffness.	70
Figure 6.8: BBR specimen preparation mold comparison: m-value.	70
Figure 6.9: BBR specimen preparation mold comparison: Percent difference in results.	70
Figure 7.1: Concentric cylinder geometry with 10-mm bob.	72
Figure 7.2: Int. temperature: Shear modulus comparison at 25°C.	74
Figure 7.3: Int. temperature: Phase angle comparison at 25°C.	74
Figure 7.4: Int. temperature: $G^*\times\sin(\delta)$ comparison at 25°C.	74
Figure 7.5: Int. temperature: Difference in $G^*\times\sin(\delta)$ between concentric cylinder and parallel plate. ...	74
Figure 8.1: MSCR: Average percent recovery at 64°C.	79
Figure 8.2: MSCR: Non-recoverable creep compliance at 64°C.	79
Figure 8.3: MSCR: Percent difference in APR between concentric cylinder and parallel plate.	79
Figure 8.4: MSCR: Percent difference in J_{nr} between concentric cylinder and parallel plate.	79
Figure 9.1: High-temperature grade and true grade results.	82
Figure 9.2: High temperature (unaged): Shear modulus.	83
Figure 9.3: High temperature (unaged): Phase angle.	83
Figure 9.4: High temperature (unaged): $G^*/\sin(\delta)$	83
Figure 9.5: High temperature (unaged): Difference between concentric cylinder and parallel plate.	83
Figure 9.6: High temperature (RTFO-aged): Shear modulus.	84
Figure 9.7: High temperature (RTFO-aged): Phase angle.	84
Figure 9.8: High temperature (RTFO-aged): $G^*/\sin(\delta)$	84
Figure 9.9: High temperature (RTFO-aged): Difference between concentric cylinder and parallel plate.	84
Figure 9.10: Low temperature: Creep stiffness.	87
Figure 9.11: Low temperature: m-value.	87

Figure 9.12: Unsieved vs. sieved: High temperature performance grade. 89

Figure 9.13: Unsieved vs. sieved: Percent difference in $G^*/\sin(\delta)$ 89

Figure 9.14: Unsieved vs. sieved: Correlation between true performance grade. 89

Figure 10.1: Air-void contents of gyratory-compacted specimens. 92

Figure 10.2: Air-void contents of rolling wheel-compacted specimens. 93

Figure 10.3: Dynamic shear modulus master curves. 94

Figure 10.4: Flexural dynamic modulus master curves. 96

Figure 10.5: Flexural complex modulus at 10 Hz loading frequency. 96

Figure 10.6: Cumulative permanent axial strain versus number of cycles (52°C). 97

Figure 10.7: Average flow number values for evaluated mixes (52°C). 98

Figure 10.8: Number of cycles to 1, 3, and 5% permanent axial strain. 98

Figure 10.9: Fatigue regression model for SOL-680. 100

Figure 10.10: Fatigue regression model for CAL-26. 100

Figure 10.11: Fatigue regression model for SB-154. 100

Figure 10.12: Fatigue regression models for all mixes. 100

Figure 10.13: Calculated fatigue life at 200, 400, and 600 μ strain. 101

Figure 10.14: SCB fracture energy. 102

Figure 10.15: SCB flexibility index. 102

LIST OF ABBREVIATIONS

AASHTO	American Association of State Highway and Transportation Officials
AMPT	Asphalt mix performance tester
AMRL	AASHTO Materials Reference Laboratory
ANOVA	Analysis of variance
APP	Asphalt plant-produced
APR	Average percent recovery
AR	Asphalt rubber
ASTM	American Society for Testing and Materials
BBR	Bending beam rheometer
Caltrans	California Department of Transportation
C_{ss}	Conversion factor
CRM	Crumb rubber modifier
CS	Chip seal
CT	Caltrans test
DGAC	Dense-graded asphalt concrete
DSR	Dynamic shear rheometer
E^*	Dynamic modulus
FTIR	Fourier Transformed Infrared Spectroscopy
FTIR-ATR	Fourier transformed infrared spectroscope in attenuated total reflection mode
G^*	Complex shear modulus
GTR	Ground tire rubber
HSD	Honest significant difference
J_{NR}	Non-recoverable creep compliance
LP	Laboratory-produced
LVDT	Linear variable displacement transducer
MSCR	Multiple stress creep recovery
PAV	Pressurized aging vessel
PG	Performance grade
PM	Polymer-modified
PP	Parallel plate
PPRC	Partnered Pavement Research Center
RAC	Rubberized asphalt concrete
RAP	Recycled asphalt pavement
RHMA-G	Gap-graded rubberized hot mix asphalt
RHMA-O	Open-graded rubberized hot mix asphalt
RPM	Revolutions per minute
RTFO	Rolling thin-film oven
SCB	Semicircular beam
SBR	Styrene-butadiene rubber
SHRP	Strategic Highway Research Program
TFO	Thin-film oven

TR	Tire rubber
UCPRC	University of California Pavement Research Center
UM	Unmodified
δ	Phase angle
μ strain	Microstrain

TEST METHODS CITED IN THE TEXT

- AASHTO M 320 Standard Specification for Performance-Graded Asphalt Binder
- AASHTO M 332 Standard Specification for Performance-Graded Asphalt Binder Using Multiple Stress Creep Recovery (MSCR) Test
- AASHTO PP 61 Standard Practice for Developing Dynamic Modulus Master Curves for Hot Mix Asphalt (HMA) Using the Asphalt Mixture Performance Tester (AMPT)
- AASHTO R 28 Standard Practice for Accelerated Aging of Asphalt Binder Using a Pressurized Aging Vessel (PAV)
- AASHTO TP 124 Provisional Standard Method of Test for Determining the Fracture Potential of Asphalt Mixtures Using Semicircular Bend Geometry (SCB) at Intermediate Temperature
- AASHTO T 166 Standard Method of Test for Bulk Specific Gravity (Gmb) of Compacted Hot Mix Asphalt (HMA) Using Saturated Surface-Dry Specimens
- AASHTO T 240 Standard Method of Test for Effect of Heat and Air on a Moving Film of Asphalt (Rolling Thin-Film Oven Test)
- AASHTO T 269 Standard Method of Test for Percent Air Voids in Compacted Dense and Open Asphalt Mixtures
- AASHTO T 313 Standard Method of Test for Determining the Flexural Creep Stiffness of Asphalt Binder Using the Bending Beam Rheometer
- AASHTO T 315 Standard Method of Test for Determining the Rheological Properties of Asphalt Binder Using a Dynamic Shear Rheometer
- AASHTO T 321 Standard Method of Test for Determining the Fatigue Life of Compacted Asphalt Mixtures Subjected to Repeated Flexural Bending
- AASHTO T 331 Bulk Specific Gravity (Gmb) and Density of Compacted Hot Mix Asphalt (HMA) Using Automatic Vacuum Sealing Method
- AASHTO T 350 Standard Method of Test for Multiple Stress Creep Recovery (MSCR) Test of Asphalt Binder Using a Dynamic Shear Rheometer (DSR)
- AASHTO T 378 Standard Method of Test for Determining the Dynamic Modulus and Flow Number for Asphalt Mixtures Using the Asphalt Mixture Performance Tester (AMPT)
- ASTM D8 Standard Terminology Relating to Materials for Roads and Pavements
- ASTM D36 Standard Test Method for Softening Point of Bitumen (Ring-and-Ball Apparatus)
- ASTM D92 Standard Test Method for Flash and Fire Points by Cleveland Open Cup Tester
- ASTM D217 Standard Test Methods for Cone Penetration of Lubricating Grease
- ASTM D297 Standard Test Methods for Rubber Products—Chemical Analysis
- ASTM D445 Standard Test Method for Kinematic Viscosity of Transparent and Opaque Liquids (and Calculation of Dynamic Viscosity)
- ASTM D2007 Standard Test Method for Characteristic Groups in Rubber Extender and Processing Oils and Other Petroleum-Derived Oils by the Clay-Gel Absorption Chromatographic Method
- ASTM D5329 Standard Test Methods for Sealants and Fillers, Hot-Applied, for Joints and Cracks in Asphalt Pavements and Portland Cement Concrete Pavements
- ASTM D7741 Standard Test Method for Measurement of Apparent Viscosity of Asphalt-Rubber or Other Asphalt Binders by Using a Rotational Handheld Viscometer
- CT 208 Method of Test for Apparent Specific Gravity of Fine Aggregates
- CT 385 Method of Test for Sampling and Testing Crumb Rubber Modifier
- CT 388 Method of Test for Sampling and Reheating Asphalt Rubber Binder Field Samples Prior to Viscosity Testing in Accordance to ASTM D 7741

CONVERSION FACTORS

SI* (MODERN METRIC) CONVERSION FACTORS				
APPROXIMATE CONVERSIONS TO SI UNITS				
Symbol	When You Know	Multiply By	To Find	Symbol
LENGTH				
in	inches	25.4	Millimeters	mm
ft	feet	0.305	Meters	m
yd	yards	0.914	Meters	m
mi	miles	1.61	Kilometers	Km
AREA				
in ²	square inches	645.2	Square millimeters	mm ²
ft ²	square feet	0.093	Square meters	m ²
yd ²	square yard	0.836	Square meters	m ²
ac	acres	0.405	Hectares	ha
mi ²	square miles	2.59	Square kilometers	km ²
VOLUME				
fl oz	fluid ounces	29.57	Milliliters	mL
gal	gallons	3.785	Liters	L
ft ³	cubic feet	0.028	cubic meters	m ³
yd ³	cubic yards	0.765	cubic meters	m ³
NOTE: volumes greater than 1000 L shall be shown in m ³				
MASS				
oz	ounces	28.35	Grams	g
lb	pounds	0.454	Kilograms	kg
T	short tons (2000 lb)	0.907	megagrams (or "metric ton")	Mg (or "t")
TEMPERATURE (exact degrees)				
°F	Fahrenheit	5 (F-32)/9 or (F-32)/1.8	Celsius	°C
ILLUMINATION				
fc	foot-candles	10.76	Lux	lx
fl	foot-Lamberts	3.426	candela/m ²	cd/m ²
FORCE and PRESSURE or STRESS				
lbf	poundforce	4.45	Newtons	N
lbf/in ²	poundforce per square inch	6.89	Kilopascals	kPa
APPROXIMATE CONVERSIONS FROM SI UNITS				
Symbol	When You Know	Multiply By	To Find	Symbol
LENGTH				
mm	millimeters	0.039	Inches	in
m	meters	3.28	Feet	ft
m	meters	1.09	Yards	yd
km	kilometers	0.621	Miles	mi
AREA				
mm ²	square millimeters	0.0016	square inches	in ²
m ²	square meters	10.764	square feet	ft ²
m ²	square meters	1.195	square yards	yd ²
ha	Hectares	2.47	Acres	ac
km ²	square kilometers	0.386	square miles	mi ²
VOLUME				
mL	Milliliters	0.034	fluid ounces	fl oz
L	liters	0.264	Gallons	gal
m ³	cubic meters	35.314	cubic feet	ft ³
m ³	cubic meters	1.307	cubic yards	yd ³
MASS				
g	grams	0.035	Ounces	oz
kg	kilograms	2.202	Pounds	lb
Mg (or "t")	megagrams (or "metric ton")	1.103	short tons (2000 lb)	T
TEMPERATURE (exact degrees)				
°C	Celsius	1.8C+32	Fahrenheit	°F
ILLUMINATION				
lx	lux	0.0929	foot-candles	fc
cd/m ²	candela/m ²	0.2919	foot-Lamberts	fl
FORCE and PRESSURE or STRESS				
N	newtons	0.225	Poundforce	lbf
kPa	kilopascals	0.145	poundforce per square inch	lbf/in ²

*SI is the symbol for the International System of Units. Appropriate rounding should be made to comply with Section 4 of ASTM E380 (Revised March 2003)

Blank page

1. INTRODUCTION

1.1 Background

1.1.1 Use of Rubberized Asphalt Concrete

Each year the United States generates nearly 300 million scrap tires, the approximate equivalent of one passenger car tire per person per year (1). Most of these tires end up in landfills, with the consequent environmental impacts. One tire disposal solution grinds the tires into crumbs that are incorporated into asphalt binders used to produce rubberized asphalt concrete (RAC), which includes gap- and open-graded rubberized hot mix asphalt (RHMA-G and RHMA-O, respectively). RAC is commonly used in California, Arizona, Texas, Florida, and New Jersey. Successful, documented use (2) of this material has created growing interest in many other states.

The maximum allowable crumb rubber particle size in asphalt rubber binders differs among the states (e.g., California and Arizona specify rubber particles passing the #8 [2.36 mm] sieve, while Florida limits the maximum size to the #30 [5 mm] sieve). Crumb rubber particle size in asphalt rubber chip seal applications is typically limited to that passing the #18 (1 mm) sieve to prevent clogging of binder spray nozzles.

In addition to recognizing the environmental benefits of recycling tires into asphalt concrete, research has also shown that RAC, when used in overlays, has better resistance to the fatigue and reflective cracking caused by traffic and exposure to temperature extremes than conventional dense-graded asphalt concrete (DGAC). Studies have also shown that half-thickness RAC used in overlays on cracked pavement can typically provide the same reflective cracking life as full thickness DGAC overlays (3-5).

1.1.2 Production of Rubber-Modified Binders

In California, crumb rubber from scrap tires is generally added to asphalt binder in a so-called wet process. Wet-process rubber-modified binder can be produced at an asphalt plant, a nearby distribution center (field blending), or at a supplier's terminal or a refinery (terminal blending). Two forms of modified binder are currently produced: *asphalt rubber binder* and *tire rubber-modified binder*.

- Asphalt rubber binder, by ASTM definition, must contain 15 percent or more rubber by weight of the binder. California Department of Transportation (Caltrans) specifications require 18 to 22 percent. The rubber particles have a coarse gradation (between 250 μm and 2.36 mm) and extender oils are often used to promote digestion. Larger particles are typically not fully digested into the binder.
- Tire rubber-modified binders typically contain less than 10 percent rubber, and the rubber particles are usually smaller than 250 μm . These binders have similar characteristics to polymer-modified binders and can be characterized accordingly using existing Superpave performance-grading (PG) procedures (AASHTO M 320). In California, these binders must meet Caltrans PG-M modified binder specifications.

The significant differences in the constituents and production procedures of asphalt rubber binders result in a product very different from unmodified asphalt binders and therefore different approaches are required to test and characterize them.

The Superpave PG procedures noted above were developed for asphalt binders that contain no additives or particles, and are therefore often inappropriate for testing asphalt rubber binders. Consequently, current quality control testing of asphalt rubber binders is limited to rotational viscosity (Haake) and cone penetration. For this reason, it is generally agreed that alternative binder grading procedures consistent with Superpave PG procedures are needed to characterize asphalt rubber binders. The research discussed in this report focuses on the development of these performance grading procedures for wet-process asphalt rubber binders.

1.1.3 Crumb Rubber Modifier Production

Crumb rubber modifier (CRM) (also known as *ground tire rubber* [GTR]) is produced by grinding waste tires. The two main methods used are *ambient grinding* and *cryogenic fracturing*. In the ambient grinding process, the scrap tires are cut to small pieces and then shredded and ground at ambient temperature into small crumbs. The ambient grinding method results in irregular-shaped rubber particles with rough surfaces. In cryogenic fracturing, the cut scrap tire pieces are frozen with liquid nitrogen and then fractured into small crumbs. Cryogenic fracturing usually results in cubical-shaped rubber particles with smooth surfaces.

1.1.4 Current Caltrans Asphalt Rubber Binder Specifications

Current Caltrans specifications for the constituents of asphalt rubber binder, asphalt rubber binder reaction design profile, and the criteria for quality control and acceptance are summarized in Table 1.1, Table 1.2, and Table 1.3, respectively. Asphalt rubber binder quality is characterized based on rotational viscosity (Haake), cone penetration, resilient properties, and softening properties. The asphalt rubber binder must meet the specified limits in Table 1.3 after at least 45 minutes of reaction time between the asphalt binder and the crumb rubber.

According to the ASTM D8 test method, a minimum of 15 percent CRM by weight of the asphalt binder is required to meet the definition of asphalt rubber binder. However, Caltrans specifications require a CRM content between 18 and 22 percent by weight of the asphalt rubber binder, of which 25 percent must be natural rubber. An extender oil must be added at a rate of two to six percent by weight of the base asphalt binder to facilitate the reaction between the asphalt binder and rubber particles (1).

Current Caltrans specifications also require crumb rubber particles finer than 2.36 mm (100 percent passing the #8 sieve). Cryogenic grinding is only permitted as a first step for the separation of metals and fibers, after which larger rubber particles are ground at ambient temperatures to meet the required sizes.

Table 1.1: Caltrans Specifications for Asphalt Rubber Binder Constituents

Component	Characteristic	Test Method	Value
Base asphalt binder	Viscosity, m ² /s (× 10 ⁻⁶) at 100°C	ASTM D445	X ± 3 ^a
	Flash point, Cleveland Open Cup (°C)	ASTM D92	>207
	Asphaltenes (% by mass)	ASTM D2007	<0.1
	Aromatics (% by mass)	ASTM D2007	>55
Crumb rubber modifier ^b	Scrap tire crumb rubber gradation (% passing #8 sieve)	CT 385	100
	High natural rubber gradation (% passing #10 sieve)	CT 385	100
	Wire in CRM (% max.)	CT 385	0.01
	Fabric in CRM (% max.)	CT 385	0.05
	CRM particle length (in. max.) ^c	--	3/16
	CRM specific gravity ^c	CT 208	1.1 – 1.2
	Natural rubber content in high natural rubber (%) ^c	ASTM D297	40.0 – 48.0
^a The symbol “X” is the proposed extender oil viscosity. “X” must be from 19 to 36. A change in “X” requires a new asphalt rubber binder design. ^b CRM must be ground and granulated at ambient temperature. If steel and fiber are cryogenically separated, this must occur before grinding and granulating. If cryogenically produced, M particles must be large enough to be ground or granulated and not pass through the grinder or granulator. ^c Test at mix design and for certificate of compliance.			

Table 1.2: Asphalt Rubber Binder Reaction Design Profile

Characteristic	Test Method	Minutes of Reaction ^{a,b}							Value
		45	60	90	120	240	360	1440	
Cone penetration @ 77°F (0.10 mm)	ASTM D217	X				X		X	25 – 70
Resilience @ 77°F (% rebound)	ASTM D5329	X				X		X	>18
Field softening point (°F)	ASTM D36	X				X		X	125 – 165
Viscosity @ 375°F, (centipoise)	ASTM D7741 ^c	X	X	X	X	X	X	X	1,500 – 4,000
^a Six hours (360 minutes) after CRM addition, the oven temperature is reduced to 275°F for 16 hours. After the 16-hour (1,320-minute) cool down after CRM addition, the binder is reheated to the reaction temperature expected during production for sampling and testing at 24 hours (1,440 minutes). ^b “X” denotes required testing. ^c Sample prepared according to CT 388									

Table 1.3: Caltrans Specifications for Asphalt Rubber Binder Quality Control and Acceptance

Characteristic	Test Purpose	Test Method	Value	
			Minimum	Maximum
Cone penetration @ 77°F (0.10 mm)	Acceptance	ASTM D217	25	70
Resilience @ 77°F (% rebound)	Acceptance	ASTM D5329	18	--
Field softening point (°F)	Acceptance	ASTM D36	125	165
Viscosity @ 375°F, (centipoise)	Quality control	ASTM D7741 ^a	1,500	4,000
^c Sample prepared according to CT 388				

For each Caltrans project, asphalt rubber binder producers must propose a design and profile for the binder that will be used. The proposed design must specify the materials to be used including base binder, extender oil, and crumb rubber. The asphalt rubber binder profile serves as a production quality indicator and is not used as a performance specification. The profile illustrates the characteristics of the binder over a 24-hour (1,440-minute) reaction period.

1.2 Problem Statements

A number of limitations to the current asphalt rubber binder specification have been identified through a review of the literature and discussions with stakeholders. These include the following:

- The current Caltrans specification for wet-process asphalt rubber binders focuses mainly on measuring viscosity at the plant using a handheld rotational viscometer. Temperature control requirements during testing are limited, which can influence results given that asphalt binder properties are highly influenced by temperature. While viscosity is an important parameter for the pumpability and workability of the binder and ultimately of the mix, it does not directly relate to the in-service performance of the binder within a rubberized asphalt concrete mix or a rubberized asphalt surface treatment. Additionally, due to the particulate phase of these binders, viscosity measurements alone lack sufficient accuracy to completely describe their complex behavioral and performance properties.
- Although cone penetration grading and resilience properties do provide a means to evaluate the stiffness and resilience of asphalt rubber binders, the Superpave performance grading testing procedure moved away from these tests because they have several limitations, including the following:
 - + They are empirical tests that measure a binder's viscous and elastic properties but the tests do not necessarily correlate with field performance.
 - + The tests only measure a binder's properties at a single intermediate temperature, and thereby fail to provide an accurate indication of its properties at typical high and low service temperatures, or of its temperature susceptibility (change of stiffness with change of temperature).
 - + The tests do not address the effects of short-term aging (during mixing and compaction) and long-term aging (during service life) on binder properties.
- Softening point generally indicates the phase change temperature of binders and may not be sufficient for comprehensive performance/rheological characterization.
- Rheological testing using a dynamic shear rheometer (DSR) and a bending beam rheometer (BBR) is now considered standard practice for evaluating performance-related characteristics of unmodified, polymer-modified, and tire rubber-modified asphalt binders. However, the standard parallel plate geometry used in a DSR test is potentially inappropriate for measuring the properties of asphalt rubber binders produced per Caltrans specifications. When an asphalt rubber binder is tested in a DSR using parallel plate geometry with a 1-mm or 2-mm gap, incompletely digested rubber particles can contact both the top and bottom plates and interfere with the torque and strain measurements. This interference results in the rheology of the rubber particles dominating the measurement and potentially providing misleading information about the rheology of the asphalt rubber binder as a whole. A potential consequence of this misleading information can be the choice/use of an inappropriate binder for a given climatic region. According to AASHTO T 315 (*Standard Method of Test for Determining the Rheological Properties of Asphalt Binder Using a Dynamic Shear Rheometer*), the gap size between the plates should be at least four times the maximum particle size to provide reliable results (i.e., an 8-mm gap, with correspondingly adjusted plate diameter, would be required for 2.0 mm [#10] crumb rubber particles). However, the maximum gap size recommended by rheologists is about 5 mm, to ensure a satisfactory linear shear rate through the asphalt binder sample sandwiched between the plates. Although increasing the gap size is a potential solution for

dealing with the larger rubber particle sizes, this increase can introduce other problems, such as poor repeatability, unacceptable temperature gradients, difficulty in trimming the specimen, uncontrollable edge effects, and potentially misleading results. When testing with parallel plate geometry, the modulus of the asphalt binder is proportional to the sample radius to the power of four. Consequently, a two percent reduction in radius due to incorrect trimming implies a potential 16 percent reduction in the measured modulus.

- Other limitations of the current performance grading testing procedures when testing asphalt rubber binders include:
 - + Short-term aging in a rolling thin-film oven (RTFO) does not uniformly coat the bottle at the current testing temperature because the asphalt rubber binder is more viscous, and it is difficult to remove the aged binder from the bottle.
 - + Long-term aging of asphalt rubber binder in a pressurized aging vessel (PAV) is questionable, since the test was developed for unmodified binders and has not been validated for asphalt rubber binders.
 - + Low-temperature testing of asphalt rubber specimens in the bending beam rheometer is questionable, since the viscous, particulate-rich binders are difficult to pour into the specimen preparation mold. The test method and interpretation of its results also need to be studied in greater detail to confirm their appropriateness for testing asphalt rubber binder.
- The actual grading limits developed for unmodified and polymer-modified asphalt binders may not be appropriate asphalt rubber binder performance indicators as they may not reflect the contribution of the binder rheology in terms of the rutting, fatigue, and low-temperature cracking performance of RAC mixes.

To resolve these issues, there is a need for alternative testing configurations and procedures that can better evaluate the performance characteristics of field-blended wet-process asphalt rubber binders using the same or similar Superpave PG parameters as for unmodified, polymer-modified (PM), and tire rubber-modified (TR) asphalt binders. These alternate methods can then be used to establish performance-based contract acceptance criteria for the production of asphalt rubber binders, which will in turn lead to more reliable performance in the field.

1.3 Project Objectives

The objective of this study is to recommend appropriate contract acceptance criteria for wet-process asphalt rubber binders used in gap- and open-graded mixes using current Superpave PG equipment with testing procedures that have been modified where appropriate. This objective will be met by completing the following tasks in a series of phases (Figure 1.1). Work that had been completed at the time of preparing this report is noted.

1. Review relevant literature on the topic. Contact DSR equipment manufacturers and discuss test requirements and alternative geometries. (The literature is summarized in Chapter 2).

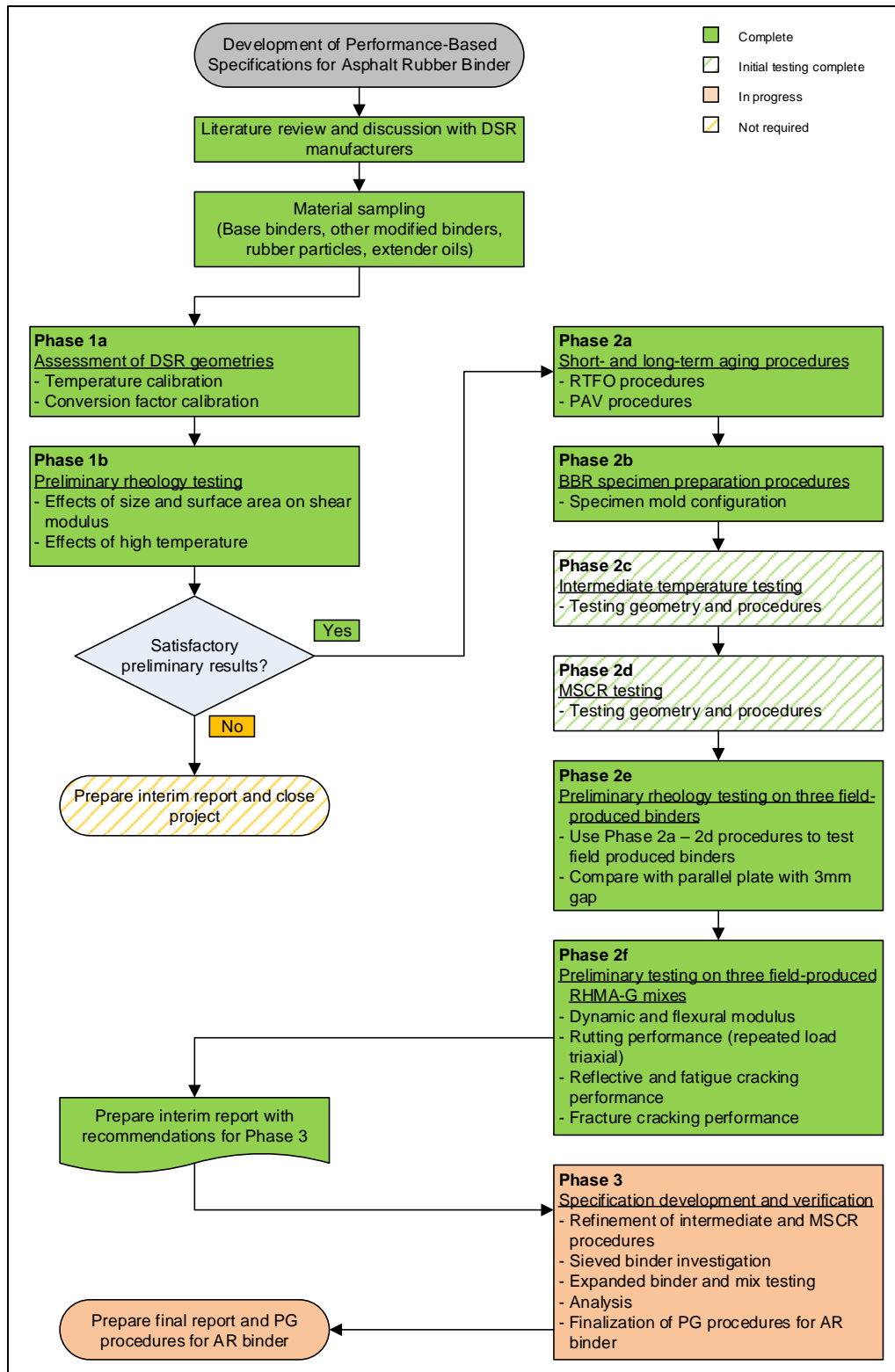


Figure 1.1: Flowchart of project tasks/phases.

2. Collect samples of asphalt binder, crumb rubber particles, and extender oil for laboratory preparation of asphalt rubber binders. On completion of initial screening tests, identify completed and current

projects where asphalt rubber binder samples can be collected for additional testing. Prepare laboratory-conditioned samples for testing with a DSR.

3. Evaluate the use and ability of the alternative concentric cylinder DSR geometry to provide realistic and repeatable results for unmodified, polymer-modified (PM), and tire rubber-modified (TR) binders that are comparable to results from the same tests using conventional parallel plate geometries. The performance of these binders is routinely measured with parallel plate geometry in terms of the Superpave performance grading system. (This testing was completed in Phase 1a and is discussed in Chapter 3).
4. Compare the abilities of the parallel plate and concentric cylinder geometries for testing asphalt rubber binder containing crumb rubber particles of various sizes, and evaluate the effects of different crumb rubber particles and asphalt rubber binder properties on test results. (This testing was completed in Phase 1b and is discussed in Chapter 4).
5. Evaluate and refine short- and long-term aging procedures for asphalt rubber binders. (This testing was completed in Phase 2a and is discussed in Chapter 5).
6. Evaluate and refine specimen preparation procedures for low-temperature testing of asphalt rubber binders in a BBR. (This testing was completed in Phase 2b and is discussed in Chapter 6).
7. Evaluate whether the concentric cylinder geometry is appropriate for intermediate-temperature and multiple stress creep recovery (MSCR) testing. (Preliminary testing on this task was completed in Phase 2c and Phase 2d, respectively, and is discussed in Chapters 7 and 8. Additional testing is in progress as part of Phase 3 and will be documented in a later report).
8. Evaluate the high-, intermediate-, and low-temperature rheological properties of field-sampled asphalt rubber binders using the refined procedures developed in Tasks 1 through 7, and interpret the test results in conjunction with results from tests on field-sampled gap-graded mixes prepared with the same binders. (Preliminary testing was completed in Phase 2e and Phase 2f, respectively and is discussed in Chapters 9 and 10. Additional testing is in progress as part of Phase 3 and will be documented in a later report.)
9. Suggest provisional performance grading criteria and provisional contract acceptance criteria for wet-process asphalt rubber binders (This task is dependent on results from all previous tasks and will be documented in a later report).
10. Prepare provisional procedures for conducting the recommended tests and interpreting the test results. (Proposed test methods are provided in Appendix A. Interpretation of results will be documented in a later report).
11. Prepare reports documenting this research effort, with recommendations for specification language and, if required, recommendations for further research to validate the provisional performance grading and contract acceptance criteria.

This report provides an update on work completed to date on all tasks/phases.

Although this study focused on testing asphalt rubber binders used in gap- and open-graded mixes, the results are relevant for asphalt rubber binders used in chip seals and other surface treatments. However, to prevent clogging of spray nozzles the maximum rubber particle size used in these applications is typically limited to that passing the #18 (1 mm) sieve, which is considerably smaller than the #8 (2.36 mm) maximum size used in binders used in gap- and open-graded mixes.

1.4 Measurement Units

Caltrans recently returned to the use of US standard measurement units, however, the Superpave performance grading system is a metric standard and uses metric units. In this report, both English and metric units (provided in parentheses after the English units) are provided in the general discussion. Metric units are used in the reporting of performance grading test results. A conversion table is provided on page xxiii.

2. LITERATURE REVIEW

2.1 Status Quo on Performance-Related Testing of Asphalt Rubber Binders

Limited research has been performed to characterize asphalt rubber binders using the Superpave Performance Grading procedures (6-11). These studies used the standard Superpave (AASHTO M 320) procedures to measure rheological properties using a dynamic shear rheometer (DSR) and bending beam rheometer (BBR) and to investigate the influence of rubber type and size, rubber content, base binder type, and reaction time and temperature on these properties. Asphalt rubber binder aging has also been evaluated to a limited extent by testing binders aged in a rolling thin-film oven (RTFO) and a pressure aging vessel (PAV) (6). However, most of this testing was conducted on binders produced with rubber particles between 0.4 mm and 0.6 mm (passing the #30 and #40 mesh sieves), with one study looking at particles passing the 1.4 mm (#14) sieve. These particles are considerably smaller than those used to produce asphalt rubber binders in California.

Bahia and Davis (6) performed one of the first studies to characterize asphalt rubber binders (prepared with rubber particles passing the 1.19 mm [#16] sieve) using Superpave testing procedures. They proposed increasing the gap size between the parallel plates to 2 mm to better compensate for the effect of the rubber particles, but still not meeting the generally recommended minimum gap that is four times the size of the particles being tested. This modification to the test has since been adopted by other researchers working with asphalt binders prepared with rubber particle gradations that do not exceed 1 mm. This modification is not considered appropriate for California given that the state's considerably larger rubber particles (passing the 2.36 mm [#8] sieve) would require a gap size of at least 8 mm to meet the 1:4 particle size to gap size ratio requirement. This gap size is not feasible for testing asphalt binders because the binder will flow out of the plates during the test.

2.2 Identifying an Alternative to Parallel Plate Testing

Discussions with binder-testing equipment manufacturers and other practitioners researching asphalt binder rheology (12), and a review of the literature indicated that the use of a concentric cylinder (or *cup-and-bob*) geometry would be the most appropriate system for testing the properties of asphalt rubber binders. Therefore, although other options for testing were not excluded from this literature review, it is mainly focused on this geometry. The literature review also focused on the potential effects of different crumb rubber modifier (CRM) properties on asphalt binder performance, with particular attention given to the method of CRM preparation, the particle size and surface area, the CRM content in the asphalt binder, and the methods used to age the asphalt rubber binder before testing.

2.2.1 Concentric Cylinder Geometry (Cup-and-Bob)

The DSR concentric cylinder measuring system proposed for evaluating asphalt binders has two cylinders: the inner cylinder is called the bob and the outer one is called the cup (Figure 2.1).

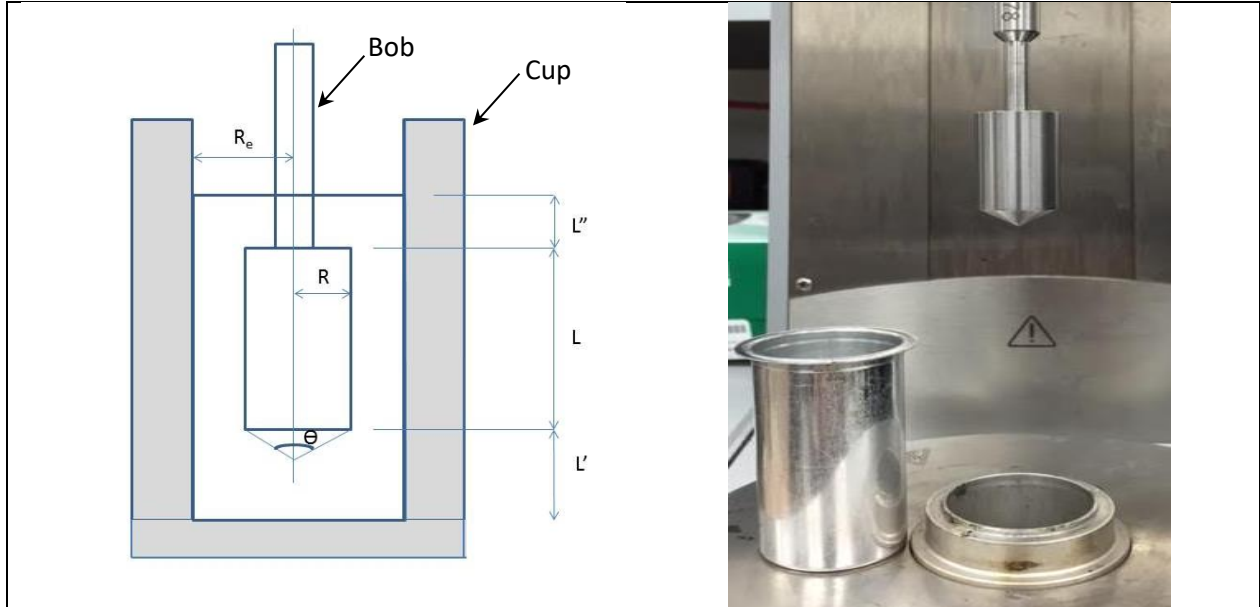


Figure 2.1: Concentric cylinder geometry.

This concentric cylinder geometry is commonly used to measure the viscosity of substances such as paints, adhesives, and various food types that may not be homogenous or that contain particulates. Only limited research has been undertaken on using the concentric cylinder geometry to measure complex shear modulus (G^*) and phase angle (δ)—the Superpave performance grading (PG) system’s main measurement parameters—to assess the high-temperature properties of unmodified and polymer-modified asphalt binders because the Superpave procedure uses parallel plate geometry with 1-mm or 2-mm gaps. However, by varying the cup and/or bob size, the concentric cylinder geometry can accommodate a gap as large as 7 mm, making it more appropriate than the parallel plate geometry for testing asphalt rubber binders with larger constituent particles. The shear stress and shear strain calculations used to interpret the data from the concentric cylinder geometry are shown in Equations 2.1 and 2.2 (13).

$$\tau = \frac{T}{2\pi LR^2} \quad (2.1)$$

$$\gamma = \frac{\theta R_e}{(R - R_e)} \quad (2.2)$$

where:

τ = shear stress (Pa)

γ = shear strain (%)

T = torque (mNm)

L = length of the bob (mm)
 R_e = radius of the cup (mm)
 R = radius of the bob (mm)
 θ = angular rotation of the bob (radians)

The concentric cylinder geometry is controlled by the surface area and radius of the bob and the inside surface area and radius of the cup, in a similar way to the parallel plate geometry, which is controlled by the surfaces and radius of the two plates. Any binder at the bottom of the cup or that overtops the bob can be ignored. Unlike the parallel plate geometry, which requires trimming of the sample that can lead to operator error (depending on the operator's skill level), the concentric cylinder geometry does not require trimming of the sample.

Baumgardner and D'Angelo (12) evaluated the concentric cylinder approach using a DSR to compare the performance grade (PG) properties of unmodified, polymer-modified, and wet-process asphalt rubber binders. They concluded that the concentric cylinder geometry can provide results ($G^*/\sin(\delta)$) similar to those obtained using parallel plate geometry. Cheng et al. (14) also investigated the $G^*/\sin(\delta)$ of unmodified binders using concentric cylinder geometry, and the results indicated a good correlation between the concentric cylinder and parallel plate geometries. However, only a limited number of binders were evaluated in both studies, and calibration factors between the two approaches were not discussed.

2.3 Effects of Crumb Rubber Modifier on Asphalt Binder Performance

Adding crumb rubber to an asphalt binder significantly impacts the binder's performance-related properties and increases its viscosity at pumping and mixing temperatures. At high temperatures, the complex shear modulus and the associated strain at failure of asphalt rubber binders are also higher than those of unmodified binders. The presence of rubber in the asphalt binder has less of an influence on the low-temperature properties (6) and test results are generally similar to those of unmodified binders.

2.3.1 Effect of Crumb Rubber Production Method

The chosen tire-grinding method (ambient grinding versus cryogenic fracturing) influences the shape of the rubber crumbs, their texture, their surface area, and other physical properties, with ambient grinding typically producing rubber crumbs with more irregular shapes, a rougher texture, and typically a larger surface area than cryogenically fractured rubber. As a consequence, the properties of rubberized binders can differ depending on the CRM production method used (15). Binder testing results have shown that asphalt rubber binders produced with cryogenically fractured rubber have more settlement, higher temperature sensitivity, and less resistance to low-temperature cracking and to drain-down than binders produced with rubber ground at ambient temperatures. However, it should be noted that the low-temperature indicator (m-

value) in the PG system was not shown to be statistically different for binders produced with rubber crumbs from the two different processes (16).

2.3.2 Effect of Crumb Rubber Particle Size, Shape, and Surface Area

The particle size, shape, and surface area of crumb rubber can affect the viscosity and performance-related properties of asphalt binders (15-18), and different researchers have obtained different results. West (15), Lee (16), and Kim et al. (17) found that crumb rubber particles with higher surface areas and more irregular shapes (i.e., those produced at ambient temperatures) tended to produce rubberized binders with higher viscosities, while Shen et al. (18) reported opposite results. Lee's findings concluded that particles with higher surface areas absorb more light fractions from the base asphalt binders, leading to the higher viscosity of the modified binder. Shen concluded that both particle size and surface area have statistically significant effects on the viscosity of rubberized binders, with particle size having a larger impact on viscosity than surface area.

2.3.3 Effect of Crumb Rubber Content

Asphalt binders modified with higher rubber contents have higher viscosities than those with lower rubber contents (15,19). Higher rubber contents also have significant effects on the high-temperature performance property (the value of $G^*/\sin(\delta)$) of asphalt binders (19). Lee et al. (16) also reported that mixes produced with binders with higher crumb rubber contents had improved fatigue resistance compared to those with lower crumb rubber contents.

2.3.4 Effect of Laboratory Aging Method

The Superpave performance grading system characterizes asphalt binders at three critical aging stages. Unaged binders are tested to characterize the virgin binder prior to mixing with aggregates. Short-term-aged binders conditioned in a rolling thin-film oven (RTFO) are tested to characterize the binder after asphalt concrete production and placement. Long-term-aged binders conditioned in both RTFO and pressure aging vessel (PAV) are tested to characterize binders that have been in service for 7 to 15 years after placement.

The high viscosities of asphalt rubber binders can have implications when conducting these performance-grading tests. In the RTFO test, a binder's high viscosity at the test temperature may prevent it from coating the entire bottle at the start of the test, prevent it from flowing in the bottle during the test period, and/or spilling out of the bottle instead of coating it (12). This coating issue defeats the original design purpose of the RTFO test, which requires that binders must keep moving in the RTFO bottle to avoid skin formation and to ensure uniform aging, conditions representative of those in the asphalt plant. High-viscosity rubberized binders are also difficult to scrape from the RTFO bottle after the test is completed.

The difference between the thin-film oven (TFO) test and the RTFO test was investigated by Jeong (19) and Zupanick (20). Zupanick analyzed the AASHTO Materials Reference Laboratory (AMRL) database, which includes more than 2,000 TFO and RTFO tests completed in laboratories throughout the United States. Using viscosity, penetration, and weight change as the measured parameters, Zupanick concluded that the TFO and RTFO tests are not interchangeable, contradicting earlier studies and industry practice. The data indicated that the RTFO test is more severe and precise than the TFO test in terms of the increase in binder viscosity. However, these results were not consistent for all the samples, with TFO-aged samples tending to have lower viscosities than RTFO-aged samples when the original binders were softer. This was attributed to the higher viscosities reducing natural convection in the TFO pan, and to skin formation on the binder during the TFO test. The study did not consider dynamic shear modulus, phase angle, or low-temperature properties.

Blank page

3. Phase 1a: ASSESSMENT OF DSR TESTING GEOMETRIES

3.1 Introduction

This chapter discusses the testing of selected performance-graded unmodified, polymer-modified, and tire rubber-modified (i.e., meeting Caltrans PG-M specifications) asphalt binders using parallel plate (PP) and concentric cylinder (CC) geometries to determine whether equivalent results can be obtained from each geometry for a range of binders with different properties. Note that although polymer-modified and tire rubber-modified binders are considered in the same category in the Caltrans specifications, the method of modification is used throughout this report to distinguish the two binders. Before this testing could be undertaken, appropriate temperature and conversion factor calibrations needed to be developed to interpret and relate results from the two geometries.

3.1.1 Temperature Calibration and Thermal Equilibrium

Asphalt binder performance is very sensitive to testing temperature, and therefore accurate temperature control of each measuring system is critical for testing. Each system must be calibrated appropriately to ensure that temperature control is correct. Since the two measuring systems have different geometries, each requires a different temperature calibration process. For both systems, three testing temperatures (40°C, 65°C, and 90°C) are typically calibrated to ensure accuracy. To check the vertical temperature gradient in the concentric cylinder configuration, four measurements are taken: at the top of the cup, at the middle of the cup close to the bob, at the middle near the cup edge, and at the bottom of the cup. This temperature gradient should not differ by more than 0.1°C from top to bottom, a value comparable to the requirements of the parallel plate testing system.

The concentric cylinder test requires significantly more binder than the parallel plate test. The parallel plate test with 25 mm diameter plates and 1 mm, 2 mm, and 3 mm gap sizes require 1.2 g, 2.4 g, and 3.6 g, respectively, while a concentric cylinder system with a 17 mm bob requires 22 g. As a result, testing with the concentric cylinder takes longer to reach temperature equilibrium than the parallel plate.

For the remainder of this study, temperature calibration and thermal equilibrium were strictly controlled following the above conventions in all tests discussed in this report.

3.1.2 Calibration of the Conversion Factor (C_{ss})

A series of laboratory tests were conducted in this part of the study to compare the results obtained from the concentric cylinder and parallel plate testing geometries. The effects of different operators, different binder types (unmodified, polymer-modified, or tire rubber-modified), binder source, and aging condition (unaged,

rolling thin-film oven [RTFO] aged, and in certain instances, thin-film oven [TFO] aged) on complex shear modulus and phase angle were all investigated.

The two cylinders (i.e., the cup and the bob) used in the concentric cylinder testing system have different diameters and therefore nonlinear behavior, unlike the parallel plate system, which uses two plates that have the same dimensions. The presence of relatively large partially digested rubber particles in the asphalt rubber binder also requires a corresponding increase in gap size in the cup-and-bob geometry. Therefore, an appropriate conversion factor must be applied to relate test results obtained with the concentric cylinder geometry (larger gap) to those obtained with the parallel plate geometry (smaller gap). When small gaps are used, the change in shear stresses between the cup and the bob is very small (assumed linear) and thus, the representative shear stress is the average shear stress between the cup and the bob. Because the shear stress is assumed to be linear, the conversion factor only depends on the geometric dimensions of the specific concentric cylinder configuration. In these instances, a fixed conversion factor can be used.

When using larger-gap concentric cylinders, the linear assumption of shear stress between the two cylinders is no longer appropriate and binder-specific conversion factors need to be determined based on the asphalt binder's complex viscosity, angular frequency, strain, and torque. The conversion factor for a large-gap concentric cylinder configuration can be calculated using Equation 3.1 (*Anton Paar, personal communication*), which provides comparable results between the concentric cylinder and parallel plate geometries in terms of complex shear modulus (G^*) and phase angle (δ). Calibration is required for each asphalt binder with different complex viscosity or torque values.

$$C_{ss} = \frac{\eta[\omega(\gamma/100)]}{T} \quad (3.1)$$

where,

- C_{ss} = conversion factor
- η = complex viscosity from parallel plate (Pa.S)
- ω = angular frequency (rad/s)
- γ = strain (%)
- T = torque from concentric cylinder (mNm)

3.2 Testing Plan

3.2.1 Testing with Binder-Specific Conversion Factors

Unmodified and modified binders were tested with a DSR to investigate the effects of varying conversion factors on the measurements from the concentric cylinder geometry. In this stage, the experiment was separated into the following three tasks:

- Task 1: Testing of three unmodified PG 64-16 binders by three different operators with three replicates. Binders were obtained from three California-based oil refineries (Refineries #1, #2, and #3).

- Task 2: Testing of one PG 64-28M polymer-modified and one PG 64-28M tire rubber-modified binder by three different operators with three replicates. Binders were obtained from one California-based oil refinery (Refinery #3).
- Task 3: Testing of two unmodified PG 64-16 binders, one PG 64-28M polymer-modified binder, and one PG 64-28M tire rubber-modified binder, all subjected to RTFO aging. No replicates were tested in this task. The unmodified binders were sourced from two refineries (#1 and #2) and the polymer- and tire-modified binders were sourced from one refinery (#3). It should be noted that TR-modified binders have much smaller rubber particles (maximum size of 300 μm [#50]) than asphalt rubber binders and due to their more complete digestion are not susceptible to the problems with RTFO aging discussed in Section 2.3.4; this permits direct comparison using the two DSR configurations.

3.2.2 Testing with a Fixed Conversion Factor

Testing of a standard fluid with viscosity similar to an asphalt binder was identified as the most appropriate method for determining a representative fixed conversion factor that could be used to compare the results obtained with the two testing geometries. A Cannon Instrument Company certified viscosity reference standard S600 was selected to obtain this conversion factor (*Anton Paar, personal communication*). Based on the test results, a fixed conversion factor value of 72 was selected for the testing described in this report.

Three unmodified binders (PG 58-22 [Refinery #1], PG 64-16 [Refinery #2], and PG 70-10 [Refinery #1]) were assessed to investigate the effects of this fixed conversion factor. Both unaged and short-term oven-aged binders were tested. Short-term aging was performed using both the RTFO and TFO in an attempt to address the issues discussed in Section 2.3.4 with regard to aging rubberized binders. A single operator conducted the experiments (with three replicates), which was determined to be sufficient given that the results obtained by the three different operators in Tasks 1 through 3 were not significantly different.

3.3 Test Results

3.3.1 Testing with Binder-Specific Conversion Factors

Table 3.1 presents the conversion factors determined for the asphalt binders evaluated in Tasks 1 through 3 (see Section 3.2.1).

Table 3.1: Specific Conversion Factors for the Evaluated Asphalt Binders

Asphalt Binder		Conversion Factor	
Source	Performance Grade	Original	RTFO-Aged
Refinery #1	64-16	70	64
Refinery #2	64-16	67	81
Refinery #3	64-16	71	50
Refinery #1	64-28M (PM)	80	78
Refinery #1	64-28M (TR)	91	81
PM = polymer modified		TR = tire rubber modified	

The conversion factors were calculated from Equation 3.1 using complex viscosity measurements at 64°C tested with both parallel plate (1-mm gap) and concentric cylinder geometries. The conversion factors were found to be different for the various evaluated asphalt binders and changed considerably with short-term RTFO aging in some cases (e.g., PG 64-16). The DSR test results are listed in Table B.1 through Table B.4 in Appendix B and are summarized in the following sections.

Task 1: Unmodified Binders

The boxplots of complex shear modulus (G^*), phase angle (δ), and $G^*/\sin(\delta)$ at 64°C for the three different unmodified binders are shown in Figure 3.1 through Figure 3.3. Based on these results, the complex shear modulus values appeared to be very similar between the two geometries, but with slightly different phase angles (less than 0.5° difference). The differences in $G^*/\sin(\delta)$ between the concentric cylinder and parallel plate geometries were therefore also very small. For reference, the high PG limits of unaged and RTFO-aged binders are the temperatures at which $G^*/\sin(\delta)$ are equal to 1.0 kPa and 2.2 kPa, respectively.

The differences in results for the three operators are shown in Figure 3.4. The results obtained by Operator #1 and Operator #2 are very close, but the results obtained by Operator #3 were slightly different for both geometries. The points in Figure 3.4 are scattered evenly for both concentric cylinder and parallel plate, indicating that the repeatability of results when using the concentric cylinder geometry is similar to that when testing with the parallel plate system.

Analysis of variance (ANOVA) was used to investigate the difference in results between the two testing geometries. $G^*/\sin(\delta)$ was the dependent variable and geometry was the independent variable. Binder source was selected as a blocking factor (i.e., arranging experimental units in groups [blocks] that are similar to each other where a blocking factor is a source of variability that is not of primary interest in the study). The analysis results are shown in Table 3.2, and indicate that the measurements of $G^*/\sin(\delta)$ between the concentric cylinder and the parallel plate were not significantly different at a 95 percent confidence interval. With a varied (i.e., binder specific) conversion factor, the results obtained when using the concentric cylinder geometry were not statistically significantly different (at the same confidence interval) from the results obtained when using the parallel plate geometry.

Table 3.2: Unmodified Binders: ANOVA Results of $G^*/\sin(\delta)$ with Varied Conversion Factor ($\alpha=0.05$)

Parameter	Df	Sum Sq	Mean Sq	F Value	Pr (>F)
Geometry	1	0.0006	0.0006	0.294	0.59
Source	2	0.9808	0.4904	240.582	<2e-16
Residuals	50	0.1019	0.0020	-	-

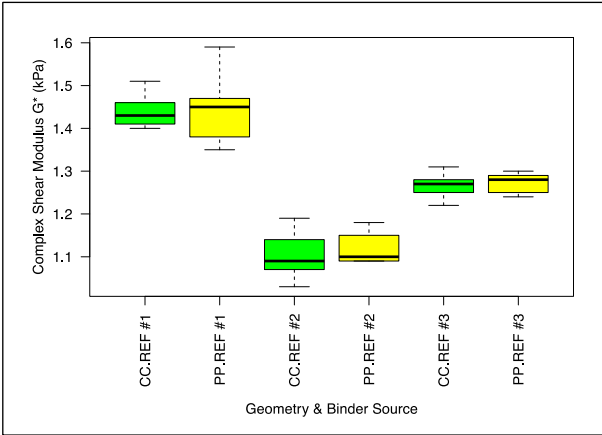


Figure 3.1: Unmodified binders: G^* with varied conversion factor at 64°C.
(CC = concentric cylinder, PP = parallel plate)

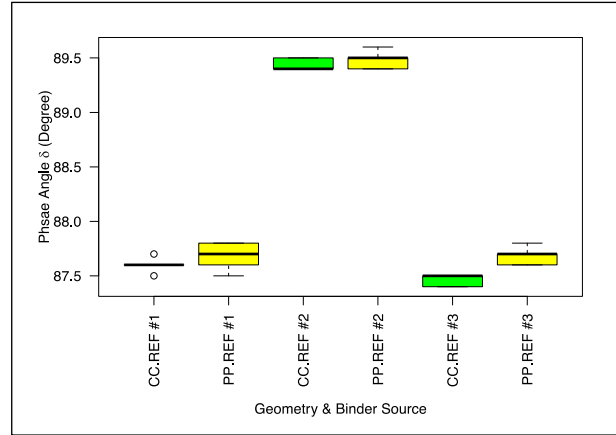


Figure 3.2: Unmodified binders: δ with varied conversion factor at 64°C.

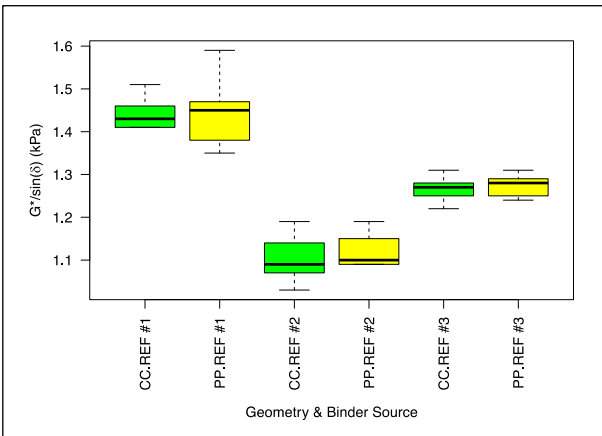


Figure 3.3: Unmodified binders: $G^*/\sin(\delta)$ with varied conversion factor at 64°C.

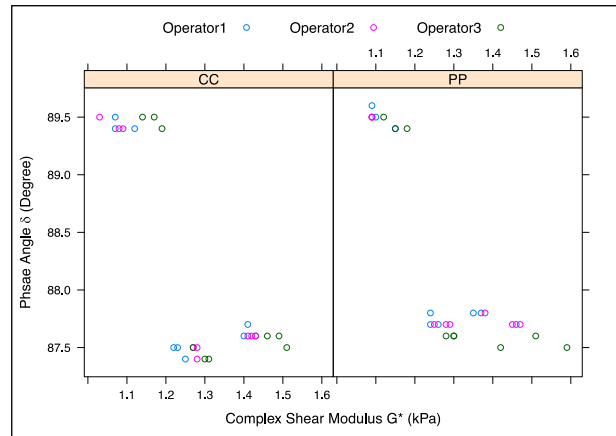


Figure 3.4: Unmodified binders: G^* against δ with varied conversion factor at 64°C.

Task 2: Modified Binders

The boxplots of complex shear modulus, phase angle, and $G^*/\sin(\delta)$ at 64°C are shown in Figure 3.5 through Figure 3.7. The polymer-modified binder complex shear modulus measured using the concentric cylinder geometry was lower than that using the parallel plate system, whereas the opposite was observed for the complex shear modulus of the tire rubber-modified binder. The modified binders' phase angles recorded with the concentric cylinder geometry were also higher than those measured with the parallel plate geometry. Trends similar to those recorded for the complex shear moduli were also recorded for $G^*/\sin(\delta)$ for both geometries. This was expected, given that differences in phase angle have less influence on $G^*/\sin(\delta)$ values than do differences in the complex shear modulus. Results obtained by the three different operators are shown in Figure 3.8. The data points are scattered relatively evenly between the operators, with the phase angles measured with the concentric cylinder geometry slightly higher than those recorded using the parallel plate geometry.

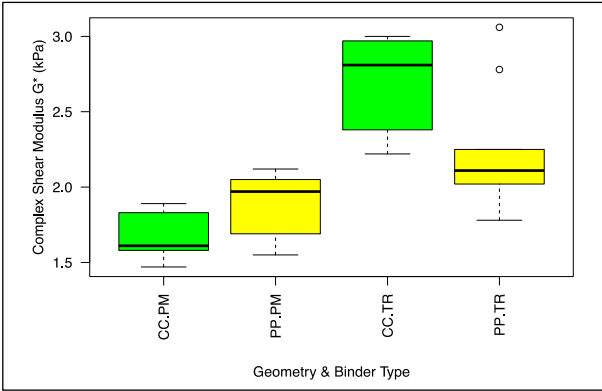


Figure 3.5: Modified binders: G^* with varied conversion factor at 64°C.

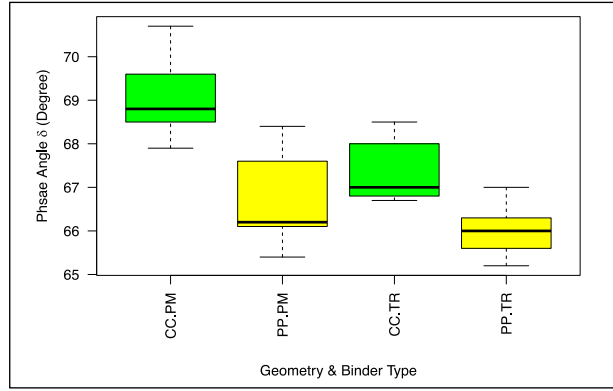


Figure 3.6: Modified binders: δ with varied conversion factor at 64°C.

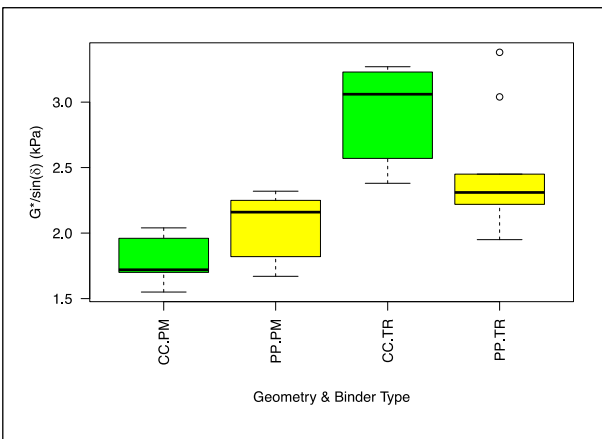


Figure 3.7: Modified binders: $G^*/\sin(\delta)$ with varied conversion factor at 64°C.

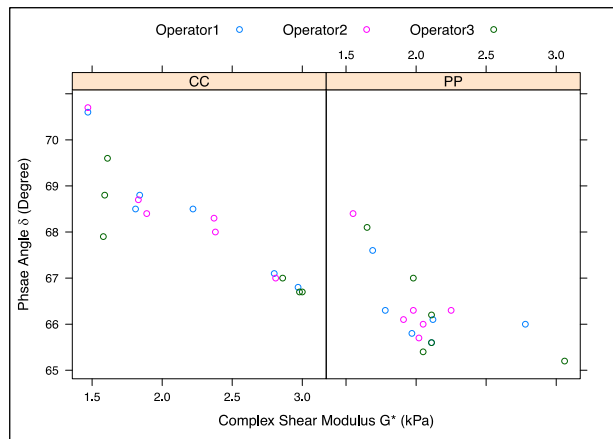


Figure 3.8: Modified binders: G^* against δ with varied conversion factor at 64°C.

The ANOVA results are shown in Table 3.3. $G^*/\sin(\delta)$ was the dependent variable and geometry was the independent variable. Binder type was again selected as a blocking factor. The ANOVA results, at a 95 percent confidence interval, indicate that the measurements of $G^*/\sin(\delta)$ using the concentric cylinder and parallel plate geometries were not significantly different. When using a binder specific conversion factor, the results obtained using the concentric cylinder geometry were not statistically significantly different than those obtained when using the parallel plate geometry.

Table 3.3: Modified Binders: ANOVA Results of $G^*/\sin(\delta)$ with Varied Conversion Factor ($\alpha=0.05$)

Parameter	Df	Sum Sq	Mean Sq	F value	Pr (>F)
Geometry	1	0.106	0.106	0.751	0.393
Binder type	1	5.282	5.282	37.542	6.6e-07
Residuals	33	4.643	0.141	-	-

Task 3: RTFO-Aged Unmodified and Modified Binders

The boxplots of complex shear modulus, phase angle, and $G^*/\sin(\delta)$ at 64°C for the RTFO-aged unmodified and modified binders are shown in Figure 3.9 through Figure 3.11. The results appeared to be similar for

both geometries. Both modified binders had higher complex shear modulus than the unmodified binders, as expected, despite their having the same high temperature ratings. Both modified binders also had lower phase angles than the unmodified binders, which led to higher $G^*/\sin(\delta)$ values. When the results obtained by the three different operators (Figure 3.12) were compared, only one data point from Operator #1 was higher, with the rest of the data points similar among the operators.

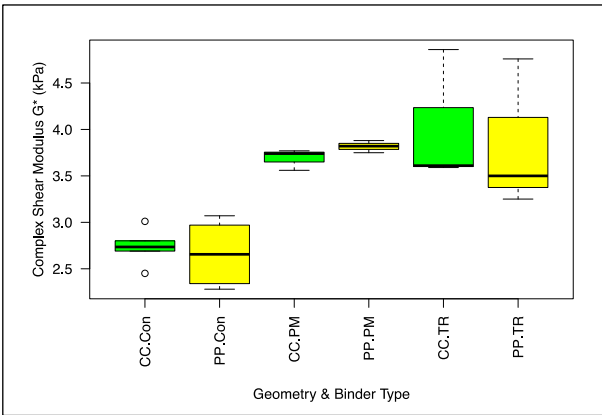


Figure 3.9: RTFO-aged binders: G^* with varied conversion factor at 64°C.
(CC = concentric cylinder, PP = parallel plate)

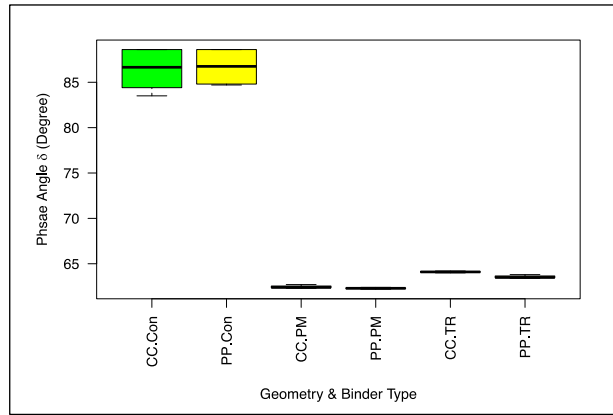


Figure 3.10: RTFO-aged binders: δ with varied conversion factor at 64°C.

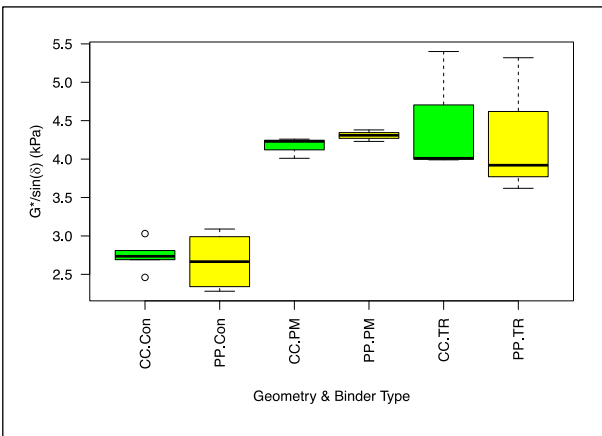


Figure 3.11: RTFO-aged binders: $G^*/\sin(\delta)$ with varied conversion factor at 64°C.

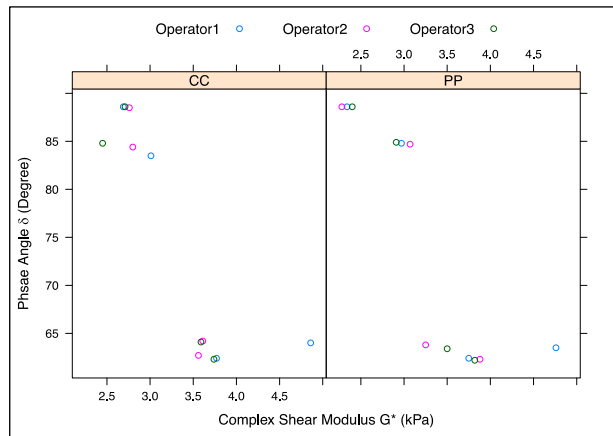


Figure 3.12: RTFO-aged binders: G^* against δ with varied conversion factor at 64°C.

The ANOVA results are shown in Table 3.4. $G^*/\sin(\delta)$ was the dependent variable and geometry was the independent variable in the analysis. Binder type was again selected as a blocking factor. The statistical analysis indicated that $G^*/\sin(\delta)$ measured with the two geometries was not significantly different at a 95 percent confidence interval.

Table 3.4: RTFO-Aged Binders: ANOVA Results of $G^*/\sin(\delta)$ with Varied Conversion Factor
($\alpha=0.05$)

Parameter	Df	Sum Sq	Mean Sq	F Value	Pr (>F)
Geometry	1	0.013	0.013	0.064	0.802
Binder type	2	15.40	7.701	39.25	1.19e-07
Residuals	20	3.924	0.196	-	-

3.3.2 Testing with Fixed Conversion Factor

As discussed in Section 3.2.2, a fixed conversion factor of 72, determined by testing a *Cannon* certified viscosity reference standard material (S600), was used in this phase of the testing. DSR test results using the parallel plate and the concentric cylinder systems are listed in Table B.4 in Appendix B and summarized below.

Unmodified Binders

Test results for the unaged and short-term aged binders at their PG temperature (58°C, 64°C, and 70°C) are shown in Figure 3.13 through Figure 3.15. The complex shear moduli and phase angles were similar between the two geometries. RTFO aging was found to be more severe than TFO aging on the selected binders, as expected. The test results are separated by performance grade in Figure 3.16. The measurements obtained from both geometries were close for all the tested binders.

The ANOVA results are shown in Table 3.5. $G^*/\sin(\delta)$ was the dependent variable and geometry and aging condition were the independent variables. The results indicate that testing geometry was not a significant factor on $G^*/\sin(\delta)$ while aging condition was a significant factor, as expected. The results also show that the concentric cylinder geometry with a fixed conversion factor can provide results that are not statistically significantly different at a 95 percent confidence interval from those obtained using the parallel plate geometry. However, a significant difference was found between RTFO-aged and TFO-aged binders based on the Tukey Honest Significant Difference (HSD) parameter (Figure 3.17), with RTFO aging being more severe than TFO aging.

Table 3.5: Unmodified Binders: ANOVA Results of $G^*/\sin(\delta)$ with Fixed Conversion Factor
($\alpha=0.05$)

Parameter	Df	Sum Sq	Mean Sq	F Value	Pr (>F)
Geometry	1	0.033	0.033	1.223	0.274
Binder type	2	17.15	8.575	315.28	2e-16
Residuals	50	1.360	0.027	-	-

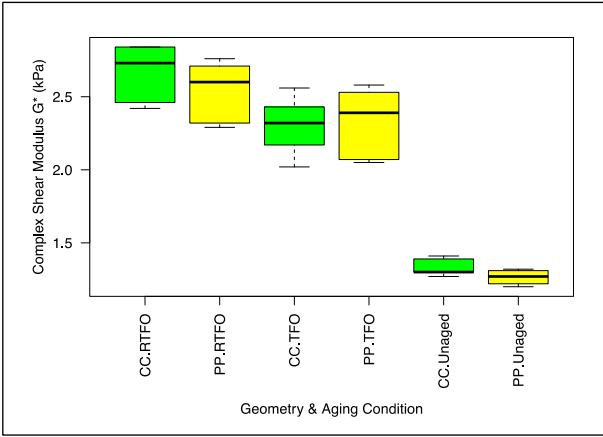


Figure 3.13: Unmodified binders, unaged and aged: G^* with fixed conversion factor.
(CC = concentric cylinder, PP = parallel plate)

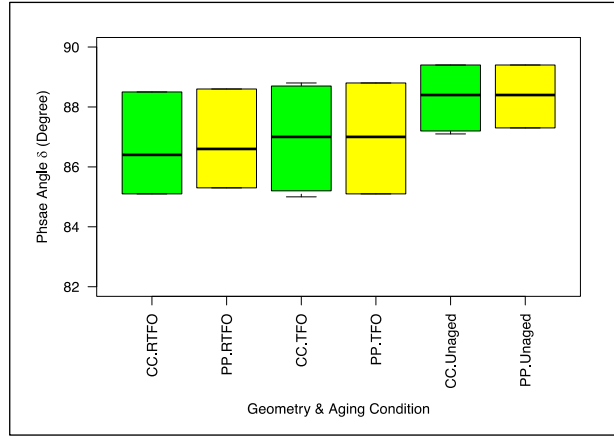


Figure 3.14: Unmodified binders, unaged and aged: δ with fixed conversion factor.

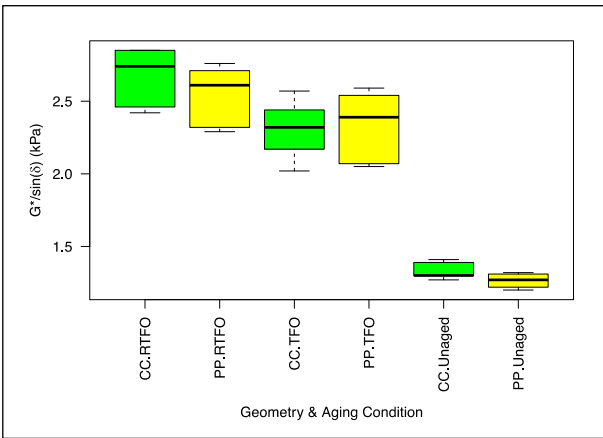


Figure 3.15: Unmodified binders, unaged and aged: $G^*/\sin(\delta)$ with fixed conversion factor.

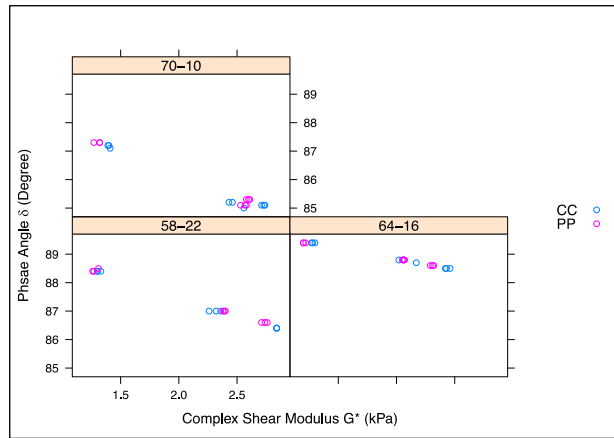


Figure 3.16: Unmodified binders, unaged and aged: G^* against δ with fixed conversion factor.

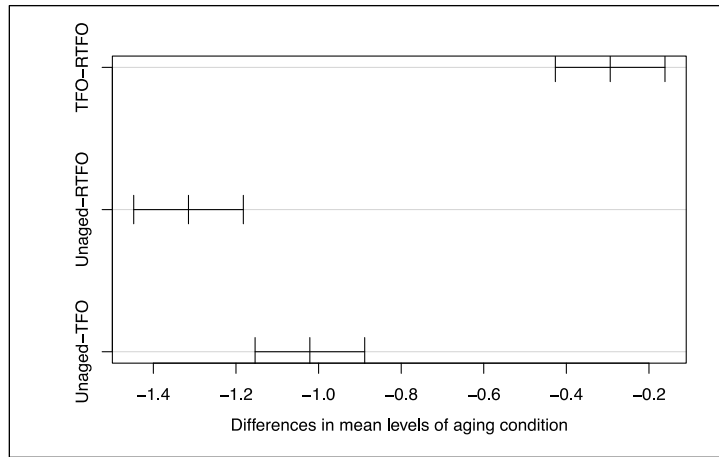


Figure 3.17: Tukey HSD with varied aging condition (95% confidence interval).

3.3.3 Testing at Two Different High Temperatures

DSR tests were repeated on the seven different binders (three PG 64-16 unmodified binders, two PG 64-28 polymer-modified binders, and two PG 64-28 tire rubber-modified binders) at 64°C and 70°C to further compare the two geometries. The unaged and RTFO-aged binders were tested at both temperatures. All testing was performed by a single operator. The averages of two test replicates are shown in Figure 3.18 through Figure 3.31. Whiskers on the $G^*/\sin(\delta)$ plots indicate the standard error for the replicate tests and show that there was very little variability among measurements. The percent difference in the $G^*/\sin(\delta)$ was calculated using Equation 3.2.

$$\frac{CC[G^*/\sin(\delta)] - PP[G^*/\sin(\delta)]}{CC[G^*/\sin(\delta)]} \times 100 \quad (3.2)$$

The results were consistent with those discussed earlier, with only the PG 64-28TR binder from Refinery #3 showing a large difference between concentric cylinder and parallel plate at the unaged stage. This was considered to be a testing anomaly, but the test was not repeated due to limited binder quantities. The percentage differences in $G^*/\sin(\delta)$ between the results of all the unaged and RTFO-aged binders tested with the two geometries at 64°C were all within the 6.4 percent benchmark listed in AASHTO T 315 (i.e., the acceptable percentage difference between two test results). However, when the binders were tested at 70°C, the differences between the two geometries were more variable at the unaged stage, with three of the seven binders (including the PG 64-28TR binder from Refinery #3) exceeding the 6.4 percent difference limit and the parallel plate geometry generally recording lower values than the concentric cylinder geometry.

3.4 Phase 1a Findings and Recommendations

Although comparatively different complex shear moduli, and consequently $G^*/\sin(\delta)$ values for unaged polymer-modified and tire rubber-modified binders were measured using the concentric cylinder and parallel plate geometries, this part of the study has indicated that the results obtained from testing the same unmodified, polymer-modified, and tire rubber-modified binders in both concentric cylinder and parallel plate geometries in a DSR are generally not statistically different. Based on these results, the concentric cylinder geometry was considered as a potentially appropriate alternative to parallel plates for quantifying the properties of asphalt rubber binders used in gap- and open-graded asphalt mixes, and specifically for further comparative tests to assess the performance properties of asphalt binders containing crumb rubber particles larger than 250 μm (i.e., particles retained on the #60 sieve).

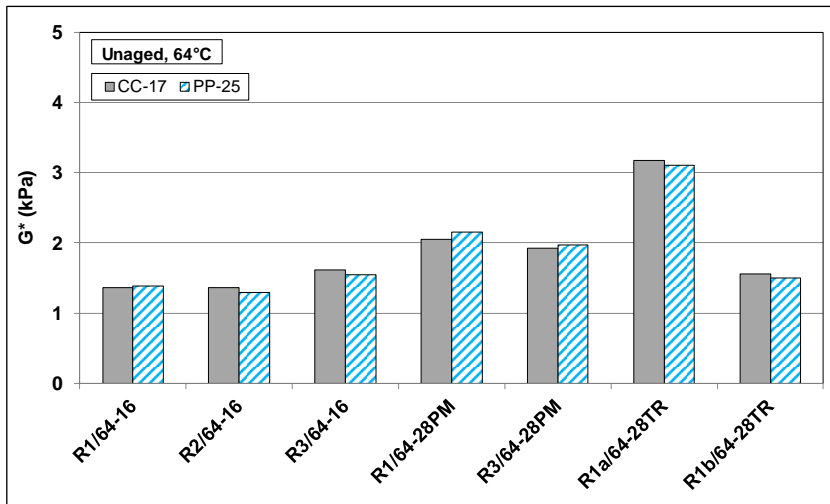


Figure 3.18: High temperature (unaged): Shear modulus tested at 64°C.

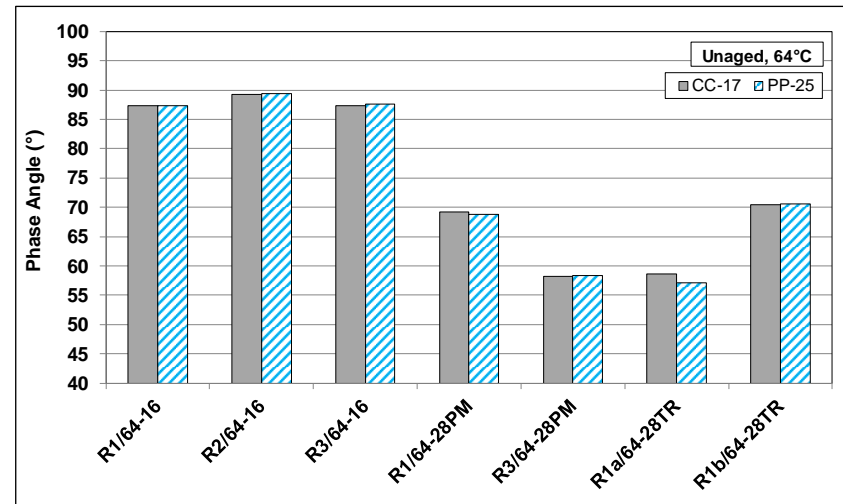


Figure 3.19: High temperature (unaged): Phase angle tested at 64°C.

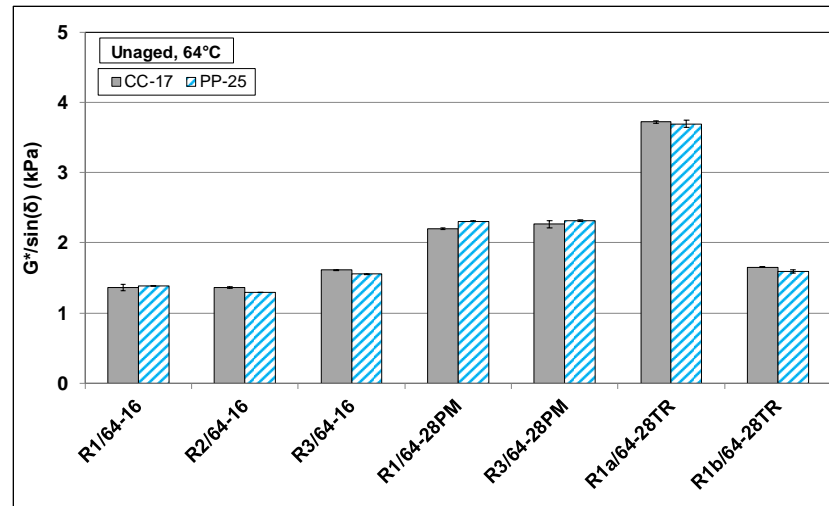


Figure 3.20: High temperature (unaged): $G^*/\sin(\delta)$ tested at 64°C.

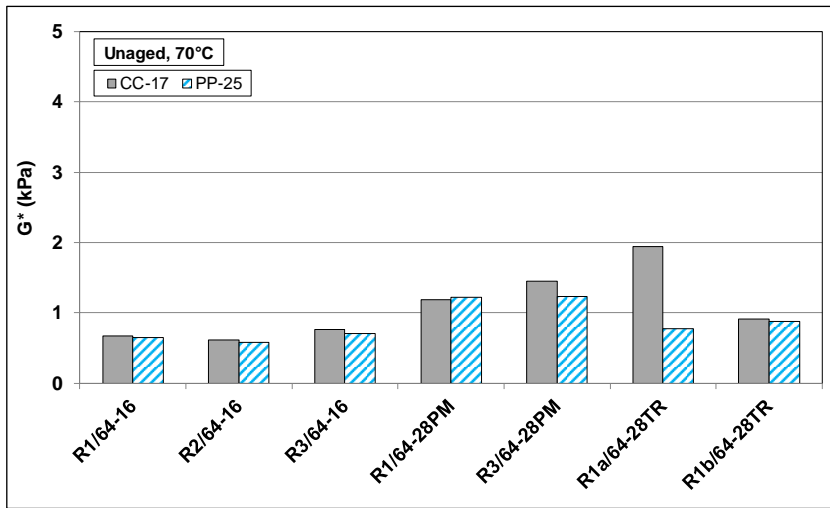


Figure 3.21: High temperature (unaged): Shear modulus tested at 70°C.

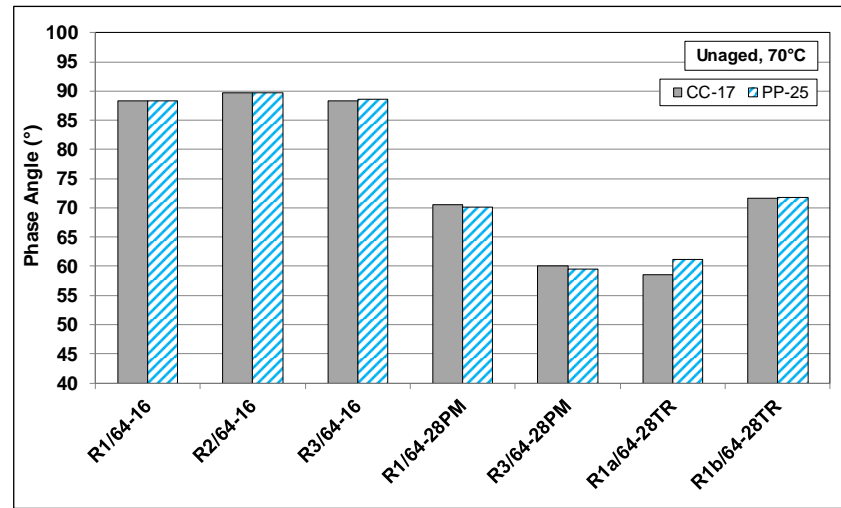


Figure 3.22: High temperature (unaged): Phase angle tested at 70°C.

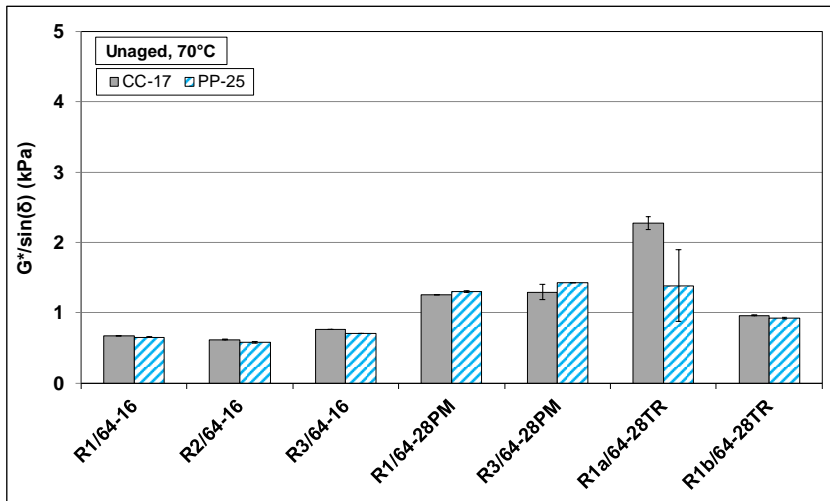


Figure 3.23: High temperature (unaged): $G^*/\sin(\delta)$ tested at 70°C.

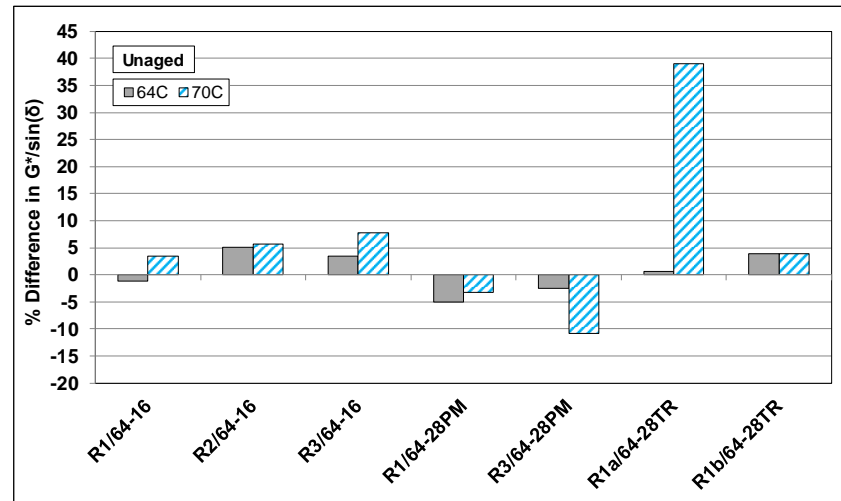


Figure 3.24: High temperature (unaged): Difference between concentric cylinder & parallel plate.

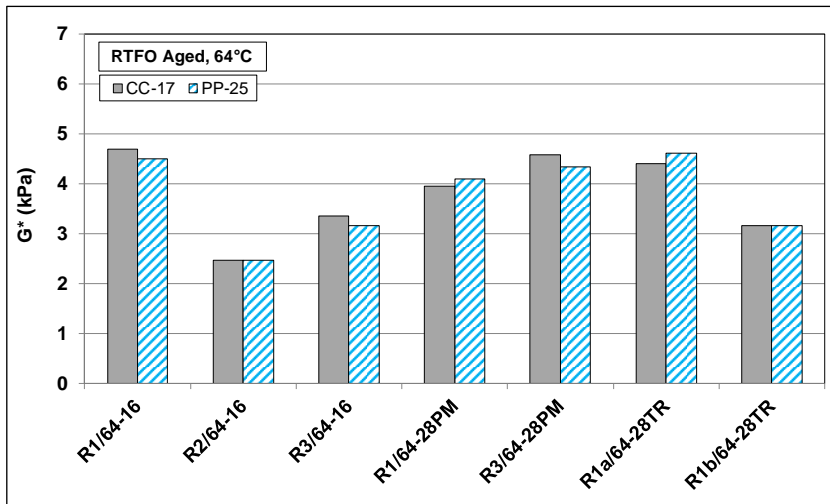


Figure 3.25: High temperature (RTFO-aged): Shear modulus tested at 64°C.

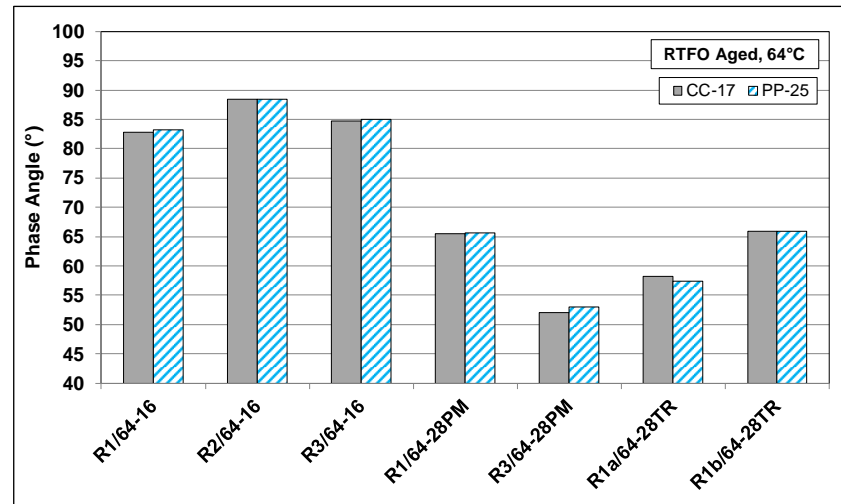


Figure 3.26: High temperature (RTFO-aged): Phase angle tested at 64°C.

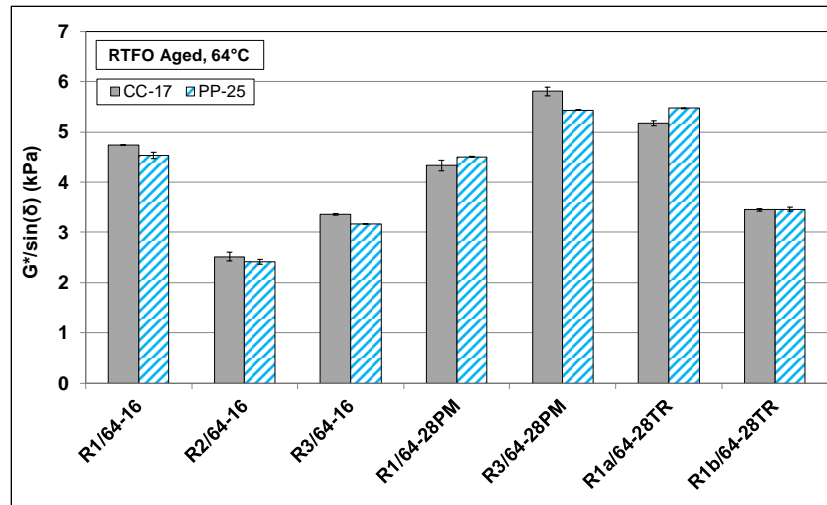


Figure 3.27: High temperature (RTFO-aged): $G^*/\sin(\delta)$ tested at 64°C.

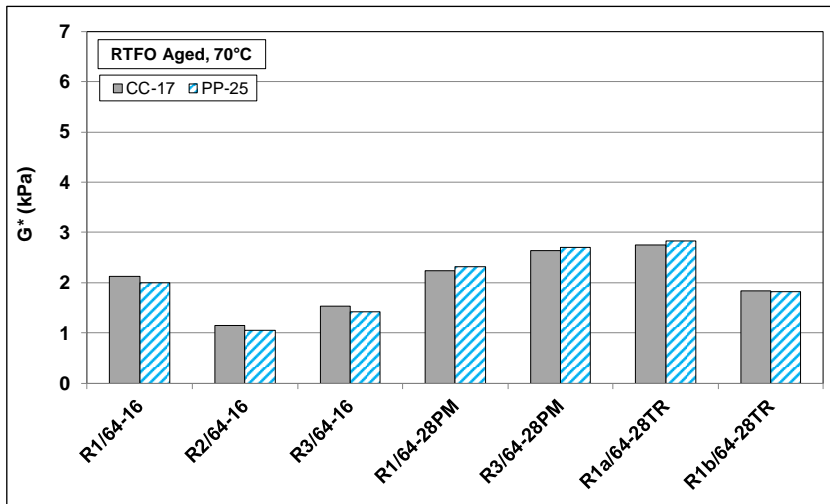


Figure 3.28: High temperature (RTFO-aged): Shear modulus tested at 70°C.

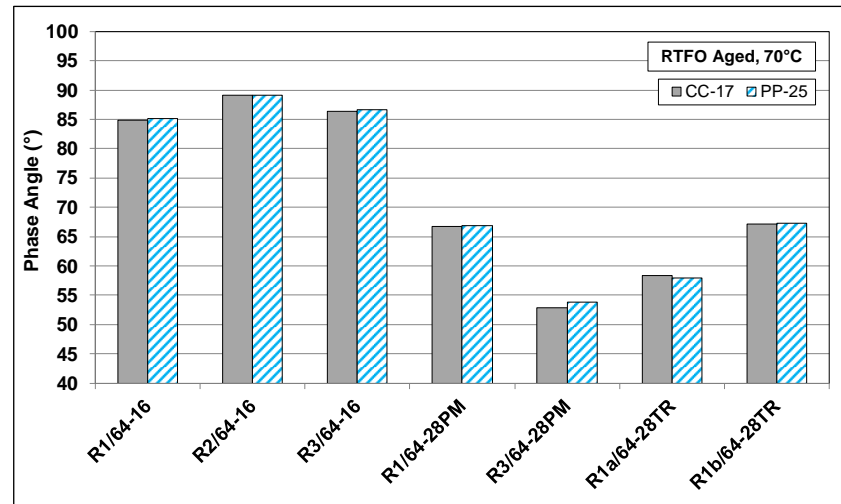


Figure 3.29: High temperature (RTFO-aged): Phase angle tested at 70°C.

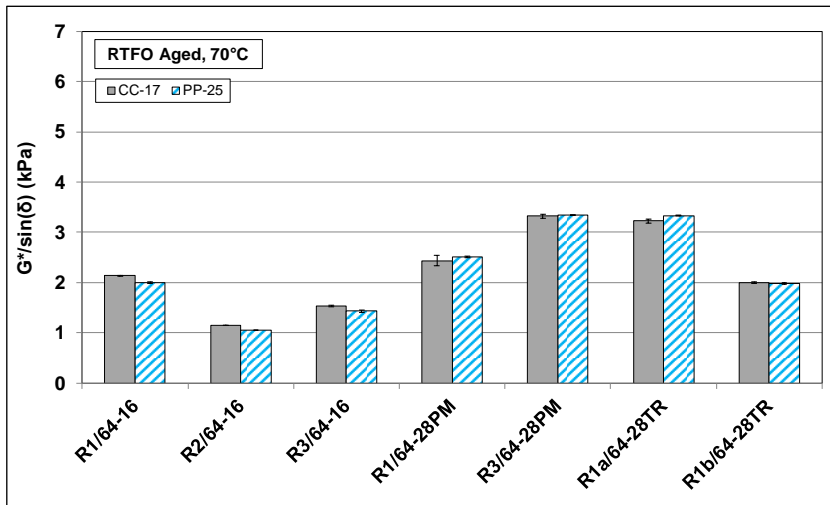


Figure 3.30: High temperature (RTFO-aged): $G^*/\sin(\delta)$ tested at 64°C.

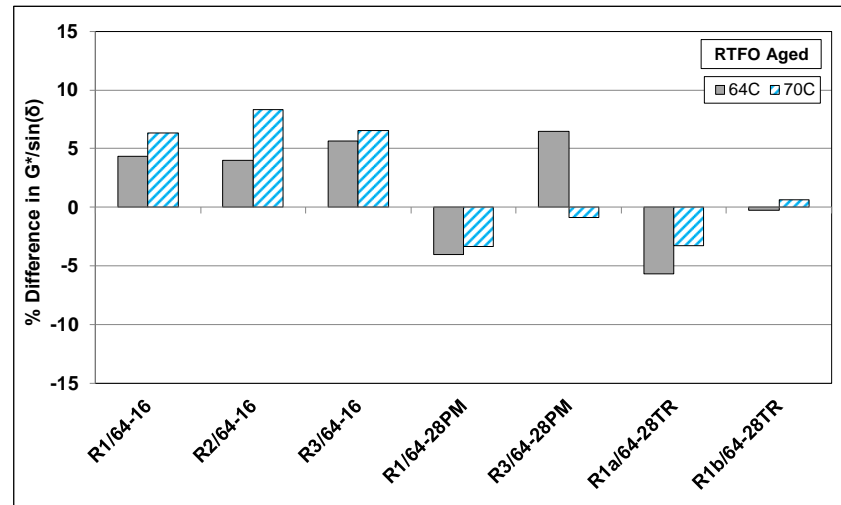


Figure 3.31: High temperature (RTFO-aged): Difference between concentric cylinder & parallel plate.

4. Phase 1b: PRELIMINARY RHEOLOGY TESTING

4.1 Introduction

Preliminary testing on unmodified, polymer-modified, and tire rubber-modified binders using the concentric cylinder and parallel plate geometries in a dynamic shear rheometer to determine performance-related properties indicated that both geometries provided statistically similar results. Based on these results, this next part of the study evaluated the two geometries for measuring the performance properties of asphalt rubber binders produced according to Caltrans specifications for use in gap- and open-graded asphalt mixes. The study assessed six crumb rubber particle size ranges, and focused on particles smaller and larger than 250 μm (i.e., retained on the #60 sieve). This particle size was chosen because it has been identified as a key size, above which the particles may influence the results of the parallel plate geometry with 1-mm and 2-mm gaps.

Earlier research on rubberized asphalt concrete indicated that several factors related to the crumb rubber modifier (CRM) can potentially influence the behavior and performance of the asphalt rubber binder, and consequently that of the mix or surface treatment that includes it. These factors include the grinding method used to produce the CRM, its particle size and surface area, the crumb rubber content of the asphalt binder, and whether an extender oil was used in its preparation. This part of the study therefore also focused on how some of these factors might influence the performance grading of asphalt rubber binders, and whether these factors impact test results from the two geometries.

4.2 Testing Plan

Table 4.1 summarizes the sampling and testing experiment for the materials assessed in this part of the study. The binders were produced in the laboratory to provide full control over the different variables being assessed.

Table 4.1: Experimental Design Factors and Factorial Levels for Phase 1b

Factor	Factorial Level	Details
Asphalt binder source and grade	1	PG 64-16 (sourced from Refinery #1)
Extender oil content (%)	2	0 (Type I) and 4 (Type II)
Rubber production method	2	Ambient and cryogenic
Rubber content (% by weight of base binder)	1	20
Rubber gradation (μm)	6	75–106, 106–150, 150–180, 180–250, 250–425, 425–850 (#200–140, 140–100, 100–80, 80–60, 60–40, 40–20)
Testing temperature ($^{\circ}\text{C}$)	2	76 and 82 ($\sim 169^{\circ}\text{F}$ and 180°F)
Aging condition	1	Unaged

Surface area of the crumb rubber particles was not included as a variable in the experiment. However, the surface area of particles sampled from the products of the two different grinding types was measured and

its effect on the asphalt rubber binder's shear modulus was determined. Additional variables identified but not incorporated in this part of the testing included different binder sources, different extender oil contents, additional larger crumb rubber gradings (i.e., gradings with particle sizes closer to 2.36 mm [#8]), and different aging conditions.

A total of 48 binders were tested following the testing plan detailed in Table 4.1. The gap used in the concentric cylinder geometry was fixed at 6 mm regardless of rubber particle sizes. Two gap sizes, based on two crumb rubber particle sizes, were used for the parallel plate geometry testing with the 25-mm diameter plates:

- 1-mm gap for maximum particle sizes smaller than 250 μm ($>$ #60 mesh)
- 2-mm gap for maximum particle sizes larger than 250 μm ($<$ #60 mesh)

4.3 Binder Preparation

The asphalt rubber binders were produced in the laboratory by blending the individual components in a high shear mixer (Figure 4.1) at two speeds over 60 minutes at a temperature of 190°C (374°F). The blending occurred at 5,000 revolutions per minute (RPM) for the first 30 minutes and was slowed to 2,500 RPM for the remaining 30 minutes. This ensured that the crumb rubber particles were appropriately swelled and had sufficient reaction with the light compounds of the asphalt binder. This mixing process was considered to be appropriately representative of plant production for the purposes of this study. During plant production, the crumb rubber, extender oil, and base binder are first mixed at high revolutions to maximize dispersion of the rubber particles, followed by mixing at lower RPMs to ensure good reaction between the rubber particles and the asphalt binder. The different asphalt rubber binders were produced in batches, stored in quart containers, and then reheated just prior to testing. In this phase of testing, comparisons were not made with plant-produced asphalt rubber binders; instead the focus was on ensuring that the preparation process was consistent for all binder samples.



Figure 4.1: High shear mixer.

4.4 Comparison of Testing Geometries with Three Rubber Particle Size Ranges

The test results comparing asphalt rubber binders with three different size ranges (180–250 μm , 250–425 μm , and 425–850 μm) are listed in Table B.5 in Appendix B and summarized in Table 4.2. Plots comparing the two geometries in terms of complex shear modulus (G^*), phase angle (δ), and $G^*/\sin(\delta)$ are shown in Figure 4.2, Figure 4.3, and Figure 4.4, respectively.

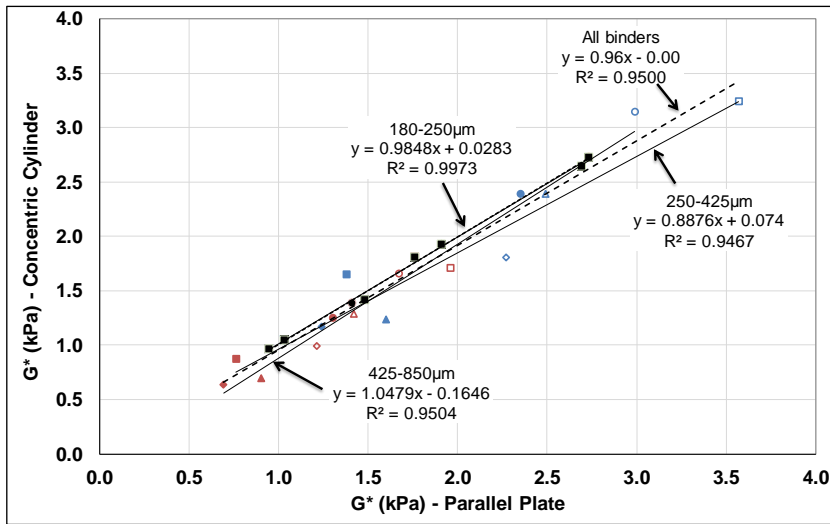


Figure 4.2: Comparison of G^* results for concentric cylinder and parallel plate.

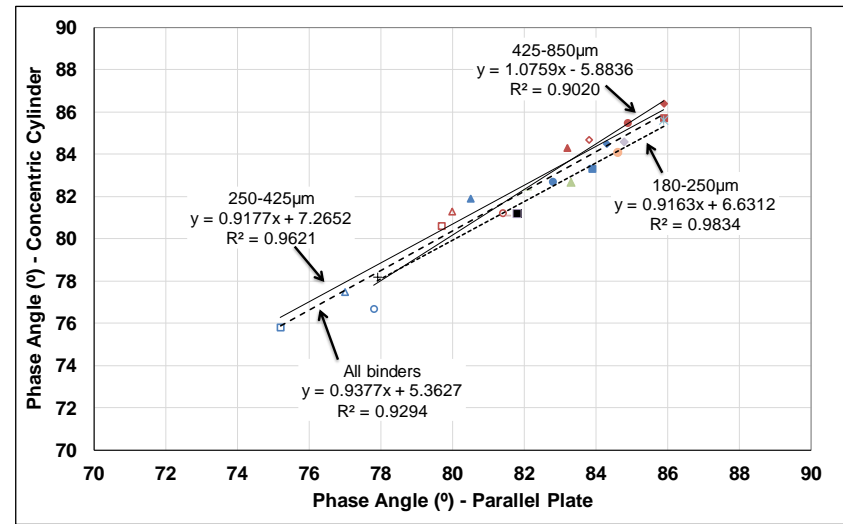


Figure 4.3: Comparison of phase angle results for concentric cylinder and parallel plate.

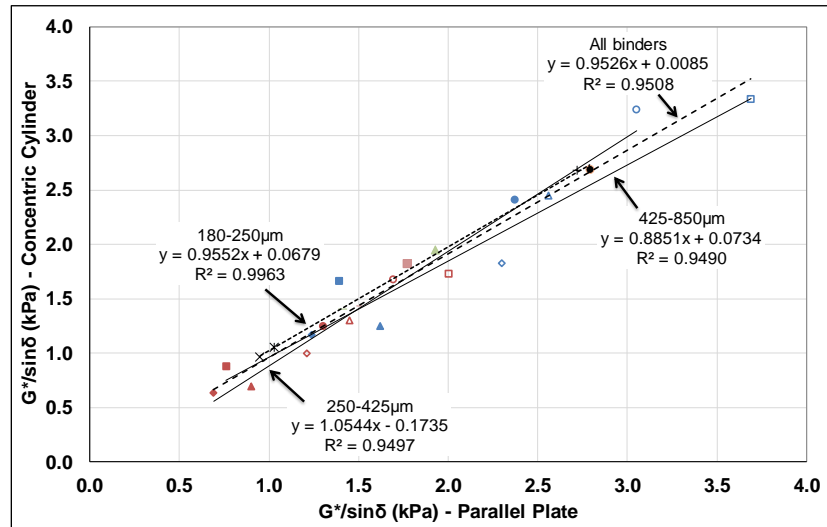


Figure 4.4: Comparison of $G^*/\sin(\delta)$ results for concentric cylinder and parallel plate.

The plots show each testing point, and trend lines for the results from each binder and for the combined results from the three binders. Regression equations comparing the results from the two testing geometries for individual size ranges and for the three binders combined are also included.

Table 4.2: Summary of Statistical Comparisons between Testing Geometries

Particle Size Range		Correlation Between Geometries (R^2)		
μm	#mesh	G^* (kPa)	δ ($^\circ$)	$G^*/\sin(\delta)$ (kPa)
180-250	60-80	0.9973	0.9834	0.9963
250-425	40-60	0.9467	0.9621	0.9497
425-850	20-40	0.9504	0.9020	0.9490
Combined		0.9500	0.9294	0.9508

The results obtained from testing the three asphalt rubber binders, each with a different maximum crumb rubber particle size, show a strong correlation between the two testing geometries for the finer particle size range (180 – 250 μm), but increasingly poorer correlations with increasing particle size. The poorer correlations observed with the larger size ranges were attributed to the increasing influence of the proximity of the larger rubber particles to the parallel plates.

Based on the results presented in Chapter 3 and those presented above, the concentric cylinder geometry can be considered as a potentially appropriate alternative geometry to parallel plates for quantifying the properties of asphalt rubber binders that meet Caltrans specifications. This observation specifically applies for further comparative tests to assess the performance properties of binders containing crumb rubber particles larger than 250 μm (i.e., particles retained on the #60 sieve).

4.5 Effect of Crumb Rubber Particle Size on Rheological Properties

This part of the experiment evaluated the impact of CRM particles on the rheological properties of the asphalt rubber binders. The test results are summarized in Table B.6 (concentric cylinder) and Table B.7 (parallel plate) in Appendix B. The $G^*/\sin(\delta)$ measurements at 76°C and 82°C against crumb rubber particle size for Type I (no extender oil) and Type II (with extender oil) asphalt rubber binders are plotted in Figure 4.5 through Figure 4.8. Crumb rubber particles produced under both ambient and cryogenic conditions were included in the analysis. In these plots, the maximum crumb rubber particle size (in microns [μm]) was selected to represent a particle size group. The results indicate that both the method used to produce the crumb rubber particles (i.e., grinding at ambient or cryogenic temperature) and the presence of an extender oil influenced the rheological properties of asphalt rubber binders. Key observations include the following:

- $G^*/\sin(\delta)$ measured with concentric cylinder geometry were generally higher than the $G^*/\sin(\delta)$ measured with parallel plate geometry, and generally showed slightly less variation.
- Higher $G^*/\sin(\delta)$ were recorded at the lower test temperature (76°C), as expected.
- There was less variation in the $G^*/\sin(\delta)$ determined at the higher temperature (82°C) over the range of different particle sizes compared to the $G^*/\sin(\delta)$ recorded at the lower temperature.

- The differences in the $G^*/\sin(\delta)$ were small for the different testing variables for crumb rubber particles in the size ranges less than 250 μm compared to the differences observed for the size ranges greater than 250 μm .
- $G^*/\sin(\delta)$ increased with increasing crumb rubber particle size if the rubber was ground at ambient temperature, but decreased if they were cryogenically ground.
- Asphalt rubber binders produced with an extender oil (Type II binders) had higher $G^*/\sin(\delta)$ than those produced with no modification (Type I binders).
- The $G^*/\sin(\delta)$ of the binders with cryogenically ground rubber particles in the 425 μm to 850 μm size range were lower than those of the same binders produced with smaller rubber particles; an opposite trend was observed for binders produced with particles ground at ambient temperature.

4.6 Effect of Crumb Rubber Particle Surface Area on Rheological Properties

The surface area of crumb rubber particles produced at ambient and cryogenic temperatures were measured by an independent accredited laboratory (*Quantachrome Instruments*). The results are listed in Table 4.3 and show that the surface area of the cryogenically produced particles was greater than that of the particles produced at ambient temperatures, indicating that particles produced in the two processes have different shapes. The difference in surface areas increased with decreasing particle size, as expected, with differences between the two processes most significant on particle sizes smaller than 250 μm (#60). It is worth noting that two different gasses (nitrogen and krypton) were used for the surface area measurements. Choice of gas is usually dependent on the surface texture of the particles being evaluated. The observed differences in results could be attributed to this choice of gas.

Table 4.3: Surface Area of Rubber Particles Produced at Ambient and Cryogenic Temperatures

Crumb Rubber Particle Size		Surface Area (m^2/g)	
(μm)	(# mesh)	Ambient	Cryogenic
425 – 850	#40 – 20	0.035 ^{Kr}	0.039 ^{Kr}
250 – 425	#60 – 40	0.036 ^{Kr}	0.052 ^{Kr}
180 – 250	#80 – 60	0.077 ^{Kr}	0.231 ^{Kr}
150 – 180	#100 – 80	0.278 ^{Ni}	0.186 ^{Ni}
106 – 150	#140 – 100	0.131 ^{Ni}	0.245 ^{Ni}
75 – 106	#200 – 140	0.138 ^{Ni}	0.668 ^{Ni}

Kr : Krypton gas was used to measure surface area. Ni: Nitrogen gas was used to measure surface area.

The DSR with concentric cylinder geometry test results are summarized in Figure 4.9 through Figure 4.12. The following observations were made:

- Higher $G^*/\sin(\delta)$ were recorded at the lower test temperature (76°C), as expected.
- There was less variation in the $G^*/\sin(\delta)$ determined at the higher temperature (82°C) over the range of surface area than in the $G^*/\sin(\delta)$ recorded at the lower temperature (76°C).
- Asphalt rubber binders containing cryogenically produced crumb rubber had higher $G^*/\sin(\delta)$ than binders containing crumb rubber produced at ambient temperatures. The increase in $G^*/\sin(\delta)$ can be attributed to the higher surface area, which indicates the presence of more cubical CRM particles in the cryogenic process.

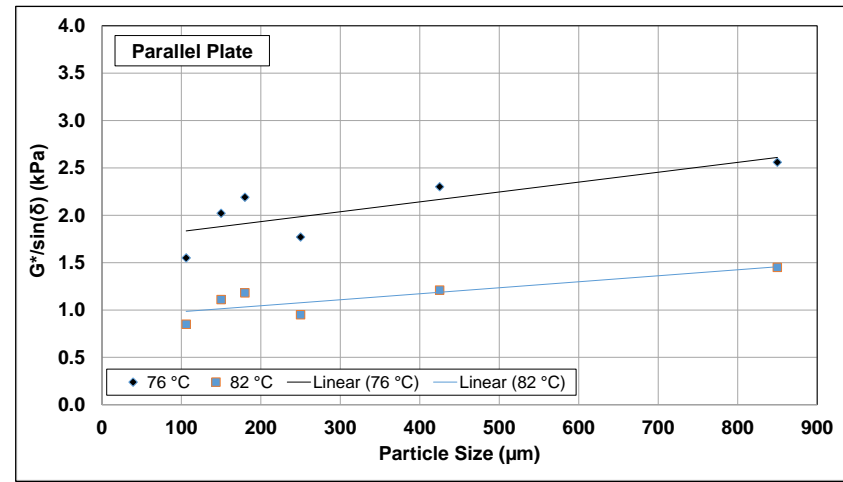
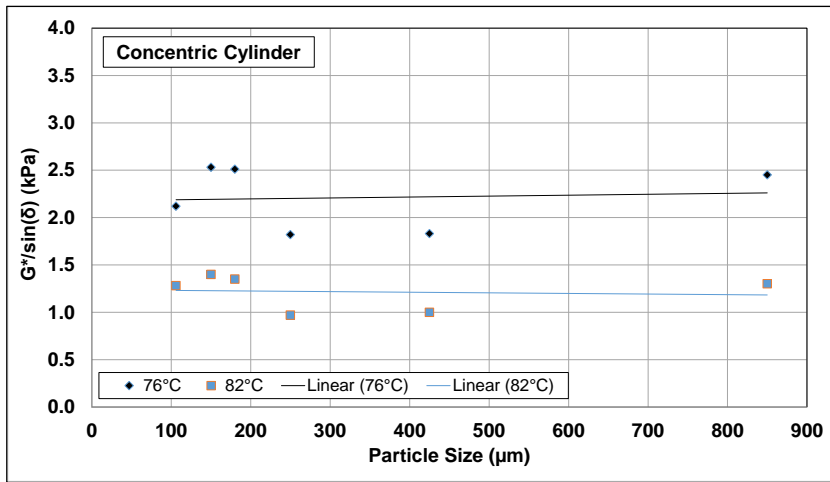


Figure 4.5: $G^*/\sin(\delta)$ versus particle size for Type I ambient rubber binder.

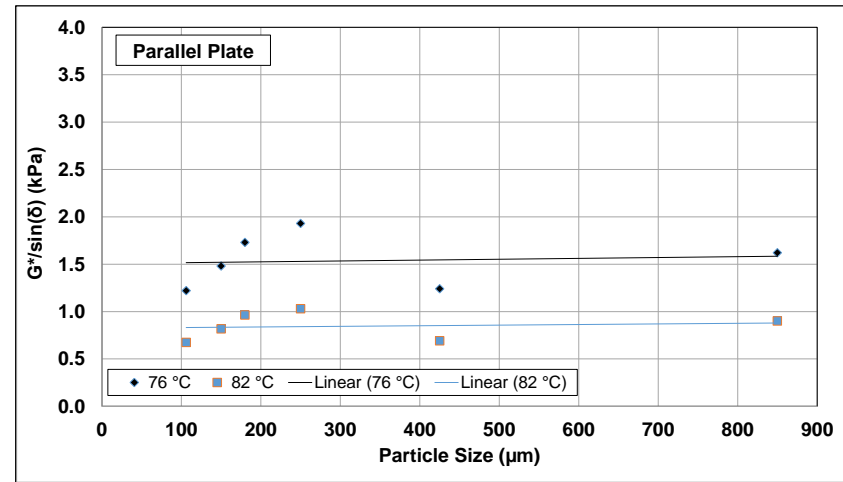
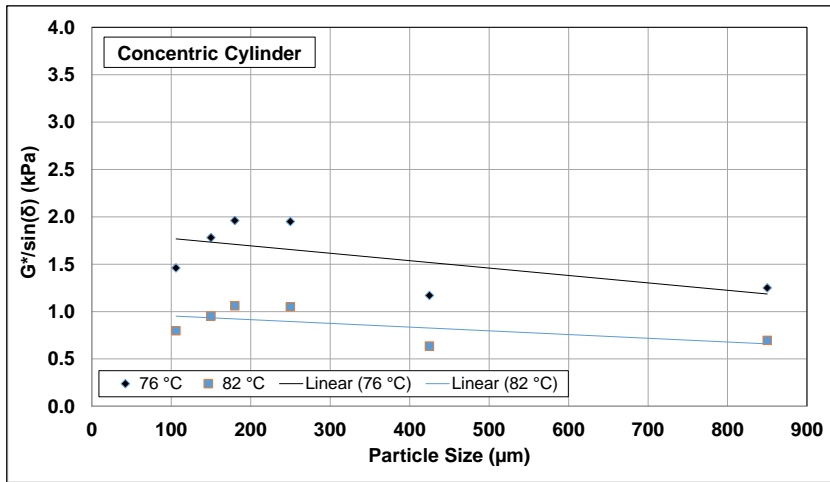


Figure 4.6: $G^*/\sin(\delta)$ versus particle size for Type I cryogenic rubber binder.

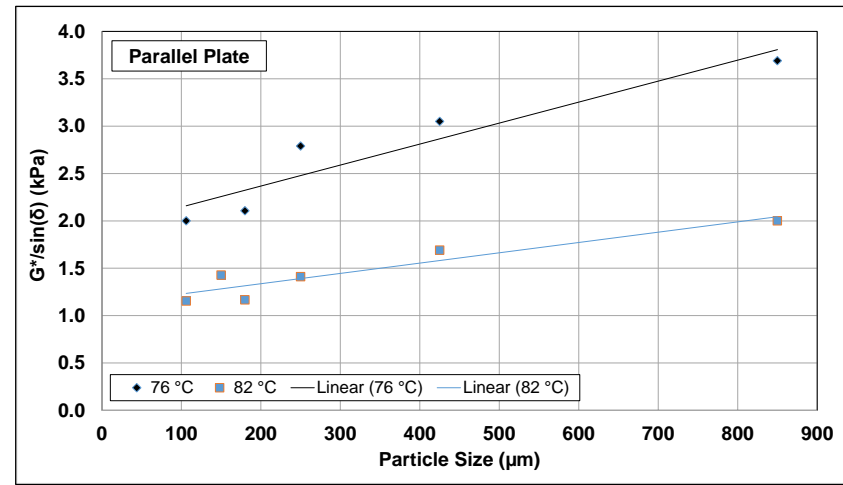
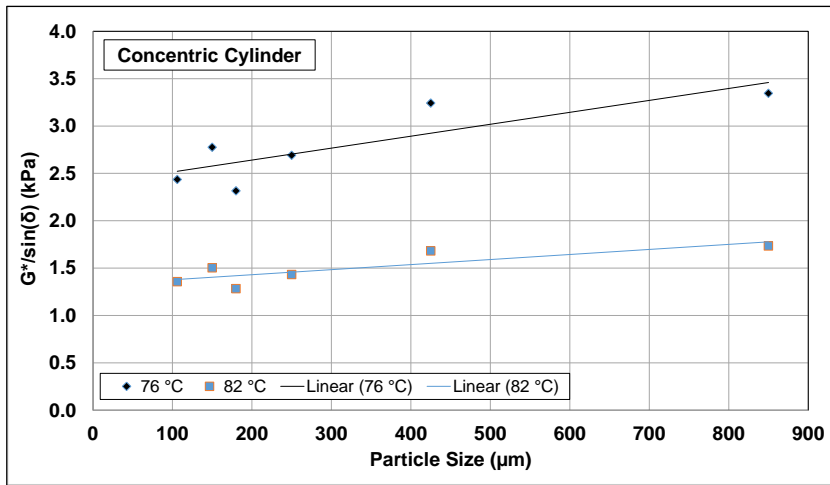


Figure 4.7: $G^*/\sin(\delta)$ versus particle size for Type II ambient rubber binder.

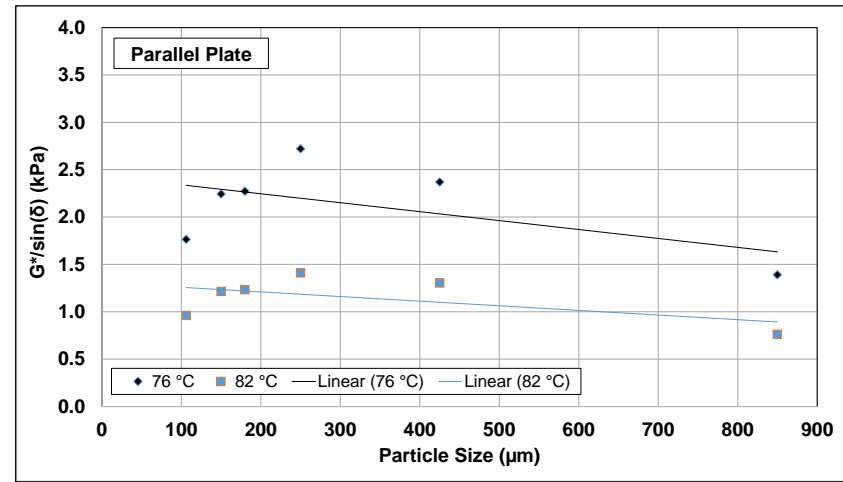
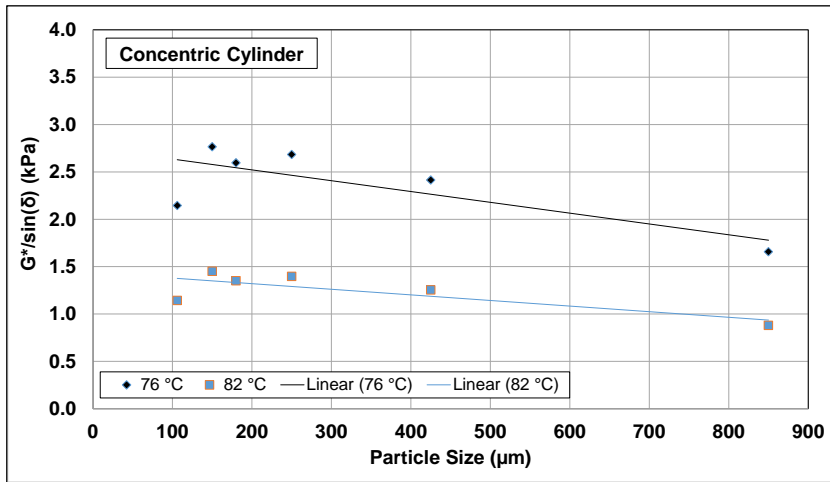


Figure 4.8: $G^*/\sin(\delta)$ versus particle size for Type II cryogenic rubber binder.

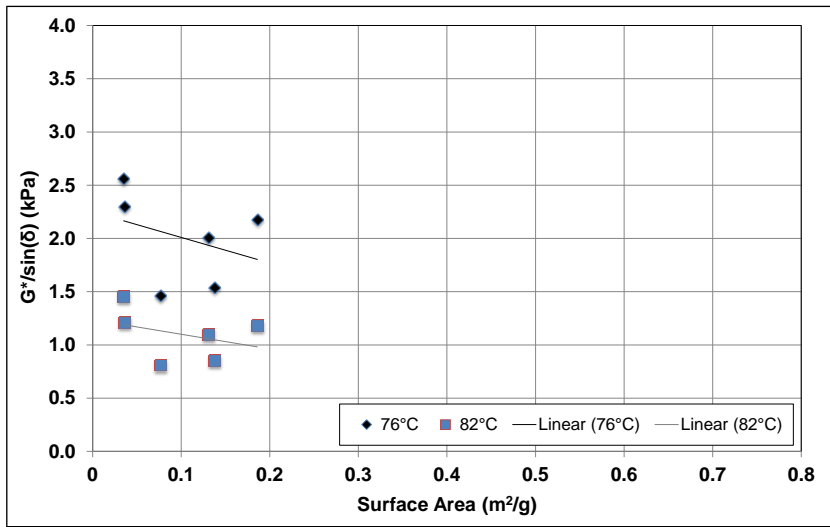


Figure 4.9: $G^*/\sin(\delta)$ versus surface area for Type I ambient rubber binder.

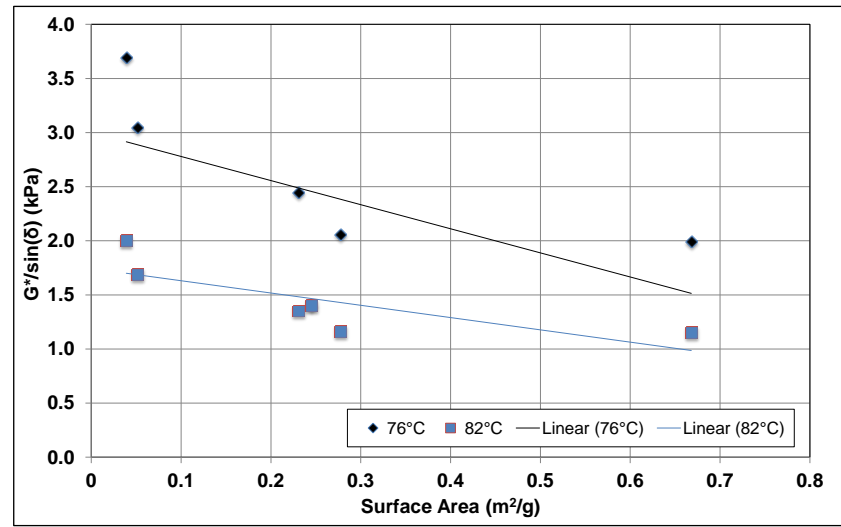


Figure 4.10: $G^*/\sin(\delta)$ versus surface area for Type I cryogenic rubber binder.

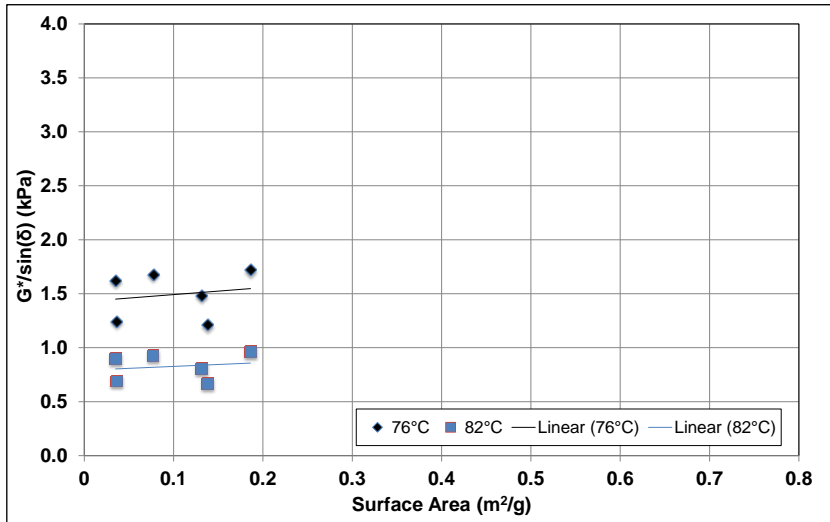


Figure 4.11: $G^*/\sin(\delta)$ versus surface area for Type II ambient rubber binder.

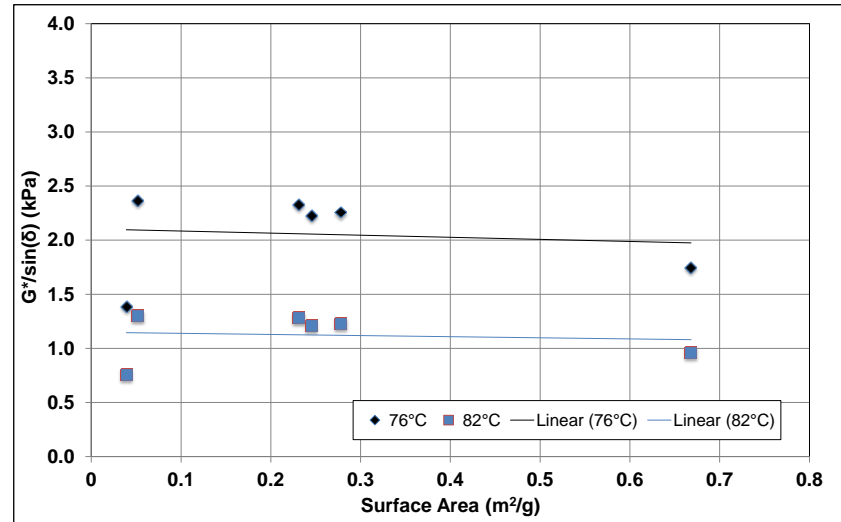


Figure 4.12: $G^*/\sin(\delta)$ versus surface area for Type II cryogenic rubber binder.

- Within a specific grinding process (i.e., ambient and cryogenic), the surface area did not significantly influence the $G^*/\sin(\delta)$ of the asphalt rubber binder if an extender oil was used. When no extender oil was used, some influence of surface area was evident, with $G^*/\sin(\delta)$ dropping with increasing surface area.

4.7 Effect of Crumb Rubber Particle Size on High Temperature Grade

The true high temperatures of the performance grade (i.e., the actual high temperature grade determined as opposed to the value to the nearest 6°C used in the PG system) for the binders tested at 82°C are listed in Table B.8 and summarized in Figure 4.13 and Figure 4.14.

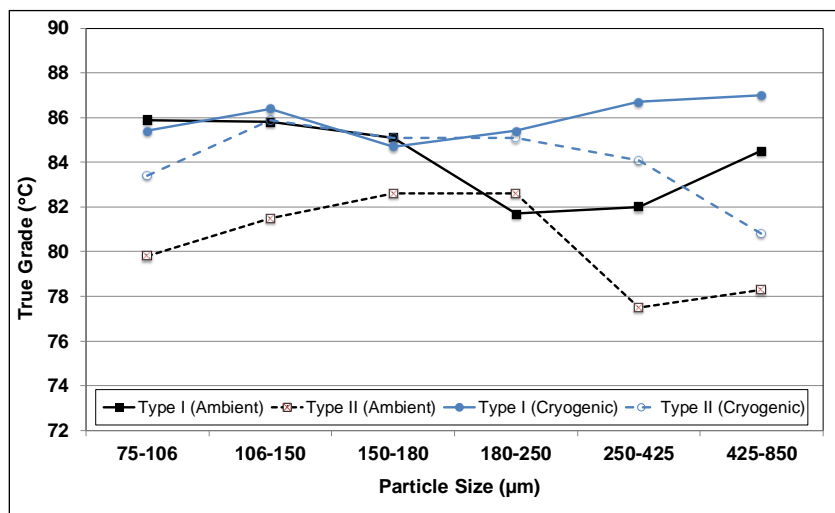


Figure 4.13: Concentric Cylinder: Plot of true temperature grade vs. rubber particle size.

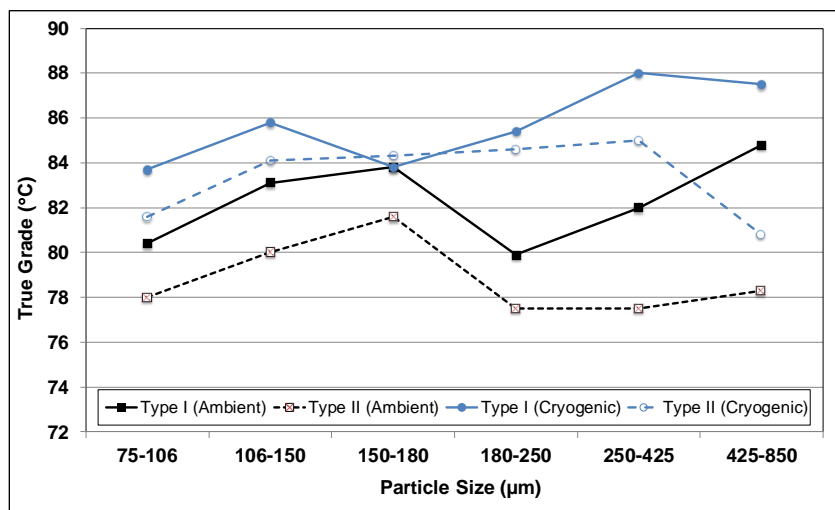


Figure 4.14: Parallel Plate: Plot of true temperature grade vs. rubber particle size.

Examination of the data presented in the figures led to the following observations:

- The true grades measured with concentric cylinder geometry were higher than those measured with the parallel plate geometry for binders with particle sizes smaller than 250 μm , and lower for binders with particle sizes larger than 250 μm .
- Type I binders mostly had higher true grades than Type II binders. The same trends were observed for both testing geometries.
- Binders produced with cryogenically crushed rubber particles mostly had higher true grades than binders produced with particles crushed at ambient temperatures. The more cubical nature of the cryogenically crushed particles may also have influenced the results of tests done using the parallel plate geometry.
- There was considerable variability in the results indicating that the degree of digestion of the rubber particles probably had an influence on the results.

4.8 Comparison of Concentric Cylinder and 3-mm Gap Parallel Plate Geometries

A Caltrans-Industry Task Group investigated the use of the parallel plate geometry with a 3-mm gap as an alternative procedure for determining the performance grade properties of asphalt rubber binders. Part of this investigation included a round-robin study covering 16 laboratories that tested three different asphalt rubber binders prepared by one supplier (21). The binder details and CRM gradations are summarized in Table 4.4 and Table 4.5, respectively. All three binders were prepared with rubber particles smaller than 1.4 mm (passing the #14 sieve) according to chip seal binder requirements. This maximum size is considerably smaller than the 2.36 mm specified for asphalt rubber binders used in gap- and open-graded mixes. The UCPRC participated in the round-robin study, but tested the supplied binders using both the 25-mm parallel plate with 3-mm gap and concentric cylinder geometries.

Table 4.4: Round-Robin Study Binder Details

Sample	Base Binder		Extender Oil (%)	CRM Scrap (%)	CRM Natural (%)	Binder/CRM (%)
	Grade	Source				
A	PG 70-10	Valero	2	17.00	5.00	78/22
B	PG 64-16	San Joaquin	2	15.75	5.25	79/21
C	PG 64-22	VSSE	2	13.5	4.40	82/18

Table 4.5: Round-Robin Study Rubber Details

Sieve Size	Sample A and B		Sample C		Specification	
	CRM Scrap (%)	CRM Natural (%)	CRM Scrap (%)	CRM Natural (%)	CRM Scrap (%)	CRM Natural (%)
#8	100	100	100	100	100	100
#10	100	100	100	100	98-100	100
#16	50	100	48	100	45-75	95-100
#30	11	72	2	39	2-20	35-85
#50	3	21	0	16	0-6	10-30
#100	1	4	0	2	0-2	0-4
#200	0	1	0	0	0	0-1

Test results comparing the two geometries are summarized in Figure 4.15 through Figure 4.18. The percent difference in $G^*/\sin(\delta)$ shown in Figure 4.18 was determined using Equation 3.2. Results from the two geometries were different in all instances; however, there was no consistent trend in these differences. $G^*/\sin(\delta)$ values for the asphalt rubber binders produced with the PG 70-10 and PG 64-22 base binders measured with the concentric cylinder were higher (12 to 16 percent) than those measured with the parallel plate at all testing temperatures. The opposite was observed for the binders produced with the PG 64-16 base binder (8 to 10 percent lower). No specific binder properties listed in Table 4.4 and Table 4.5 are likely to have contributed to these observations.

4.9 Phase 1b Findings and Recommendations

This stage of the study covered DSR testing with parallel plate and concentric cylinder geometries to assess the influences of selected crumb rubber properties (particle size and surface area), of production method (at ambient or cryogenic temperature), and of the use of extender oils on the performance properties of asphalt rubber binders. The results obtained from testing three asphalt rubber binders, each with different maximum crumb rubber particle size, show a strong correlation between the two testing geometries for the finer particle size range (180 – 250 μm), but increasingly weaker correlations with increasing particle size. These weaker correlations in the larger size ranges were attributed to increasing influence of the proximity of the larger incompletely digested rubber particles to the parallel plates. The results indicate that both the method used to produce the crumb rubber particles (i.e., grinding at ambient or cryogenic temperatures) and whether an extender oil was used influenced the shear modulus of asphalt rubber binders. Asphalt rubber binders containing cryogenically produced crumb rubber had higher $G^*/\sin(\delta)$ than binders containing crumb rubber produced at ambient temperatures. Particle surface area did not significantly influence the $G^*/\sin(\delta)$ of the asphalt rubber binder if an extender oil was used (Type II binders). When no extender oil was used, some influence of surface area was evident, with $G^*/\sin(\delta)$ dropping with increasing surface area. The presence of incompletely digested rubber particles appeared to influence the variability of the results.

A recommended test method for asphalt rubber binder performance grading using the concentric cylinder geometry in a DSR is provided in Appendix A.

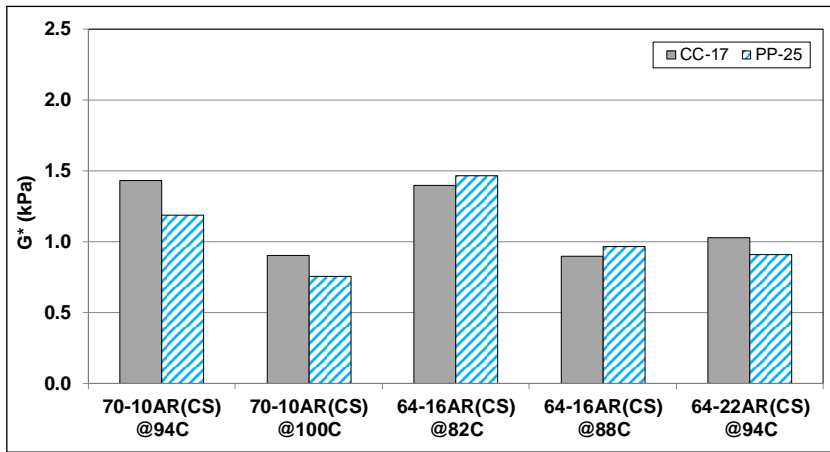


Figure 4.15: Comparison of G^* for concentric cylinder and parallel plate with 3-mm gap.

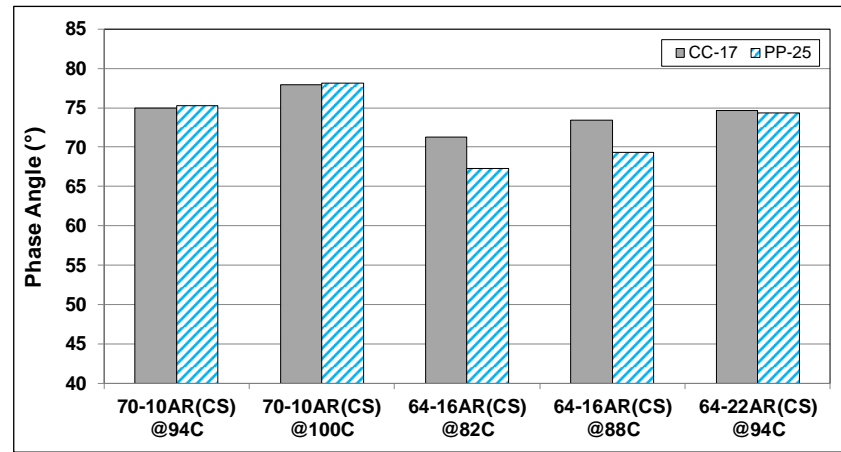


Figure 4.16: Comparison of phase angle for concentric cylinder and parallel plate with 3-mm gap.

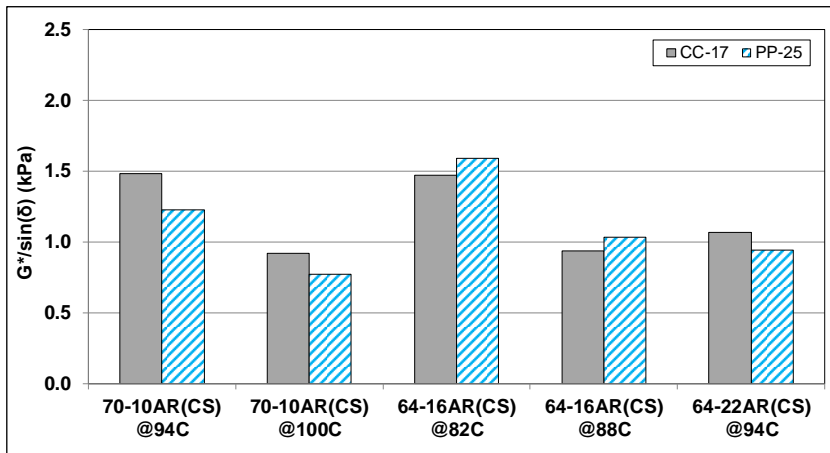


Figure 4.17: Comparison of $G^*/\sin(\delta)$ for concentric cylinder and parallel plate with 3-mm gap.

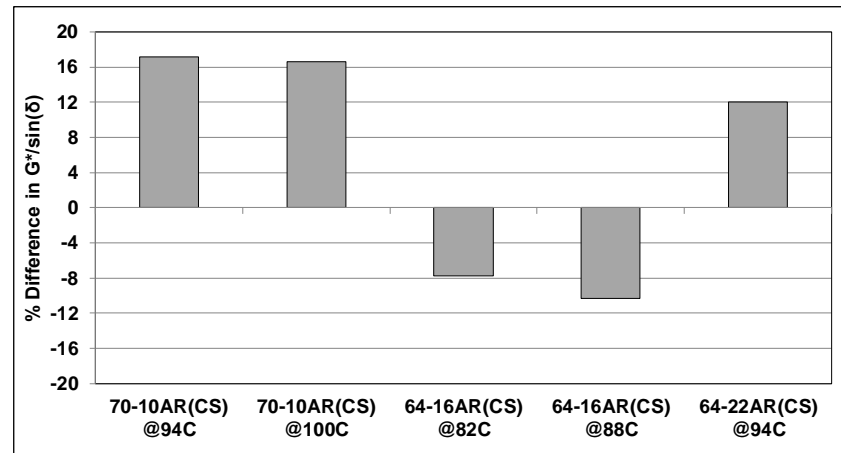


Figure 4.18: Difference between $G^*/\sin(\delta)$ for concentric cylinder and parallel plate with 3-mm gap.

5. Phase 2a: SHORT- AND LONG-TERM AGING PROCEDURES

5.1 Introduction

Evaluating highly viscous binders, including asphalt rubber binders, with the rolling thin-film oven (RTFO, AASHTO T 240) test is known to be problematic because of the limited rolling action of the binder during the test, and the consequent poor distribution and inconsistent film thickness during aging. Options suggested for improving binder flow (22) include placing steel rods inside the bottles and tilting the oven, but preliminary testing at the UCPRC indicates that these approaches were ineffective for asphalt rubber binders that meet Caltrans specifications. Alternative procedures were therefore investigated.

The standard AASHTO RTFO test, which is carried out on a 35 g (1.2 oz.) sample at 163°C (325°F), was developed for testing unmodified asphalt binders that are typically heated to between 135°C and 190°C (275°F and 374°F) before mixing with aggregate. However, according to Caltrans specifications, asphalt rubber binders should be heated to between 190°C and 220°C (374°F and 428°F) prior to mixing with aggregate and consequently the standard RTFO testing temperature is theoretically too low to be representative of asphalt rubber mix production temperatures and potentially too low to mobilize the asphalt rubber binder sufficiently to coat the bottle uniformly. The 35 g sample size used in the conventional RTFO test is based on the required amount of binder to coat the bottle with a uniform film thickness for an unmodified binder of approximately 10 µm, which in turn corresponds to the thickness required, in combination with time and temperature, to achieve a level of aging representative of that occurring between start of production at the plant and end of compaction of the layer on the road (23,24). This 35 g sample size is therefore potentially inappropriate for asphalt rubber binders, given that adding between 18 and 22 percent rubber by weight of the binder will effectively reduce the quantity of base asphalt binder tested by approximately 10 g. This reduction in volume will potentially influence full coating of the RTFO bottle and/or the resulting film thickness, and reduce the amount of binder available for testing in the DSR and BBR. Given the nature of asphalt rubber binder with its incompletely digested rubber particles, thicker films on the RTFO bottles were expected. Research by Glover, et al. (25) found that film thickness did not directly affect the mechanism of oxidation reactions, and that satisfactory short-term aging could be achieved by adjusting the duration of heating.

The AASHTO RTFO test standard also recommends turning the bottles manually to precoat them with binder before loading them in the oven, but the standard does not require complete coating, and observations indicate that between 70 and 80 percent coverage is typical for conventional unmodified binders. However, since pretest bottle-coating with asphalt rubber binders is generally very poor, this study investigated bottle preheating to determine if this could improve coverage and reduce the variability of results.

After completion of the RTFO test at 163°C, the standard AASHTO pressure aging vessel (PAV, AASHTO R 28) test is carried out on 50 g ± 0.5 g (1.8 oz) samples poured into a pan. The PAV test is conducted for 20 hours at 100°C and 2.1 MPa pressure. Although no changes to the test duration, temperature, and pressure parameters are required because these are intended to simulate field conditions, sample preparation procedures (sample size, binder temperature, and pouring technique) were investigated.

Based on the concerns noted above and results of a literature review that indicated that no similar research had already been undertaken, a decision was made to modify the RTFO and PAV test parameters—specifically the RTFO and PAV sample sizes and RTFO testing temperatures—to ensure that they are more suited to the properties of the asphalt rubber binder and more representative of rubberized asphalt concrete mix production and postconstruction performance. Therefore, 190°C (the lowest mix production temperature listed in the Caltrans specifications) was provisionally selected for the RTFO testing temperature and PAV sample preparation, 45 g was provisionally selected as the RTFO sample size, and 63 g was provisionally selected as the PAV sample size. Higher temperatures were not considered due to safety concerns. The 45 g and 63 g sample sizes were initially selected to provide equivalent quantities of the base asphalt binder to the standard tests to ensure film thicknesses in the RTFO bottles and PAV pans equivalent to those used in testing unmodified asphalt binders.

Ideally, any changes to laboratory-aging procedures should be validated by comparing the rheological properties of laboratory-aged binders to those of binders chemically extracted and recovered from mix sampled during paving (to verify short-term aging procedures) and from cores sampled from roads of different ages (to verify long-term aging procedures). However, asphalt rubber binders cannot be effectively extracted because the extraction process separates the rubber particles from the base binder and consequently, the measured properties are typically those of the base binder and not those of the asphalt rubber binder. The processes and results discussed in this chapter are therefore considered only in terms of the intent of the original testing procedures.

5.2 Short-Term Aging Procedures

5.2.1 Testing Plan

Table 5.1 summarizes the sampling and testing factorial for the materials assessed in this part of the study. Asphalt rubber binders were produced in the laboratory as described in Section 4.3. RTFO testing duration and air flow were set at 85 minutes and four bars, respectively, for all tests. All RTFO bottles were visually inspected to assess coating, and approximations of film thickness were made using a dental posterior probe. All DSR testing on the aged binders was performed using a concentric cylinder geometry with a 17-mm diameter bob. Shear modulus, phase angle, and true high PG limit were determined. For an unaged binder,

the high PG limit is the temperature at which $G^*/\sin(\delta)$ is equal to 1.0 kPa. The high PG limit of an RTFO-aged binder is the temperature at which $G^*/\sin(\delta)$ is equal to 2.2 kPa.

Table 5.1: Phase 2a: Experimental Design Factors and Factorial Levels for Short-Term Aging

Factor	Factorial Level	Details
Asphalt binder source and grade	1	PG 64-16 (sourced from Refinery #1)
Extender oil content (%)	2	0 and 4
Rubber content (%)	1	18
Rubber gradation (μm)	2	< 250 and 250 to 2,360
Sample size (g)	2	35 and 45
Testing temperature ($^{\circ}\text{C}$)	2	163 and 190
Bottle preheating	2	No preheating and preheating to 190°C for 10 minutes

Changes in the chemical composition of the binders after RTFO-aging were assessed using a *Bruker Alpha* Fourier transformed infrared spectroscope in attenuated total reflection mode (FTIR-ATR). All binder samples were preheated at 163°C for 10 minutes in sealed containers (to limit additional aging) to lower their viscosity for sample preparation. A small sample of the heated binder was applied directly onto the FTIR optics and spectra were recorded in reflective mode from $4,000\text{ cm}^{-1}$ to 400 cm^{-1} at a resolution of 4 cm^{-1} , averaging 24 scans for each measurement. Nine individual spectra were recorded for each sample.

Each spectrum was analyzed to assess chemical composition changes after RTFO aging. Changes in carbonyl (C=O) and sulfoxide (S=O) were of primary interest. The *carbonyl area* is commonly defined as the band around the $1,680\text{ cm}^{-1}$ peak, while the *sulfoxide area* is the band around $1,030\text{ cm}^{-1}$. The spectra were normalized using the aliphatic peak at $2,923\text{ cm}^{-1}$ as a reference since it is generally agreed that these structures are not affected by aging over time. The respective carbonyl and sulfoxide areas were calculated by tangentially integrating the band around the peak as represented in Equation 5.1. Lower and upper wave number limits were set at $1,670\text{ cm}^{-1}$ and $1,720\text{ cm}^{-1}$ respectively for carbonyl and at 981 cm^{-1} and $1,048\text{ cm}^{-1}$ for sulfoxide. Figure 5.1 shows an example of an FTIR testing spectrum with highlighted carbonyl and sulfoxide areas.

$$I_i = \int_{w_{l,i}}^{w_{u,i}} a(w) dw - \frac{a(w_{u,i}) + a(w_{l,i})}{2} \cdot (w_{u,i} - w_{l,i}) \quad (5.1)$$

where:

- I_i = index of area i , i being either carbonyl or sulfoxide
- $w_{l,i}$ = lower wave number integral limit of area i
- $w_{u,i}$ = upper wave number integral limit of area i
- $a(w)$ = absorbance as a function of wave number

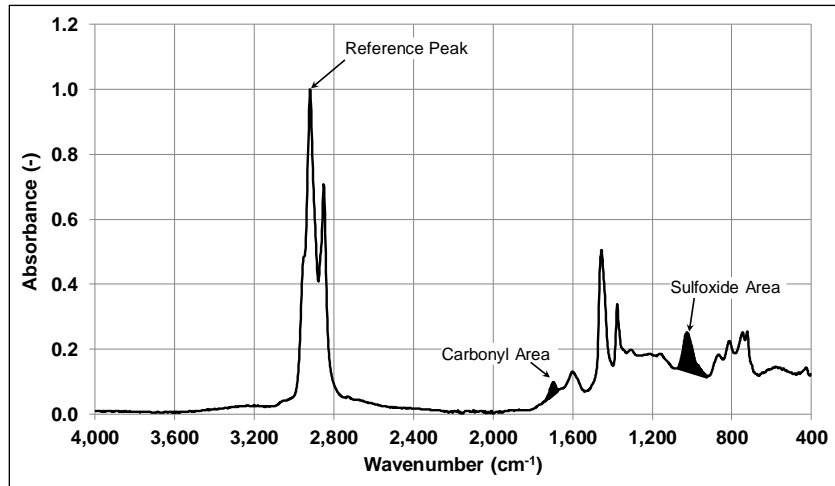


Figure 5.1: Example normalized FTIR absorbance spectrum with carbonyl and sulfoxide areas.

5.2.2 Preheating RTFO Bottles Prior to Pouring Binder

Figure 5.2 shows RTFO bottles that were not preheated prior to pouring the asphalt rubber binder and bottles that were preheated for 10 minutes at 190°C prior to pouring the binder. The photographs clearly show the improved coating due to the heating. Although preheating the bottles might have a negligible effect in terms of additional aging of the binder, the reduced time that elapses prior to full coating of the bottle during testing is believed to provide more consistent aging of the sample over the duration of the test.

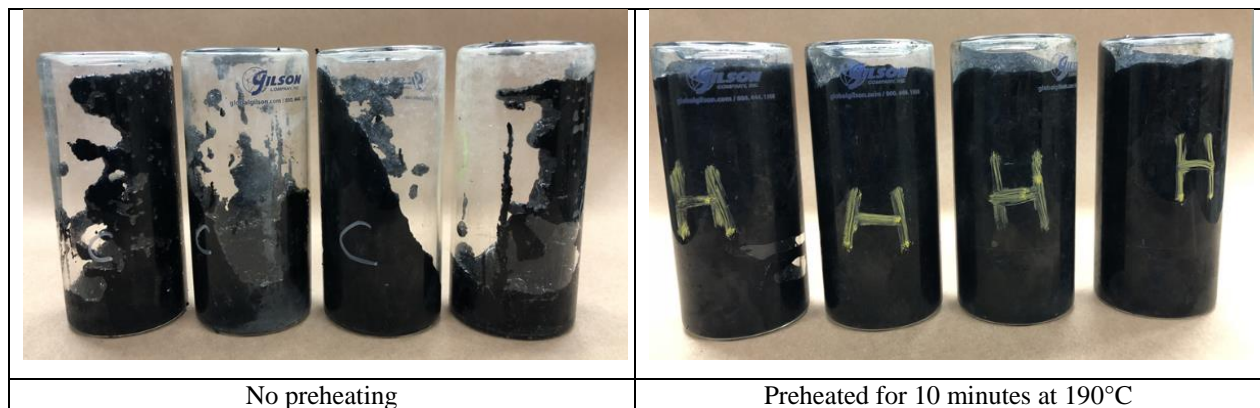


Figure 5.2: Effect of preheating on precoating of RTFO bottles.

5.2.3 Visual Inspection of RTFO Bottles after Aging

Figure 5.3 shows RTFO bottles after testing according to the standard method (AASHTO T 240, 35 g sample tested at 163°C) and after testing of a larger sample (45 g) at the proposed higher temperature (190°C).

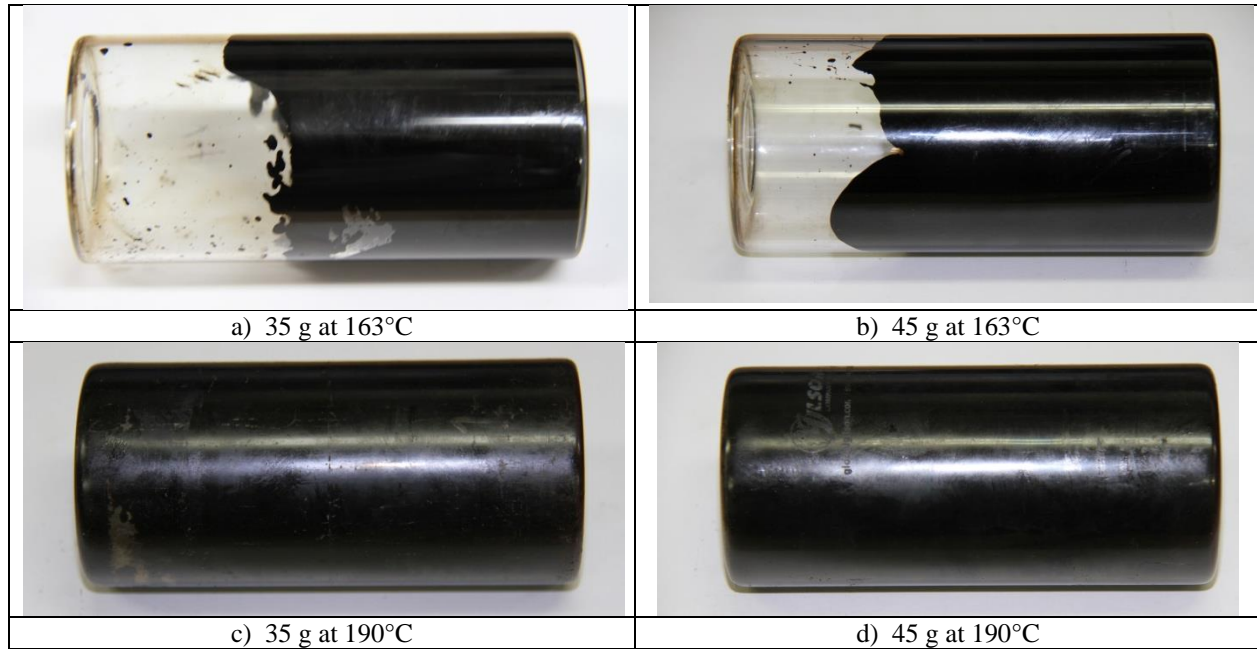


Figure 5.3: Effect of RTFO test parameters on bottle coating.

Based on the information gathered during the RTFO aging experiments, the following observations were made:

- Testing asphalt rubber binders according to AASHTO T 240 resulted in partial, non-uniform coating of the bottle, which implies that aging of the binder was also non-uniform (Figure 5.3a). Estimated film thickness within the bottle based on measurements with the dental probe ranged between 250 μm and 1 mm.
- Increasing the sample size to 45 g and testing at 163°C resulted in more of the bottle surface being coated, but the coating was still not uniform, which again implies that aging of the binder was also non-uniform (Figure 5.3b). Estimated film thicknesses were similar to those measured on the 35 g samples.
- Maintaining the sample size at 35 g and increasing the test temperature to 190°C significantly improved coating of the bottle, although some partially coated areas were still observed near the top of the bottle (Figure 5.3c). This improved coating implies that aging of the binder was more uniform; however, the small sample size was still a concern in terms of representative base asphalt binder content in the bottle and having sufficient binder for testing. Estimated film thicknesses did not appear to change.
- Increasing the sample size to 45 g and the temperature to 190°C provided complete and uniform coating of the bottle (Figure 5.3d), which implies that uniform aging of the binder was also achieved. Using these parameters, the base asphalt binder content is also representative of that prescribed in AASHTO T 240, and sufficient quantities can be produced in a single run for binder testing. Estimated film thicknesses were marginally lower than those recorded in the other tests, but thickness appeared to be more consistent over the entire bottle.
- Testing the asphalt rubber binder at the higher temperature facilitates removing it from the bottle and preparing it for testing.

- Testing at higher temperatures increases safety risks for personnel, and staff training needs to cover these additional risks.
- Testing at the higher-temperature resulted in more smoke and increased odor levels, so laboratory ventilation systems may need upgrading to accommodate the changes.

Although bottle leakage was reported in the literature, this was not observed during any testing at 190°C or with 45 g of binder during this phase of the study. Possible solutions to this problem include setting the carriage angle at -1° , which is still within the acceptable tolerance in the AASHTO T 240 specification, and/or using bottles with smaller openings.

5.2.4 Effects of RTFO Test Parameters on High Temperature Properties

Test results for assessing the effects of RTFO test parameters on binder shear modulus, phase angle, and $G^*/\sin(\delta)$ are summarized in Table C.1 in Appendix C.

Binder Shear Modulus and $G^*/\sin(\delta)$

Figure 5.4 and Figure 5.6 show the shear modulus and $G^*/\sin(\delta)$ values, respectively, measured at 64°C for unaged and RTFO-aged binders for the different scenarios listed in Table 5.1. A review of the test results led to the following observations:

- The shear modulus of all the binders increased after RTFO aging, as expected. Shear modulus increased by between 1.5 and 2.0 times when aged at 163°C and by between 3.0 and 5.0 times when aged at 190°C.
- Increasing the sample size reduced the shear modulus slightly on the base binder, had no effect on the asphalt rubber binder produced with fine rubber particles ($<250\ \mu\text{m}$), and increased the stiffness slightly when coarse rubber particles ($>250\ \mu\text{m}$) were used.
- Asphalt rubber binder samples produced with extender oil had lower shear moduli than the same binder formulations produced without extender oil. Sample size and RTFO temperature did not appear to influence the effect of the extender oil.
- Rubber particle size had a significant effect on shear modulus. Binders produced with coarser rubber particles were between 30 and 40 percent stiffer than the binders produced with finer rubber particles. This increase is most likely due to stiffness changes in the rubber particles being less sensitive to oxidative aging and temperature changes than the asphalt.

Binder Phase Angle

Figure 5.5 shows the phase angles measured on the unaged and RTFO-aged binders. The following observations were made:

- RTFO aging of the binders decreased the phase angle in all instances, as expected, with trends opposite those shown in the shear modulus results.
- Increasing the RTFO temperature to 190°C decreased the phase angle significantly more than did testing at 160°C.

- The asphalt rubber binders had lower phase angles than the unmodified binders, as expected. The asphalt rubber binders produced with coarse particles had smaller phase angles than the binders produced with fine rubber particles; this result was attributed to the predominance of the larger incompletely digested particles.
- Increasing the sample size had minimal effect on phase angle.
- Asphalt rubber binder samples produced with extender oil had slightly larger phase angles than the same binder formulations produced without extender oil. Sample size and RTFO temperature did not appear to influence the effect of the extender oil.
- Asphalt rubber binders produced with coarse rubber particles had smaller phase angles than the binders produced with fine particles. This implies that despite the smaller surface area, the larger particles likely absorbed more of the binder's light components, thereby enhancing the elastic properties of the asphalt rubber binder.

High PG Limit

Figure 5.7 shows the true high PG for the unaged and RTFO-aged binders. A review of the data led to the following observations:

- When tested according to AASHTO T 240, the high PG limit did not change significantly after RTFO aging when compared to the unaged binders with the same formulations.
- Increasing the test temperature to 190°C resulted in an increase of about 6°C in high PG limit, which is equal to one PG bump.
- Sample size had minimal effect on the high PG limit.
- Adding extender oil reduced the high PG limits of the unmodified binder and the asphalt rubber binder produced with fine rubber particles. It had limited effect on the asphalt rubber binder produced with the coarse rubber particles at 190°C.
- The performance grades of the AR binders were notably higher than those of the base binder, indicating that the presence of rubber particles has a significant impact on the test results. It is not clear whether this is a true reflection of expected field performance when ambient temperatures are very high.

5.2.5 Effect of RTFO Test Parameters on Binder Chemistry

Figure 5.8 shows FTIR spectra (wavelengths from 2,000 cm^{-1} to 600 cm^{-1}) of all the analyzed samples. The spectra are stacked for each binder type starting with the unaged sample on the bottom, followed by the 35 g and 45 g samples aged at 163°C, and then the 35 g and 45 g samples aged at 190°C. The carbonyl and sulfoxide bands are labeled in the spectra. A review of the data led to the following observations:

- The carbonyl bands have indistinct peaks, which implies a small change after RTFO aging. This is consistent with other studies, which indicate that bigger changes in the carbonyl peak are usually only observed after pressure vessel aging in the laboratory or long-term field aging (26,27). The sulfoxide band showed more distinct peaks in both unaged and RTFO-aged stages.

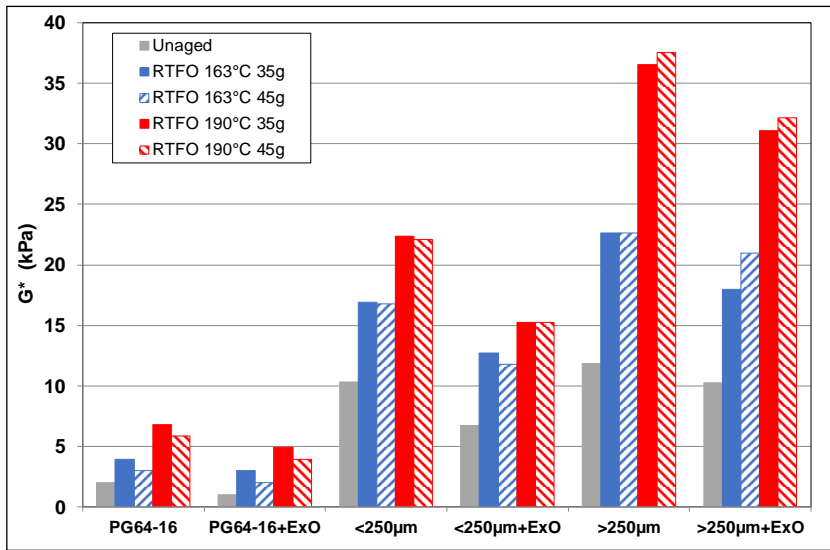


Figure 5.4: Effect of RTFO test parameters on shear modulus tested at 64°C.

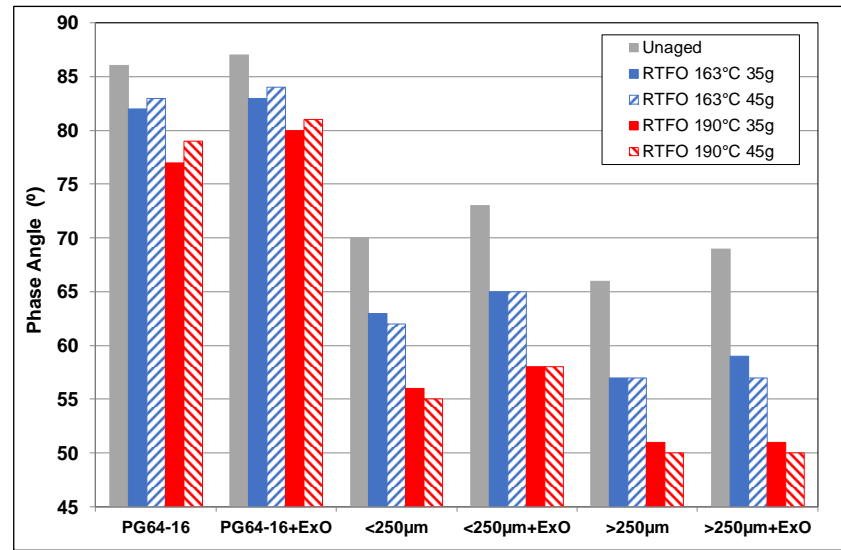


Figure 5.5: Effect of RTFO test parameters on phase angle tested at 64°C.

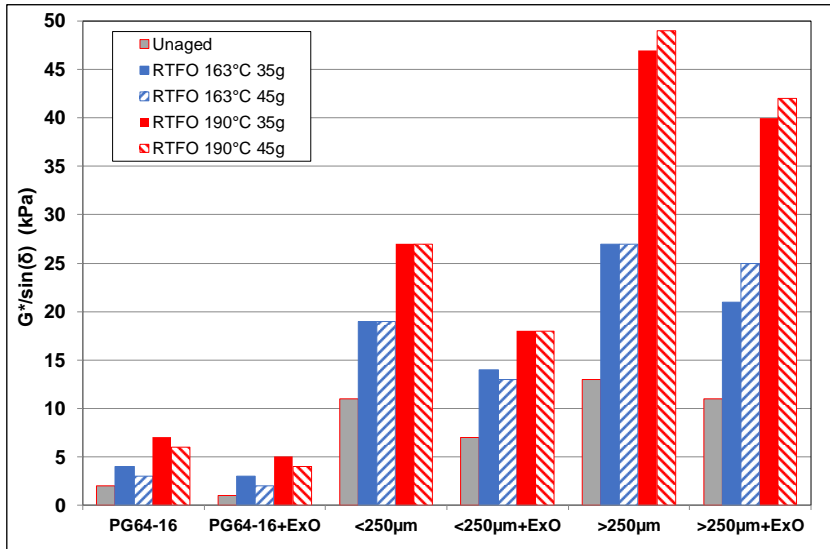


Figure 5.6: Effect of RTFO test parameters on $G^*/\sin(\delta)$.

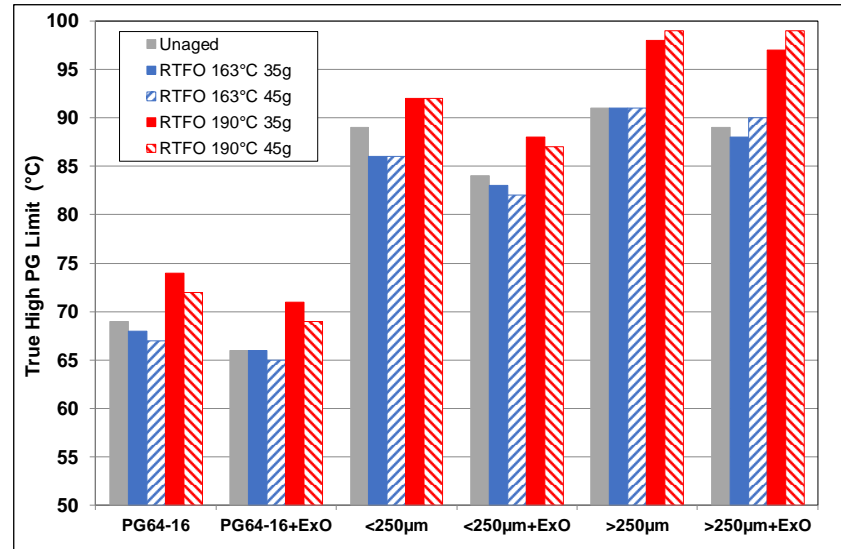


Figure 5.7: Effect of RTFO test parameters on true high PG limit.

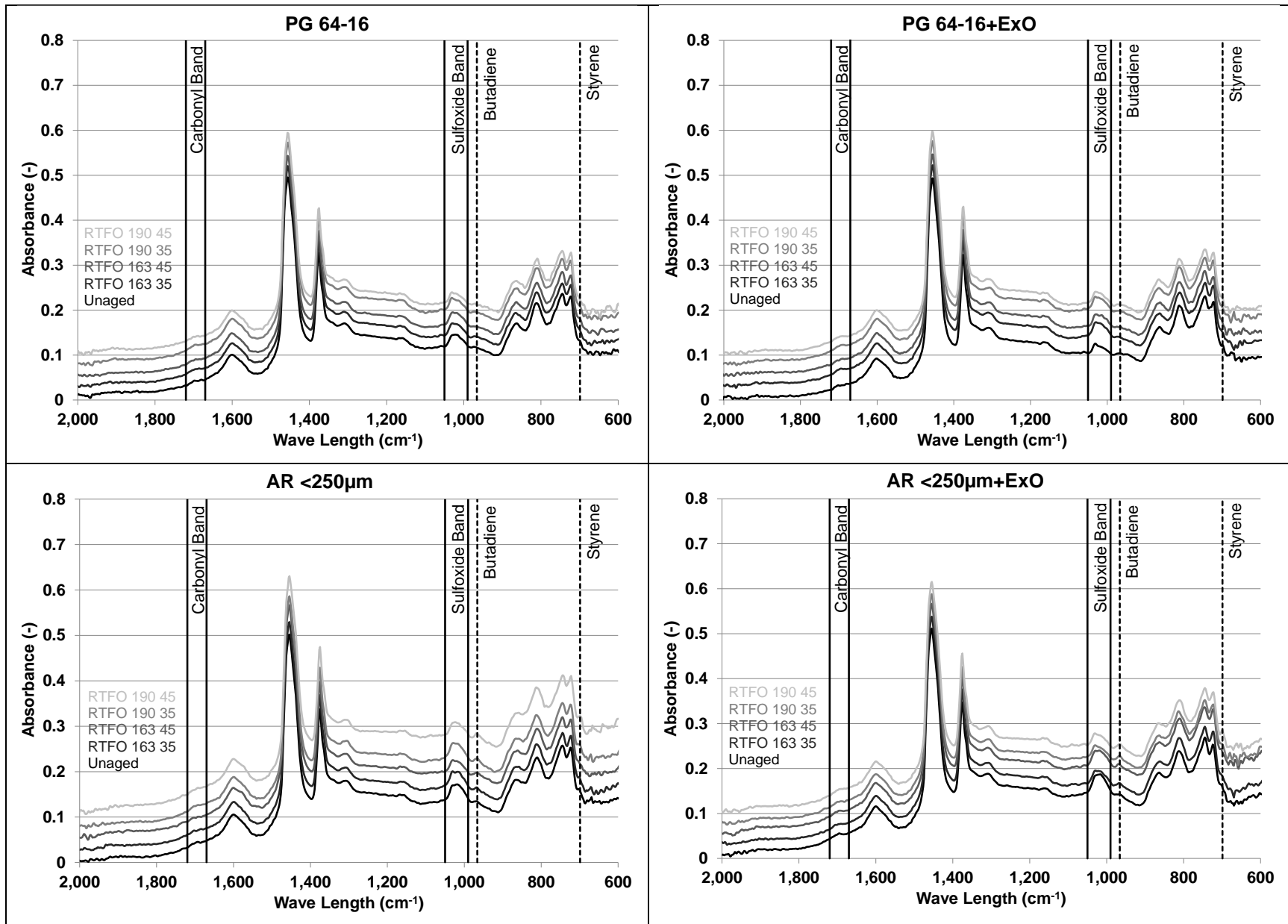


Figure 5.8: Effect of RTFO test parameters on binder chemistry.

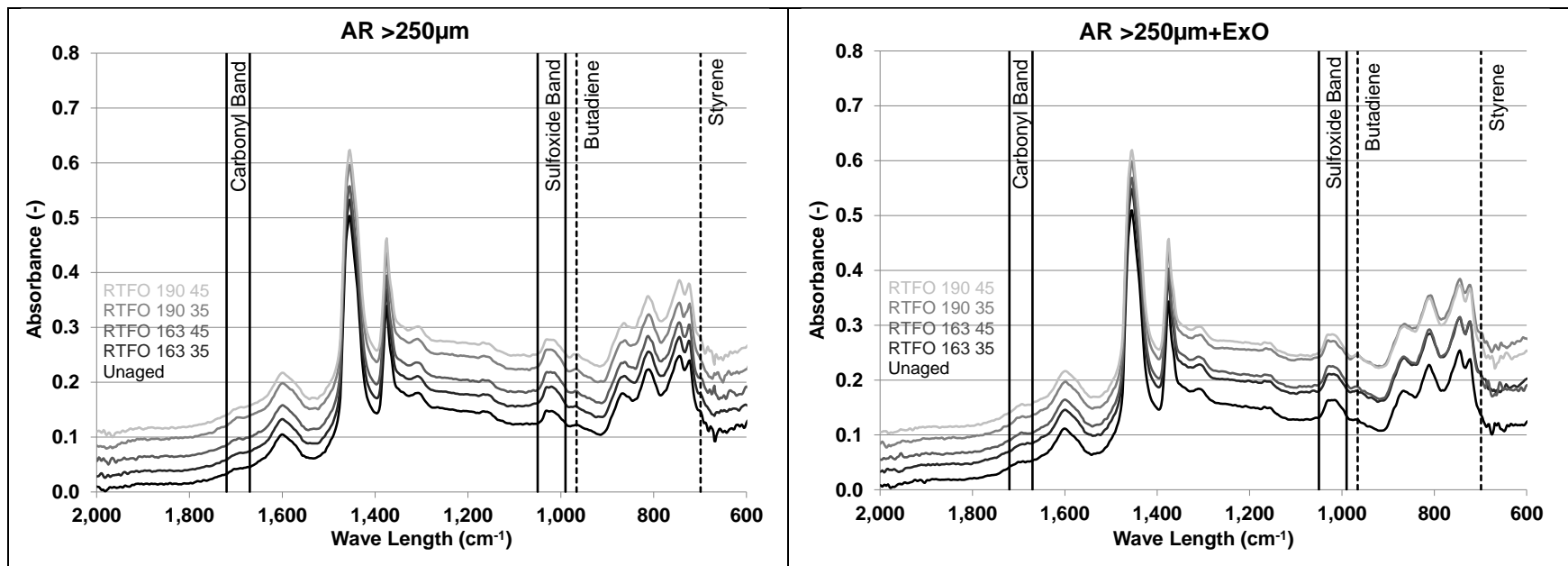


Figure 5.8: Effect of RTFO test parameters on binder chemistry (*continued*).

- Additional chemical structures were observed in the asphalt rubber binders, as expected, and are attributed to the rubber itself. Distinct absorbance maxima are visible at 966 cm^{-1} and 699 cm^{-1} , which represent trans-butadiene and polystyrene, respectively (28), both of which are known constituents of tire rubber. The respective absorbance maxima tended to increase with RTFO aging. To analyze the changes in the styrene-butadiene rubber (SBR) in the asphalt rubber binders in more detail, a butadiene index with wavenumbers of 950 cm^{-1} to 981 cm^{-1} was calculated using Equation 5.1. The butadiene band was selected since the styrene band at 699 cm^{-1} is close to the aromatic component bands, which complicates defining unbiased integration boundaries.

The changes in the indices relative to the respective index of the unaged base binder were evaluated to describe and interpret changes in the oxidized structures. The results are summarized in Figure 5.9 through Figure 5.11. In all plots, the index is set to 100 percent for the unaged base binder and indices of all other samples are shown as a percentage relative to this index value.

Figure 5.9 shows relative changes in the carbonyl index. A review of the data led to the following observations:

- Some inconsistencies were noted in the results of the asphalt rubber binder produced with fine rubber particles and no extender oil. The results from the standard RTFO test method were considerably lower than expected and these were therefore excluded from the analysis.
- There was a notable difference in the change in carbonyl content (increased oxidation) after RTFO aging of the unmodified binder and the unmodified binder with extender oil using the standard test method. Increasing the RTFO temperature further increased the change in carbonyl content. However, there was less change in carbonyl content when the sample size increased. Adding extender oil had limited effect on the change in carbonyl content of the unmodified binder.
- The asphalt rubber binders had a higher carbonyl content than the unmodified base binder, and this was attributed to aging that occurred during heating of the binder while the rubber particles were blended. Standard RTFO-aging had a mostly limited effect on the change in carbonyl content. Increasing the RTFO temperature had a further small, positive change. Adding extender oil and increasing the sample size both resulted in additional small positive changes. Asphalt rubber binder produced with larger rubber particles had larger carbonyl content changes than the binder produced with small particles for all testing conditions, indicating that the larger surface area of the finer particles contributed to a lower rate of oxidation.

Figure 5.10 shows relative changes in the sulfoxide index. These changes showed trends similar to those discussed for the carbonyl content, except that the extent of the change was generally lower.

Figure 5.11 summarizes the changes in the butadiene index. The following observations were made:

- There was limited change in the unmodified base binder, as expected, given that there was no polymer modification in this binder. Adding extender oil appears to have had a minor influence, and this was attributed to the chemical formulation of the oil.

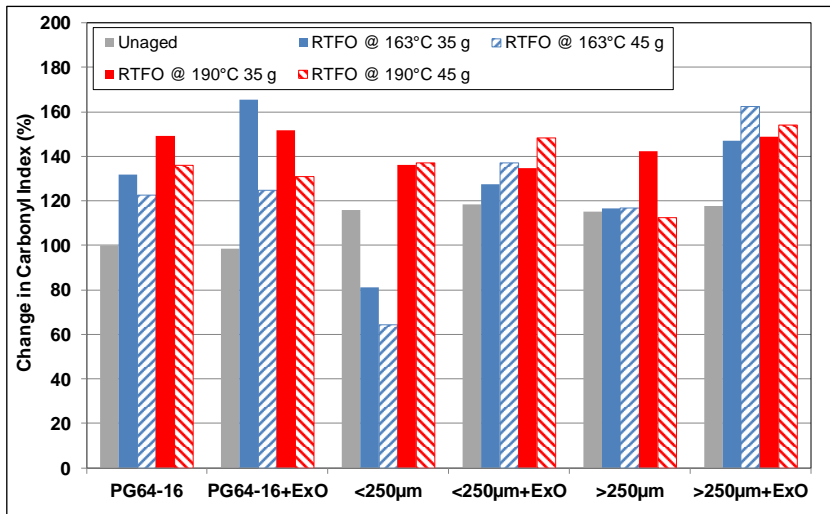


Figure 5.9: Effect of RTFO test parameters on carbonyl index.

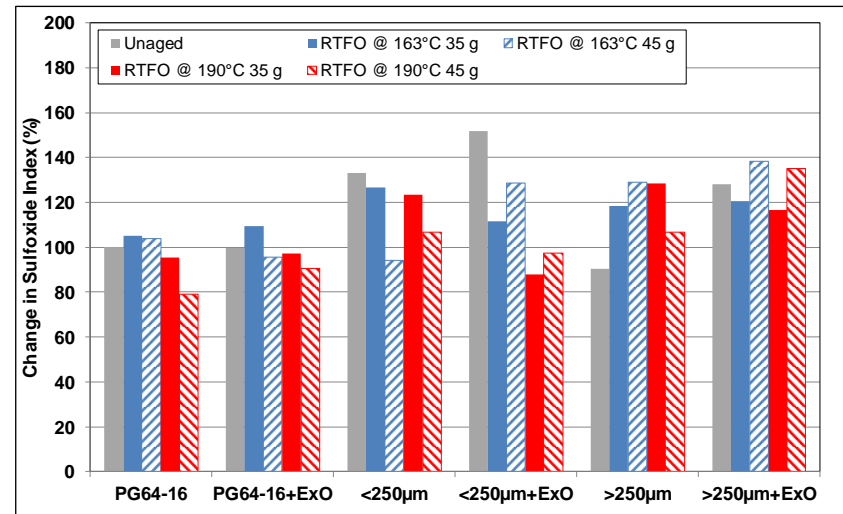


Figure 5.10: Effect of RTFO test parameters on sulfoxide index.

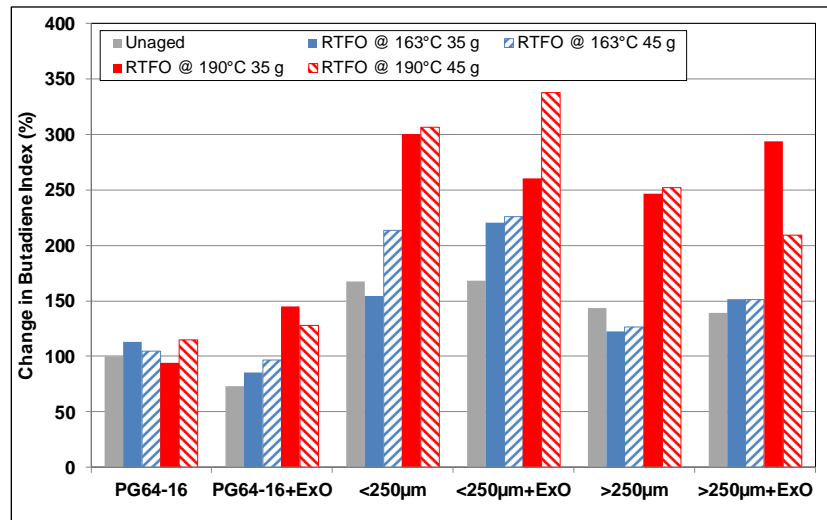


Figure 5.11: Effect of RTFO test parameters on butadiene index.

- The influence of the rubber on changes in the butadiene index is clear for all the asphalt rubber binders. Changes in butadiene index were larger in the binders produced with fine rubber particles for all testing parameters. Producing the asphalt rubber binders with extender oil had limited effect on change in butadiene index.
- RTFO aging at 190°C resulted in significantly greater changes in the butadiene index of the asphalt rubber binders than the aging at 163°C.
- The butadiene index data corresponds to the rheology results discussed above in terms of stiffness and viscoelasticity. RTFO-aged asphalt rubber binders were stiffer but more elastic than the unmodified binders. Increasing the RTFO temperature to 190°C resulted in a corresponding increase in stiffness and elasticity. Given that the changes in carbonyl and sulfoxide content were relatively small compared to the changes in butadiene content, activation of the butadiene and other polymeric compounds in the rubber at the higher aging temperature may have contributed to these rheological changes.

5.3 Long-Term Aging Procedures

5.3.1 Testing Plan

Table 5.2 summarizes the sampling and testing factorial for the materials assessed in this part of the study. Given that the PAV testing procedure did not need modification for particle size, three plant-produced asphalt rubber binders were selected to assess the PAV specimen preparation procedure. The binders were short-term aged following the revised RTFO procedure discussed above (45 g sample aged at 190°C in preheated bottles) prior to pouring into the PAV pans. Three samples sizes were considered. Bending beam rheometer (BBR) specimens were fabricated using the PAV-aged binder samples prepared using the traditional (50 g ± 0.5 g) and modified methods. All pans were visually assessed to determine coating. Film thicknesses were measured with a Vernier caliper.

Table 5.2: Phase 2a: Experimental Design Factors and Factorial Levels for Long-Term Aging

Factor	Factorial Level	Details
Asphalt source (plant-produced)	3	Projects in Solano, Calaveras, and Santa Barbara counties
RTFO aging temperature (°C)	1	190 (consistent with short-term aging)
Sample size (g)	3	50 (control), 63, and 72
Pan preheating treatments	2	No preheating, preheating to 190°C for 10 minutes

5.3.2 Visual Inspection of PAV Pans with 50 g Samples

Traditional PAV specimen (AASHTO R 28) preparation procedures require pouring the heated binder evenly over a pan at room temperature. However, despite heating the asphalt rubber binders to 190°C (instead of 163°C), this pouring process did not result in even distribution of binder, or full coverage of the pan, because of the viscous nature of the binder and the reduced quantity of base asphalt used per pan (i.e., less base asphalt because of the addition of up to 22 percent rubber particles [Figure 5.12]). Incomplete coverage was also noted in most pans after completion of PAV aging of samples prepared using the standard

50 g \pm 0.5 g sample size. Some separation of binder from the incompletely digested rubber particles close to the edges of the pan in the areas of incomplete coverage was also observed (Figure 5.13).

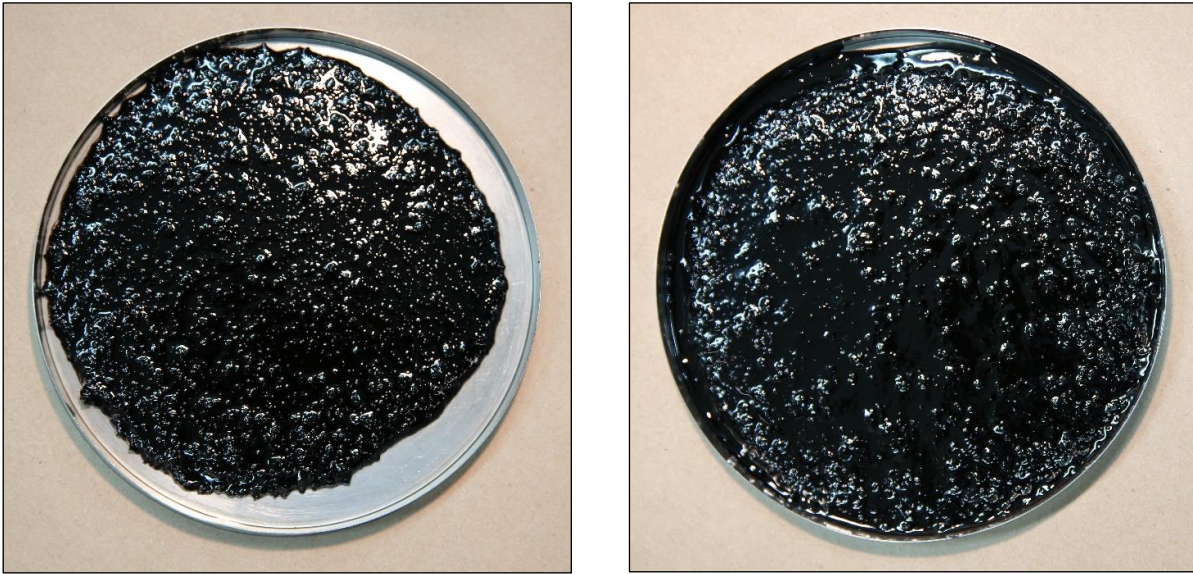


Figure 5.12: Binder coverage of a 50 g sample before and after PAV aging.

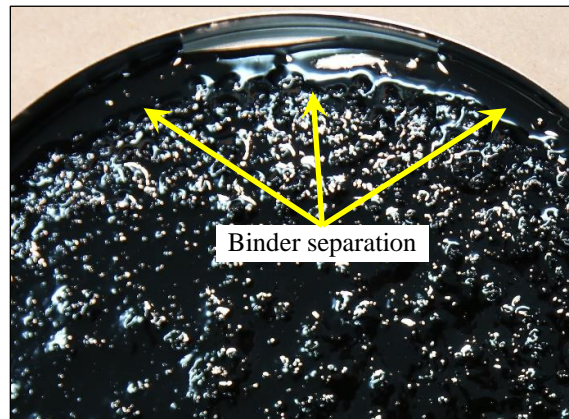


Figure 5.13: Binder separation at edge of pan after PAV aging.

Film thicknesses measured after pouring at nine fixed locations in the pan (Figure 5.14) revealed pan coverage of about 80 percent and a range of thicknesses between 0 mm (in areas where the binder did not flow) and 5.0 mm. Thickness at the pouring point in the center of the pan was 5 mm, but the average thickness for all nine points was only 0.9 mm, indicating that limited flow had occurred. This average is 2.3 mm less than the recommended average of 3.2 mm listed in AASHTO R 28. Observations of the same pan after PAV aging revealed that the binder had spread more evenly with a coverage of 99 percent, and that film thicknesses ranged between 0 mm and 4.6 mm, with an average of 2.1 mm (Figure 5.15). Film thickness at the pouring point was still well above the recommended average thickness, while overall average thickness was still well below. Multiple repetitions of this exercise revealed similar results.

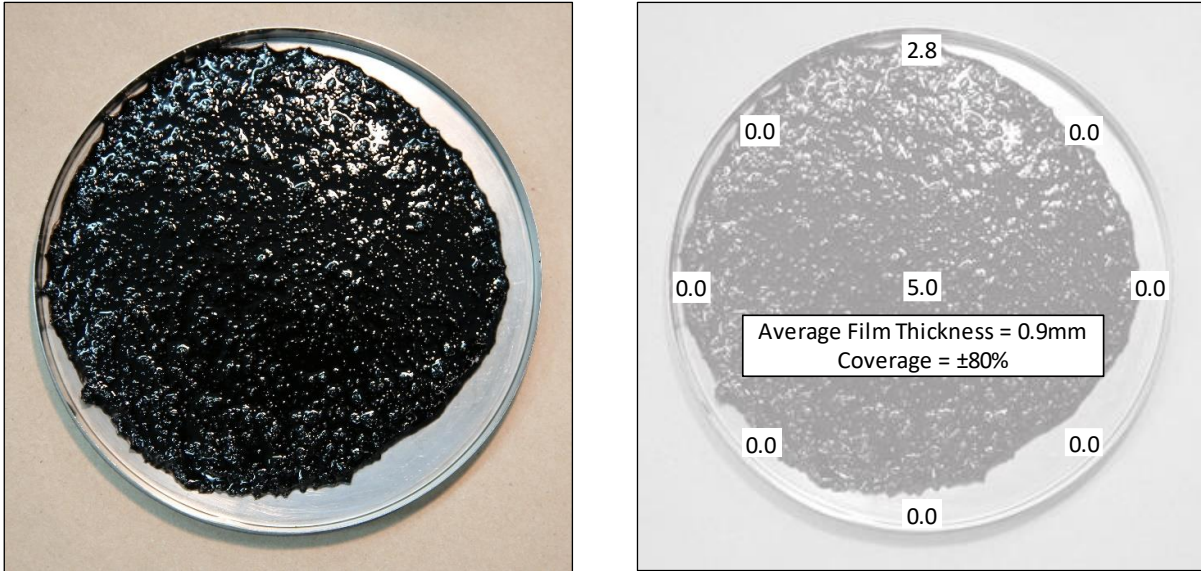


Figure 5.14: Binder coverage and thickness after pouring a 50 g sample.

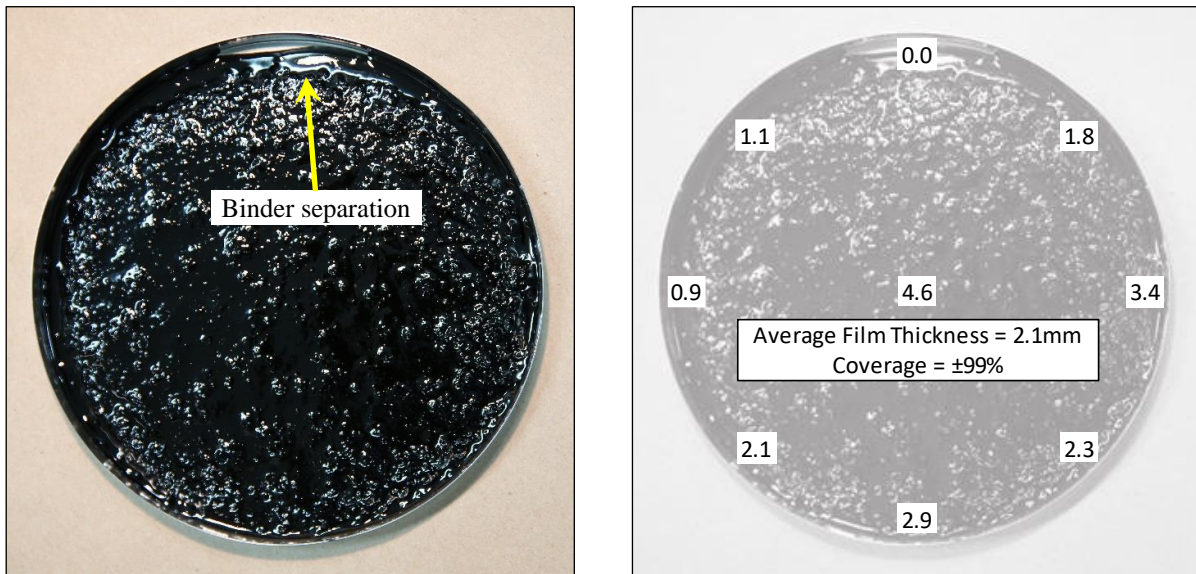


Figure 5.15: Binder coverage and thickness after PAV aging a 50 g sample.

Preheating the pan to 190°C for 10 minutes prior to pouring the asphalt rubber binder increased the pan coverage to about 97 percent (Figure 5.16). Preheating also led to better flow as indicated by the thickness of 3.2 mm at the central pouring point, but although average thickness of all nine points was marginally higher at 1.9 mm, it was still well below the required 3.2 mm. After PAV aging, pan coverage improved to 100 percent, and average thickness increased to 2.7 mm, indicating a more even film thickness over the pan (Figure 5.17). Some binder separation was still noted around the edges of the pan.

Based on these observations, it was concluded that a 50 g sample is insufficient to satisfy the minimum film thickness of 3.2 mm specified in AASHTO R 28. This raised concerns given that recent research on binder

aging (29) indicated that every 0.5 mm change in thickness below 3.2 mm could cause a variation of between 10 and 19 percent in the shear modulus measured after aging. The study also showed that only the upper portion of the binder film aged during the 20-hour process and therefore thicker films would result in larger quantities of less-aged binder. A series of modified sample preparation procedures were therefore investigated and are discussed in the following sections.

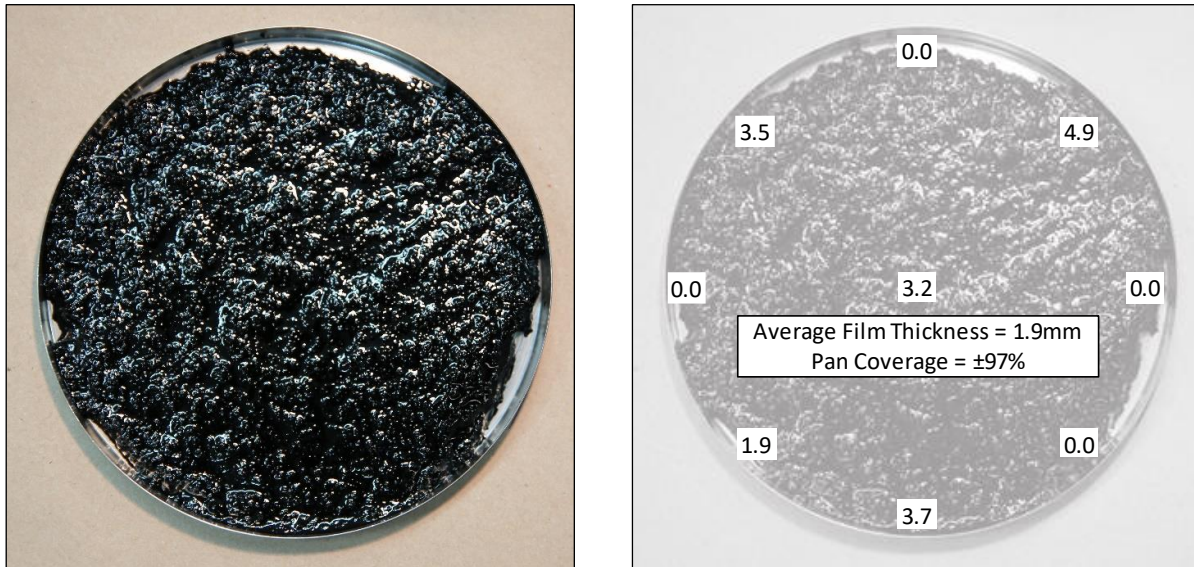


Figure 5.16: Binder coverage and thickness after pouring a 50 g sample into preheated pan.

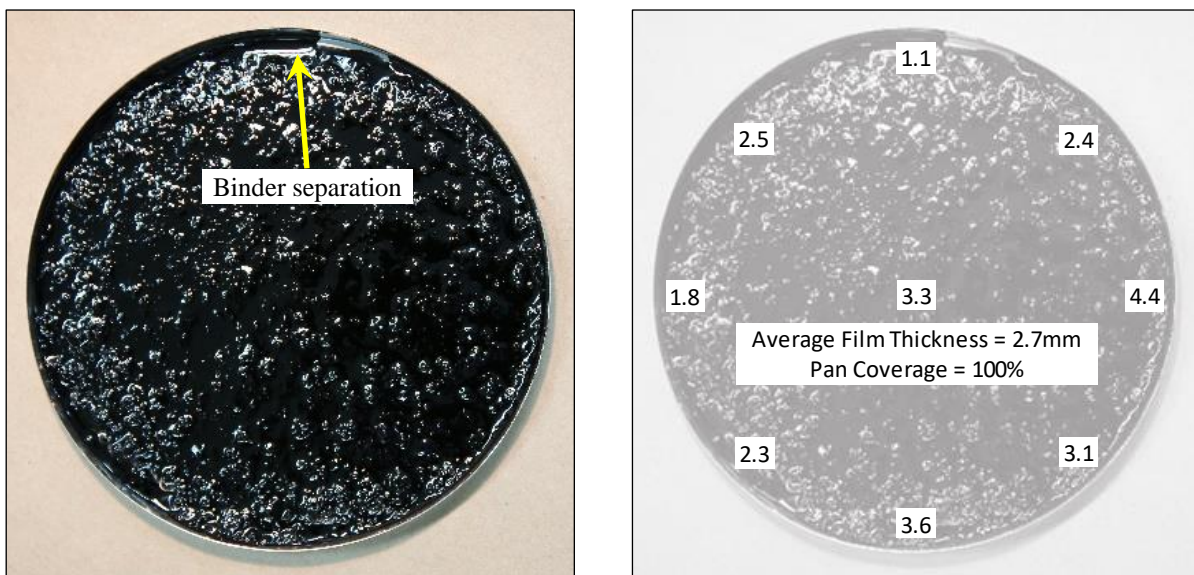


Figure 5.17: Binder coverage and thickness after PAV-aging a 50 g sample in preheated pan.

5.3.3 Modified Sample Preparation Procedures

A series of experiments were carried out to assess different sample sizes, pouring procedures, and spreading techniques. These included the following:

- Method #1: Standard AASHTO R 28 procedure, which was used as a control.
- Method #2: Same as Method #1, with the pans preheated to 190°C for 10 minutes and constantly agitated during pouring to facilitate even coating over the pan surfaces. Based on the initial findings presented in Section 5.3.2, this was also considered as a control.
- Method #3: Increasing the sample size from 50 g to 63 g to account for the rubber particles (calculated at approximately 20 percent rubber by weight of binder), increasing the binder heating temperature to 190°C (i.e., the RTFO temperature), and quickly pouring the binder into the pan in a continuous spiral pattern, starting at the center of the pan and moving toward its outside edge. Preliminary observations from this process indicated that although the larger sample resulted in more complete distribution than the smaller sample, the binder did not spread evenly across the pan, with ridges evident in the pouring overlap areas. Attempting to facilitate spreading with a spatula resulted in improved but incomplete distribution of the binder, with some gaps caused by the spatula.
- Method #4: Same as Method #3, with manual agitation of the pan during and after pouring. Distribution with a spatula was not attempted. Observations from this process indicated that the combination of the larger sample and constant agitation of the pan resulted in more complete distribution compared to the 50 g sample, with a relatively even coverage across the pan. However, some small gaps were still noted around the edges on some pans.
- Method #5: Same as Method #4, with the pan heated to 190°C prior to pouring the binder. Visually, this method appeared to provide the most even binder distribution. Thickness measurements after pouring revealed a range of between 2.9 mm at one point on the edge of the pan and 4.6 mm in the center, with an average depth of 3.5 mm (Figure 5.18), slightly above the AASHTO R 28 recommended thickness. Thickness measurements after PAV-aging ranged between 2.9 mm and 4.4 mm, with an average thickness of 3.6 mm, indicating that further leveling of the sample to a more constant thickness had occurred during the aging process (Figure 5.19). Similar results were achieved on different pans with an average film thickness of 3.7 mm measured on three pans after pouring and 3.8 mm after PAV-aging. These results were slightly higher than the target thickness of 3.2 mm, but were considered satisfactory given the potential effect of the incompletely digested rubber particles on film thickness. Since the 63-g sample size was calculated as an optimal increase to account for the rubber particles, further testing with a smaller sample size was not considered appropriate.
- Method #6: Heating the pan to 190°C and pouring the binder until full coverage of the pan was achieved without any agitation. The weight of the binder required to achieve full coverage was then determined; in this instance 72 g. Thickness measurements after pouring revealed a range between 4.1 mm and 4.8 mm, with an average depth of 4.4 mm, which is 1.2 mm thicker than the AASHTO R 28 recommended thickness.

Methods #1, #2, #5 and #6 were selected for further testing to compare DSR intermediate-temperature and BBR low-temperature test results with those results tested with the standard 50 g PAV-aged samples (Method #1).

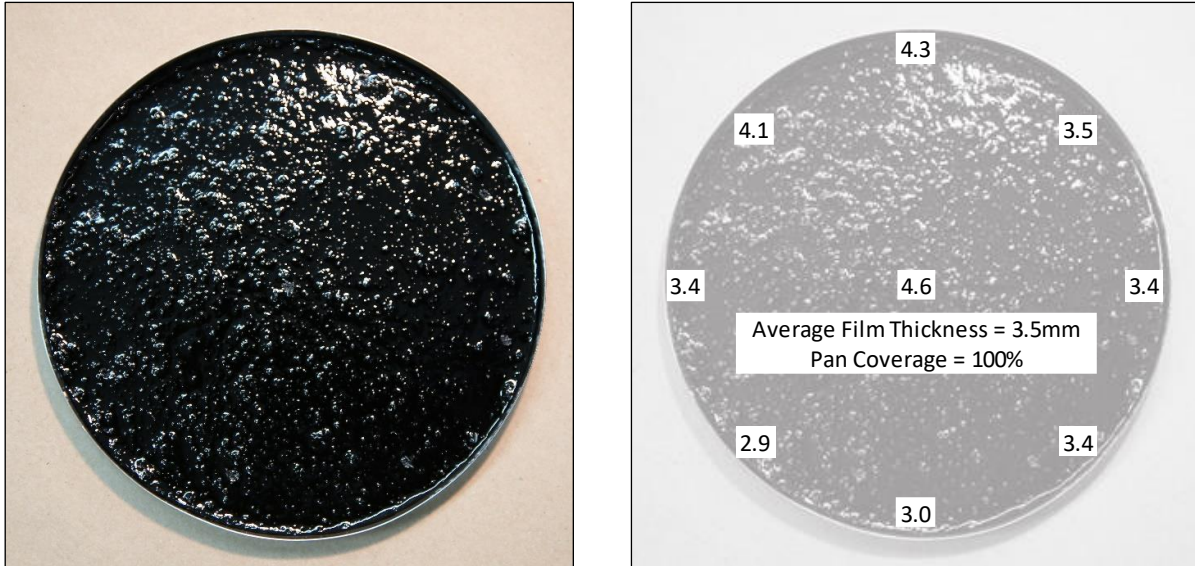


Figure 5.18: Binder coverage and thickness after pouring a 63 g sample in preheated pan.

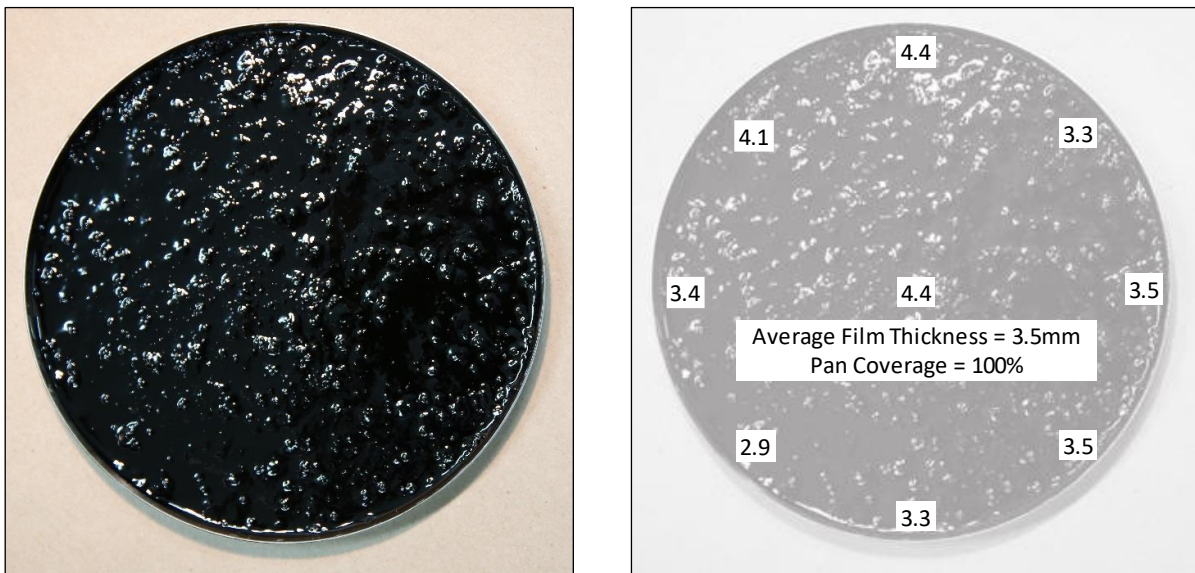


Figure 5.19: Binder coverage and thickness after PAV-aging a 63 g sample in preheated pan.

5.3.4 Preliminary Intermediate-Temperature Test Results

Preliminary intermediate-temperature testing was conducted following the procedure discussed in Chapter 7. The PAV-aged binders were uniformly mixed prior to taking the sample for DSR testing. Test results are provided in Table C.2 in Appendix C and summarized in Table 5.3 and in Figure 5.20. Whiskers on the plots indicate the standard error for the three replicate DSR tests done for each preparation method. The standard errors show some variability between the replicate tests for some methods.

Table 5.3: Phase 2a: Intermediate-Temperature Test Results

Source	Test	Preparation Method							
		Method #1 (Control)		Method #2		Method #5		Method #6	
		Avg.	SD	Avg.	SD	Avg.	SD	Avg.	SD
FB1	Shear modulus (kPa)	3,877	266	2,880	565	4,130	201	3,263	47
	Phase angle (°)	44	0	48	3	44	0	47	0
	$G^* \times \sin(\delta)$ (kPa)	2,685	175	2,122	336	2,875	123	2,373	31
FB2	Shear modulus (kPa) Phase angle (°) $G^* \times \sin(\delta)$ (kPa)	No result; machine torque limits were exceeded							
FB3	Shear modulus (kPa)	8,875	215	7,473	971	5,730	120	5,993	387
	Phase angle (°)	32	0	32	0	34	0	35	0
	$G^* \times \sin(\delta)$ (kPa)	4,696	130	3,931	493	3,229	74	3,392	200

FB = Field Binder Avg. = Average; SD = Standard Deviation

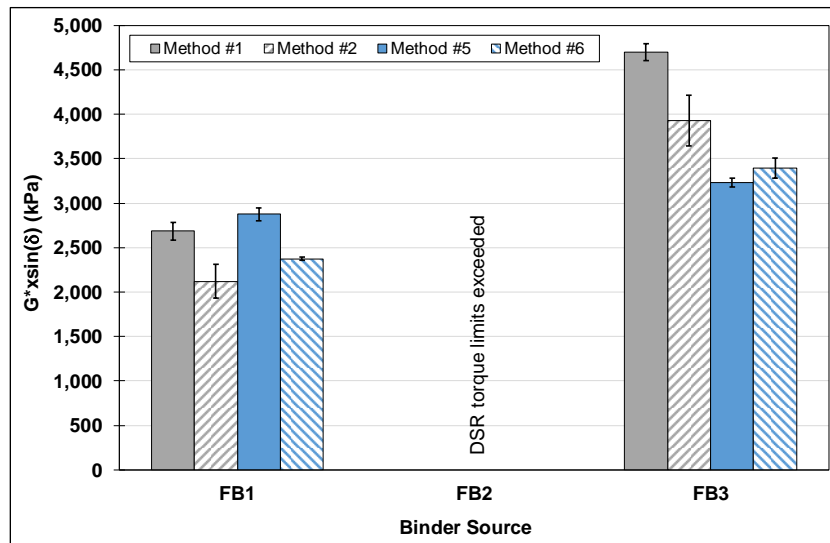


Figure 5.20: Intermediate-temperature ($G^* \times \sin(\delta)$) test results for different PAV preparation methods.

Tests on FB2 could not be completed because the torque limits of the DSR were exceeded as a result of the binder’s very stiff nature at the testing temperature (i.e., the cup twisted in the holder). The results obtained were somewhat inconsistent across the FB1 and FB3 binders. The results for FB3 showed the expected trends, with Methods #1 and #2 having higher $G^* \times \sin(\delta)$ values (i.e., less binder spread unevenly over the pan) than Methods #5 and #6 (i.e., more binder spread evenly over the pan), respectively. The results for FB1 had less variation between the four methods, with no distinct trends. Standard deviations were relatively large in some instances (specifically for Method #2), and if this is taken into consideration along with differences in the degree of rubber particle digestion and distribution of these particles across the pan, then the results appear reasonable. ANOVA results are shown in Table 5.4. The analysis indicated that $G^* \times \sin(\delta)$ measured on samples prepared with the different methods were significantly different at a 95 percent confidence interval (i.e., PAV preparation method influenced the intermediate-temperature results).

Table 5.4: ANOVA Results of $G^* \times \sin(\delta)$ for PAV Preparation Procedures
($\alpha=0.05$)

Parameter	Df	Sum Sq	Mean Sq	F Value	F Critical
Between Groups	3	999,443	333,147	5.564	4.066
Within Groups	8	479,022	59,877	-	-

5.3.5 Preliminary Low-Temperature Test Results

Using the proposed mold configuration discussed in Chapter 6 (Bending Beam Rheometer [BBR] Specimen Preparation Procedures), four sets of BBR specimens, each with three replicates, were fabricated from the same plant-produced binders used for the intermediate-temperature tests. All BBR tests were conducted at -12°C . Test results are provided in Table C.3 in Appendix C and summarized in Table 5.5 and in Figure 5.21 and Figure 5.22. Whiskers on the plots indicate the standard error for the three replicate BBR tests done for each preparation method.

Table 5.5: Phase 2a: Low-Temperature Test Results

Source	Test	Preparation Method							
		Method #1 (Control)		Method #2		Method #5		Method #6	
		Avg.	SD	Avg.	SD	Avg.	SD	Avg.	SD
FB1	Stiffness (MPa)	63.8	3.2	60.4	3.0	67.5	8.8	57.5	9.7
	m-Value	0.365	0.009	0.361	0.002	0.355	0.007	0.371	0.005
FB2	Stiffness (MPa)	39.6	2.5	39.6	2.5	43.0	7.4	56.5	0.5
	m-Value	0.319	0.01	0.319	0.008	0.326	0.005	0.317	0.014
FB3	Stiffness (MPa)	49.7	5.7	44.7	11.2	40.3	8.1	49.0	3.9
	m-Value	0.265	0.02	0.288	0.003	0.305	0.002	0.292	0.008

FB = Field Binder Avg. = Average, SD = Standard Deviation

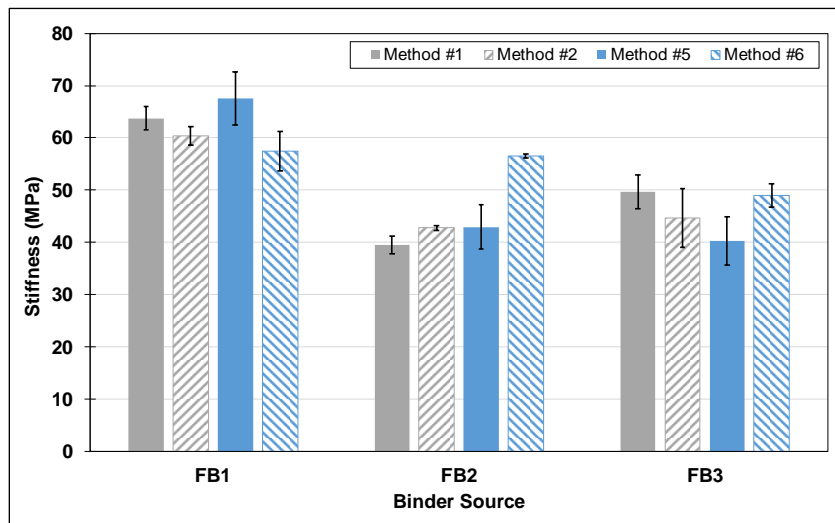


Figure 5.21: Low-temperature stiffness test results for different PAV preparation methods.

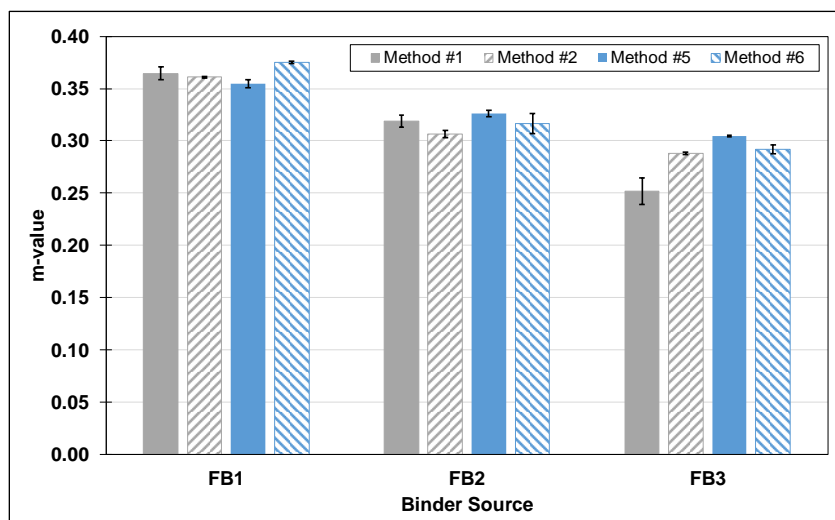


Figure 5.22: Low-temperature m-value test results for different PAV preparation methods.

The results indicate that there was some variability in the stiffness (S) measurements across the four methods and between the replicates tested within each method. The m-value test results were more consistent with less variability among the four methods and between the replicates tested within each method. The reasons for the variability, taking into consideration that only three binders were tested, are the same as those discussed under intermediate-temperature testing.

5.4 Short- and Long-Term Aging Procedure Test Summary

This phase of the study investigated modifications to the AASHTO T 240 RTFO and AASHTO R 28 PAV tests to improve the representability of short- and long-term aging that asphalt rubber binders are subjected to during mix production and during service life. The following modifications were included:

- RTFO testing
 - + Preheating the bottles at 190°C for 10 minutes to improve the uniformity of bottle coating.
 - + Increasing the sample size from 35 g to 45 g to account for the rubber particles, to ensure that the same amount of the base asphalt binder is tested, and to ensure that sufficient binder is available for rheology testing.
 - + Increasing the RTFO test temperature from 163°C to 190°C to better represent rubberized asphalt concrete mix production temperatures.
- PAV sample preparation (Method #5)
 - + Preheating the pans at 190°C for 10 minutes prior to pouring to facilitate more even spread of the binder over the pan to the required thickness.
 - + Increasing the sample size from 50 g to 63 g to account for the rubber particles, to ensure that the same amount of the base asphalt binder is tested, and to ensure that sufficient binder from a single PAV test is available for rheology testing.
 - + Increasing the sample preparation temperature from 163°C to 190°C to be consistent with the temperature of the RTFO-aged binder.

- + Altering the pouring procedure and agitating the pan during pouring to facilitate even spread of the binder over the pan to the required thickness.

A review of the test results generated from this experiment led to the following observations:

- RTFO testing
 - + Complete coating of the bottle was achieved with the larger sample at the higher temperature. Although coating was satisfactory using the smaller sample at the higher temperature, insufficient material was produced for the desired rheology testing. Film thickness on the bottle was relatively even, but marginally thicker than that measured during aging of conventional unmodified binders due to the presence of the incompletely digested rubber particles.
 - + Aging at 190°C increased the shear modulus of the asphalt rubber binder and reduced the phase angle, as expected. The true high temperature PG typically increased by about 6°C, which equates to a one-grade bump. Sample size and extender oil had limited effect on these parameters.
 - + Rubber particle size had a notable effect on all test results, which is consistent with findings from the literature.
 - + The measured carbonyl and sulfoxide indices for unaged and RTFO-aged binders showed clear trends with respect to the effect of aging temperature and sample size, as expected. Ongoing testing will attempt to compare laboratory- and plant-produced binders to determine whether the proposed revised aging procedure is representative of aging conditions during plant production, storage, transport to the project, and placement.
 - + The butadiene index appears to increase with increasing rubber content and could be a useful potential indicator of the level of modification in asphalt rubber binders. This index also changed with increasing RTFO-aging temperature and the larger sample size, which implies that some rubber modification may have continued during aging.
 - + The performance grades of the AR binders were notably higher than the base binder, indicating that the presence of rubber has a significant impact on the test results. It is not clear whether this is a true reflection of likely performance in the field during very high ambient temperatures.
- PAV preparation procedures (Method #5)
 - + Complete coating of the pan was achieved with the 63 g sample, and the average film thickness after pouring and after PAV aging met the requirements listed in AASHTO R 28.
 - + Following this method provides an additional 130 g of aged binder per PAV test compared to following the standard method (i.e., 10 pans of 63 g versus 10 pans of 50 g), which provides sufficient binder for both intermediate-temperature testing (using the concentric cylinder geometry) and low-temperature testing. This is considered to be an important advantage given that one PAV test takes 20 hours, excluding preparation time.
- Preliminary intermediate-temperature DSR testing of PAV-aged binder
 - + No clear trends were observed from the preliminary intermediate-temperature test results on three binders for the different preparation procedures. Only two of the three binders could be tested due to torque limitations of the DSR. The results from one of the binders were consistent with expectations. PAV preparation procedures did not appear to have a significant effect on the test results of the second binder.
- Preliminary low-temperature BBR testing of PAV-aged binder

- + No clear trends were observed from the stiffness testing results on three binders. Little variation between the different PAV preparation methods across the three binders was observed when variations between replicates within each method were considered.
- + The m-value did not appear to be significantly affected by the PAV preparation method.

Although only limited DSR and BBR testing was conducted in this phase of the research, the modifications proposed above are considered to be appropriate in reflecting the original intent and mechanisms of the tests. There is unfortunately no documented procedure to verify the appropriateness of the evaluated procedures given that asphalt rubber binders cannot be effectively extracted and recovered from loose field mixes or core samples removed from highways.

The proposed modifications to the RTFO test were followed in most instances in the testing conducted in the next phases of the research. Assessment of PAV preparation procedures followed both the standard and modified (Method #5) procedures to gather more information before any recommendations towards adopting a modified procedure can be made.

Suggested test method language that covers the proposed modifications to the RTFO testing procedure, as an addendum to AASHTO T 240, is provided in Appendix A. Suggested test method language covering the proposed modifications to the PAV test procedure will be prepared once the modifications have been finalized.

Blank page

6. Phase 2b: BBR SPECIMEN PREPARATION PROCEDURES

6.1 Introduction

Asphalt rubber binders are tested in a bending beam rheometer (BBR) the same way that unmodified binders are tested, although problems have arisen with the preparation of testable asphalt rubber beam specimens with regular dimensions. The standard procedure (AASHTO T 313) requires pouring heated asphalt binder into the 6.25 mm opening of a 127 mm × 12.7 mm × 6.25 mm mold. However, pouring viscous asphalt rubber binders with swollen, incompletely digested rubber particles through this 6.25 mm opening and achieving a consistent specimen that meets the required beam dimensions is very difficult. Common problems include the binder not filling all the corners and trapped air that leads to bubbles inside the specimen (Figure 6.1).

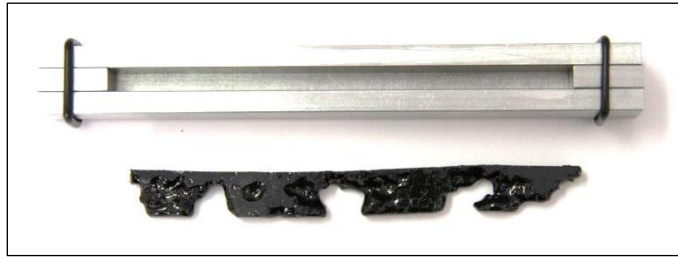


Figure 6.1: Asphalt rubber specimen prepared with conventional BBR mold and method.

A number of deviations from the standard method have reportedly been experimented with, but no formalized procedures have been published. These deviations include:

- Preheating the BBR molds. This has some positive effect on the end result, but could lead to an expansion of the mold that may affect the beam's dimensions.
- Heating the asphalt rubber binder to a higher temperature to make it flow more easily and to ensure uniform flow of the binder inside the mold. This approach has limited effect on the end results and can lead to additional binder aging, which could negatively influence the low-temperature grading of the binder.
- Placing the mold in an oven for five to ten minutes after the binder has been poured to promote uniform flow in the mold. Although reasonable results can be achieved following this process, heating of the mold and additional heating of the binder can lead to expansion of the mold and further aging of the binder. Irregular shaped beams may still result depending on the number and size of the air bubbles after the binder is poured, given that binder consolidation in one area can result in creation of new space in other parts. Topping up the mold with additional binder to fill these spaces is not considered to be appropriate.

6.2 Modified Specimen Mold Configuration

After careful review of the above procedure, changing the mold orientation (i.e., pouring the binder through the wider 12.7 mm opening) was considered to be the most appropriate approach to avoid subjecting the binder to any additional heating. New molds were fabricated to satisfy this pouring orientation (Figure 6.2). This new orientation simplified binder pouring and allowed for easier binder flow into the corners. However, specimen trimming is a little more challenging given the increased trimmed surface area. This is not considered to be a significant issue. A photograph of a beam produced with the modified mold configuration is shown in Figure 6.3.

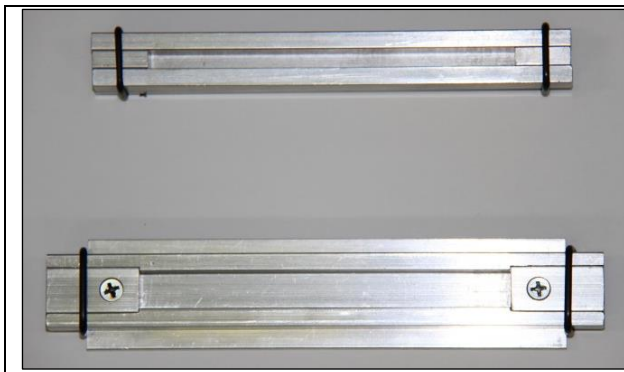


Figure 6.2: Standard (top) and modified (bottom) BBR specimen mold configurations.

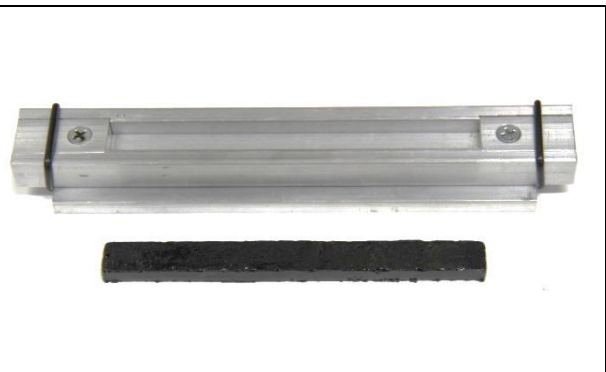


Figure 6.3: Modified mold configuration and beam specimen.

Asphalt rubber beams produced with the modified mold were consistently uniform in shape and dimensions with no visible air bubbles. However, when producing multiple beams from the same binder sample for replicate tests, it was noted that the incompletely digested rubber particles were distributed unevenly among the three molds due to gravitational effects, with a larger percentage of particles dropping into the first mold than into the second and third molds. Some air bubbles were also evident in the third specimen produced, and these were attributed to the binder being more viscous after some cooling at this stage of the process (Figure 6.4).



Figure 6.4: Air pockets noted on third replicate specimen.

Based on the above observations, a single base with three adjacent molds was fabricated (Figure 6.5); this configuration allows for rapid, even pouring of the binder across all three molds. Although some binder is wasted because of overflow during the pouring process, the improved beam specimen consistency outweighed this disadvantage.



Figure 6.5: Modified mold configuration to produce three beam specimens in a single pour.

A series of tests on beams produced with the standard and modified molds using unmodified, polymer-modified, tire-rubber modified, and asphalt rubber binders was carried out to check if there were any differences in the measured results.

6.3 Testing Plan

Table 6.1 summarizes the sampling and testing plan for the materials assessed in this part of the study.

Table 6.1: Phase 2b: Experimental Design Factors and Factorial Levels

Factor	Factorial Level	Details
Mold configuration	2	Standard and modified
Unmodified binder (UM)	3	PG 64-16 (sourced from Refineries #1, #2, and #3)
Polymer-modified binder (PM)	2	PG 64-28M (sourced from Refineries #1 and #2)
Tire rubber-modified binder (TR)	2	PG 64-22M (sourced from Refinery #1)
Asphalt rubber binder (AR)	3	Asphalt plant-produced (APP), modified mold configuration only
Chip seal asphalt rubber binder (CS)	3	Laboratory-produced (LP), modified mold configuration only

The experimental plan included three unmodified (UM) binders, two polymer-modified (PM) binders, two refinery-produced tire rubber-modified (TR, meeting Caltrans PG-M specifications) binders, three asphalt plant-produced (APP) asphalt rubber binders meeting standard Caltrans specifications, and three laboratory-produced (LP) asphalt rubber binders meeting chip seal (CS) binder specifications. Laboratory-produced binders were prepared as described in Section 4.3. All binders were tested according to AASHTO T 313 after first being aged in a rolling thin-film oven (RTFO) and then in a pressurized aging vessel (PAV). Unmodified, polymer-modified, and tire rubber-modified binders were tested at 10°C higher than the low PG limit, while the asphalt rubber binders were tested at 10°C higher than the low PG limit of the base binder. RTFO aging of asphalt rubber binders was done according to the revised method proposed in

Chapter 5 (45-g sample aged at 190°C). PAV aging was conducted according to the standard procedure (i.e., sample size of 50 g) for 20 hours at 100°C and 2.1 MPa pressure. Unmodified, polymer-modified, and tire rubber-modified binders were tested using beams produced in both the standard and modified mold configurations, while asphalt rubber binders were tested using beams produced with the modified single beam mold configuration only.

6.4 Testing Results

Two replicate beams of each binder were tested. Potential variation between the results of replicate asphalt rubber binder specimens produced in the single beam mold was attributed to some unevenness of the top of the beam specimens after trimming caused by inconsistent blade movements as shown in Figure 6.6. It is believed that this problem would be overcome with the use of the three-beam mold, faster pouring, more appropriate trimming-blade selection, and the experience of the individual doing the trimming.

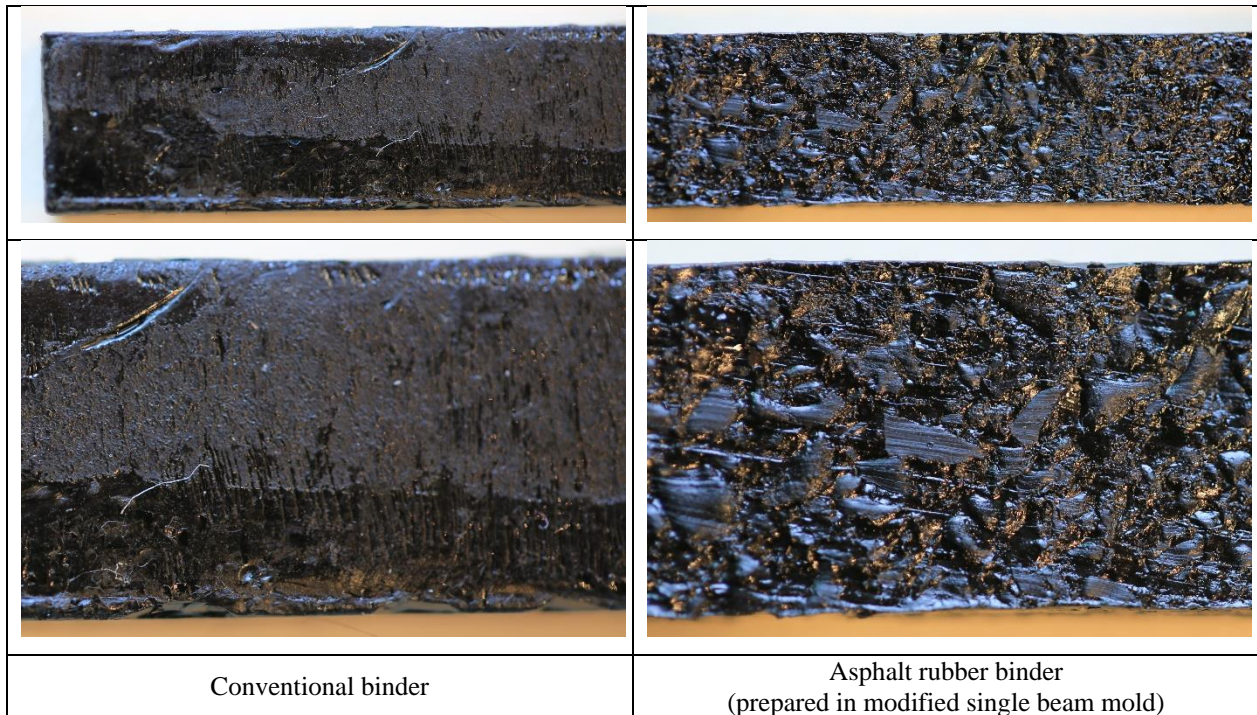


Figure 6.6: Uneven surface of asphalt rubber beam specimen after trimming.

Test results are summarized in Table C.4 in Appendix C. The averages of the creep stiffness and m-value of beams produced with the standard and modified configuration molds are shown in Figure 6.7 and Figure 6.8, respectively. Whiskers on the plots indicate the standard error for the two replicate BBR tests done for each preparation method. The percent difference in the stiffness and m-value was calculated using Equation 6.1 and the results are shown in Figure 6.9.

$$\frac{\text{Modified mold value} - \text{Standard mold value}}{\text{Modified mold value}} \times 100 \quad (6.1)$$

Some variability was apparent between the two test results for each binder. Three of the seven average stiffness results exceeded the listed 7.2 percent limit, while one m-value exceeded the 2.9 percent limit. These observations indicate that the mold configuration used to prepare beam specimens could affect the measured rheological properties of the binder and that the low-temperature PG could change if the modified configuration was used instead of the standard configuration. This was attributed to the inconsistencies on the surface of the specimens discussed above. Improvements in specimen trimming along with new variance limits will be determined in ongoing testing to accommodate these inconsistencies.

Suggested test method language that covers the proposed modifications to the specimen preparation procedures for BBR testing, as an addendum to AASHTO T 313, is provided in Appendix A.

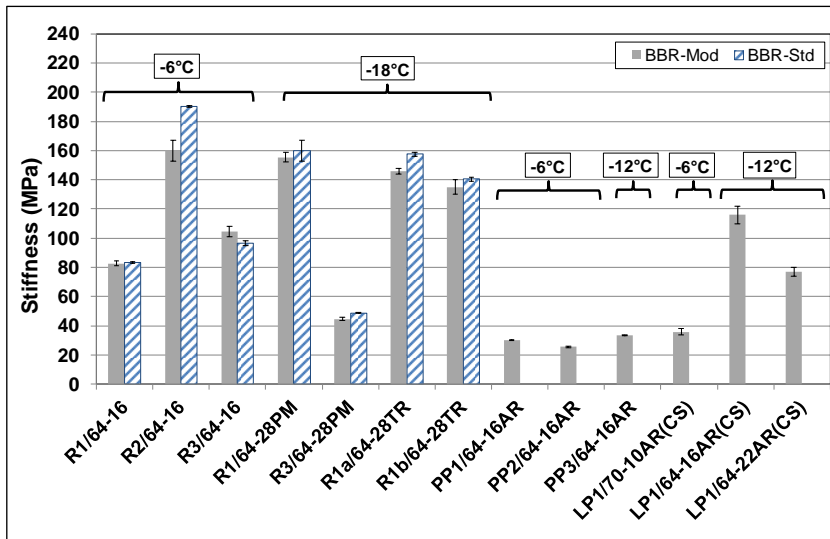


Figure 6.7: BBR specimen preparation mold comparison: Creep stiffness.

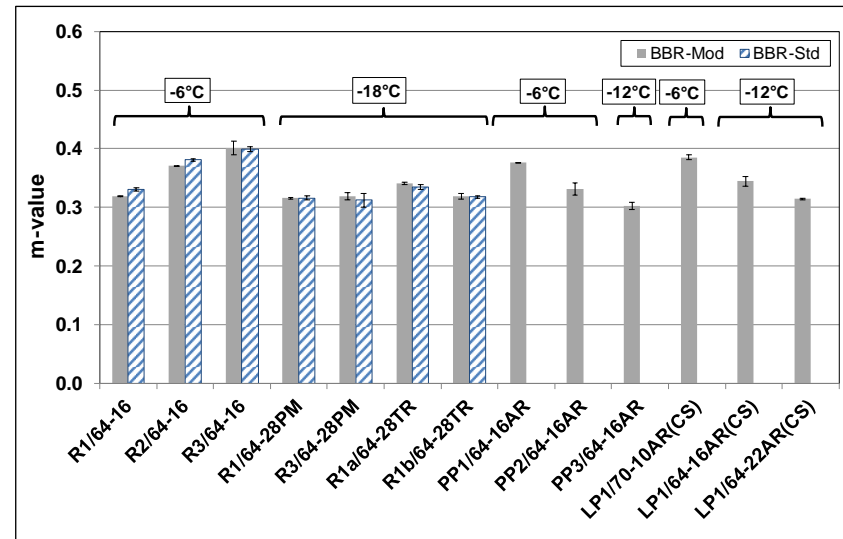


Figure 6.8: BBR specimen preparation mold comparison: m-value.

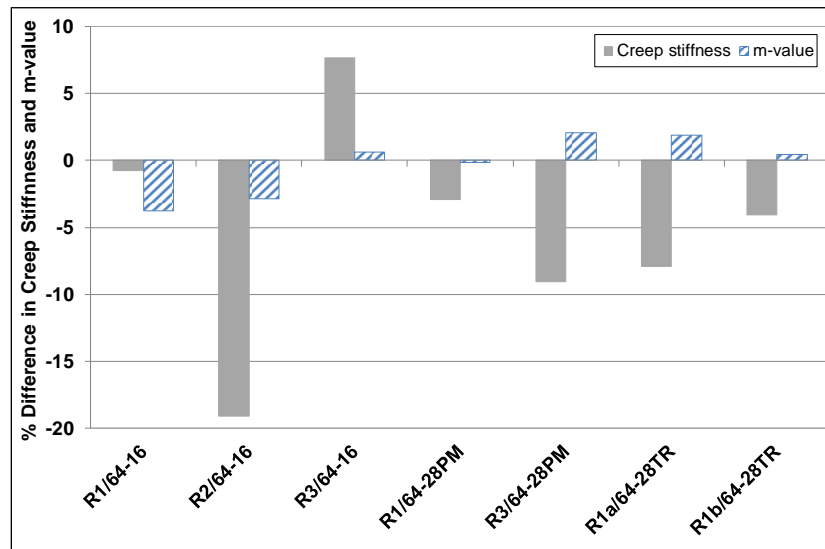


Figure 6.9: BBR specimen preparation mold comparison: Percent difference in results.

7. Phase 2c: INTERMEDIATE-TEMPERATURE TESTING

7.1 Introduction

In addition to testing at high and low temperatures, the Superpave binder grading procedure also requires determination of the intermediate-temperature performance grade (PG) of the binder that has been aged in both the rolling thin film oven (RTFO) and in the pressurized aging vessel (PAV). The intermediate PG of a binder is the temperature at which $G^* \times \sin(\delta)$ is equal to or greater than 5,000 kPa. The standard AASHTO M 320 method specifies dynamic shear rheometer (DSR) testing with a parallel plate geometry with an 8-mm plate diameter and a 2-mm gap between the plates. The smaller plate size allows testing of the much stiffer aged binders without exceeding the testing capabilities of the DSR. The stiffness of aged binders tested at typical intermediate testing temperatures of 15°C through 30°C is usually more than five times that of the RTFO-aged binders tested in the high temperature testing range. Therefore, testing in a 25-mm plate geometry would exceed the capabilities of DSRs typically used for high temperature testing. This smaller plate geometry is not applicable for testing asphalt rubber binders with particle sizes larger than 250 μm for the same reasons that were discussed in earlier chapters. The concentric cylinder geometry (30-mm cup/17-mm bob) used for high temperature testing is also not appropriate for the same reasons that the 25-mm plate geometry cannot be used. Therefore, a different bob size that would give similar results to the 8-mm parallel plate geometry was investigated.

7.2 Testing Geometry

Anton Paar MCR 301 and MCR 302 DSRs were used for preliminary intermediate-temperature testing of binders using the concentric cylinder and parallel plate geometries. Based on discussions with the equipment manufacturers, a 30-mm disposable cup and 10-mm bob concentric cylinder configuration (Figure 7.1) was selected as the setup most likely to be appropriate for the anticipated binder stiffness in the typical intermediate-temperature range. This setup has a 9.5 mm gap between the inside edge of the cup and the outside edge of the bob. The disposable cups used were the same as those used for high-temperature testing. Preliminary dynamic viscosity tests using a Cannon N27e9 standard oil were performed in close collaboration with rheologists from the DSR manufacturer to determine the geometry stress and strain correction factors and testing details, including sample size and location of the bob in the cup. All tests were done at 25°C and results were compared against the specified values provided by Cannon.

Based on the satisfactory results of this preliminary testing, the 30-mm cup/10-mm bob configuration was selected for further testing. Approximately 25 g of unmodified binder and 27 g of asphalt rubber binder is required to fill the cup, slightly more than that used for high-temperature tests (24 g and 26 g, respectively), because of the smaller bob size and associated additional shrinkage/consolidation of the sample during

testing. The same procedure of marking the top level inside the cup used in the high temperature tests is followed for intermediate-temperature tests.



Figure 7.1: Concentric cylinder geometry with 10-mm bob.

Due to the torque limitation of the MCR 301 and MCR 302 DSRs, the lowest temperature at which reliable data could be obtained for asphalt rubber binders was determined to be 16°C. Therefore, the proposed configuration on these DSRs was considered to be suitable for testing in a temperature range between 16°C and 46°C.

7.3 Testing Plan

Table 7.1 summarizes the sampling and testing plan for the materials assessed in this part of the study. The experimental plan included the same three unmodified binders, two polymer-modified binders, and two terminal-produced tire rubber-modified asphalt rubber binders evaluated in previous phases. Three plant-produced asphalt rubber binders from three different asphalt plants and three laboratory-produced asphalt rubber chip seal binders were also tested. The parallel plate gap size was increased to 3 mm. All binders were tested after aging in an RTFO and then in a PAV. For the purposes of this limited preliminary comparison of the two geometries, all binders were tested only at 25°C. Determination of the actual intermediate temperature for each binder was not attempted in this phase of the study. RTFO aging of asphalt rubber binders was done according to the revised method proposed in Chapter 5 (45-g sample aged at 190°C in preheated bottles). PAV aging was conducted according to the standard method (for 20 hours at 100°C

and 2.1 MPa pressure) as the revised procedure discussed in Chapter 5 was still under development at the time of this testing.

Table 7.1: Phase 2c: Experimental Design Factors and Factorial Levels

Factor	Factorial Level	Details
Test temperature	1	25°C
Unmodified binder (UM)	3	PG 64-16 (sourced from Refineries #1, #2 and #3)
Polymer-modified binder (PM)	2	PG 64-28M (sourced from Refineries #1 and #2)
Tire rubber-modified binder (TR)	2	PG 64-28M (sourced from Refineries #2 and #3)
Asphalt rubber binder (AR)	3	Asphalt plant-produced (APP)
Chip seal asphalt rubber binder (CS)	3	Laboratory-produced (LP)

7.4 Testing Results

The test results are summarized in Table C.5 in Appendix C. Shear modulus, phase angle, and $G^* \times \sin(\delta)$ test results from the preliminary testing at 25°C are shown in Figure 7.2 through Figure 7.4. Whiskers on the plots indicate the standard error for the two replicate DSR tests. The percent differences in $G^* \times \sin(\delta)$ between the concentric cylinder and parallel plate geometries, calculated using Equation 7.1 are shown in Figure 7.5.

$$\frac{CC[G^* \times \sin(\delta)] - PP[G^* \times \sin(\delta)]}{CC[G^* \times \sin(\delta)]} \times 100 \quad (7.1)$$

A review of the data led to the following observations:

- Differences in shear modulus values between the two geometries were generally low (between -9 percent [i.e., the concentric cylinder result was 9 percent lower than the parallel plate result] and +15 percent [i.e., the concentric cylinder result was 15 percent higher than the parallel plate result] for binders tested with the 8-mm plate/2-mm gap configuration and between -16 percent and +30 percent for the 8-mm plate/3-mm gap configuration). The concentric cylinder values were slightly higher than the parallel plate values for the unmodified and polymer-modified binders, and slightly lower for the tire rubber-modified binders.
- Differences in phase angle values between the concentric cylinder and 8-mm plate/2-mm gap configuration were generally low (between -5 percent and 0 percent [i.e., the concentric cylinder phase angle was slightly lower than the parallel plate in all instances]). There was a larger difference in the phase angles measured with the concentric cylinder and 8-mm plate/3-mm gap configuration, with values ranging between -9 percent and +16 percent. The chip seal binders showed a larger variation than the asphalt rubber binders.
- Differences in $G^* \times \sin(\delta)$ values (as shown in Figure 7.5) showed the same trends as the shear modulus results, as expected. Differences between the concentric cylinder and 8-mm plate/2-mm gap configuration varied between -12 percent and +12 percent, and between -8 percent and +27 percent for the concentric cylinder and 8-mm plate/3-mm gap configuration. Given that the differences were not consistent across the different binders tested, it is not clear what factors influenced the test results.

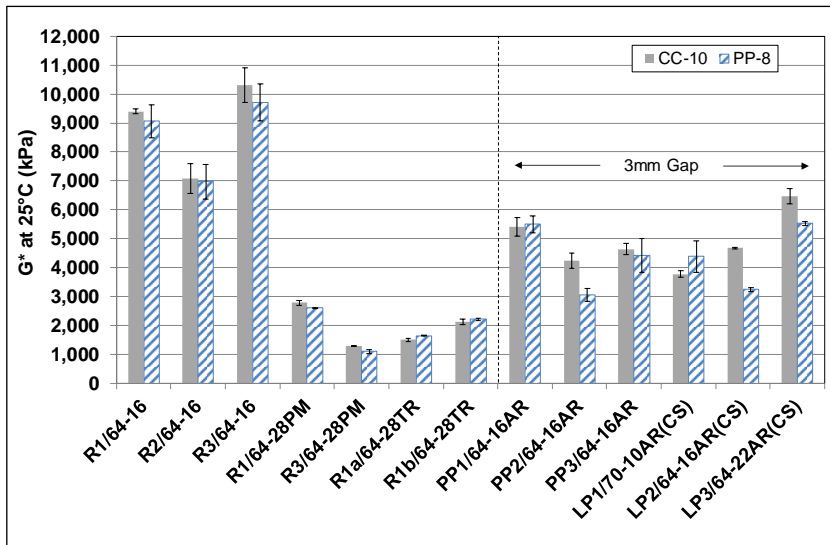


Figure 7.2: Int. temperature: Shear modulus comparison at 25°C.

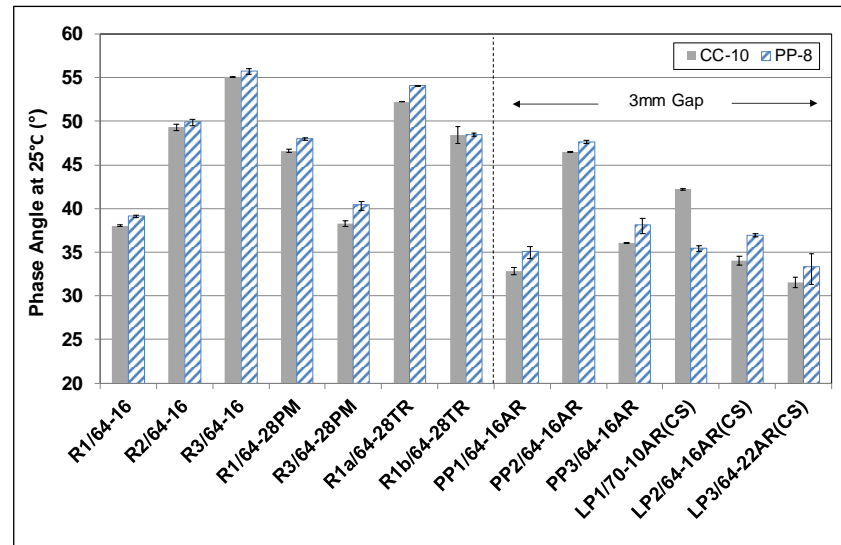


Figure 7.3: Int. temperature: Phase angle comparison at 25°C.

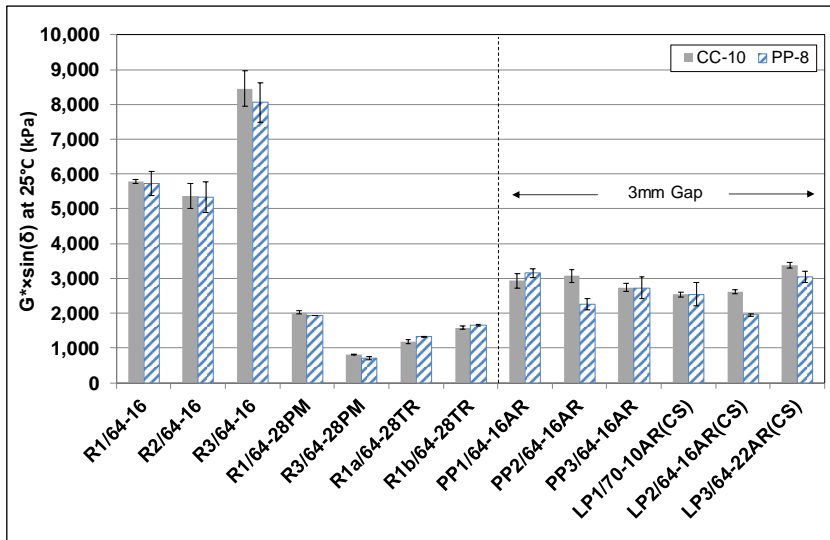


Figure 7.4: Int. temperature: $G^* \times \sin(\delta)$ comparison at 25°C.

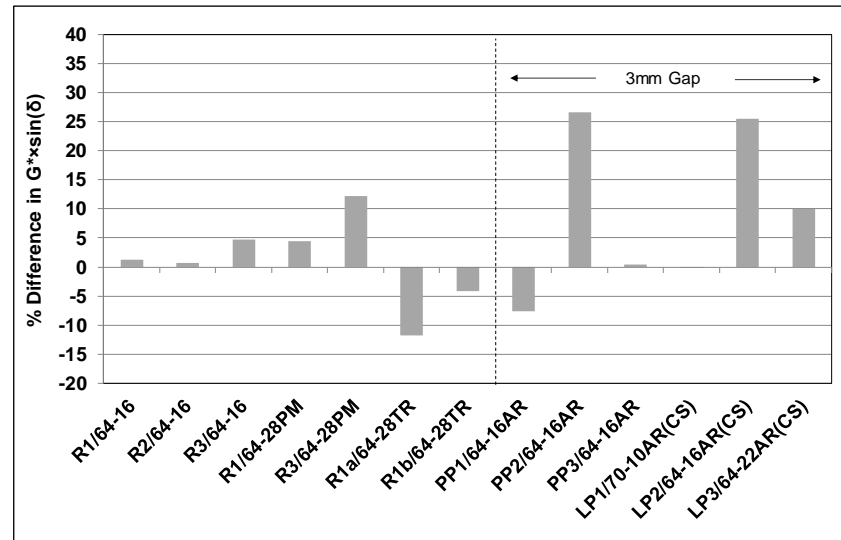


Figure 7.5: Int. temperature: Difference in $G^* \times \sin(\delta)$ between concentric cylinder and parallel plate.

- Concentric cylinder test results on the plant-produced asphalt rubber binders indicated that shear modulus and $G^* \times \sin(\delta)$ values fell between those of the unmodified binders and the polymer and tire rubber-modified binders. The $G^* \times \sin(\delta)$ values at 25°C were considerably lower than the 5,000 kPa threshold, indicating that the intermediate temperatures for asphalt rubber binders are likely to be below 25°C.
- Variability between replicates tested with each geometry was inconsistent across the different binders. Results for the three unmodified base binders had the highest variability between replicates

The results indicate that the concentric cylinder geometry is potentially suitable for testing intermediate temperatures of asphalt rubber binders. However, given that all testing in this phase of the study was conducted at 25°C, the test setup will require more testing with a representative set of asphalt rubber binders to determine whether it is appropriate for determining actual intermediate temperatures. Refinements to the testing geometry (i.e., different bob sizes) and testing procedures will also be investigated during this testing. This testing is planned for Phase 3 of the study.

Blank page

8. Phase 2d: MULTIPLE STRESS CREEP RECOVERY TESTING

8.1 Introduction

The multiple stress creep recovery (MSCR) test is gaining popularity as an alternative to elastic recovery, and toughness/tenacity tests to assess the rutting performance of modified asphalt binders. A number of state transportation agencies now require MSCR testing as part of their PG specifications. A single MSCR test can provide information on both performance and formulation of the asphalt binder.

The MSCR test and specification for unmodified, polymer-modified, and tire rubber-modified binder (AASHTO T 350 and AASHTO M 332) uses a dynamic shear rheometer (DSR) with a 25-mm parallel plate with 1-mm gap configuration to apply creep/recovery cycles of one-second creep followed by nine-second recovery cycles. A stress of 0.1 kPa is applied for the first 10 creep/recovery cycles followed by a stress of 3.2 kPa for an additional 10 cycles. The material response in the MSCR test is significantly different than its response in the standard high-temperature DSR test, in which $G^*/\sin(\delta)$ is measured by applying an oscillating load to the binder at very low strain. The $G^*/\sin(\delta)$ parameter does not accurately represent the ability of modified binders to resist rutting because the polymer networks are insufficiently activated at these low strains. In the MSCR test, the higher levels of applied stress and strain better capture both the stiffening effects of the polymer and the delayed elastic (or recovery) effects. The average percent recovery (APR) and non-recoverable creep compliance (J_{nr}) are reported.

8.2 Testing Plan

Table 8.1 summarizes the sampling and testing plan for the materials assessed in this part of the study. Three tested modified asphalt binders were the same as those used to assess intermediate-temperature testing procedures discussed in Chapter 7 and included two polymer-modified binders, two terminal-produced tire rubber-modified asphalt rubber binders, and three plant-produced asphalt rubber binders.

Table 8.1: Phase 2d: Experimental Design Factors and Factorial Levels

Factor	Factorial Level	Details
Polymer-modified binder (PM)	2	PG 64-28M (sourced from Refineries #1 and #2)
Tire rubber-modified binder (TR)	2	PG 64-28M (sourced from Refineries #2 and #3)
Asphalt rubber binder (AR)	3	Asphalt plant-produced (APP)

All binders were tested using the 30-mm cup/17-mm bob concentric cylinder and 25-mm parallel plate geometry. Conventional binders were tested with a 2-mm parallel plate gap and the asphalt rubber binders were tested with a 3-mm gap. Standard RTFO procedures were used for conventional binders, and the modified procedures (i.e., 45 g sample tested at 190°C discussed in Chapter 5) were followed for the asphalt rubber binders. For the purposes of this limited comparison of the two geometries, all binders were tested

only at 64°C, which is the high-temperature PG of the polymer-modified binders, tire rubber-modified binders and the base binders used to produce the asphalt rubber binders. Determination of the actual average percent recovery and non-recoverable creep compliance is typically done at the actual high-temperature grade and consequently it was accepted that the values for the asphalt rubber binders would not be representative of the actual binder performance.

8.3 Testing Results

Test results are summarized in Table C.6 in Appendix C. Average percent recovery and non-recoverable creep compliance from the preliminary testing at 64°C are shown in Figure 8.1 and Figure 8.2. Whiskers on the plots indicate the standard error for the two replicate DSR tests. The percent differences in average percent recovery and non-recoverable creep compliance (J_{nr}) between the concentric cylinder and parallel plate geometries calculated using Equation 8.1, are shown in Figure 8.3 and Figure 8.4.

$$\frac{CC[J_{nr}] - PP[J_{nr}]}{CC[J_{nr}]} \times 100 \quad (8.1)$$

A review of the data led to the following observations:

- The average percent recovery varied among the binders, but similar trends were observed in terms of the differences between the recovery at 0.1 kPa and 3.2 kPa. The differences in results between the two stress levels for asphalt rubber binders from Plant #1 and Plant #3 were higher than the other binders.
- The percent difference in average percent recovery at 0.1 kPa between the concentric cylinder and parallel plate geometries for the polymer-modified and tire rubber-modified binders was small (between zero and 4 percent), with the concentric cylinder geometry recording slightly higher recoveries than the parallel plate geometry. The difference was slightly larger for the tests at 3.2 kPa (between zero and 14 percent), but the trends were the same.
- Variability in average percent recovery between replicates of the same sample was very small.
- The difference in recovery between the two geometries for the asphalt rubber binders was considerably larger than the other binders, and in all but one instance, the recoveries recorded with the parallel plate geometry were higher than those recorded with the concentric cylinder geometry. It is not clear whether the differences were related to the degree of digestion of the rubber particles or to the 3-mm parallel gap being inappropriate to accurately measure creep recovery.
- The non-recoverable creep compliance varied considerably across the different binders. Creep compliance at 3.2 kPa was higher than that at 0.1 kPa for all binders, as expected.
- There were large differences in the non-recoverable creep compliances of the two polymer-modified binders and also between the two tire rubber-modified binders. Two of the asphalt rubber binders had very low compliances compared to the third asphalt rubber binder and the polymer-modified and tire rubber-modified binders.

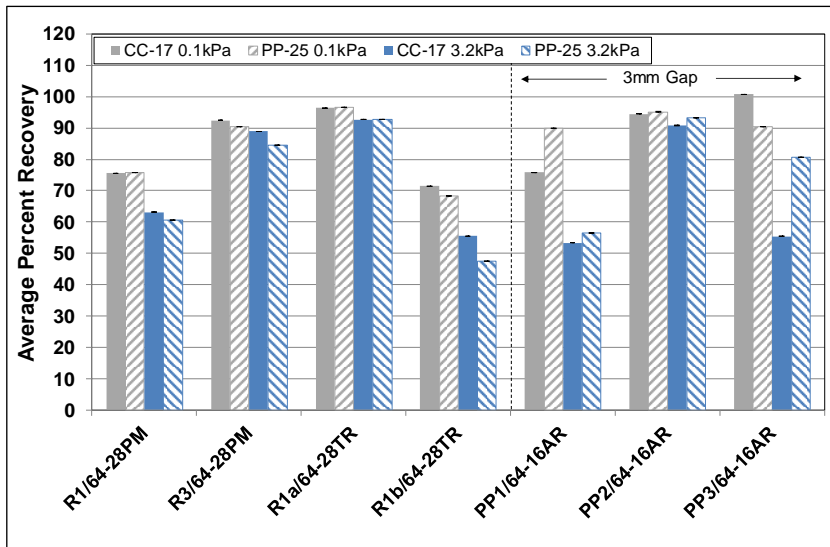


Figure 8.1: MSCR: Average percent recovery at 64°C.

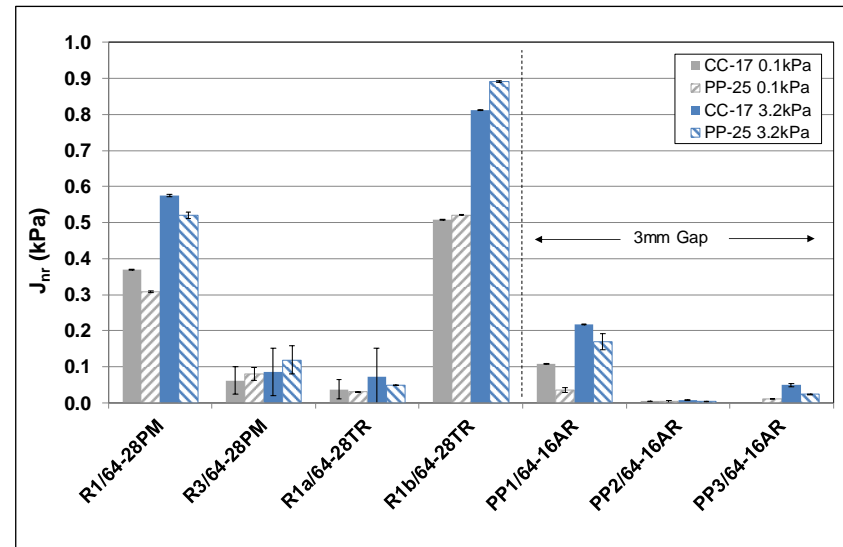


Figure 8.2: MSCR: Non-recoverable creep compliance at 64°C.

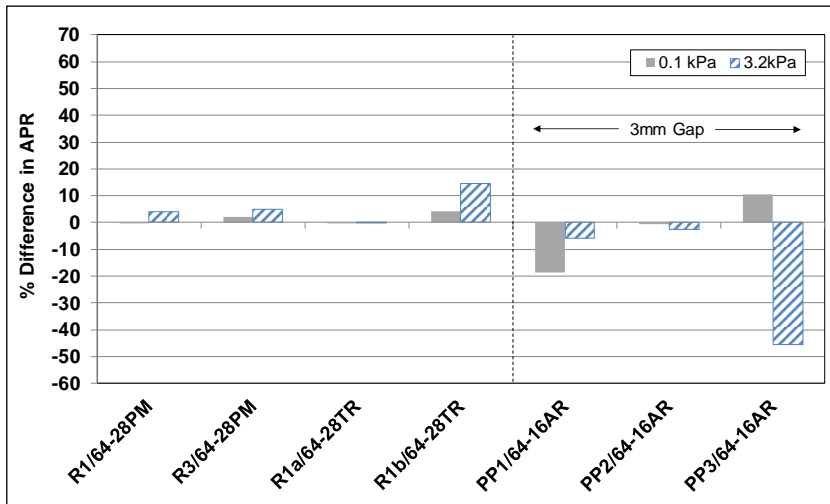


Figure 8.3: MSCR: Percent difference in APR between concentric cylinder and parallel plate.

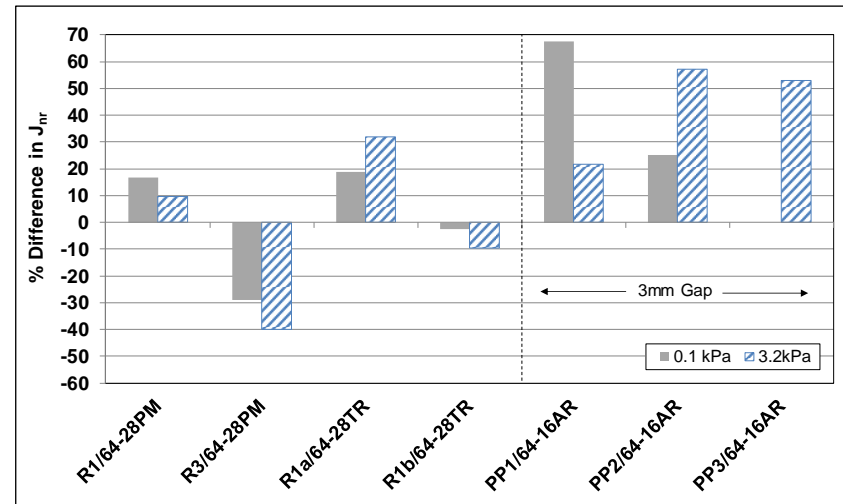


Figure 8.4: MSCR: Percent difference in J_{nr} between concentric cylinder and parallel plate.

- Variability in non-recoverable creep compliance between replicates of the same sample differed between binders. There was considerable variability between replicates in one of the polymer-modified and one of the tire rubber-modified binders.
- The percent difference in non-recoverable creep compliance between the two geometries also varied considerably with no clear trends.

Based on these observations, it is clear that additional testing is required before any conclusions on the appropriateness of using the concentric cylinder geometry for testing multiple stress creep compliance can be drawn. This evaluation will continue in Phase 3 when field binders are tested.

9. Phase 2e: RHEOLOGY TESTING OF PLANT-PRODUCED BINDERS

9.1 Introduction

This chapter covers preliminary rheological testing to determine the high-, intermediate-, and low-temperature performance grades of three plant-produced asphalt rubber binders using the proposed testing procedures discussed in Chapters 4 through 8. Further testing on up to 30 plant-produced binders that will be collected during the 2019 and 2020 paving seasons is planned for Phase 3 of this study.

9.2 Testing Plan

The experimental plan included three plant-produced asphalt rubber binders produced at asphalt plants supplying gap-graded rubberized hot mix asphalt (RHMA-G) mixes for overlay projects on three different California highways: SOL-680, CAL-26, and SB-154. Samples of crumb rubber, base binder, asphalt rubber binder, and loose mix samples were collected.

Crumb rubber samples were subjected to a grading analysis to check maximum particle size and particle size distribution against Caltrans specifications. Base binder PG was verified. High- and intermediate-temperature tests were conducted on the three plant-produced binders using both concentric cylinder and 25-mm parallel plate with 3-mm gap geometries. Short- and long-term aging were carried out according to the revised methods discussed in Chapter 5. Specimens for the low-temperature tests were fabricated using the modified mold configuration discussed in Chapter 6. Multiple stress creep recovery tests were not conducted on these materials given that further development of the testing procedure was deemed necessary (as discussed in Chapter 8).

9.3 Crumb Rubber Particle Size Distribution

Samples of waste tire rubber and high natural rubber were collected from two of the three projects (CAL-26 and SB-154). Scrap tire and high natural rubber gradations were both checked to confirm that they met Caltrans specifications. Samples were mixed in a ratio of 75 percent waste tire rubber to 25 percent high natural rubber, in line with Caltrans specifications. The gradation of the combined sample was then checked for reasonableness (Caltrans specifications do not require a gradation of the combined rubber). The results are summarized in Table 9.1.

Table 9.1: Phase 2e: Rubber Particle Gradations used in Plant-Produced Binders

Sieve Size		% Passing		
(mm)	(US)	SOL-680	CAL-26	SB-154
2.36	#8	Not tested	100	100
2.00	#10		99.2	99.4
1.18	#16		72.5	71.1
0.600	#30		41.2	38.2
0.300	#50		11.1	12.4
0.150	#100		1.9	2.6
0.075	#200		0.0	0.1

9.4 High-Temperature Testing

Results of the high-temperature grade tests on the three binders are listed in Table C.7 through Table C.12 in Appendix C and summarized in Table 9.2. Plots of the test results are shown in Figure 9.1 through Figure 9.9. In Figure 9.1, bars on the true grade data indicate the range (highest and lowest) of temperatures measured across the three replicate specimens tested. The whiskers shown in Figure 9.2 through Figure 9.4 and Figure 9.6 through Figure 9.8 show the variability (standard error) between replicate tests of the same binder sample. The percent difference in $G^*/\sin(\delta)$ between the concentric cylinder and parallel plate geometries, calculated using the formula in Equation 3.2, are shown in Figure 9.5 and Figure 9.9 for unaged and RTFO-aged samples, respectively. Only those temperatures with measurements from both geometries are shown.

Table 9.2: Phase 2e: High-Temperature Grade and True Grade Results

Source	Base Binder	Concentric Cylinder (°C)			Parallel Plate with 3-mm Gap (°C)		
		High PG	True Grade		High PG	True Grade	
			Mean	Std. Dev.		Mean	Std. Dev.
SOL-680	64	88	91.3	1.0	88	92.4	0.4
CAL-26	64	94	94.9	0.4	94	98.1	1.5
SB-154	64	88	93.3	0.3	94	100.9	3.1

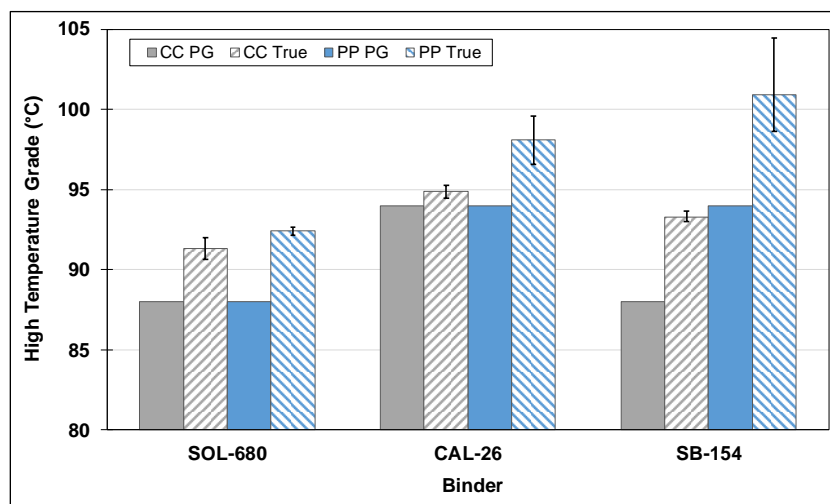


Figure 9.1: High-temperature grade and true grade results.

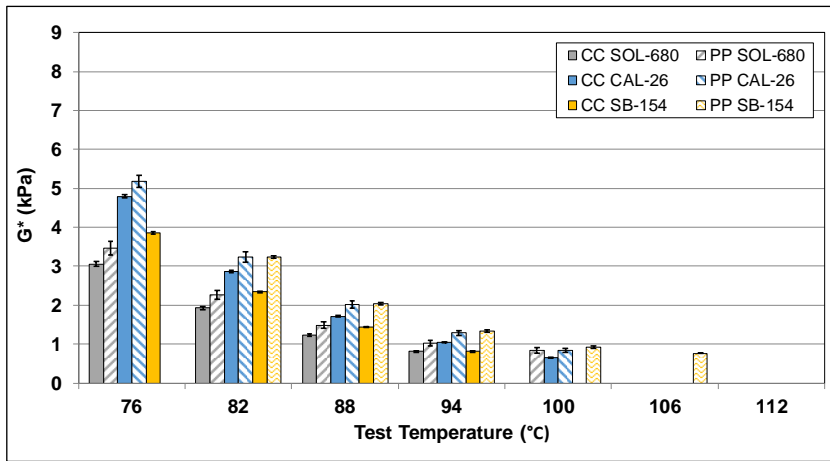


Figure 9.2: High temperature (unaged): Shear modulus.

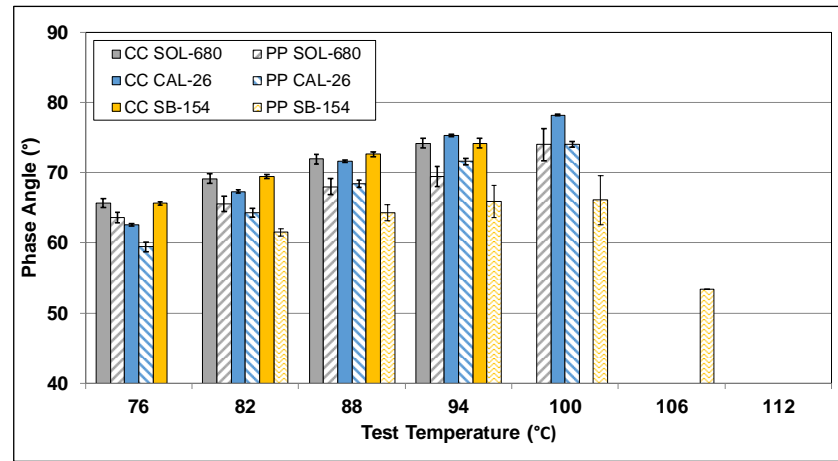


Figure 9.3: High temperature (unaged): Phase angle.

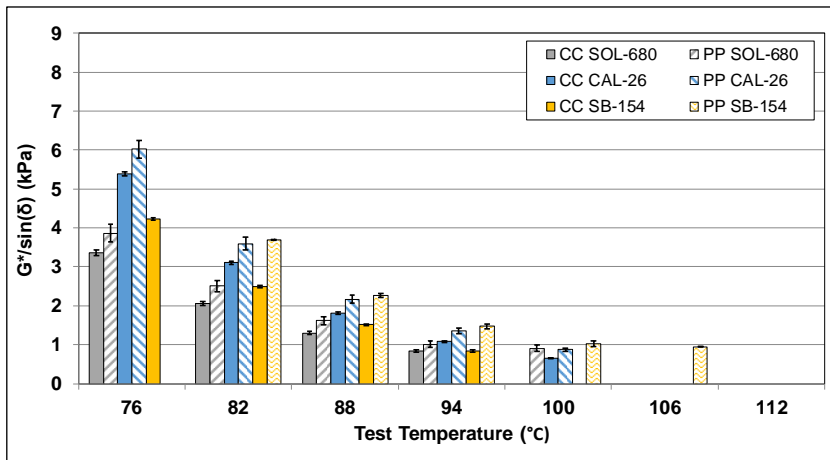


Figure 9.4: High temperature (unaged): $G^*/\sin(\delta)$.

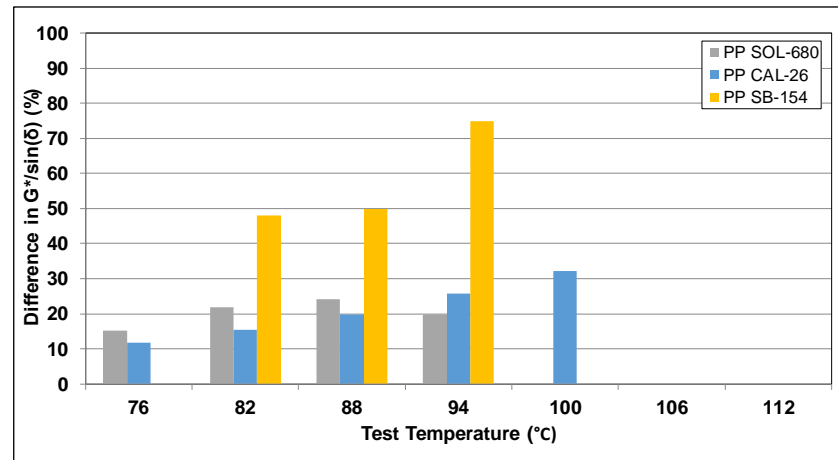


Figure 9.5: High temperature (unaged): Difference between concentric cylinder and parallel plate.

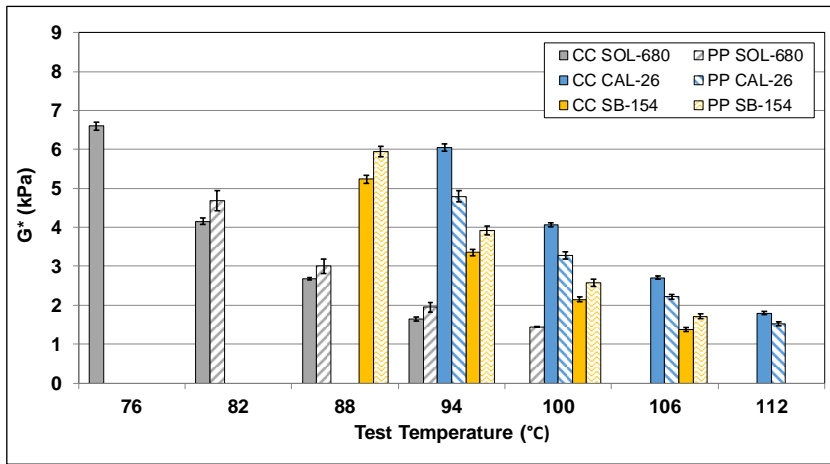


Figure 9.6: High temperature (RTFO-aged): Shear modulus.

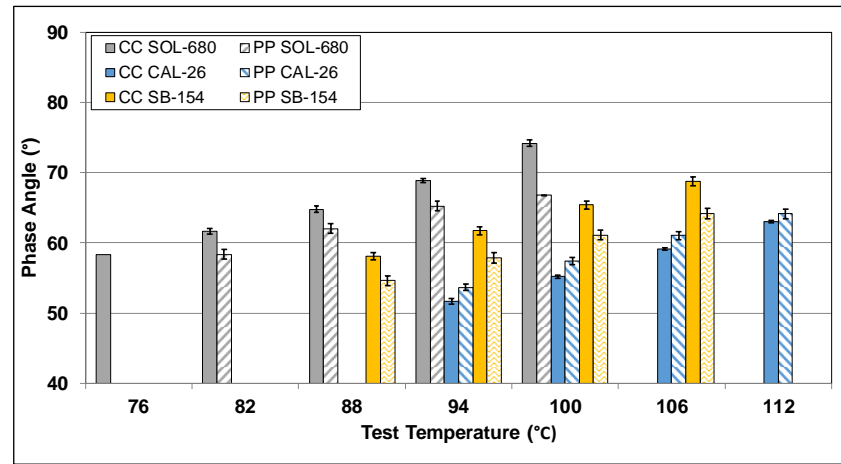


Figure 9.7: High temperature (RTFO-aged): Phase angle.

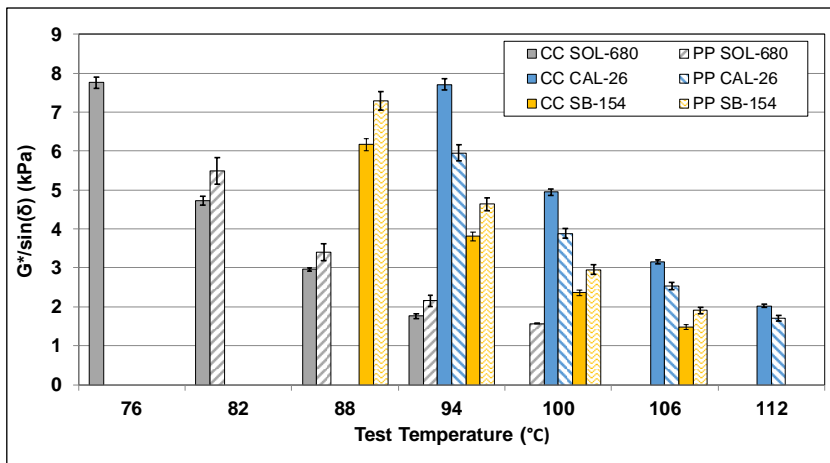


Figure 9.8: High temperature (RTFO-aged): $G^*/\sin(\delta)$.

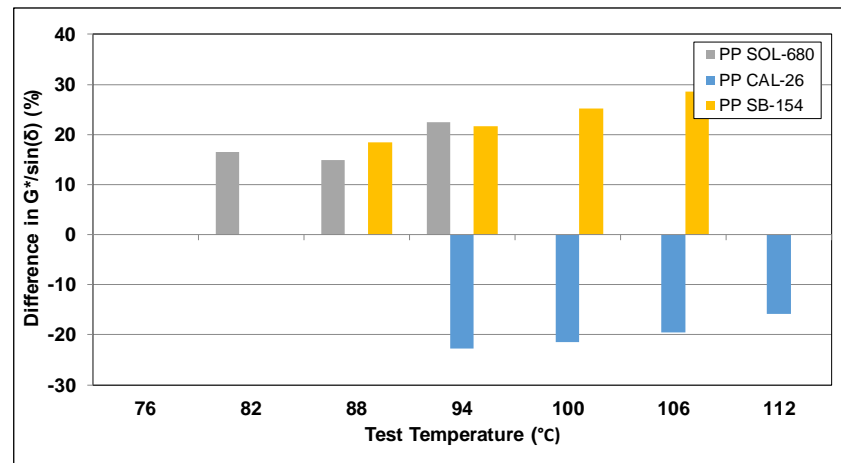


Figure 9.9: High temperature (RTFO-aged): Difference between concentric cylinder and parallel plate.

A review of the data led to the following observations:

- Concentric cylinder
 - + An increase of four grades higher than the base binder was recorded for two of the asphalt rubber binders (SOL-680 and SB-154) and an increase of five grades was recorded for the third (CAL-26).
 - + Mean true grade results show that all three asphalt rubber binders were relatively close and fell in a range between 91°C and 95°C.
 - + Variation in the results from the three replicates in each test was small.
 - + The incompletely digested rubber particles clearly had a significant influence on the results when compared to the base binder.
 - + All results were higher than the maximum grade of 82°C listed in the AASHTO M 320 standard.
- Parallel plate geometry
 - + The same grade increases recorded for the tests with the concentric cylinder were observed for the tests with the parallel plate geometry.
 - + The mean true grade results for all three asphalt rubber binders were relatively close and fell in a range between 92°C and 105°C, a range approximately 7°C higher than the concentric cylinder measurements.
 - + Variation in the results for the three replicates of each asphalt rubber binder tested with the parallel plate geometry was notably larger than the variation recorded when testing with the concentric cylinder.
- Difference between concentric cylinder and parallel plate
 - + Figure 9.5 shows that the $G^*/\sin(\delta)$ values of unaged samples measured with the parallel plate geometry were consistently higher than those determined in the concentric cylinder geometry. Different trends among the different binders were also apparent (i.e., the difference between the two geometries was much higher for the SB-154 binder when compared to the SOL-680 and CAL-26 binders).
 - + For the RTFO-aged binders, $G^*/\sin(\delta)$ values determined with the parallel plate geometry were again considerably higher than those determined with the concentric cylinder geometry for the SOL-680 and SB-154 binders (Figure 9.9). However, values determined with the concentric cylinder geometry were consistently higher than those determined using the parallel plate geometry for the CAL-26 binders.

9.5 Intermediate-Temperature Testing

Results of the intermediate-temperature grade tests cannot be reported until completion of further testing to refine the concentric cylinder testing approach. Further analysis will be done after testing in the planned third phase of this study during which a larger number of plant-produced binders will be assessed.

9.6 Low-Temperature Testing

Results of the low-temperature grade tests on the three asphalt rubber binders are listed in Table C.13 in Appendix C and summarized in Table 9.3. Plots of the test results are shown in Figure 9.10 and Figure 9.11.

Table 9.3: Phase 2e: Low-Temperature Grade Results

Source	Base Binder	Bending Beam Rheometer (°C)		
		Low PG	True Grade	
			Mean	Std. Dev.
SOL-680	-16	-28	-30.5	2.3
CAL-26	-16	-22	-24.5	0.9
SB-154	-16	-16	-18.6	1.5

A review of the data led to the following observations:

- Stiffness values were well below the AASHTO M 320 criteria for determining the low-temperature grade (i.e., $S \leq 300$ MPa) and consequently grades were dictated by the m-value (i.e., m-value ≥ 0.30). The presence of incompletely digested rubber particles probably contributed to the lower stiffness values.
- The acceptable ranges between two test results for the same unmodified binder as listed in AASHTO T 313 (7.2 percent for stiffness and 2.9 percent for m-value) were exceeded in most instances. These larger differences between results were attributed in part to the rougher beam surfaces after trimming and to variation in the number, size, and degree of digestion of the rubber particles in each beam. Revised acceptance ranges for asphalt rubber binders will be suggested, if appropriate, after completion of further testing on additional plant-produced binders in Phase 3.
- The AASHTO M 320 procedure contains no recommendations for asphalt rubber binders. The minimum low-temperature grade in the standard table for conventional binders with a high-temperature grade equal to or greater than 76°C is -22°C, which was achieved for the SOL-680 (changed from -16°C to -28°C after modification) and CAL-26 (changed from -16°C to -22°C) asphalt rubber binders. The SB-154 binder low-temperature grade did not differ from that of the base binder.
- Other factors that may influence results, and specifically the variability, which may require further investigation, include whether changes in the properties of the incompletely digested rubber particles occur at very low temperatures (i.e., in the range of glass transition), whether different rubber type (e.g., synthetic versus natural rubber) have different coefficients of thermal expansion, and whether the properties of the rubber particles are in any way effected by the type of temperature control medium used in the BBR (i.e., ethanol for the testing discussed in this report).

9.7 Performance Grade Summary

The performance grades of the three asphalt rubber binders tested in this experiment are summarized in Table 9.4. Testing with both geometries provided the same high-temperature grade despite the noted variability in test results discussed above.

Table 9.4: Phase 2e: Performance Grade Summary

Source	Base Binder	Concentric Cylinder	Parallel Plate
SOL-680	64-16	88-28	88-28
CAL-26	64-16	94-22	94-22
SB-154	64-16	88-16	88-16

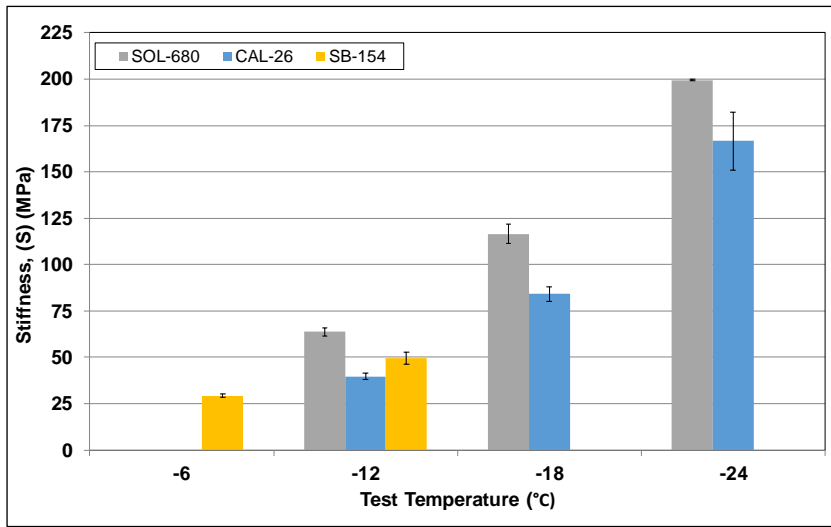


Figure 9.10: Low temperature: Creep stiffness.

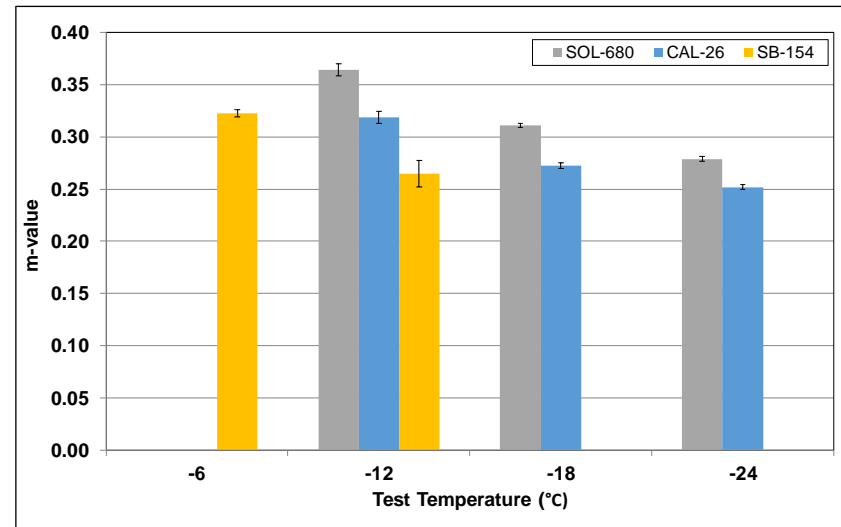


Figure 9.11: Low temperature: m-value.

9.8 Effect of Incompletely Digested Rubber Particles on Performance Grading

9.8.1 Introduction

Asphalt rubber binders typically contain visible, incompletely digested rubber particles. In gap- or open-graded mixes, these particles are unlikely to coat the aggregates, but will instead be squeezed into the gaps as part of the mastic between the aggregates. Given that these incompletely digested particles appear to dominate rheology test results, considering them as part of a homogenous binder may not be appropriate when determining performance grades. The results discussed in the previous chapters also indicate that the presence of these particles likely contributes to higher variability in the measured properties.

A small study was therefore conducted to determine the extent to which these incompletely digested particles might affect performance grading results. This was achieved by comparing results from the three plant-produced asphalt rubber binders discussed in Section 9.4 with results produced using the same binders but with particles larger than 300 μm ($> \#50$ sieve) removed by sieving. Preliminary testing was limited to high-temperature grading only. Sieved binders were tested using a 25-mm parallel plate geometry with a 2-mm gap according to the standard AASHTO T 315 method, while the unsieved binders were tested in the concentric cylinder geometry. Results for high-temperature grade, percent difference in $G^*/\sin(\delta)$, and correlation between true high temperature grade are shown in Figure 9.12, Figure 9.13, and Figure 9.14, respectively. The percent difference was calculated using the formula in Equation 9.1.

$$\frac{\text{Unsieved}[G^*/\sin(\delta)] - \text{Sieved}[G^*/\sin(\delta)]}{\text{Unsieved}[G^*/\sin(\delta)]} \times 100 \quad (9.1)$$

A review of the data led to the following observations:

- The high-temperature performance grades of the sieved binders were consistently two grades lower than those determined for the unsieved binders, indicating that the incompletely digested particles had a significant influence on the test results.
- The percent decrease in $G^*/\sin(\delta)$ between the sieved with the unsieved binders was significant.
- The correlation between the true high temperatures of the binders tested with both geometries was strong, indicating that testing sieved binders in a standard parallel plate geometry may be an appropriate alternative to testing unsieved binders in the concentric cylinder geometry.

Given that the variability of incompletely digested rubber particles in asphalt rubber binder samples leads to considerable variability in high-, intermediate-, and low-temperature test results, testing sieved binders may be a more appropriate approach to performance grade testing of these binders. This approach could also be used to develop a relationship between test results from unsieved and sieved binders as a means to determine representative performance grades for asphalt rubber binders. Sieved asphalt rubber binders will therefore be included as part of the scheduled testing of additional plant-produced binders in Phase 3 of this study.

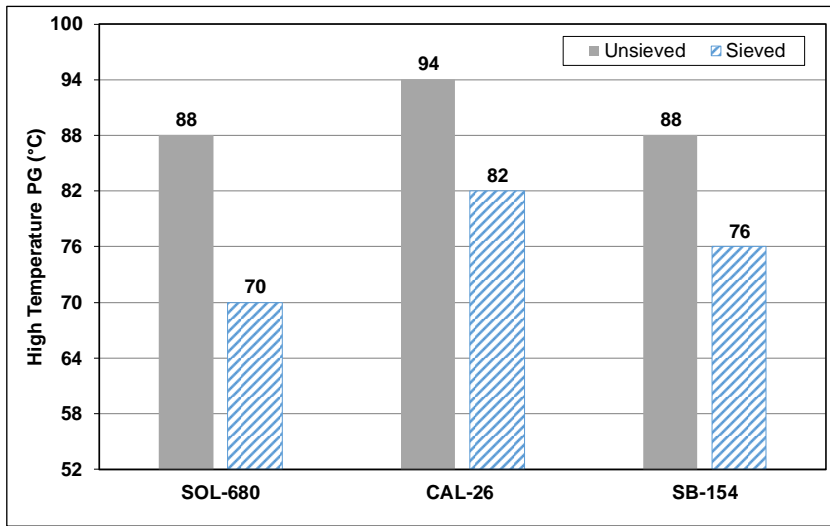


Figure 9.12: Unsieved vs. sieved: High temperature performance grade.

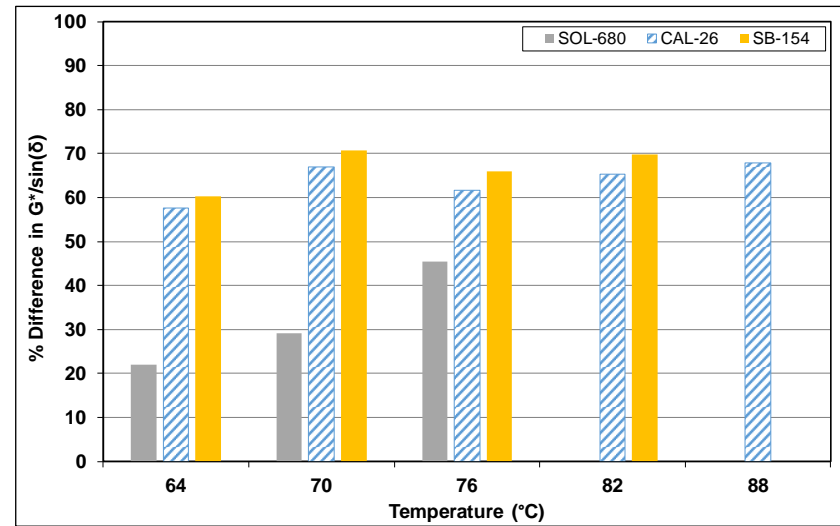


Figure 9.13: Unsieved vs. sieved: Percent difference in $G^*/\sin(\delta)$.

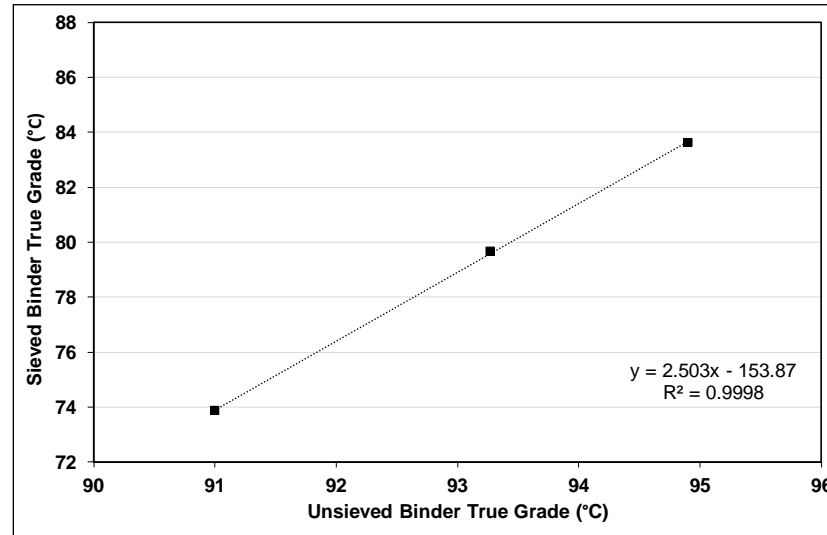


Figure 9.14: Unsieved vs. sieved: Correlation between true performance grade.

Blank page

10. Phase 2f: TESTING OF PLANT-PRODUCED RHMA-G MIXES

10.1 Introduction

This chapter presents preliminary mix testing to develop a database of stiffness, permanent deformation, and cracking properties against which binder properties can be assessed. These comparisons will ultimately be used to determine whether the performance grades determined from the binder testing are representative of actual expected mix performance or whether they need to be adjusted. Additional asphalt rubber binders will be collected in the 2019 and 2020 paving seasons from at least 25 projects. Loose mixes will be collected from five of these projects for mix testing. Selection of projects will be based on location to ensure good aggregate, binder, and asphalt plant representation.

10.2 Testing Plan

10.2.1 Materials

Loose gap-graded rubber hot mix asphalt (RHMA-G) mix was sampled from the same three field projects listed in Section 9.2, namely; SOL-680, CAL-26, and SB-154.

10.2.2 Testing Program

Table 10.1 lists the test methods and brief details about the test parameters used to conduct performance-related testing on the three RHMA-G mixes sampled from the three projects.

Table 10.1: Phase 2f: Tests Performed on Plant-Produced Mixes

Test	Replicates	Air Voids (%) ¹	Test Variables
<u>Stiffness</u> <ul style="list-style-type: none"> Dynamic modulus - AASHTO T 378 	3	7.0 ± 1.0	<ul style="list-style-type: none"> 1 temperature sequence (4, 20, 45°C) 1 stress level¹ No confining pressure
<u>Stiffness</u> <ul style="list-style-type: none"> Beam flexural frequency sweep - AASHTO T 321 	2	7.0 ± 1.0	<ul style="list-style-type: none"> 3 temperatures (10, 20, 30°C) 2 strain levels (100 µstrain at 10 and 20°C; 200 µstrain at 30°C)
<u>Rutting Performance</u> <ul style="list-style-type: none"> Flow number from repeated load triaxial results - AASHTO T 378 	3	7.0 ± 1.0	<ul style="list-style-type: none"> 1 temperature (52°C) 1 deviator stress (600 kPa [87 psi])² 1 contact stress (30 kPa [4 psi]) No confining pressure
<u>Cracking Performance</u> <ul style="list-style-type: none"> Beam fatigue - AASHTO T 321 	3	7.0 ± 1.0	<ul style="list-style-type: none"> 1 temperature (20°C) 3 strain ranges (high, medium, low) based on the mix stiffness 1 frequency (10 Hz)
<u>Cracking Performance</u> <ul style="list-style-type: none"> Semicircular Beam (SCB) test - AASHTO TP 124 	3	7.0 ± 1.0	<ul style="list-style-type: none"> 1 temperature (25°C)
¹ Based on saturated surface-dry bulk specific gravity ² Deviator stress controlled by AMPT software to get 75 to 125 µstrain peak-to-peak axial strain.			

10.2.3 Specimen Preparation

Specimen preparation details for the different tests were as follows:

- Asphalt Mix Performance Tester (AMPT) tests were conducted on specimens with 100 mm (4 in.) diameter and 150 mm (6 in.) height, cored from 150 mm and 175 mm gyratory-compacted specimens.
- Beam fatigue specimens were cut from ingots compacted with a steel-wheel roller to target air-void contents of 7.0 ± 1.0 percent. The beams were 380 mm (15 in.) in length, 50 mm (2 in.) in height, and 63 mm (2.5 in.) in width.
- Semicircular bend (SCB) specimens were cut from gyratory-compacted specimens with 150 mm (6 in.) diameter and 175 mm (7 in.) height. Two 50-mm (2-in.) thick discs were cut from the compacted specimen, from which four SCB specimens were cut. A 15 mm \times 1.5 mm notch was cut into each SCB specimen.

10.3 Specimen Air-Void Contents

Air-void contents were determined according to AASHTO T 269. Bulk specific gravity was determined using both saturated surface-dry (AASHTO T 166) and automatic vacuum sealing methods (AASHTO T 331). Air-void contents (based on saturated surface-dry bulk specific gravity) for the specimens compacted in a Superpave gyratory compactor (cylindrical AMPT and SCB specimens) and with a rolling-wheel compactor (beam specimens) are listed in Table C.14 and Table C.15, respectively in Appendix C. Averages and standard deviations are shown in Figure 10.1 and Figure 10.2, respectively. Whiskers on the data show the lowest and highest air-void contents of the three replicates. All specimens were within the target limits (7.0 ± 1.0 percent) and there was little variation between specimens, indicating that consistent compaction was achieved. Any potential influences of air-void content were considered during analysis of the results.

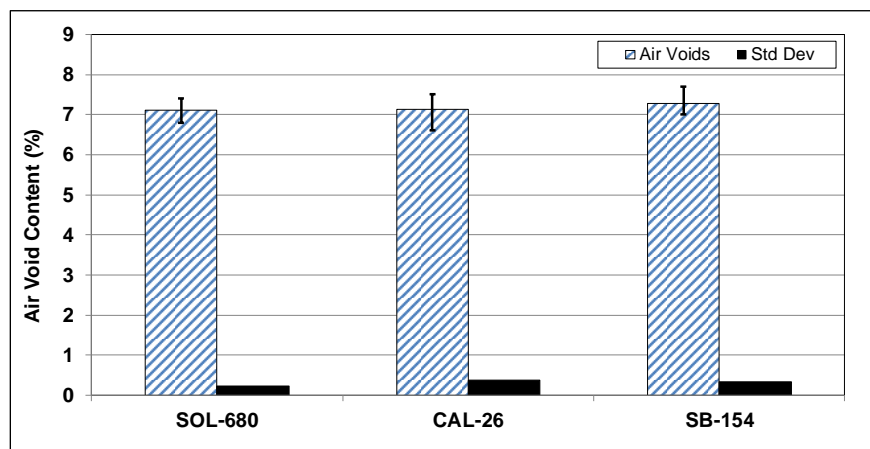


Figure 10.1: Air-void contents of gyratory-compacted specimens.

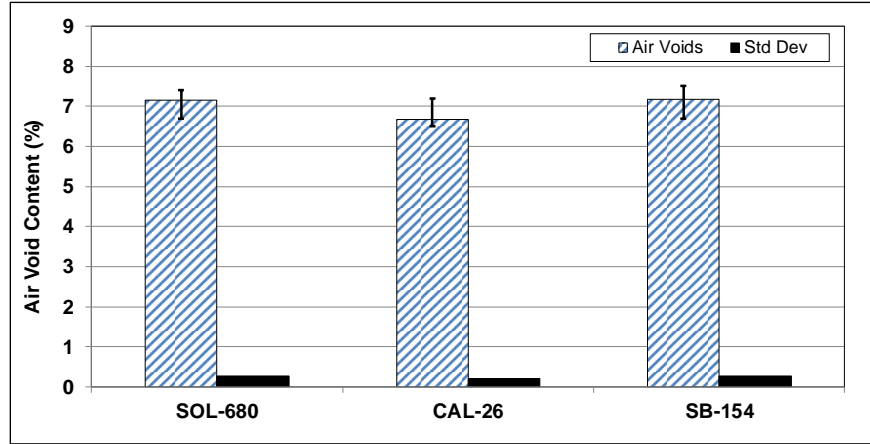


Figure 10.2: Air-void contents of rolling wheel-compacted specimens.

10.4 Mix Stiffness: AMPT Dynamic Modulus

Tests to determine dynamic modulus (E^*) and phase angle of the RHMA-G mixes were performed using an AMPT at 10 Hz, 1 Hz, and 0.1 Hz when testing at 4°C and 20°C (39°F and 68°F) and at 10 Hz, 1 Hz, 0.1 Hz, and 0.01 Hz when testing at 45°C (113°F). In this test, the specimen is subjected to a haversine axial-compressive load with fixed amplitude under controlled-strain conditions. The axial deformation of the specimen during cyclic loading is measured using three linear variable displacement transducers (LVDTs) mounted around the specimen 120° apart. The dynamic modulus is calculated by dividing the peak stress (σ_{\max}) by the peak strain (ϵ_{\max}) during each loading cycle. Three replicate specimens from each mix were tested.

Dynamic modulus master curves were developed using Equation 10.1 through Equation 10.3. The measured modulus values were used to construct master curves at the reference temperature of 20°C by fitting the data to the sigmoidal function shown in Equation 10.1. The testing frequencies at any testing temperature were converted to the reduced frequency at the reference temperature using the time-temperature superposition principle (Equation 10.2) with the aid of an Arrhenius shift factor (Equation 10.3).

$$\log(|G^*(f_r)|) = \delta + \frac{\alpha}{1 + e^{\beta + \gamma \times \log(f_r)}} \quad (10.1)$$

where: $\delta, \alpha, \beta,$ and γ are sigmoidal function parameters
 f_r is the reduced frequency at reference temperature T_r .

$$\log(f_r) = \log(a_T(T)) + \log(f) \quad (10.2)$$

where: f is the testing frequency at testing temperature T (°C)
 f_r is the reduced frequency at reference temperature T_r (°C)

$$\log(a_T(T)) = \frac{E_a}{Ln(10) \times R} \left(\frac{1}{T} - \frac{1}{T_r} \right) \quad (10.3)$$

where: $a_T(T)$ is the shift factor value for temperature T (°K)
 E_a is an activation energy term (Joules [J]/mol)
 R is the universal gas constant (J/(mol·K))
 T_r is the reference temperature (°K)

The parameters of the sigmoidal function as well as the activation energy term in the Arrhenius shift factor equation were estimated using the *Solver* feature in *Microsoft Excel*® by minimizing the sum of square error between predicted and measured values.

10.4.1 Testing Results

Test results are listed in Table C.16 in Appendix C. Table 10.2 lists the function parameters (Equation 10.1) and activation energy term used in the Arrhenius shift factor equation (Equation 10.3) to determine the master curves for the evaluated mixes, which are shown in Figure 10.3.

Table 10.2: Phase 2f: Dynamic Modulus Master Curve Parameters

Mix	Master Curve Parameters				
	δ (MPa)	α	β	γ	Ea (kJ/mol)
SOL-680	0.00	4.25	-1.72	-0.41	200,000
CAL-26	0.96	3.34	-1.17	-0.40	200,000
SB-154	0.00	4.25	-1.45	-0.34	200,000

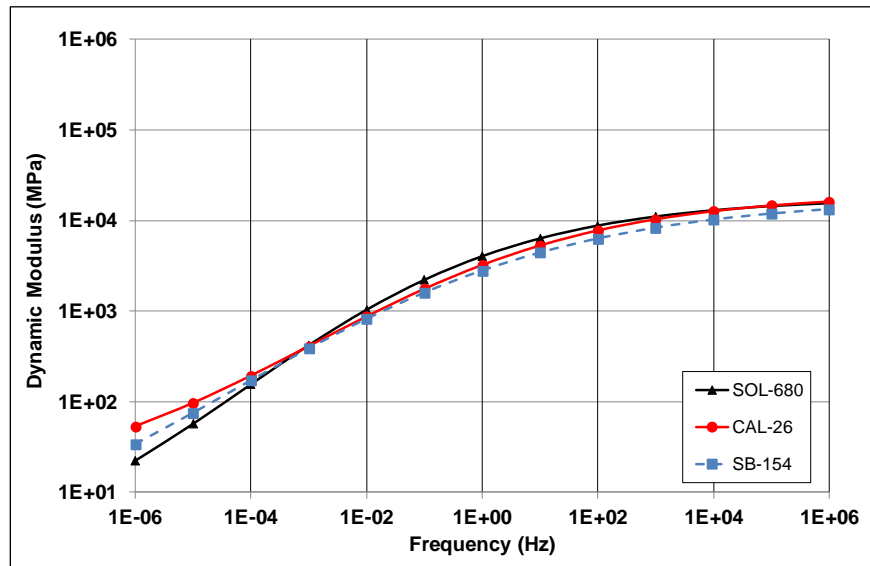


Figure 10.3: Dynamic shear modulus master curves.

The stiffness results were similar for all three mixes and were consistent with those measured on typical RHMA-G mixes.

10.5 Mix Stiffness: Flexural Modulus

Four-point-bending beam frequency sweep tests were conducted to measure the stiffness (flexural dynamic modulus) of the RHMA-G beams under different frequencies and various temperatures. Two replicates were tested at temperatures of 10°C, 20°C, and 30°C and over frequencies of 15, 10, 5, 2, 1, 0.5, 0.2, 0.1, 0.05, 0.02 and 0.01 Hz. Tests were performed in strain control mode (100 µstrain at 10°C and 20°C, and 200 µstrain at 30°C).

A sigmoidal function similar to that used to determine the dynamic modulus was used to construct the flexural dynamic modulus master curve at a reference temperature of 20°C. The shift factor equation used for generating the master curves is shown in Equation 10.4.

$$\text{Log } a_T(T) = C \times (T - T_r) \quad (10.4)$$

where:

C is the shift factor constant

T_r is the reference temperature and T is the testing temperature (°C)

Table 10.3 lists the sigmoidal function parameters used for the evaluated mixes.

Table 10.3: Phase 2f: Flexural Modulus Master Curve Parameters

Mix	Master Curve Parameters			
	δ (kPa)	α	β	γ
SOL-680	1.553	2.464	-0.955	-0.594
CAL-26	0.317	3.876	-1.076	-0.358
SB-154	-0.335	4.376	-1.694	-0.371

10.5.1 Testing Results

Test results are listed in Table C.17 in Appendix C. Figure 10.4 shows the flexural dynamic modulus master curves for the different RHMA-G mixes and Figure 10.5 shows the flexural complex modulus at temperatures between -20°C and +80°C (-4°F and 176 F) at a loading frequency of 10 Hz.

A review of the data led to the following observations:

- Results from the flexural dynamic modulus testing showed trends similar to those from the AMPT dynamic modulus testing discussed in Section 10.4.1. The stiffness results were similar for all three mixes and were consistent with those measured on typical RHMA-G mixes.

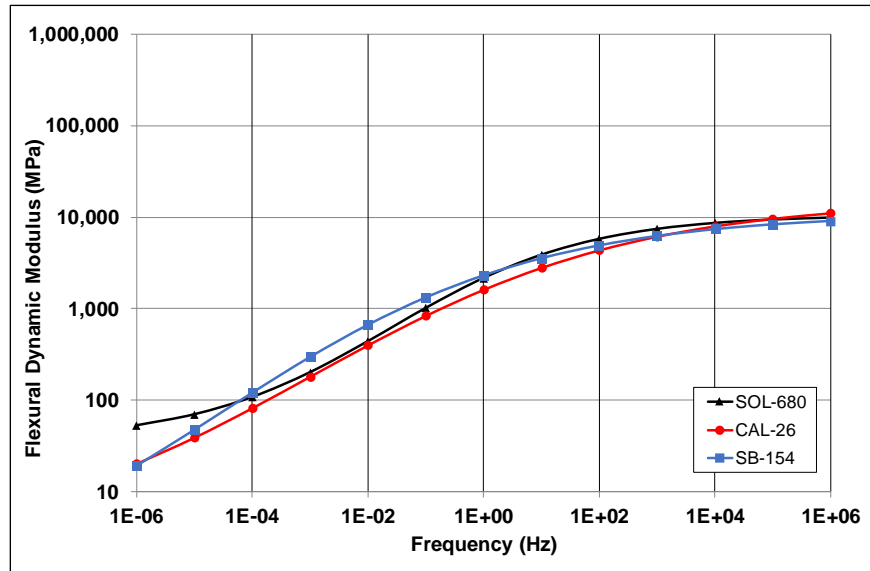


Figure 10.4: Flexural dynamic modulus master curves.

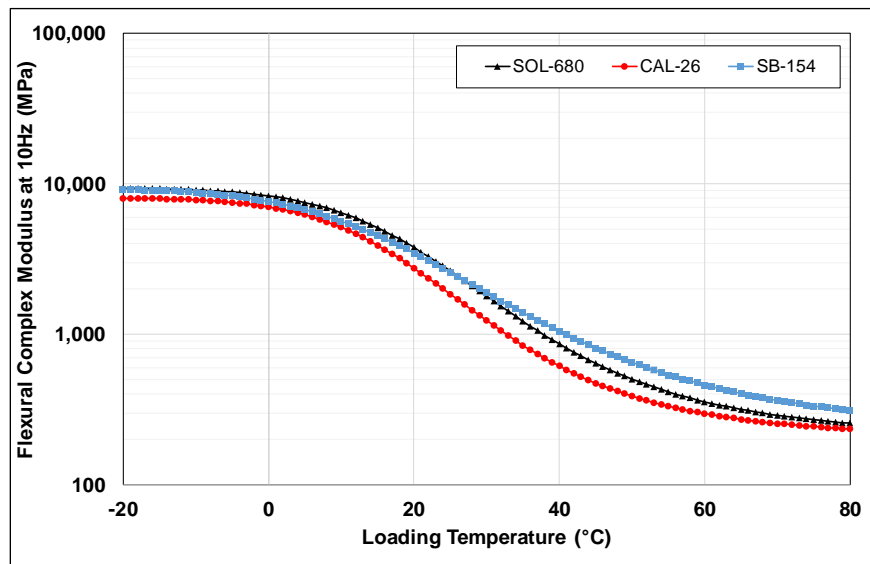


Figure 10.5: Flexural complex modulus at 10 Hz loading frequency.

10.6 Rutting Performance: Unconfined Repeated Load Triaxial

The flow number test (AASHTO T 378) provides an indication of the resistance of an asphalt mix to permanent deformation (rutting). The accumulation of permanent deformation is assumed to occur in primary, secondary, and tertiary phases. Permanent strain typically accumulates rapidly in the primary phase, followed by a lower constant rate through the secondary phase, and then accumulates rapidly again in the tertiary phase. The flow number is defined as the number of cycles at which the tertiary phase starts. Higher flow number values imply that a mix has better rutting (permanent deformation) resistance. In this study, unconfined specimens were subjected to a repeated compressive deviator stress of 600 kPa (87 psi)

and a 30 kPa (4.4 psi) contact stress. The resulting cumulative permanent deformation versus the number of loading cycles was recorded with flow number calculations performed automatically by the AMPT software. The numbers of cycles to 1, 3, and 5 percent permanent axial strain were also analyzed to obtain a better understanding of the likely rutting behavior of each of the mixes. According to the test method, the selected testing temperature should be based on the adjusted high PG temperature of the binder identified for the pavement location. Since testing for specific project locations was not included as part of the workplan, all tests were performed at 52°C to obtain a good understanding of how damage accumulated during the test. Running the test at higher temperatures (e.g., 64°C, or the high PG temperatures determined in Chapter 9) could have resulted in accelerated evolution of permanent deformation, which would not provide a comprehensive indication of how damage accumulated with load repetition. Running the test at lower temperatures would extend the testing time, but would probably not provide any additional useful information.

10.6.1 Testing Results

Flow number test results are listed in Table C.18 in Appendix C. Figure 10.6 shows the relationship between cumulative permanent axial strains and the number of load cycles for all mixes evaluated. A review of the data led to the following observations:

- The repeatability of the test results met the single-operator precision specified in AASHTO T 378 for all mixes, but showed some variability between the replicate specimens in each mix, which is consistent with repeated load testing.
- The evolution rate of cumulative permanent deformation with increasing loading cycles was initially similar for all mixes, but thereafter the SOL-680 mix appeared to be more susceptible to rutting than the other two mixes.

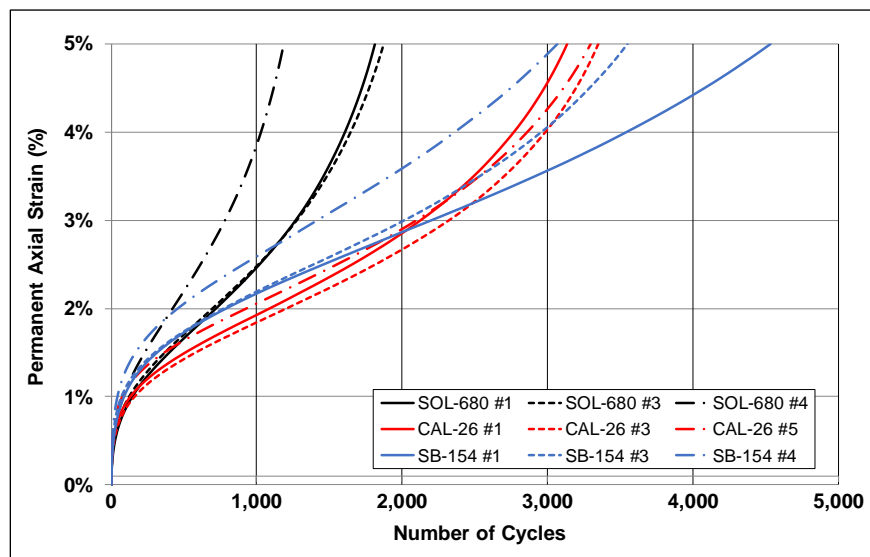


Figure 10.6: Cumulative permanent axial strain versus number of cycles (52°C).

Figure 10.7 shows the flow number values for the different mixes. Whiskers on the data show the lowest and highest flow numbers of the three replicates in each mix. The SOL-680 mix had the lowest average flow number, followed by the SB-154 and CAL-26 mixes, respectively. Although there was considerable variability between the results of the three replicates in each mix, this ranking of average flow numbers is consistent with the true high temperature grade results of the binders (Table 9.2).

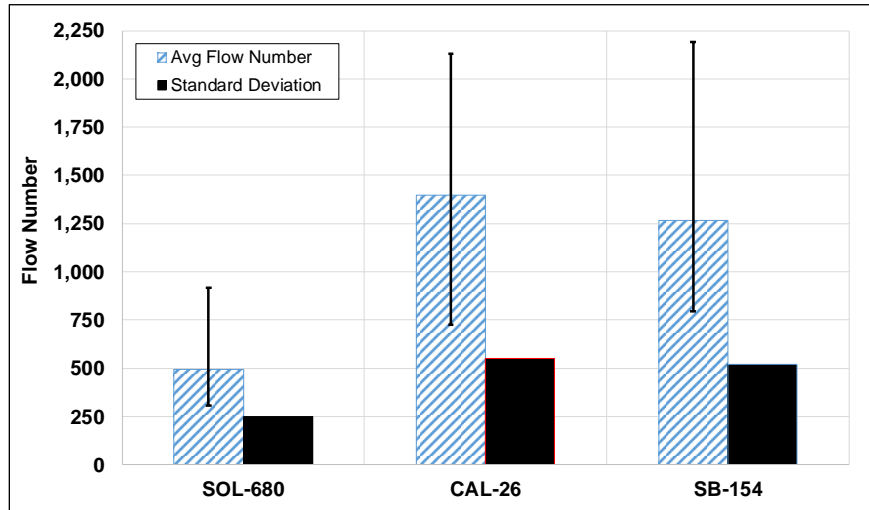


Figure 10.7: Average flow number values for evaluated mixes (52°C).

Figure 10.8 shows the number of cycles to 1, 3, and 5 percent permanent axial strain (note that the y-axis is on a log scale). Trends observed for the number of cycles to 3 and 5 percent permanent axial strain were similar to those observed for the flow number results. At lower strain levels, the difference in the number of cycles required to reach the selected strain level was much closer between the mixes (also clearly shown in Figure 10.6), with the rankings of some of the mixes different from those for the higher strain levels.

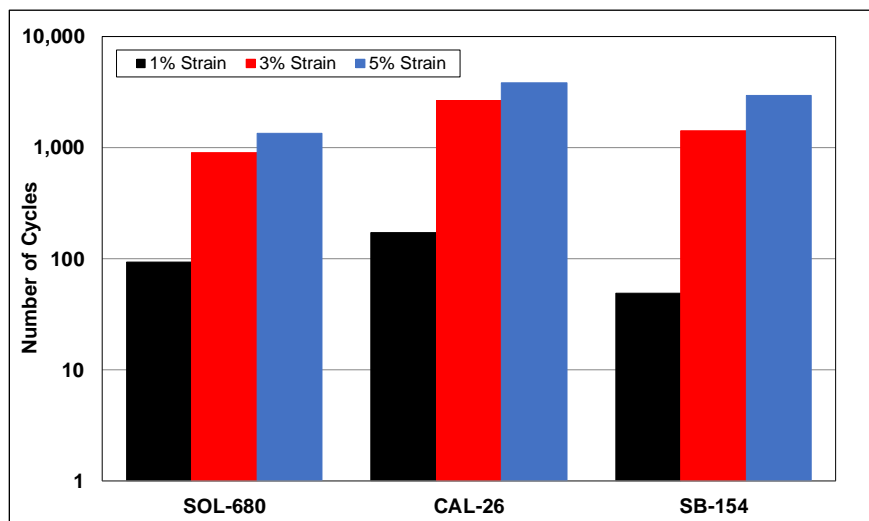


Figure 10.8: Number of cycles to 1, 3, and 5% permanent axial strain.

10.7 Fatigue/Reflective Cracking Performance: Four-Point Beam

The beam fatigue test (AASHTO T 321) provides an indication of the resistance of an asphalt mix to fatigue cracking at a constant deformation (strain). Beam specimens are subjected to four-point bending by applying sinusoidal loading at three different strain levels (high, intermediate, and low) at a frequency of 10 Hz and temperature of 20°C (68°F). The fatigue life for each strain level was selected by multiplying the maximum stiffness value for that strain level by the number of cycles at which that stiffness value occurred. Laboratory test results will generally correspond with field fatigue or reflection cracking performance for overlays thinner than about 75 mm (0.25 ft) but may not correspond with expected field performance for thicker layers of asphalt. For thicker layers, the interaction of the pavement structure, traffic loading, temperature, and mix stiffness with the controlled-strain beam fatigue results needs to be simulated using mechanistic analysis in order to rank mixes for expected field performance.

In this UCPRC study, the testing approach currently specified in AASHTO T 321 was modified to optimize the quantity and quality of the data collected. Replicate specimens were first tested at high and medium strain levels to develop an initial regression relationship between fatigue life and strain (Equation 10.5). Strain levels were selected, based on experience, to achieve fatigue lives between 10,000 and 100,000 load cycles and between 300,000 and 500,000 load cycles for high and medium strains, respectively. Additional specimens were then tested at lower strain levels selected based on the results of the initial linear regression relationship to achieve a fatigue life of about 1 million load repetitions. The final regression relationship was then refined to accommodate the measured stiffness at the lower strain level.

$$\ln N = A + B \times \varepsilon \quad (10.5)$$

where: N is fatigue life (number of cycles)
 ε is the strain level (microstrain [μ strain])
 A and B are model parameters

10.7.1 Testing Results

Plots of the fatigue models for each mix are shown in Figure 10.9 through Figure 10.11 and a comparison of the three mixes is shown in Figure 10.12. The models were considered to be generally appropriate based on the high R-squared values of the model fitting and the repeatability of the test results at each strain level. The CAL-26 mix beams had some variability at low and high strains. Calculated fatigue lives at 200 μ strain, 400 μ strain, and 600 μ strain of the three mixes are compared in Figure 10.13. Note that no mixes were tested at 200 μ strain and that fatigue life at this strain level was extrapolated.

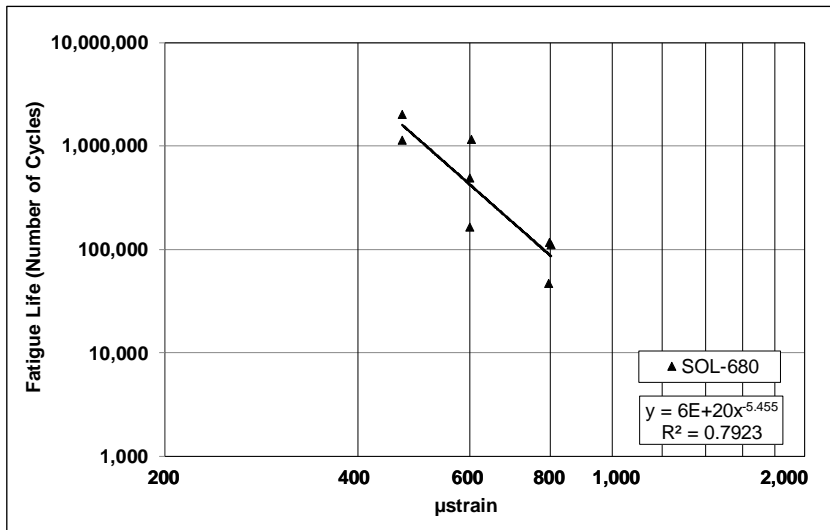


Figure 10.9: Fatigue regression model for SOL-680.

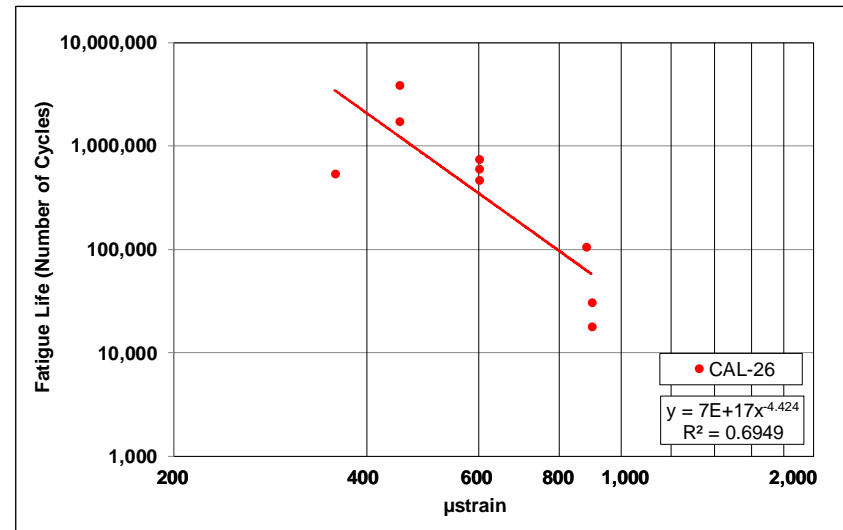


Figure 10.10: Fatigue regression model for CAL-26.

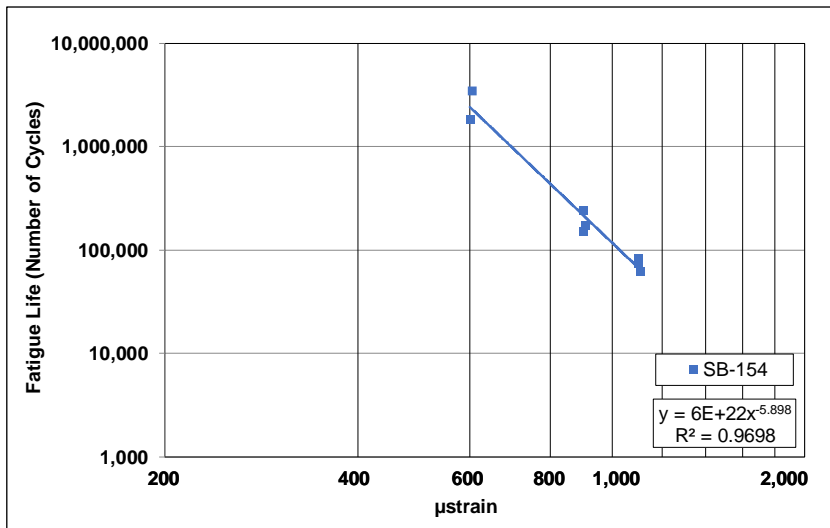


Figure 10.11: Fatigue regression model for SB-154.

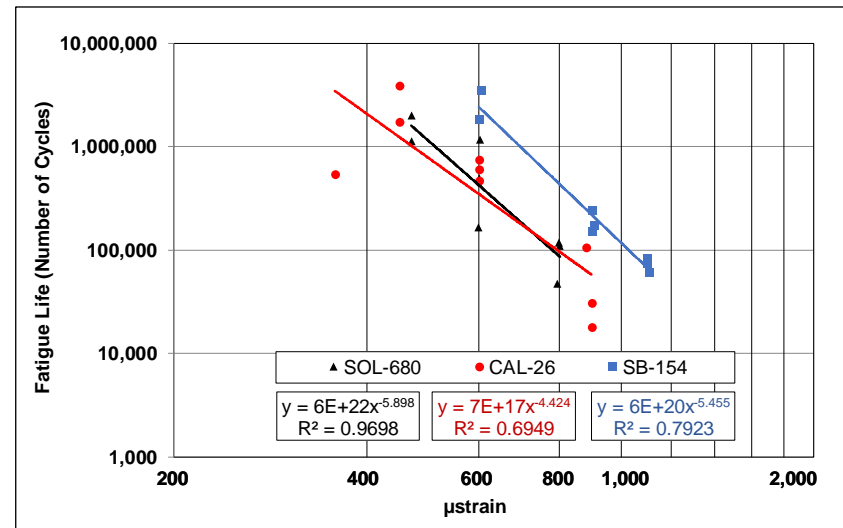


Figure 10.12: Fatigue regression models for all mixes.

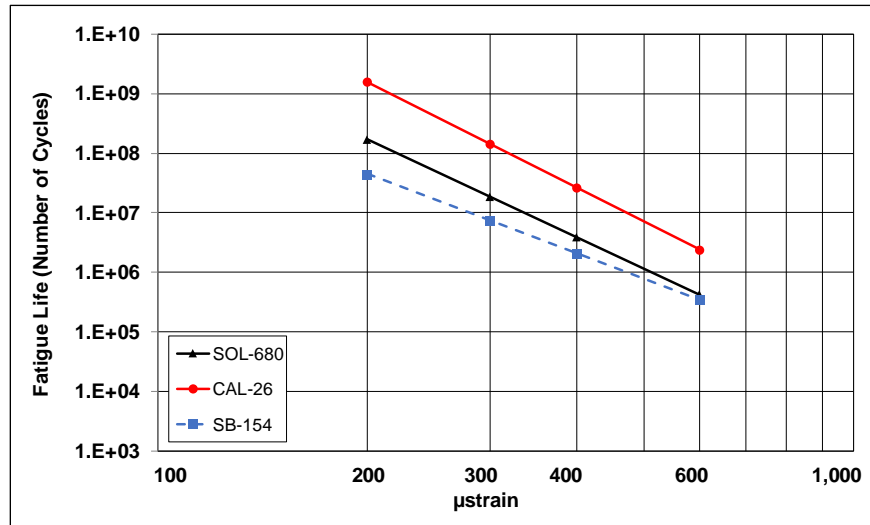


Figure 10.13: Calculated fatigue life at 200, 400, and 600 μ strain.

A review of the data led to the following observations:

- Fatigue life decreased with increasing strain level, as expected.
- The SOL-680 and SB-154 mixes had similar fatigue performance, which was somewhat lower than expected for RHMA-G mixes when the results were compared with other recent tests at the UCPRC. The CAL-26 mix had a slightly higher fatigue life, which was more consistent with other RHMA-G mixes tested.

10.8 Fatigue/Reflective Cracking Performance: Semicircular Bend

The semicircular bend (SCB) test is used to determine the fracture resistance parameters of asphalt mixtures at intermediate temperature and can be used to rank the cracking resistance of asphalt mixtures containing different binders, modifiers, aggregate gradations, and recycled asphalt pavement. The UCPRC is currently investigating the SCB and other simple cracking tests that relate to beam fatigue test results and can be used for mix design, quality control, and quality assurance purposes. The fracture energy (G_f) and flexibility index (FI) test parameters were selected to compare the performance of mixes. *Fracture energy* is the area under the load-displacement curve and shows the overall resistance of the mix to crack-related damage. The *flexibility index* is calculated from the fracture energy and post-peak slope of the load-displacement curve that represents the average crack growth rate. Increasing fracture energy and flexibility index implies increasing cracking resistance and is used to identify brittle mixes.

10.8.1 Testing Results

Test results are listed in Table C.19 in Appendix C. Average fracture energies and flexibility indices for the three mixes are shown in Figure 10.14 and Figure 10.15. Whiskers on the data show the lowest and highest

fracture energies and flexibility indices, respectively for the number of replicates tested (i.e., 8, 8, and 18 replicates for SOL-680, CAL-26, and SB-154, respectively).

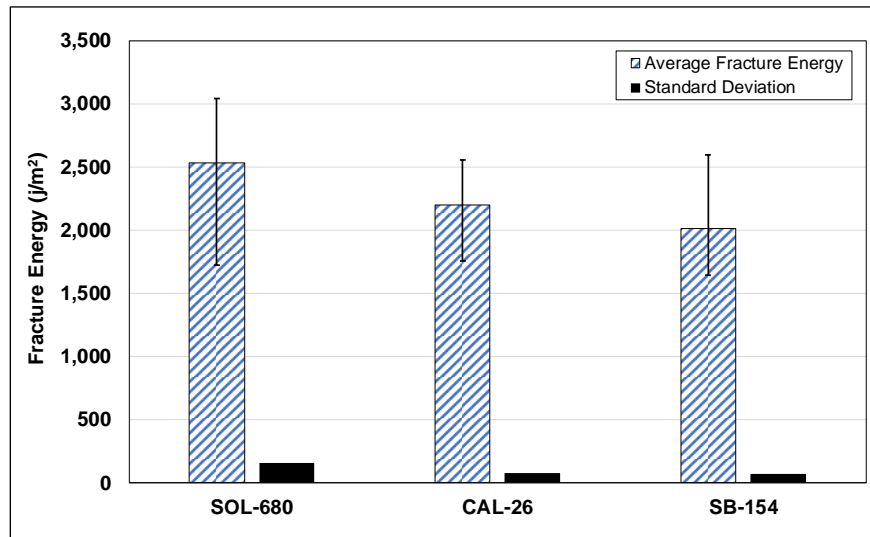


Figure 10.14: SCB fracture energy.

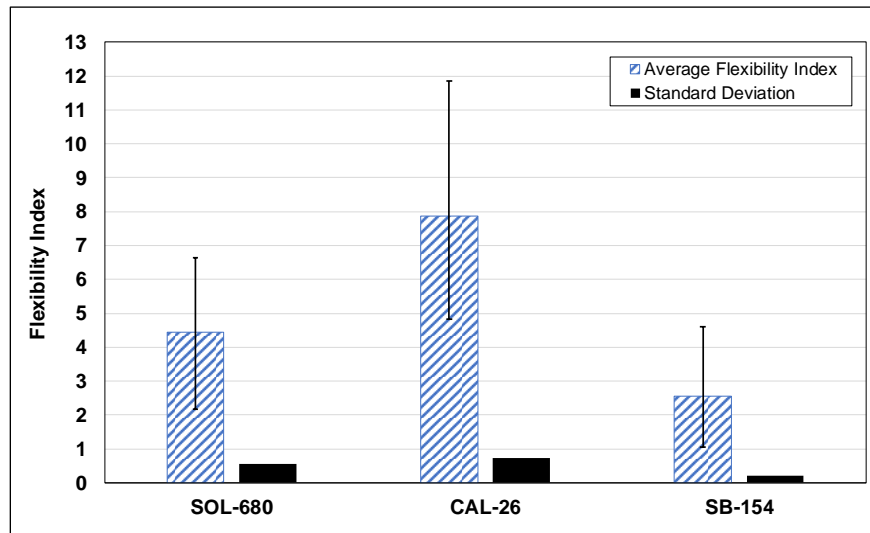


Figure 10.15: SCB flexibility index.

A review of the data led to the following observations:

- There was notable variability between mixes and between replicate specimens within each mix for both the fracture energy and flexibility index.
- The fracture energy of the SOL-680 mix was higher than the fracture energies of the CAL-26 and SB-154 mixes, which were similar. This trend differs from the beam fatigue results.
- The flexibility index of the CAL-26 mix was considerably higher than the indices of the SOL-680 and SB-154 mixes, indicating that this mix is likely to have better cracking resistance than the other two. The flexibility index results showed the same ranks and trends as the beam fatigue results.

10.9 Provisional Performance Grading Criteria for Asphalt Rubber Binders

Given that only three plant-produced asphalt rubber binders and the corresponding RHMA-G mixes produced with them were tested, it is not considered appropriate at this time to make provisional recommendations for performance grading criteria for asphalt rubber binders. As of this writing, 30 additional asphalt rubber binders from other projects (approximately 20 from RHMA-G or RHMA-O projects and approximately 10 from chip seal projects) are being collected for Phase 3 testing. The binders collected from each project will be tested in at least two different laboratories following the provisional test methods developed during this study (Appendix C). RHMA-G mixes will be collected from five of these projects in five different regions of the state to ensure a representative spread of aggregates, base binders, asphalt rubber binders, and asphalt plants. The test results will be analyzed and documented in a separate report, along with recommendations for performance grading criteria for AR binders produced as per Caltrans specifications.

Blank page

11. CONCLUSIONS AND INTERIM RECOMMENDATIONS

11.1 Project Summary

This report documents the first two phases of a three-phase study to investigate test methods for measuring the performance properties of asphalt rubber binders produced according to Caltrans specifications. The current method of rotational viscosity (Haake) testing used by Caltrans is deemed to be an insufficient measure for assessing the expected performance for asphalt rubber binders compared to the more rigorous testing requirements for unmodified, polymer-modified, and tire rubber-modified binders. The first phase of the study consisted of preliminary testing to compare two different dynamic shear rheometer (DSR) geometries, with a goal to make recommendations about whether to adopt similar testing procedures for asphalt rubber binders to supplement those currently used for unmodified and other modified binders. The second phase of the study investigated short- and long-term aging procedures, developed revised specimen preparation procedures for bending beam rheometer (BBR) testing, and conducted preliminary investigations into the use of the two DSR geometries for intermediate-temperature testing and multiple stress creep recovery (MSCR) testing. Three asphalt rubber binders, and loose mixtures produced with them, were sampled from three different field projects to assess the binder testing procedures developed and to relate the tested properties to expected field performance.

11.1.1 Phase 1: DSR Testing Geometries

The high temperature properties of unmodified and other modified asphalt binders are typically measured in tests that use a DSR with parallel plate geometry, with the gap size between the plates dependent on the size of any particulates in the binder. A 2.0 mm gap size is considered to be the maximum appropriate gap for testing asphalt binders (in order to limit variability in results due to specimen trimming and binder flow at higher temperatures), provided that no particulates in the binder exceed the AASHTO/ASTM-recommended maximum particle size of 0.25 mm (or 250 μm [#60]). In addition, DSR-manufacturers recommend that the gap between the plates should be at least four times the maximum particle size to provide reliable results. However, Caltrans specifications allow crumb rubber particles up to 2.36 mm (passing the #8 sieve), which exceeds this maximum recommended size for parallel plate testing (i.e., an 8-mm gap, with correspondingly adjusted plate diameter, would be required for 2.0 mm [#10] particle sizes). Consequently, the appropriateness of the parallel plate geometry for testing asphalt rubber binders is questionable because the rheology of the large incompletely digested rubber particles may dominate the DSR results and give misleading performance parameters for the binder properties. This study therefore assessed the concentric cylinder, an alternative geometry that can accommodate larger particles in the asphalt rubber binder. The two geometries were compared using unmodified, polymer-modified, tire rubber-modified (i.e., binders with no particulates), and wet-process asphalt rubber binders (binder containing

incompletely digested rubber particles). Binders with no particles were tested with a 1-mm gap, while the asphalt rubber binders were tested with a 3-mm parallel plate gap (to better accommodate the incompletely digested rubber particles). Key findings from the work completed to date include the following:

- The results obtained from testing the same unmodified, polymer-modified, and tire rubber-modified binders with concentric cylinder and parallel plate geometries in a DSR showed that the two geometries produced results for the same binder that were statistically similar at a 95 percent confidence interval.
- The results obtained from testing asphalt rubber binders with three different crumb rubber particle size ranges (180 μm to 250 μm , 250 μm to 425 μm , and 425 μm to 850 μm [#40 to #20, #60 to #40, and #80 to #60, respectively]) showed a strong correlation between the two testing geometries for finer particle size ranges but the correlations became weaker with increasing particle size. These weaker correlations in the larger size ranges were attributed in part to the increasing influence of the larger rubber particles in proximity of the plates. Strong correlations between the two geometries were also noted in the test results from assessments of the effects of extender oils and from tire-crushing methods (crushing at ambient versus cryogenic temperatures).

11.1.2 Phase 2a: Short- and Long-Term Aging Procedures

Phase 2a of the study investigated modifications to the AASHTO T 240 rolling thin film oven (RTFO) and AASHTO R 28 pressurized aging vessel (PAV) tests to make them more representative of short- and long-term aging that asphalt rubber binders are subjected to during mix production and during service life. Suggested modifications to the test procedures include the following:

- RTFO testing
 - + Preheating the bottles at 190°C for 10 minutes to improve the uniformity of the coating.
 - + Increasing the sample size from 35 g to 45 g to account for the rubber particles, to ensure that the same amount of the base asphalt binder is tested, and to ensure that sufficient binder is available for rheology testing.
 - + Increasing the RTFO test temperature from 163°C to 190°C to better represent rubberized asphalt concrete mix production temperatures.
- PAV sample preparation
 - + Preheating the pans at 190°C for 10 minutes prior to pouring to facilitate more even spread of the binder to the required thickness.
 - + Increasing the sample size from 50 g to 63 g to account for the rubber particles, to ensure that the same amount of the base asphalt binder is tested, and to ensure that sufficient binder from a single PAV test is available for rheology testing.
 - + Increasing the sample preparation temperature from 163°C to 190°C to be consistent with the temperature of the RTFO-aged binder.
 - + Altering the pouring procedure and agitating the pan during pouring to facilitate even spread of the binder to the required thickness.

Test results revealed the following:

- RTFO testing
 - + Complete coating of the bottle was achieved with the larger sample at the higher temperature. Although coating was satisfactory using the smaller sample at the higher temperature, insufficient material was produced for the desired rheology testing. Film thickness on the bottle was relatively even, but marginally thicker than that measured during aging of conventional unmodified binders, with these results primarily attributed to the presence of incompletely digested rubber particles.
 - + Aging at 190°C increased the shear modulus of the asphalt rubber binder, and reduced the phase angle, as expected. The true high temperature performance grade (PG) typically increased by about 6°C, which equates to a one-grade bump. Sample size and extender oil had limited effect on these parameters.
 - + Rubber particle size had a notable effect on all tests, which is consistent with findings from the literature.
 - + The measured carbonyl and sulfoxide indices for unaged and RTFO-aged binders showed clear trends with respect to the effect of aging temperature and sample size, as expected. Ongoing testing in Phase 3 will attempt to compare laboratory- and plant-produced binders to determine whether the proposed revised aging procedure is representative of aging conditions during plant production, storage, transport to the project, and placement.
 - + The butadiene index appears to increase with increasing rubber content and could be a useful potential indicator of the level of modification in asphalt rubber binders. This index also changed with increasing RTFO-aging temperature and the larger sample size, which implies that some rubber modification may have continued during aging.
- PAV preparation procedures
 - + Complete coating of the pan was achieved with the 63 g sample, and the average film thickness after pouring and after PAV aging met the requirements listed in AASHTO R 28.
 - + Following this method provides an additional 130 g of aged binder per PAV test compared to following the standard method (10 pans of 63 g versus 10 pans of 50 g), which provides sufficient binder for both intermediate-temperature testing (using the concentric cylinder geometry) and low-temperature testing. This is considered to be an important advantage given that one PAV test takes 20 hours, excluding preparation time.
- Preliminary intermediate-temperature testing of PAV-aged binder
 - + No clear trends were observed from the preliminary intermediate-temperature test results on three binders for the different preparation procedures. Only two of the three binders could be tested due to torque limitations of the DSR. The results from one of the binders were consistent with expectations. PAV preparation procedures did not appear to have a significant effect on the test results of the second binder.
- Preliminary BBR testing:
 - + No clear trends were observed from the stiffness testing results, with little variation observed between the different PAV preparation methods across the three binders tested when variation between replicates within each method were considered.
 - + The m-value did not appear to be significantly affected by PAV sample preparation method.

Although only limited DSR and BBR testing was conducted in this phase of the research, the modifications proposed above are considered to be appropriate in reflecting the original intent and mechanisms of the tests. Unfortunately, there is no documented procedure to verify the appropriateness of the procedures given that asphalt rubber binders cannot be effectively extracted and recovered for loose mix or core samples removed from highways.

11.1.3 Phase 2b: Bending Beam Rheometer Specimen Preparation Procedures

Phase 2b investigated modifications to the mold used to prepare BBR specimens. Pouring asphalt rubber binder into a standard BBR mold is very difficult given the mold's small opening and the viscosity and consistency of the binder. Modified molds that allow binder to be poured through a 12.5 mm opening (i.e., the width of the mold) instead of the standard 6.25 mm opening (i.e., the thickness of the specimen) improved the quality of the specimens in terms of dimension uniformity and absence of air bubbles. However, the specimen's wider surface area made trimming more challenging, and the specimen's rougher surface after trimming could influence the dimensions of the beam. Ongoing refinements to the trimming process are being investigated, along with the determination of new variance limits, to accommodate these inconsistencies.

BBR testing indicated that the mold configuration used to prepare beam specimens can affect the measured rheological properties of the binder and that the low-temperature performance grade could change if the modified configuration is used instead of the standard configuration. Results from the modified configuration appeared to be more consistent than those produced with the standard configuration.

11.1.4 Phase 2c: Intermediate-Temperature Testing

Preliminary intermediate-temperature test results indicated that the concentric cylinder geometry is potentially suitable for testing of asphalt rubber binders at intermediate temperatures. However, all testing in this phase of the study was conducted at 25°C, and the test setup will require more testing with a representative set of asphalt rubber binders to determine whether it is appropriate for determining actual intermediate-temperatures, and whether maximum torque ranges of the DSR are likely to be exceeded. Refinements to the testing geometry, such as different bob sizes and testing procedures will also be investigated during planned additional testing.

11.1.5 Phase 2d: Multiple Stress Creep Recovery (MSCR) Testing

Preliminary MSCR test results indicated that the concentric cylinder geometry is also potentially suitable for testing this property of asphalt rubber binders. However, given that only limited testing was undertaken and that the results were somewhat inconsistent, additional testing is required before any conclusions on the

appropriateness of using the concentric cylinder geometry for MSCR testing can be drawn. This evaluation will continue in the next phase when field binders are tested.

11.1.6 Phase 2e: Rheology Testing on Plant-Produced Binders

Preliminary rheology testing to determine the high-, intermediate-, and low-temperature performance grades of the three plant-produced asphalt rubber binders using the proposed testing procedures discussed in this report was undertaken to “test” the procedures. The following observations from the high temperature tests were made:

- Concentric cylinder
 - + An increase of four grades over the base binder was recorded for two of the asphalt rubber binders and an increase of five grades was recorded for the third.
 - + Mean true grade results showed that all three binders were relatively close and fell in a range between 91°C and 95°C.
 - + Variation in results of the three replicates in each test was small.
 - + The incompletely digested rubber particles clearly had a significant influence on the results when compared to the base binder.
 - + All results were higher than the maximum grade of 82°C listed in the AASHTO M 320 standard.
- Parallel plates with 3-mm gap
 - + The same grade increases recorded for the tests with the concentric cylinder were observed for the tests with the parallel plate.
 - + Mean true grade results showed that all three binders were relatively close and fell in a range between 92°C and 105°C, a range approximately 7°C higher than the concentric cylinder measurements.
 - + Variation in results of the three replicates for each binder was notably larger than the variation recorded when testing with the concentric cylinder.
- Difference between concentric cylinder and parallel plate
 - + For the unaged binders, $G^*/\sin(\delta)$ values measured with the parallel plate geometry were consistently higher than those determined from concentric cylinder measurements. Similar trends between the different binders were also apparent.
 - + For the RTFO-aged binders, $G^*/\sin(\delta)$ values determined with the parallel plate geometry were again considerably higher than those determined with the concentric cylinder for two of the three binders tested.
- Binder grade
 - + Testing with both geometries provided the same high-temperature grade despite the noted variations in test results discussed above.

The following observations from the low-temperature tests were made:

- Stiffness values were well below the AASHTO M 320 criteria for determining the low-temperature grade ($S \leq 300$) and consequently grades were dictated by the m-value (≥ 0.30). The presence of incompletely digested rubber particles and potential phase separation between these particles and the asphalt binder probably contributed to the low stiffness values.

- Although the acceptable ranges between two test results for the same unmodified binder as listed in AASHTO T 313 (7.2 percent for stiffness and 2.9 percent for m-value) were exceeded in most instances, the low-temperature grade of each tested binder remained the same. These larger differences between results were attributed in part to the rougher beam surfaces after trimming and to variation in the number, size, and degree of digestion of the rubber particles in each beam. Revised acceptance ranges for asphalt rubber binders will be suggested, if appropriate, after completion of further testing on additional plant-produced binders in Phase 3.
- The AASHTO M 320 procedure contains no recommendations for asphalt rubber binders. The minimum low-temperature grade in the standard table for conventional binders with a high-temperature grade equal to or greater than 76°C is -22°C, which was achieved for two of the tested binders. The low-temperature grade of the third binder did not differ from that of the base binder.
- Questions regarding other factors that may influence results, and specifically the variability between results, and that may require further investigation, include; a) whether changes in the properties of the incompletely digested rubber particles occur at very low temperatures (i.e., in the range of glass transition); b) whether different rubber particles (e.g., synthetic versus natural rubber) have different coefficients of thermal expansion, and c) whether the properties of the rubber particles are in any way effected by the type of temperature control medium used in the BBR (i.e., ethanol for the testing discussed in this report).

A small study was conducted to determine the extent to which incompletely digested particles might affect performance-grading test results. This was achieved by comparing the results from the three plant-produced asphalt rubber binders with the results produced using the same binder but with all particles larger than 300 μm (> #50 sieve) removed. Preliminary testing was limited to the high-temperature grading only. Sieved binders were tested using a 25-mm parallel plate geometry with 2-mm gap according to the standard AASHTO T 315 method. The following observations were made:

- The high temperature performance grades of the sieved binders were consistently two grades lower than those determined for the unsieved binders, indicating that the incompletely digested particles had a significant influence on the test results.
- The percent decrease in $G^*/\sin(\delta)$ when comparing the sieved with the unsieved binders was significant.
- The correlation between the true performance grades of the two types of binders was strong, indicating that testing sieved binders in a standard parallel plate geometry may be an appropriate alternative to testing unsieved binders in the concentric cylinder geometry.

Given that the variability of incompletely digested rubber particles in asphalt rubber binder samples leads to considerable variability in high-, intermediate-, and low-temperature test results, testing sieved binders may be a more appropriate approach to performance grade testing of these binders, or at least for developing a relationship between test results from unsieved and sieved binders as a means to determine a representative PG grading for asphalt rubber binders. Sieved binders will therefore be included as part of the scheduled testing of additional plant-produced binders.

11.1.7 Phase 2f: Performance Testing on Plant-Produced Mixes

Preliminary mix testing was undertaken to assess rutting and cracking performance in relation to performance grading to determine whether the rheology testing approaches provide properties that are representative of likely field performance. The following observations were made based on the testing of three plant-produced gap-graded asphalt rubber mixes:

- The dynamic and flexural moduli results were similar for all three mixes and were consistent with those measured on other RHMA-G mixes.
- The initial rates of cumulative permanent deformation with increasing loading cycles were similar for the three mixes, but thereafter one mix appeared to be more susceptible to rutting than the other two. Similar trends were recorded in the flow number tests and in tests to determine the number of cycles to three and five percent permanent axial strain. Rankings in these tests were consistent with the true high-temperature grade results of the binders.
- Two of the mixes had similar fatigue life results that were somewhat lower than expected for RHMA-G mixes, when compared with other mixes recently tested at the UCPRC. The remaining mix had a slightly higher fatigue life that was more consistent with other RHMA-G mixes tested.
- The semicircular beam flexibility index results showed the same ranking and trends as the beam fatigue results.

Given that only three plant-produced binders and the mixes produced with them have been tested to date, the database of results is considered to be insufficient for in-depth analysis purposes at this stage of the investigation.

11.2 Conclusions

Based on the results obtained to date, the concentric cylinder geometry appears to be a potentially appropriate alternative to the parallel plate geometry for quantifying the properties of asphalt rubber binders produced per Caltrans specifications, and specifically for assessing the performance properties of binders containing crumb rubber particles larger than 250 μm (particles retained on the #60 sieve). Additional testing of a larger number of binders, planned for Phase 3 of this study, is required to confirm these initial findings. The concentric cylinder geometry requires a larger binder sample for testing and it takes longer to complete than testing with the parallel plate geometry. Incompletely digested rubber particles, which have different sensitivities to temperature and applied stress and strain than the base asphalt binder, appear to dominate the test results and this will need to be factored into analyses and interpretation of rheology and mix performance test results. The proposed modifications to the short- and long-term aging procedures and to the BBR specimen preparation procedures are considered to be more aligned with the original intent of the tests and will likely reduce the variability between replicate specimens during testing.

11.3 Recommendations

Initial results from this study support the continuation of testing to assess the appropriateness of using the concentric cylinder geometry to measure the performance properties of asphalt rubber binders that are produced according to Caltrans specifications using a wet process with crumb rubber particles larger than 0.25 mm (#60 mesh). This testing should be in line with the original workplan and objectives prepared for this project, and work should continue to refine the testing procedures on additional plant-produced binders, assess the repeatability and reproducibility of measurements from any proposed test methods, and evaluate the applicability of the results to the actual performance properties of mixes produced with asphalt rubber binders. The potential influence of incompletely digested rubber particles dominating the results will need to be carefully considered in any testing and analysis procedures.

REFERENCES

1. **California Waste Tire Generation, Markets and Disposal, Staff Report.** 2003. California Integrated Waste Management Board.
2. **Status of the Nation's Highways, Bridges, and Transit: Conditions and Performance.** 2006. Washington, DC: Federal Highway Administration.
3. HARVEY, J. and Bejarano, M. 2001. Performance of Two Overlay Strategies under Heavy Vehicle Simulator Trafficking. **Transportation Research Record, Journal of the Transportation Research Board, No.1769.** (pp. 123-133).
4. JONES, D., Tsai, B.W., Ullidtz, P., Wu, R., Harvey, J.T. and Monismith, C.L. 2008. **Reflective Cracking Study: Second-Level Analysis Report.** Davis and Berkeley: University of California Pavement Research Center. (Research Report RR-2007-09).
5. JONES, D. and Harvey, J. 2009. Accelerated Pavement Testing Experiment to Assess the Use of Modified Binders to Limit Reflective Cracking in Thin Asphalt Concrete Overlays. In **Use of Accelerated Pavement Testing to Evaluate Maintenance and Pavement Preservation Treatments.** Transportation Research Circular Number E-C139, (pp. 11-31).
6. BAHIA, H.U. and Davies, R. 1994. Effect of Crumb Rubber Modifiers (CRM) on Performance Related Properties of Asphalt Binders. **Journal of the Association of Asphalt Paving Technologists, 63.** (pp. 414-424).
7. ABDELRAHMAN, M.A. and Carpenter, S.H. 1999. The Mechanism of Interaction of Asphalt Cement with Crumb Rubber Modifier. **Transportation Research Record: Journal of the Transportation Research Board, No.1661.**
8. KIM, S., Loh, S.W., Zhai, H. and Bahia, H.U. 2001. Advanced Characterization of Crumb Rubber Modified Asphalts Using Protocols Developed for Complex Binders. **Transportation Research Record: Journal of the Transportation Research Board, No.2293.**
9. SHEN, J. and Amirhanian, S.N. 2005. Influence of Crumb Rubber Modifier (CRM) Microstructures on High-Temperature Properties of CRM Binders. **International Journal of Pavement Engineering, 6 (4).**
10. PUTMAN, B.J., Thompson, J.U. and Amirhanian, S.N. 2005. High-Temperature Properties of Crumb Rubber Modified (CRM) Asphalt Binders. **Proceedings Fourth International Conference on Maintenance and Rehabilitation of Pavements and Technological Control (MAIREPAV 2005).** Belfast, UK.
11. LEE, S.J., Akisety, C.K., and Amirhanian, S.N. 2008. The Effect of Crumb Rubber Modified (CRM) on The Performance Properties of Rubberized Binders in HMA Pavements. **Journal of Construction and Building Materials, 22.** (pp 1368-1376).

12. BAUMGARDNER, G. and D'Angelo, J.A. 2012. Evaluation of New DSR Testing Geometry for Performance Testing of Crumb Rubber Modified (CRM) Binder. **Transportation Research Record: Journal of the Transportation Research Board, No.2293.** (pp. 73-79).
13. MEZGER, T.G. 2006. **The Rheology Handbook for Users of Rotational and Oscillatory Rheometers.** Vincentz Network GmbH and Co KG.
14. CHENG, D., Hicks, R.G., Fraser, B. and Garcia, M. 2014. Evaluating the Performance of Asphalt Rubber Used in California. **Proceedings 93rd Transportation Research Board Annual Meeting, Washington D.C.**
15. WEST, R.C., et al. 1998. Effect of Tire Rubber Grinding Method on Asphalt-Rubber Binder Characteristics. **Transportation Research Record: Journal of the Transportation Research Board, 1638(1).** (pp. 134-140).
16. LEE, S.-J., Akisetty, C.K. and Amirhanian, S.N. 2008. The Effect of Crumb Rubber Modifier (CRM) on the Performance Properties of Rubberized Binders in HMA Pavements. **Construction and Building Materials, 22(7).** (pp. 1368-1376).
17. KIM, S., et al. 2001. Advanced Characterization of Crumb Rubber-Modified Asphalts, Using Protocols Developed for Complex Binders. **Transportation Research Record: Journal of the Transportation Research Board, No.1767(1).** (pp. 15-24).
18. SHEN, J., et al. 2009. Surface Area of Crumb Rubber Modifier and Its Influence on High-Temperature Viscosity of CRM binders. **International Journal of Pavement Engineering, 10(5).** (pp. 375-381).
19. JEONG, K.-D., et al. 2010. Interaction Effects of Crumb Rubber Modified Asphalt Binders. **Construction and Building Materials, 24(5).** (pp. 824-831).
20. ZUPANICK, M. 1994. Comparison of the Thin Film Oven Test and the Rolling Thin Film Oven Test. **Journal of the Association of Asphalt Paving Technologists, 63.**
21. HOUSTON, S. Shatnawi, S, Teclerian, S. and Houston, G. 2017. Inter-Laboratory Study of Performance Grade Testing of Crumb Rubber Modified Asphalt Binders. **Proceedings 54th Petersen Asphalt Research Conference.** Laramie, WY: Western Research Institute.
22. BAHIA, H.U., Hanson, D.I., Zeng, M., Zhai, H., Khatri, M.A. and Anderson, R.M. 2001. **Characterization of Modified Asphalt Binders in Superpave Mix Design.** Washington DC: Transportation Research Board (NCHRP Report 459).
23. HVEEM, F.N., Zube, E. and Skog, J. 1963. Proposed New Tests and Specifications For Paving Grade Asphalts. **Association of Asphalt Paving Technologists Proceedings, Vol. 32,** (pp. 271-327).
24. LEE, D. 1969. **Durability and Durability Tests for Paving Asphalt; A State-of-The-Art Report.** Ames, IA: Iowa State University.

25. GLOVER, C.J., Davison, R.R., Vassiliev, N., Hausman, T. and Williamson, S.A. 2001. **Development of Stirred Air-Flow test (SAFT) for Improved HMA Plant Binder Aging Simulation and Studies of Asphalt Air Blowing**. College Station, TX: Texas Transportation Institute. (Report 1742-2).
26. LAMONTAGNE, J., Dumas, P., Mouillet, V. and Kister, J. 2001. Comparison by Fourier Transform Infrared (FTIR) Spectroscopy of Different Ageing Techniques: Application to Road Bitumens. **Fuel**, **80**. (pp 483 – 488).
27. MIKHAILENKO, P., Bertron, A. and Ringot, E. 2016. Methods for Analyzing the Chemical Mechanisms of Bitumen Aging and Rejuvenation with FTIR Spectrometry. **Proceedings 8th RILEM International Symposium on Testing and Characterization of Sustainable and Innovative Bituminous Materials**. (pp 203 - 214).
28. KOCEVSKI, S., Yagneswaran, S., Xiao, F., Punith, V.S. and Smith, D.W. 2012. Surface Modified Ground Rubber Tire by Grafting Acrylic Acid for Paving Applications. **Construction and Building Materials Vol. 34**. (pp 83 – 90).
29. HOFKO, B. and Hospodka, M. 2016. Rolling Thin Film Oven Test and Pressure Aging Vessel Conditioning Parameters: Effect on Viscoelastic Behavior and Binder Performance Grade. **Transportation Research Record: Journal of the Transportation Research Board, No.2574**. (pp. 111-116).

Blank page

APPENDIX A: PROVISIONAL TEST METHODS

The following provisional test methods for testing asphalt rubber binder are provided in this appendix:

- Standard Method of Test for Determining the Rheological Properties of Asphalt Binder Containing Ground Tire Rubber Particulates Using Concentric Cylinder Geometry in the Dynamic Shear Rheometer (DSR).
- Standard Method of Test for Effect of Heat and Air on a Moving Film of Asphalt Binder (Rolling Thin-Film Oven Test). Part B: Asphalt Rubber Binders.
- Standard Practice for Accelerated Aging of Asphalt Binder Using a Pressurized Aging Vessel (PAV). Part B: Asphalt Rubber Binders.
- Standard Method of Test for Determining the Flexural Creep Stiffness of Asphalt Binder Using the Bending Beam Rheometer (BBR). Part B: Asphalt Rubber Binders.

Blank page

Standard Method of Test for

**Determining the Rheological
Properties of Asphalt Binder
Containing Ground Tire Rubber
Particulates Using Concentric
Cylinder Geometry in the Dynamic
Shear Rheometer (DSR)**

AASHTO Designation: TP XX-XX



**American Association of State Highway and Transportation Officials
444 North Capitol Street N.W., Suite 249
Washington, D.C. 20001**

Determining the Rheological Properties of Asphalt Binder Containing Ground Tire Rubber Particulates Using Concentric Cylinder Geometry in the Dynamic Shear Rheometer (DSR)

AASHTO Designation: TP XX-XX



1. SCOPE

- 1.1. This test method covers the determination of the dynamic shear modulus and phase angle of asphalt rubber (AR) binders, containing incompletely digested ground tire rubber (GTR) particulates larger than 0.5 mm, when tested in dynamic (oscillatory) shear using concentric cylinder test geometry. This standard can also be used to test unmodified and polymer-modified binders. It is applicable to asphalt binders having dynamic shear modulus values in the range from 100 Pa to 20 MPa. This range in modulus is typically obtained between 16°C and 120°C at an angular frequency of 10 rad/s. This test method is intended for determining the linear viscoelastic properties of asphalt rubber binders as required for specification testing. This method is not intended as a comprehensive procedure for the full characterization of the viscoelastic properties of asphalt rubber binders at high and intermediate temperatures.
- 1.2. This standard is appropriate for unaged material or material aged in accordance with T 240 and R 28, modified for testing temperature and sample size.
- 1.3. Particulate material in the asphalt binder is limited to particles that pass through a 2.36 mm sieve.
- 1.4. *This standard may involve hazardous materials, operations, and equipment. This standard does not purport to address all of the safety concerns associated with its use. It is the responsibility of the user of this procedure to establish appropriate safety and health practices and to determine the applicability of regulatory limitations prior to use.*

2. REFERENCED DOCUMENTS

- 2.1. **AASHTO Standards:**
 - M 320 and M 332, Performance-Graded Asphalt Binder
 - R 28, Accelerated Aging of Asphalt Binder Using a Pressurized Aging Vessel (PAV)
 - R 29, Grading or Verifying the Performance Grade (PG) of an Asphalt Binder
 - R 66, Sampling Bituminous Materials
 - T 240, Effect of Heat and Air on a Moving Film of Asphalt Binder (Rolling Thin-Film Oven Test) (Modified for testing temperature and sample size)

2.2. **ASTM Standards:**

- C670, Standard Practice for Preparing Precision and Bias Statements for Test Methods for Construction Materials
- E1, Standard Specification for ASTM Liquid-in-Glass Thermometers
- E77, Standard Test Method for Inspection and Verification of Thermometers
- E563, Standard Practice for Preparation and Use of an Ice-Point Bath as a Reference Temperature
- E644, Standard Test Methods for Testing Industrial Resistance Thermometers

2.3. **Deutsche Industrie Norm (DIN) Standard:**

- 43760, Industrial Platinum Resistance Thermometers and Platinum Temperature Sensors

3. TERMINOLOGY

3.1. *Definitions:*

3.1.1. *asphalt rubber binder*—a blend of paving grade asphalt cement, ground recycled tire (i.e., vulcanized) rubber and other additives, as needed, for use as binder in pavement construction. The rubber shall be blended and interacted in the hot asphalt cement sufficiently to cause swelling of the rubber particles prior to use.

3.2. *Descriptions of Terms Specific to This Standard:*

3.2.1. *annealing*—heating the binder until it is sufficiently fluid to remove the effects of steric hardening.

3.2.2. *calibration*—process of checking the accuracy and precision of a device using NIST-traceable standards and making adjustments to the device where necessary to correct its operation or precision and accuracy.

3.2.3. *complex shear modulus (G^*)*—ratio calculated by dividing the absolute value of the peak-to-peak shear stress, τ , by the absolute value of the peak-to-peak shear strain, γ .

3.2.4. *concentric cylinder geometry* — refers to a testing geometry containing a cup (typically 29 mm inside diameter) and a measuring shaft with cylindrical cone-shaped head (referred to as the bob), which are concentric. Different bob sizes are required for binder tests at high (bob size typically 17 mm diameter) and intermediate (bob size typically 10 mm diameter) temperatures. The asphalt rubber binder sample in the cup is subjected to an oscillatory shear force applied by the immersed bob.

3.2.5. *ground tire rubber*— material derived by grinding scrap tires

3.2.6. *linear viscoelastic*—within the context of this specification refers to a region of behavior in which the dynamic shear modulus is independent of shear stress or strain.

3.2.7. *loading cycle*—a unit cycle of time for which the test sample is loaded at a selected frequency and stress or strain level.

3.2.8. *loss shear modulus (G'')*—the complex shear modulus multiplied by the sine of the phase angle expressed in degrees. It represents the component of the complex modulus that is a measure of the energy lost (dissipated during a loading cycle).

- 3.2.9. *molecular association*—a process where associations occur between asphalt binder molecules during storage at ambient temperature. Often called steric hardening in the asphalt literature, molecular associations can increase the dynamic shear modulus of asphalt binders. The amount of molecular association is asphalt specific and may be significant even after a few hours of storage.
- 3.2.10. *oscillatory shear*—refers to a type of loading in which a shear stress or shear strain is applied to a test sample in an oscillatory manner such that the shear stress or strain varies in amplitude by about zero in a sinusoidal manner.
- 3.2.11. *phase angle (δ)*—the angle in degrees between a sinusoidally applied strain and the resultant sinusoidal stress in a controlled-strain testing mode, or between the applied stress and the resultant strain in a controlled-stress testing mode.
- 3.2.12. *portable thermometer*—an electronic device that consists of a temperature detector (probe containing a thermocouple or resistive element), required electronic circuitry, and readout system.
- 3.2.13. *reference thermometer*—a NIST-traceable liquid-in-glass or electronic thermometer that is used as a laboratory standard.
- 3.2.14. *steric hardening*—see molecular association.
- 3.2.15. *storage shear modulus (G')*—the complex shear modulus multiplied by the cosine of the phase angle expressed in degrees. It represents the in-phase component of the complex modulus that is a measure of the energy stored during a loading cycle.
- 3.2.16. *temperature correction*—difference in temperature between the temperature indicated by the DSR and the test specimen as measured by the portable thermometer inserted into the cup.
- 3.2.17. *thermal equilibrium*—is reached when the temperature of the binder in the cup is constant with time.
- 3.2.18. *verification*—process of checking the accuracy of a device or its components against an internal laboratory standard. It is usually performed within the operating laboratory.

4. SUMMARY OF TEST METHOD

- 4.1. This standard contains the procedure used to measure the complex shear modulus (G^*) and phase angle (δ) of asphalt rubber binders using a dynamic shear rheometer and concentric cylinder test geometry at high and intermediate temperatures.
- 4.2. The standard is suitable for use when the dynamic shear modulus varies between 100 Pa and 20 MPa. This range in modulus is typically obtained between 16°C and 120°C at an angular frequency of 10 rad/s, dependent upon the grade, test temperature, and conditioning (aging) of the asphalt binder. AASHTO M 320 and/or M 332 guidelines shall be used for determining the high and intermediate temperature performance grading (PG) range.
- 4.3. Test geometry consists of a cup and a shaft with a cylindrical cone-shaped head (referred to as the bob). Asphalt material is poured into the cup and then the bob is immersed into the asphalt specimen. During testing, the bob is oscillated at preselected

frequencies and rotational deformation amplitudes (strain control) or torque amplitudes (stress control). The required stress or strain amplitude depends upon the value of the complex shear modulus of the asphalt binder being tested. The required amplitudes have been selected to ensure that the measurements are within the region of linear behavior.

- 4.4. The test specimen is maintained at the test temperature to within $\pm 0.1^\circ\text{C}$ by positive heating and cooling of the cup or by enclosing the cup and bob in a thermally controlled environment or test chamber.
- 4.5. Oscillatory loading frequencies using this standard can range from 1 to 100 rad/s using a sinusoidal waveform. Specification testing is performed at a test frequency of 10 rad/s. The complex modulus (G^*) and phase angle (δ) are calculated automatically as part of the operation of the rheometer using proprietary computer software supplied by the equipment manufacturer.

5. SIGNIFICANCE AND USE

- 5.1. The test temperature for this test is related to the temperature experienced by the pavement in the geographical area for which the asphalt binder is intended to be used.
- 5.2. The complex shear modulus is an indicator of the stiffness or resistance of asphalt binder to deformation under load. The complex shear modulus and the phase angle define the resistance to shear deformation of the asphalt binder in the linear viscoelastic region.
- 5.3. The complex modulus and the phase angle are used to calculate performance-related criteria in accordance with M 320 and/or M 332.

6. APPARATUS

- 6.1. *Dynamic Shear Rheometer (DSR) Test System*—Consisting of concentric cylinder geometry, an environmental chamber, a loading device, and a control and data acquisition system.
- 6.2. *Concentric Cylinder Geometry*—Stainless steel or aluminum cup (typically 29 mm inside diameter) and stainless steel shaft with cone-shaped cylindrical head (bob) with smooth ground surfaces. Different bob sizes are required for tests at high (bob size typically 17-mm diameter) and intermediate (bob size typically 10-mm diameter) temperatures.

Note 1— To obtain accurate data, the cup and bob should be concentric with each other. At present there is no suitable procedure for the user to check the concentricity except to visually observe whether or not the cup and bob are centered with respect to each other. The moveable bob should rotate without any observable horizontal or vertical wobble. This operation may be checked visually or with a dial gauge held in contact with the edge of the moveable bob while it is being rotated. There are two values that determine the operating behavior of a measuring system: centricity (horizontal wobble) and runout (vertical wobble). Typically, wobble can be detected if it is greater than ± 0.02 mm. For a new system, a wobble of ± 0.01 mm is typical. If the wobble grows to more than ± 0.02 mm with use, it is recommended that the instrument be serviced by the manufacturer.

Note 2— The exact dimensions of the cup and bob are according to DIN EN 13302 and ISO 3219 standards. This information can be obtained from the manufacturer. The ratio of cup

radius (R_e) over bob radius (R_i) is shown in Figure 1 and will differ for high (ratio of 1.74 for 17 mm bob) and intermediate (ratio of 2.89 for 10-mm bob) temperature tests.

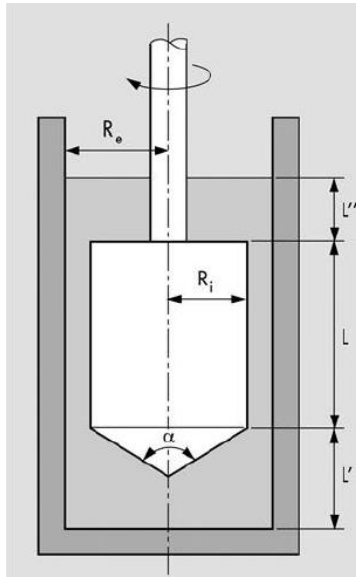


Figure 6.1—Concentric Cylinder Dimensions

- 6.2.1. *Environmental Chamber*—Used on some DSRs for controlling the test temperature, by heating or cooling (in steps or ramps), to maintain a constant specimen temperature. The medium for heating and cooling the specimen in the environmental chamber shall not affect the properties of the asphalt binder containing GTR particulates. The temperature in the chamber may be controlled by the circulation of fluid such as water, conditioned gas such as nitrogen, or by a suitable arrangement of solid-state Peltier elements surrounding the sample with a hood to prevent temperature loss from the top of the cup. When forced air is used, a suitable drier must be included to prevent condensation of moisture in the cup, on the bob, and on other fixtures and, if operating below freezing temperatures, the formation of ice. The environmental chamber and the temperature controller shall control the temperature of the specimen, including thermal gradients within the sample, to an accuracy of $\pm 0.1^\circ\text{C}$. The chamber shall completely enclose the cup and bob to minimize thermal gradients.

Note 3—A circulating bath unit, separate from the DSR, that pumps the bath fluid through the test chamber may be required if a fluid medium is used. The flow rate of the bath media should not be modified once the temperature settings have been adjusted to the desired value. Media lines should be periodically inspected and cleaned or replaced if necessary to remove obstructions.

- 6.2.1.1. *Temperature Controller*—Capable of maintaining specimen temperatures within $\pm 0.1^\circ\text{C}$ for test temperatures ranging from 16°C to 120°C .
- 6.2.1.2. *Internal Temperature Detector for the DSR*—A platinum resistance thermometer (PRT) mounted within the environmental chamber as an integral part of the DSR, with a range of 16°C to 120°C , and with a resolution of 0.1°C (see Note 4). This thermometer shall be used to control the temperature of the test specimen in the cup and shall provide a continuous readout of temperature during the mounting, conditioning, and testing of the specimen. The PRT shall be calibrated as an integral unit with its respective meter or electronic circuitry.

Note 4—PRTs meeting DIN Standard 43760 (Class A) or equal are recommended for this purpose.

- 6.2.2. *Loading Device*—Capable of applying a sinusoidal oscillatory load to the specimen at a frequency of 10.0 ± 0.1 rad/s. If frequencies other than 10 rad/s are used, the frequency shall be accurate to 1 percent. The loading device shall be capable of providing either a stress-controlled or strain-controlled load. If the load is strain-controlled, the loading device shall apply a cyclic torque sufficient to cause an angular rotational strain accurate to within $100\text{E-}06$ rad of the strain specified. If the load is stress controlled, the loading device shall apply a cyclic torque accurate to within 10 mNm of the torque specified. Total system compliance at 100 Nm of torque shall be less than 2 mrad/Nm. The manufacturer of the device shall certify that the frequency, stress, and strain are controlled and measured with an accuracy of one percent or less in the range of this measurement.
- 6.2.3. *Control and Data Acquisition System*—Capable of providing a record of temperature, frequency, deflection angle, and torque. Devices used to measure these quantities shall meet the accuracy requirements specified in Table 1. In addition, the system shall calculate and record the shear stress, shear strain, complex shear modulus (G^*), and phase angle (δ). The system shall measure and record G^* , in the range of 100 Pa to 20 MPa, to an accuracy of 1.0 percent or less, and the phase angle, in the range of 0 to 90 degrees, to an accuracy of 0.1 degree.

Table 4—**Control and Data Acquisition System Requirements**

Property	Accuracy
Temperature	0.1°C
Frequency	1%
Torque	10 mN·m
Deflection angle	100E-06 rad

- 6.3. *Balance* — A balance with a capacity of 2,000 g readable to 0.1 g for determining the mass of asphalt binder.
- 6.4. *Wiping Material*—Clean cloth, paper towels, cotton swabs, or other suitable material as required for wiping the cylinders and bobs.
- 6.5. *Cleaning Solvents*—Mineral oil, citrus-based solvents, mineral spirits, toluene, or similar solvent as required for cleaning the cup and bob, if a non-disposable cup is used. Acetone for removing the solvent residue from the cleaned surfaces is also necessary.
- 6.6. *Reference Thermometer*—Either IST—traceable liquid-in-glass thermometer(s) or NIST-traceable electronic thermometric device(s). This temperature standard shall be used to standardize the portable thermometer (Section 9.3).
- 6.6.1. *Liquid-in-Glass Thermometer*—NIST-traceable thermometer(s) with a suitable range and subdivisions of 0.1°C. The thermometer(s) shall be a partial immersion thermometer(s) within an ice point and standardized in accordance with ASTM E563.
- 6.6.1.1. *Optical Viewing Device (Optional)*—For use with liquid-in-glass thermometers that enhances readability and minimizes parallax when reading the liquid-in-glass reference thermometer.
- 6.6.2. *Electronic Thermometer*—Incorporating a resistive detector (Note 4) with an accuracy of $\pm 0.05^\circ\text{C}$ and a resolution of 0.01°C . The electronic thermometer shall be standardized at least once per year using a NIST-traceable reference standard in accordance with ASTM E77.

- 6.7. *Portable Thermometer*—A standardized portable thermometer consisting of a resistive detector, associated electronic circuitry, and digital readout. The thickness of the detector shall be no greater than 2.0 mm such that it can be inserted into the gap between the side of the cup and the bob. The reference thermometer (see Section 6.6) may be used for this purpose if its detector fits within the dummy specimen as required by Section 9.4.1.

7. HAZARDS

- 7.1. Standard laboratory caution should be used in handling the hot asphalt binder when preparing test specimens.

8. PREPARATION OF APPARATUS

- 8.1. Prepare the apparatus for testing in accordance with the manufacturer's recommendations. Specific requirements will vary for different DSR models and manufacturers.
- 8.2. Use of disposable cups is recommended. Inspect the cup and discard if it has any damage including but not limited to dents and deformations, internal scratches, or damage to the rim. Inspect the surfaces of the test bobs and discard any bobs with jagged or rounded edges or deep scratches. Clean any asphalt binder residue from the bob (and cup if a non-disposable cup is used) with an organic solvent such as mineral oil, mineral spirits, or a citrus-based solvent. Remove any remaining solvent residue by wiping the surfaces with a cotton swab or a soft cloth dampened with acetone. If necessary, use a dry cotton swab or soft cloth to ensure that no moisture condenses on the cup or bob.
- 8.3. Mount the cleaned and inspected test cup and bob on the test fixtures and tighten firmly.
- 8.4. Select the testing temperature according to the grade of the asphalt binder or according to the preselected testing schedule (see Note 5). Allow the DSR to reach a stabilized temperature within $\pm 0.1^\circ\text{C}$ of the test temperature.
- Note 5**—M 320 and R 29 provide guidance on the selection of test temperatures.

9. VERIFICATION AND CALIBRATION

- 9.1. Verify the DSR and its components at least every 6 months and when the DSR or concentric cylinder system is newly installed, when the DSR is moved to a new location, or when the accuracy of the DSR or any of its components is suspect. Four items require verification—the test bob diameter, DSR torque transducer, portable thermometer, and DSR test specimen temperature. Verify the DSR temperature transducer before verifying the torque transducer.
- 9.2. *Verification of Bob Diameter*—Measure the diameters to the nearest 0.01 mm. Maintain a log of the measured diameters as part of the laboratory quality control program so that the measurements are clearly identified with the specific bobs. Enter the actual measured dimensions into the DSR software for use in calculations.

Note 6—Decreasing bob diameter (i.e., smaller than specified) or increasing bob diameter (i.e., larger than specified) can result in increasing or decreasing percent errors in the complex modulus.

- 9.3. *Verification of Portable Thermometer*—Verify the portable thermometer (used to measure the temperature in a silicone mold placed in the cup), using the laboratory reference thermometer. A portable thermometer shall consider the combination of the meter (readout device) and the thermistor (temperature probe) as a single unit, and must be verified as such.
- 9.3.1. *Recommended Verification Procedure*—Bring the reference thermometer into intimate contact with the detector from the portable thermometer and place them in a thermostatically controlled and stirred water bath (Note 7). Ensure that deionized water is used to prevent electrical conduction from occurring between the electrodes of the resistive temperature sensitive element. If deionized water is not available, encase the reference thermometer and detector of the portable thermometer in a waterproof plastic bag prior to placement in the bath. Obtain measurements at intervals of approximately 6°C over the range of test temperatures allowing the bath to reach thermal equilibrium at each temperature. If the readings of the portable thermometer and the reference thermometer differ by 0.1°C or more, record the difference at each temperature as a temperature correction, and maintain the corrections in a log as part of the laboratory quality control program.
- Note 7**—A recommended procedure for the high-temperature range is to use a stirred water bath that is controlled within $\pm 0.1^\circ\text{C}$ such as the viscosity bath used for ASTM D2170/D2170M or D2171/D2171M. For a low-temperature bath, an ice bath or controlled-temperature bath may be used. Bring the probe from the portable thermometer into contact with the reference thermometer, and hold the assembly in intimate contact. A rubber band works well for this purpose. Immerse the assembly in the water bath, and bring the water bath to thermal equilibrium. Record the temperature on each device when thermal equilibrium is reached.
- Note 8**—If the readings from the two devices differ by 0.5°C or more, the calibration or operation of the portable thermometer may be suspect, and it may need to be recalibrated or replaced. A continuing change in the temperature corrections with time may also make the portable thermometer suspect.
- 9.4. *Test Specimen Temperature Correction*—Thermal gradients within the rheometer can cause differences between the temperature of the test specimen and the temperature indicated by the DSR thermometer (also used to control the temperature of the DSR). The DSR thermometer shall be checked at an interval no greater than six months. When these differences are 0.1°C or greater, determine a temperature correction by using a thermal detector mounted in a silicone rubber mold (Section 9.4.1).
- 9.4.1. *Method Using Silicone Rubber Specimen*—For the entire range of test temperatures, place the silicone specimen with the thermocouple onto the bob and bring the cup and bob assembly to the testing position in the temperature controller unit so that the silicone rubber makes complete contact with the surfaces of the cup and the bob. Complete contact is needed to ensure proper heat transfer across the cup, bob, and silicone specimen. Determine any needed temperature correction as per Section 9.4.2.
- 9.4.2. *Determination of Temperature Correction*—Obtain simultaneous temperature measurements with the DSR thermometer and the portable thermometer at 6°C increments to cover the range of test temperatures. At each temperature increment, after thermal equilibrium has been reached, record the temperature indicated by the portable thermometer and the DSR thermometer to the nearest 0.1°C. Temperature equilibrium is reached when the temperature indicated by both the DSR thermometer

and the portable thermometer do not vary by more than 0.1°C over a 5-minute period. Obtain additional measurements to include the entire temperature range that will be used for measuring the dynamic shear modulus.

- 9.4.3. *Plot Correction Versus Specimen Temperature*—Using the data obtained in Section 9.4, prepare a plot of the difference between the two temperature measurements versus the temperature measured with the portable thermometer (example in Figure 2). This difference is the temperature correction that must be applied to the DSR temperature controller to obtain the desired temperature in the test specimen in the cup. Report the temperature correction at the respective test temperature from the plot and report the test temperature in the cup as the test temperature. Alternatively, the instrument operating system options may be updated to incorporate these temperature corrections.

Note 9—The difference between the two temperature measurements may not be a constant for a given rheometer but may vary with differences between the test temperature and the ambient laboratory temperature as well as with fluctuations in ambient temperature. The difference between the two temperature measurements is caused in part by thermal gradients in the test specimen and fixtures.

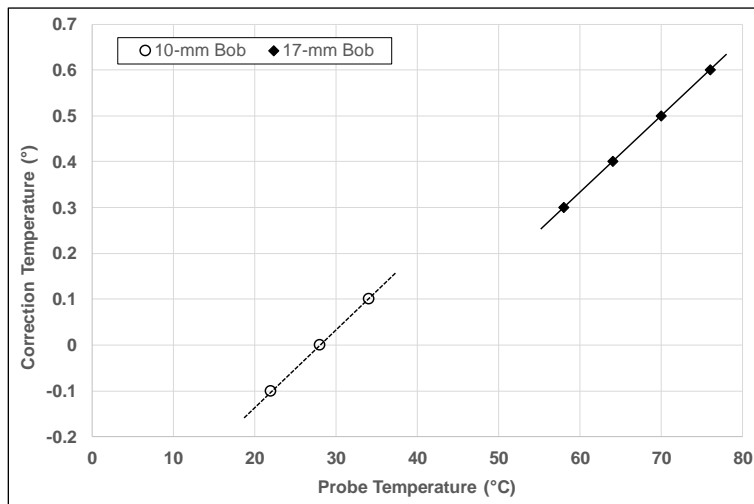


Figure 2—Example Determination of Temperature Correction

- 9.5. *Verification of DSR*—Verify the accuracy of the torque transducer and angular displacement transducer.

Note 10—A newly installed or reconditioned instrument should be verified on a weekly basis using the procedures in Section 9.5 until acceptable verification has been demonstrated. Maintaining the data in the form of a control chart where the verification measurements are plotted versus calendar date is recommended (see Appendix X2).

- 9.5.1. *Verification of Torque Transducer*—Verify the calibration of the torque transducer a minimum of once every six months using a reference fluid or manufacturer-supplied fixtures when the calibration of the torque transducer is suspect or when the dynamic viscosity, as measured for the reference fluid, indicates that the torque transducer is not in calibration.

- 9.5.1.1. *Verification of Torque Transducer with Reference Fluid*—The complex viscosity measured with the DSR shall be within 3 percent of the capillary viscosity as reported by the manufacturer of the reference fluid; otherwise, the calibration of the torque

transducer shall be considered suspect. Calculate the complex viscosity as the complex modulus, G^* , divided by the angular frequency in rad/s. Recommended practice for using the reference fluid is given in Appendix X3.

$$\text{Percent Variance} = \left[\frac{(\eta_a - \eta_b)}{\eta_a} \right] \times 100 \quad (1)$$

where:

η_a = the standard capillary viscosity as reported by the supplier of the reference fluid;
and

η_b = the measured viscosity as calculated from the complex modulus, G^* , divided by the angular frequency in rad/s.

Note 11—A suitable reference fluid is available from Cannon Instrument Company as Viscosity Standard Number N2700000SP. The viscosity of the standard is reported in mPa/s. Convert the viscosity measurements to mPa/s before calculating the percent variance.

- 9.5.1.2. *Verification of Torque Transducer with Fixtures*—Verify the calibration of the torque transducer using the manufacturer-supplied fixtures in accordance with the instructions supplied by the manufacturer. Suitable manufacturer-supplied fixtures are not widely available. If suitable fixtures are not available, this requirement shall be waived.
- 9.5.2. *Verification of Angular Displacement Transducer*—If manufacturer-supplied fixtures are available, verify the calibration every six months or when the calibration of the DSR is suspect. If suitable fixtures are not available, this requirement shall be waived.
- 9.5.3. If the DSR cannot be successfully verified according to Section 9.5, it shall not be used for testing in accordance with this standard until it has been successfully calibrated by the manufacturer or other qualified service personnel.

10. PREPARING SAMPLES AND TEST SPECIMENS

- 10.1. *Preparing Test Samples*—If unaged binder is to be tested, obtain test samples according to R 66.
- 10.2. *Preparing Disposable Cups*—Mark the required binder height on the inside of the cup according to the DSR manufacturer's requirements. This mark must not be higher than 1 mm above the top of bob.
- Note 12**— The binder quantity required in the cup depends on the bob size. Tests with larger bob sizes (e.g., 17 mm for high temperature tests) typically require between 22 and 24 g of binder. Tests with smaller bob sizes (e.g., 10 mm for intermediate temperature tests) typically require between 30 and 32 g. The bob must be fully submerged in the binder, but the binder must not be more than 1 mm above the top of the bob.
- 10.3. *Mounting the Bob*—Mount the appropriate sized bob (size will differ for the high- and intermediate-temperature tests) onto the DSR and lower it to the testing position. Close the hood or environmental chamber and then preheat the proportional temperature controller to 135°C. Raise the bob again immediately prior to placing the cup with binder into the temperature controller.
- 10.4. *Determining Binder Weight*—Place the marked cup onto the scale. Pour heated binder up to the mark. Note the weight to nearest 0.1g. Pour this weight of binder into each of the replicate cups that will be tested. Repeat this process for each binder tested.

- 10.5. *Transferring the Specimen and Inserting the Bob*—Immediately after pouring the binder into the cup, transfer the cup into the temperature controller unit using the DSR manufacturers supplied cup holder. Gently lower the bob into the asphalt to the testing position as specified by the equipment manufacturer.

Note 13—This procedure may vary based on the manufacturer’s recommendations.

11. TESTING PROCEDURE

- 11.1. Bring the specimen to the test temperature $\pm 0.1^\circ\text{C}$.
- 11.1.1. When testing a binder for compliance with M 320 and/or M 332, select the test temperature from the appropriate table in M 320/M 332.
- 11.1.2. When conducting a temperature sweep, start at a midrange test temperature and increase or decrease the test temperature to cover the desired range of test temperatures. (See Sections 6 and 7 in R 29.)
- 11.2. Set the temperature controller to the desired test temperature, including any offset as required by Section 9.4.4. Allow the temperature indicated by the resistance temperature detector (RTD) to come to the desired temperature. The test shall be started only after the temperature has remained at the desired temperature $\pm 0.1^\circ\text{C}$ for at least 20 minutes.

Note 14—It is impossible to specify a single equilibration time that is valid for DSRs produced by different manufacturers. The design (fluid bath or air oven) of the environmental control system and the starting temperature will dictate the time required to reach the test temperature. Reaching temperature equilibrium with the concentric cylinder geometry will take longer than the time needed when using the parallel plate geometry. Care should be taken to avoid extended heating to minimize effects of hardening. It is suggested that an additional specimen of each binder is prepared to determine the time required to reach equilibrium for that binder. Use this time for the tests on each replicate specimen. The method for determining the correct thermal equilibrium time is described in Appendix X9.

- 11.3. *Strain Control Mode*—When operating in a strain-controlled mode, determine the strain value according to the value of the complex modulus. Control the strain within 20 percent of the target value calculated by Equation 2.

$$\gamma = \frac{12}{(G^*)^{0.29}} \quad (2)$$

where:

γ = shear strain in percent, and

G^* = complex modulus in kPa.

- 11.3.1. When testing specimens for compliance with M 320 and/or M 332, select an appropriate strain value from Table 2. Software is available with the dynamic shear rheometers that will control the strain automatically without control by the operator.

Table 5—Target Strain Values

Material	kPa	Strain, percent	
		Target Value	Range
Original binder	1.0 $G^*/\sin(\delta)$	12	9 to 15
RTFO residue	2.2 $G^*/\sin(\delta)$	10	8 to 12
PAV residue	5000 $G^*\sin(\delta)$	1	0.8 to 1.2

- 11.4. *Stress Control Mode*—When operating in a stress-controlled mode, determine the stress level according to the value of the complex modulus. Control the stress within 20 percent of the target value calculated by Equation 3.

$$\tau = 12.0(G^*)^{0.71} \quad (3)$$

where:

τ = shear stress in kPa, and

G^* = complex modulus in kPa.

- 11.4.1. When testing specimens for compliance with M 320 and/or M 332, select an appropriate stress level from Table 3. Software is available with the dynamic shear rheometers that will control the stress level automatically without control by the operator.

Table 6—Target Stress Levels

Material	kPa	Stress, kPa	
		Target Level	Range
Original binder	1.0 $G^*/\sin(\delta)$	0.12	0.09 to 0.15
RTFO residue	2.2 $G^*/\sin(\delta)$	0.22	0.18 to 0.26
PAV residue	5000 $G^*\sin(\delta)$	50.0	40.0 to 60.0

- 11.5. When the temperature has equilibrated, condition the specimen by applying the required strain for a recommended 10 cycles or a required range of 8 to 16 cycles at a frequency of 10 rad/s (see Note 14). Obtain a test measurement by recording data for an additional recommended 10 cycles or a range of 8 to 16 cycles. Reduce the data obtained for the second set of cycles to produce a value for the complex modulus and phase angle. Typically, a Fast Fourier Transform is used to reduce the data. Multiple measurements may be obtained to verify that the sample is properly prepared. Slipping between the bob and the binder can result in a decrease in the modulus with repeat measurements. Some asphalt binders may exhibit a reduced modulus with continued application of shear stresses (multiple measurements). The data acquisition system automatically acquires and reduces the data when properly activated. When conducting tests at more than one frequency, start testing at the lowest frequency and increase to the highest frequency.

Note 15—The standard frequency of 10 rad/s is used when testing binder for compliance with M 320 and/or M 332.

- 11.6. The data acquisition system specified in Section 6.1.4 automatically calculates G^* and δ from test data acquired when properly activated.
- 11.7. Initiate the testing immediately after preparing and pouring the specimen. The testing at subsequent temperatures should be done as quickly as possible to minimize the effect of molecular associations (steric hardening) that can cause an increase in modulus if the specimen is held in the rheometer for a prolonged period of time. When testing at multiple temperatures all testing should be completed within 4 hours.

12. INTERPRETATION OF RESULTS

- 12.1. The dynamic modulus and phase angle depend upon the magnitude of the shear strain; the modulus and phase angle for both unmodified and modified asphalt binder decrease with increasing shear strain as shown in Figure 3. A plot such as that shown

in Figure 4 can be generated by gradually increasing the load or strain amplitude, thereby producing a strain sweep. It is not necessary to generate such sweeps during normal specification testing; however, such plots are useful for verifying the limits of the linear region.

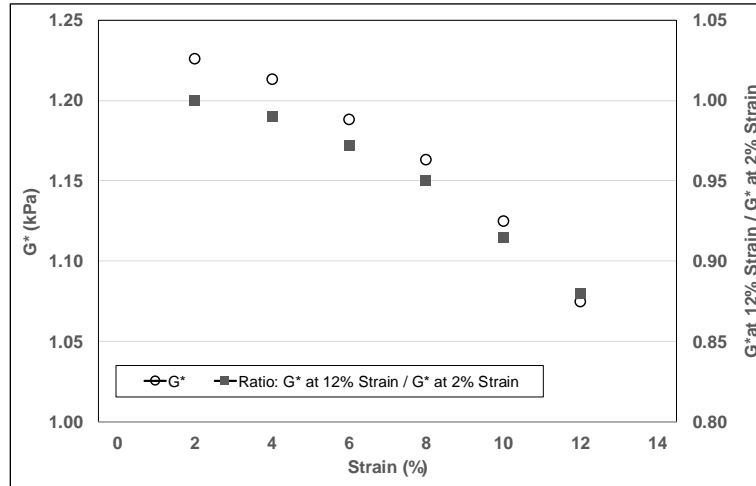


Figure 3—Example of Strain Sweep

- 12.2. A linear region may be defined at small strains where the modulus is relatively independent of shear strain. This region will vary with the magnitude of the complex modulus. The linear region is defined as the range in strains where the complex modulus is 95 percent or more of the zero-strain value.
- 12.3. The shear stress varies linearly from the edge of the bob to a maximum at the extremities of the cup perimeter. The shear stress is calculated from the applied or measured torque, measured or applied strain, and the geometry of the test specimen.

13. REPORT

- 13.1. A sample report format is given in Appendix X13. Provide a complete identification and description of the material tested including name, grade, and source.
- 13.2. Describe the instrument used for the test including the model number.
- 13.3. The strain and stress levels specified in Tables 2 and 3 have been selected to ensure a common reference point that has been shown to be within the linear region for neat and modified asphalt binders. Some systems may not be linear within this region. When this situation is observed, report the modulus at the recommended stress or strain levels but also report that the test conditions were outside the linear region.
- 13.4. *For each test, report the following:*
- 13.4.1. Test bob diameter, nearest 0.1 mm, and test cup diameter, nearest 0.1 mm;
- 13.4.2. Test temperature, nearest 0.1°C;
- 13.4.3. Test frequency, nearest 0.1 rad/s;

- 13.4.4. Strain amplitude, nearest 0.01 percent, or torque, nearest mN·m;
- 13.4.5. Complex modulus (G^*) for the 10 measurements, kPa to three significant figures;
- 13.4.6. Phase angle (δ) for the second 10 cycles, nearest 0.1 degrees; and
- 13.4.7. $G^*/\sin(\delta)$, nearest 0.01 kPa, or $G^*\sin(\delta)$, nearest whole number.

14. PRECISION AND BIAS

- 14.1. *To be completed after inter/intra laboratory study*

15. KEYWORDS

- 15.1. Dynamic shear rheometer; DSR; concentric cylinder; complex modulus; GTR, asphalt binder.

APPENDICES

(Nonmandatory Information)

X1. TESTING FOR LINEARITY

X1.1. Scope:

X1.1.1. This procedure is used to determine whether an unaged asphalt binder exhibits linear or nonlinear behavior at the upper grading temperature, e.g., 52, 58, 64, 70, 76, or 82°C. The determination is based on the change in complex shear modulus at 10 rad/s when the strain is increased from 2 to 12 percent.

X1.2. Procedure:

X1.2.1. Verify the DSR and its components in accordance with Section 9 of this standard.

X1.2.2. Prepare the DSR in accordance with Section 10 of this standard.

X1.2.3. Prepare a test specimen for testing with the high temperature test configuration as per Section 11 of this standard. Select the test temperature as the upper grading temperature for the binder in question.

X1.2.4. Determine the complex shear modulus at 2 and 12 percent strain following the test procedure described in Section 12 except as noted below. Always start with the lowest strain and proceed to the next larger strain.

X1.3. *Strain -Controlled Rheometers*—If the software provided with the DSR will automatically conduct tests at multiple strains, program the DSR to obtain the complex shear modulus at strains of 2, 4, 6, 8, 10, and 12 percent. If this automatic feature is not available, test by manually selecting strains of 2, 4, 6, 8, 10, and 12 percent strain.

X1.4. For stress-controlled rheometers, compute the starting stress based on the complex shear modulus, G^* , and shear stress, τ , as determined at the upper grading temperature during the grading of the binder. At this temperature the complex modulus, G^* , will be greater than or equal to 1.00 kPa and the shear stress, τ , will be between 0.090 and 0.150 kPa (see Table 2). Calculate the starting stress as $\tau / 6.00$ kPa. Increase the stress in five increments of $\tau / 6.00$ kPa.

Note X1—*Sample calculation*: Assume a PG 64-22 asphalt binder with $G^* = 1.29$ kPa at 64°C and $\tau = 0.135$ kPa. The starting stress will be $1.35\text{kPa}/6 = 0.225$ kPa. Test at 0.225, 0.450, 0.675, 0.900, 1.13, and 1.35 kPa, starting with 0.225 kPa.

X1.5. *Plot of Complex Modulus Versus Strain*—Prepare a plot of complex shear modulus versus percent strain as shown in Figure 3. From the plot, determine the complex shear modulus at 2 and 12 percent strain.

X1.6. Calculations:

X1.6.1. Calculate the modulus ratio as the complex shear modulus at 12 percent strain divided by the complex shear modulus at 2 percent strain.

X1.7. Report:

X1.7.1. Report the following:

X1.7.1.1. Complex shear modulus (G^*) to three significant figures;

X1.7.1.2. Strain, nearest 0.1 percent;

X1.7.1.3. Frequency, nearest 0.1 rad/s; and

X1.7.1.4. The ratio calculated by dividing the modulus at 12 percent strain by the modulus at 2 percent strain.

X1.8. *Data Interpretation:*

X1.8.1. The measurement was performed in the nonlinear range of the material if the modulus ratio as calculated in Section X1.6.1 is <0.900 and linear if ≥ 0.900 . If the measurement was performed in the nonlinear range of the material, the results obtained under this standard will be considered as invalid for grading a binder according to M 320 and/or M 332.

X2. CONTROL CHART

X2.1. *Control Charts:*

X2.1.1. Control charts are commonly used by various industries, including the highway construction industry, to control the quality of products. Control charts provide a means for organizing, maintaining, and interpreting test data. As such, control charts are an excellent means for organizing, maintaining, and interpreting DSR verification test data. Formal procedures based on statistical principles are used to develop control charts and the decision processes that are part of statistical quality control.

A quality control chart is simply a graphical representation of test data versus time. By plotting laboratory measured values for the reference fluid in a control chart format, it is easy to see when:

- The measurements are well controlled and both the device and the operator are performing properly.
- The measurements are becoming more variable with time, possibly indicating a problem with the test equipment or the operator.
- The laboratory measurements for the fluid are, on the average above or below the target (reference fluid) value.

Many excellent software programs are available for generating and maintaining control charts. Some computer-based statistical analysis packages contain procedures that can be used to generate control charts. Spreadsheets such as Microsoft's Excel can also be used to generate control charts and, of course, control charts can be generated manually. (See Table X3.1 as an example.)

X2.2. *Care in Selecting Data:*

X2.2.1. Data used to generate control charts should be obtained with care. The idea of randomness is important but need not become unnecessarily complicated. An example will show why a random sample is needed; a laboratory always measures the reference fluid at the start of the shift or workday. These measurements could be biased by start-up errors such as a lack of temperature stability when the device is first turned on. The random sample ensures that the measurement is representative of the process or the material being tested. Said another way, a random sample has an equal chance of being drawn as any other sample. A measurement or sample always taken at the start or end of the day, or just before coffee break, does not have this chance.

X3. EXAMPLE

X3.1. The power of the control chart is illustrated in Table X3.1 using the verification data obtained for the DSR. Other DSR verification data suitable for a quality control chart presentation include

measurements for determining the temperature correction, calibrating the electronic thermometer, and maintaining data from internally generated asphalt binder reference samples. For this example, the reported viscosity for the reference fluid is 271 Pa/s; hence, the calculated value for G^* is 2.71 kPa. This value for G^* is labeled as “ G^* from “Reference Fluid” in Figure X3.1. The laboratory should obtain this value on average if there is no laboratory bias.

Table X3.1—Sample Test Data

Week	Measured G^* , kPa
1	2.83
2	2.82
3	2.77
4	2.72
5	2.69
6	2.72
7	2.77
8	2.75
9	2.71
10	2.82
11	2.66
12	2.69
13	2.75
14	2.69
15	2.73
16	2.77
17	2.72
18	2.67
19	2.66
20	2.78
21	2.74
22	2.69
Average	2.73
Std. Dev.	0.051
CV %	1.86

X3.2. *Comparison of 22-Week Laboratory Average for G^* with Value Calculated from Reference Fluid:*

X3.2.1. The 22-week average of the laboratory measurements is labeled as “22-Week Laboratory Average” in Figure X3.1. Over the 22 weeks for which measurements were made, the average was 2.73 kPa. This value compares favorably with the calculated reference value, 2.71 kPa, differing on the average by only 0.7 percent. There appears to be little laboratory bias in this data.

X3.3. *Comparison of CV of Laboratory Measurements with Round-Robin CV:*

X3.3.1. From a previous round-robin study, the within laboratory standard deviation (d1s) for the fluid was reported as 0.045 (CV = 1.67 percent). The 22-week standard deviation for the measured values of G^* is 0.051 (CV = 1.86 percent), as compared to 0.045 (CV = 1.67 percent) reported from the round robin. However, it should be pointed out that the 22-week CV, 1.86 percent, also includes day-to-day variability, a component of variability not included in the round-robin d1s value. Based on this information the variability of the laboratory measurements is acceptable.

X3.4. *Variability of Measured Values:*

X3.4.1. In Figure X3.1, the value of G^* calculated from the reference fluid is shown as a solid line. Also shown are two dotted lines that represent the G^* calculated from the reference fluid ± 2 d1s

where $d1s$ is the value from the round robin. The calculated reference value for the fluid is 2.71 kPa, and the standard deviation is 0.045. Thus, a deviation of 2 $d1s$ gives values of:

$$2.71\text{kPa} \pm (2) (0.045) = 2.80 \text{ kPa}, 2.62 \text{ kPa} \quad (\text{X3.1})$$

If the laboratory procedures are under control, the equipment is properly calibrated, and there is no laboratory bias, 95 percent of the measurements should fall within the limits 2.62 kPa and 2.80 kPa. Laboratory measurements outside this range are suspect, and the cause of the outlier should be investigated. The outlier may be the result of either testing variability or laboratory bias. The measurement from Week 10 in Figure X3.1 falls outside the $\pm 2 d1s$ limits and is cause for concern such that testing procedures and verification should be investigated.

If a measurement deviates from the target, in this case G^* from the reference fluid, by more than $\pm 3 d1s$, corrective action should be initiated. The $\pm 3 d1s$ limits 99.7 percent of the measured values if the laboratory procedures are under control and the equipment is properly calibrated.

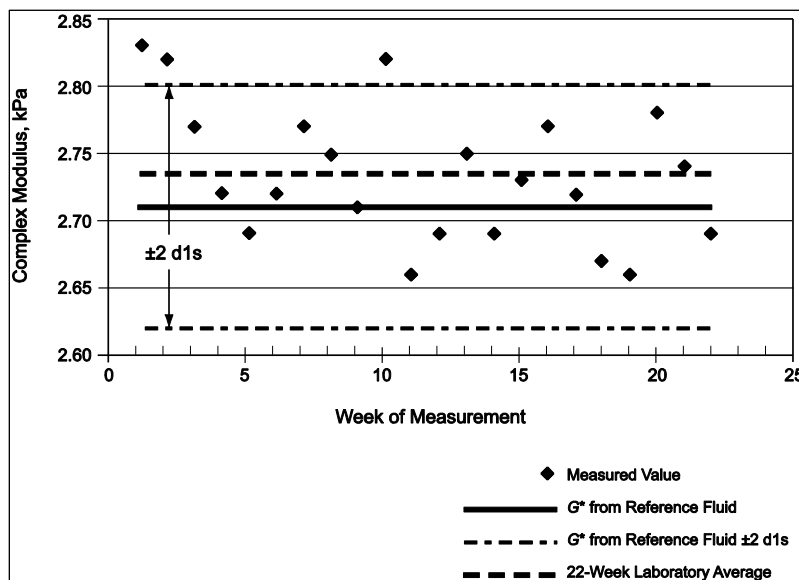


Figure X3.1—Control Chart

X3.5. Trends in Measured Value:

X3.5.1. The control chart can also be used to identify unwanted trends in the data. For example, from Weeks 1 to 5, a steady decrease in the measured value is observed. This is cause for concern and the reason for the trend should be investigated. More sophisticated rules for analyzing trends in control charts can be found elsewhere.

X4. USE OF REFERENCE FLUID

X4.1. Source of Reference Fluid:

X4.2. An organic polymer produced by Cannon Instrument Company as Viscosity Standard N2700000SP has been found suitable as reference fluid for verifying the calibration of the DSR. The viscosity of the fluid, as determined from NIST-traceable capillary viscosity measurements, is approximately 270 Pa/s at 64°C. However, the viscosity of the fluid varies from one lot to the next. The lot-specific viscosity is printed on the label of the bottle.

X5. CAUTIONS IN USING REFERENCE FLUID

- X5.1. Some items of caution when using the reference fluid are:
- The fluid cannot be used to verify the accuracy of the phase angle measurement.
 - The fluid must not be heated as heating can degrade the fluid, causing a change in its viscosity.
 - The fluid should be used for verification only after the DSR temperature measurements are verified.
 - The fluid cannot be used to calibrate the torque transducer. The manufacturer or other qualified service personnel using a calibration device designed specifically for the rheometer should perform the calibration. These calibration devices are typically not available in operating laboratories.
 - When tested at 10 rad/s, the reference fluid should be used only at 64°C and above. At lower temperatures, the fluid is viscoelastic; hence, the viscosity, η , reported on the certificate by Cannon will not match the complex viscosity $\eta^* = G^*/10$ rad/s determined from the measurement.
 - Bubbles in the fluid will have a dramatic effect on the measured value of G^* . The fluid in the bottle should be free of bubbles and care must be taken not to introduce bubbles when preparing test specimens. Recommended procedures for preparing test specimens are given in Appendix X7.

X6. CALCULATION OF G^* FROM STEADY-STATE VISCOSITY MEASUREMENTS

- X6.1. Among the different methods for converting between dynamic and steady-state viscosity of polymers, the most popular and most successful is the so-called Cox-Merz empirical rule. The rule leads, in simplified terms, to the following approximation.

$$\frac{G^*}{\omega} \sim \eta \quad (\text{X6.1})$$

where:

- G^* = the complex modulus;
- ω = the angular frequency in radians/s; and
- η = the shear rate independent capillary viscosity as reported by the supplier of the reference fluid.

For this rule to apply the measurements must be in the viscous region where the phase angle approaches 90 degrees. The value of the complex modulus is then simply 10 times the value of the capillary viscosity. For example, if the capillary viscosity is 270,000 mPa/s the complex modulus is:

$$G^*, \text{ kPa} \approx (270,000 \text{ mPa}\cdot\text{s})(1 \text{ kPa}/1,000,000 \text{ mPa})(10 \text{ rad/s}) = 2.70 \text{ kPa}\cdot\text{rad} \quad (\text{X6.2})$$

The reference fluid behaves as a viscous fluid at 64°C and above and provides very accurate estimates of G^* above 64°C. At temperatures below 58°C the fluid gives incorrect values for G^* with the error increasing as the temperature departs from 64°C. At 64°C and above G^* divided by the frequency in radians per second should be no more than 3 percent different than the viscosity printed on the bottle label. If this is the case, then the torque calibration should be considered suspect.

X7. DETERMINATION OF TIME TO THERMAL EQUILIBRIUM

X7.1. *Reason for Determining Time Required to Obtain Thermal Equilibrium:*

- X7.1.1. After the test specimen has been mounted in the DSR, it takes some time for the asphalt binder in the cup to reach thermal equilibrium. Because of thermal gradients within the test specimen, it may take longer for the test specimen to come to thermal equilibrium than the time indicated by the DSR thermometer. Therefore, it is necessary to experimentally determine the time required for the test specimen to reach thermal equilibrium.
- X7.1.2. The time required to obtain thermal equilibrium varies for different rheometers. Factors that affect the time required for thermal equilibrium include:
- X7.1.3. Design of the rheometer and whether air or liquid is used as a heating/cooling medium;
- X7.1.4. Difference between ambient temperature and the test temperature, different when testing below room temperature, and above room temperature;
- X7.2. It is not possible to specify a single time as the time required to obtain thermal equilibrium. For example, thermal equilibrium is reached much quicker with liquid-controlled rheometers than with air-cooled rheometer. This requires that the time to thermal equilibrium be established for individual rheometers, typical testing temperatures, and testing conditions.

X8. METHOD TO DETERMINE THE TIME REQUIRED TO OBTAIN THERMAL EQUILIBRIUM

- X8.1. A reliable estimate of the time required for thermal equilibrium can be obtained by monitoring the DSR temperature and the complex modulus of a sample in the cup. Because the modulus is highly sensitive to temperature, it is an excellent indicator of thermal equilibrium. The following procedure is recommended for establishing the time to thermal equilibrium:
 - X8.1.1. Place an unmodified asphalt binder specimen in the DSR and bring the test chamber or fluid to the test temperature. The modulus of the selected binder should not change with repeated shearing.
 - X8.1.2. Operate the rheometer in a continuous mode at 10 rad/s. Use the smallest strain value that gives good measurement resolution.
 - X8.1.3. Record the modulus at 30-s time intervals, and plot the modulus versus time (Figure X8.1).

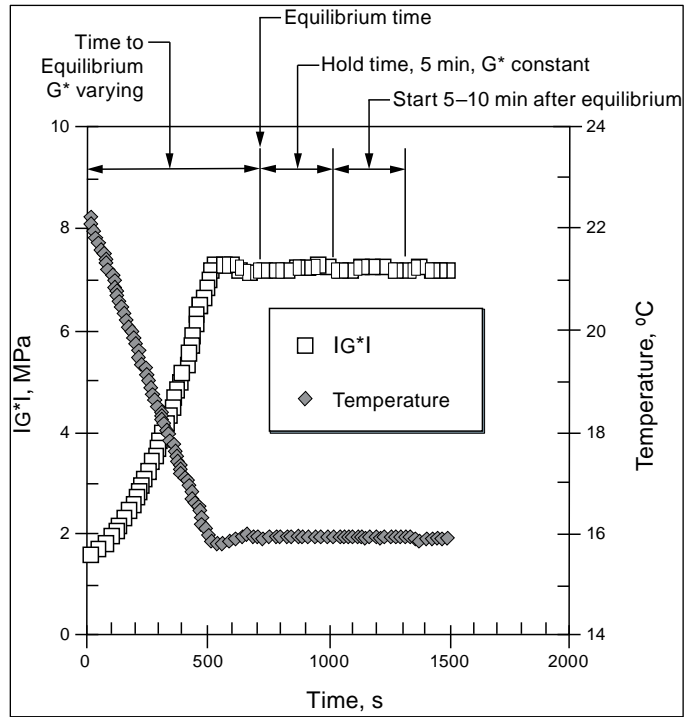


Figure X8.1—Determining Thermal Equilibrium Time

- X8.2. The time to reach thermal equilibrium is the time required to reach a constant modulus. Typically, this time will be greater than the time required to reach a constant reading on the DSR thermometer.
- X8.3. Because the time required to reach thermal equilibrium will vary with the test temperature and testing conditions, the time to thermal equilibrium should be established separately for both high- and intermediate-temperature measurements. Once the time to thermal equilibrium has been established, it does not have to be repeated unless the test conditions change.

X9. SAMPLE REPORT

Header Information:

Item	Data Group 1	Item	Data Group 2
Operator's Name:	24 Alpha-Numeric	Date of Test (dd/mm/yy):	__/__/__
Test Specimen ID No.:	18 Alpha	Time of Test (hr:min):	_:__
Project ID No.:	12 Alpha-Numeric	DSR Manufacturer:	12 Alpha-Numeric
File Name:	12 Alpha-Numeric	DSR Model:	12 Alpha-Numeric
Bob Diameter, Nearest 0.01 mm:	00.00	DSR Serial Number or Other Identifying ID No.:	18 Alpha-Numeric
Test Frequency, rad/s:	0.00	Software Version:	12 Alpha-Numeric
Test Gap, 0.01 mm:	00.00		

Test Results for Grading (Use separate column for each test temperature):

Measurements	Data Group 3	Data Group 4	Data Group 5	Data Group 6
Test Specimen Temperature, 0.1°C	0.00	0.00	0.00	0.00
Temperature Correction at Test Temperature, 0.1°C	0.00	0.00	0.00	0.00
Stress Amplitude, kPa	0.00	0.00	0.00	0.00
Strain Amplitude, percent	0.00	0.00	0.00	0.00
Complex Modulus, G^* , kPa	0.00	0.00	0.00	0.00
Phase Angle, degrees	00.0	00.0	00.0	00.0
Complex Modulus/sin(Phase Angle)	0.00	0.00	0.00	0.00
Complex Modulus \times sin(δ) (Phase Angle)	00.0	00.0	00.0	00.0
Comments generated by DSR software (Example: "This material passes.")				
At end of file, 276 alphanumeric field for operator comments and comments, if any, generated by DSR software.				

Test Results for Linearity Determination:

Measurements	Data Group 7					
Test Specimen Temperature, 0.1°C	0.00					
Temperature Correction at Test Temperature, 0.1°C	0.00					
	Data Group 8	Data Group 9	Data Group 10	Data Group 11	Data Group 12	Data Group 13
Measurements		0.00	0.00	0.00	0.00	0.00
Stress Amplitude, kPa	0.00	0.00	0.00	0.00	0.00	0.00
Strain Amplitude, percent	0.00	0.00	0.00	0.00	0.00	0.00
Complex Modulus, G^* , kPa	0.00	00.0	00.0	00.0	00.0	00.0
Phase Angle, degrees	00.0	00.0	00.0	00.0	00.0	00.0
At end of file, 276 alphanumeric field for operator comments and comments, if any, generated by DSR software.						

X10. REFERENCES

- X10.1. Anderson, D. A. and M. Marasteanu. “*Manual of Practice for Testing Asphalt Binders in Accordance with the Superpave PG Grading System.*” The Pennsylvania Transportation Institute, The Pennsylvania State University, PTI 2K07, November 1999 (Revised February 2002).
- X10.2. Anderson, D. A., C. E. Antle, K. Knechtel, and Y. Liu. *Interlaboratory Test Program to Determine the Inter- and Intra-Laboratory Variability of the SHRP Asphalt Binder Tests.* FHWA, 1997.
- X10.3. Cox, W. P. and E. H. Merz. Correlation of Dynamic and Steady Flow Viscosities. *Journal of Polymer Science*, Vol. 28, 1958, pp. 619–622.
- X10.4. Wadsworth, H., ed. *Handbook of Statistical Methods for Engineers and Scientists.* McGraw-Hill, New York, NY, 1990.

Standard Method of Test for

**Effect of Heat and Air on a Moving Film
of Asphalt Binder (Rolling Thin-Film
Oven Test)**

AASHTO Designation: T 240-13 (2017)



**American Association of State Highway and Transportation Officials
444 North Capitol Street N.W., Suite 249
Washington, D.C. 20001**

Standard Method of Test for

Effect of Heat and Air on a Moving Film of Asphalt Binder (Rolling Thin-Film Oven Test)

AASHTO Designation: T 240-13 (2017)



PART B: PROCEDURES FOR ASPHALT RUBBER BINDER

1. SCOPE

- 1.1. This test is used to measure the effect of heat and air on a moving film of asphalt rubber binder and to provide residue for additional testing. The effects of this treatment are determined from measurements of the properties of the asphalt rubber binder before and after the test.
- 1.2. The values stated in SI units are to be regarded as the standard.
- 1.3. *This standard may involve hazardous materials, operations, and equipment. This standard does not purport to address all of the safety concerns associated with its use. It is the responsibility of the user of this procedure to establish appropriate safety and health practices and to determine the applicability of regulatory limitations prior to use.*

2. REFERENCED DOCUMENTS

No change

3. SUMMARY OF TEST METHOD

- 1.1. A moving film of asphaltic material is heated in an oven for 85 min at 190°C (374°F). The effects of heat and air are determined from changes in the physical test values as measured before and after the oven treatment. The residue from this test is also used for additional testing as required in M 320 and M 332. An optional procedure is provided for determining the change in sample mass.
- 1.2. Precision values for this method have not been developed.

4. SIGNIFICANCE AND USE

- 4.1. This method indicates the approximate change in properties of asphalt rubber binder during conventional batch plant mixing at about 190°C (374°F) as indicated by viscosity and other rheological measurements. The residue from this test is also used to determine the conformance of an asphalt rubber binder to M 320 and M 332. It yields a residue that approximates the condition of the asphalt rubber binder immediately after the pavement is constructed. If the mixing temperature differs appreciably from 190°C (374°F), more or less effect on the properties will occur. This method can also be used

to determine mass change, which is a measure of asphalt rubber binder volatility and mass changes resulting from oxidation.

5. APPARATUS

No change

6. PREPARATION OF OVEN

No change

7. PROCEDURE

- 7.1. The sample as received shall be free of water. Heat the sample in its container with a loosely fitted cover in an oven not to exceed 190°C (374°F) for the minimum time necessary to ensure that the sample is completely fluid. Manually stir the sample but avoid incorporating air bubbles.
- 7.2. Place the bottles in the oven at 190°C (374°F), preferably on a rack, 10 minutes prior to pouring. When mass change is to be determined, label the containers and record the mass of two empty containers, using an analytical balance having an accuracy of 0.001 g, before the 10-minute preheating. Pour 45 g ± 3 g of the sample into each of the number of glass containers required to provide sufficient material for the tests that are to be performed on the residue.
- 7.3. Immediately after pouring the sample into a glass container, turn the container to a horizontal position. Rotate the container slowly for at least one full rotation, and attempt to precoat its cylindrical surface. It is not necessary to precoat the open end of the container, and care should be taken to prevent the sample from flowing out of the container during this step. Ensure that the asphalt rubber binder does not coat the central part of the open end of the container. Place the container horizontally in a clean cooling rack that is maintained in a draft-free, room-temperature location away from ovens or other sources of heat.
- Note 5**—Asphalt rubber binder will quickly lose temperature during bottle-coating. It is therefore important to place the container back in the oven immediately after pouring to maintain workability.
- Note 6**—Complete precoating of the bottle may take additional time for asphalt rubber binders.
- Note 7**—For maximum precision in determining mass change, the cooling rack should be in a location that is the same temperature and humidity as the balance used for measuring the mass of the containers.
- Note 8**—Static electricity may cause unstable mass measurements, due in part to the characteristics of the glass sample containers. This problem can be minimized by mounting a passive ion source inside the balance draft shield.
- 7.4. Allow the glass containers to cool in the cooling rack for at least 60 min but no more than 180 min before placing the containers in the oven.
- 7.5. When mass change is being determined, use two separate containers for this determination. After cooling, determine the mass of these containers using an analytical balance having a resolution of 0.001 g or better. Separately place each container vertically on the balance and record the mass to the full resolution of the balance.

- 7.6. With the oven at operating temperature and the airflow set at 4000 ± 300 mL/min, arrange the containers holding the asphalt rubber binder in the carriage so that the carriage is balanced. Fill any unused spaces in the carriage with empty containers. Close the door, and rotate the carriage assembly at a rate of 15 ± 0.2 r/min. Maintain the glass containers in the oven with the air flowing and the carriage rotating for 85 min. The test temperature of $190 \pm 1.0^\circ\text{C}$ ($374 \pm 2^\circ\text{F}$) shall be reached within the first 15 min—otherwise discontinue the test.
- 7.7. At the conclusion of the testing period, remove any containers for mass change determination, and place them horizontally in the cooling rack. Then remove each remaining container, one at a time, and transfer its contents to a collection container having a capacity at least 30 percent greater than the total expected volume of residue. This transfer shall be accomplished by first pouring out any residue that will flow freely from the container, and then scraping out as much of the remaining residue as practical. While the residue is being removed from each container, the oven door shall remain closed, with the heater power on, the air on, and the remaining samples rotating in the carriage. The final container shall be removed from the oven within 5 min of removal of the initial container.
- Note 9**—Any scraping tool may be used, as long as an average of 80-90 percent or more of the residue is removed from the sample containers. It has been determined that circumferential scraping tends to be more effective than lengthwise scraping.
- 7.8. After removing the residue from each of the containers, gently stir the residue in the collection container to homogenize the residue without introducing air into it.
- 7.9. If the mass change is being determined, allow the designated containers to cool on the cooling rack for at least 60 min but not more than 180 min. After cooling, determine the mass of these containers using an analytical balance having a resolution of 0.001 g or better. Separately place each container vertically on the balance, and record the mass to the full resolution of the balance.
- 7.9.1. Make a note on the report if any sample appears to have flowed out of the container. If mass has flowed from the container, do not use the container for mass change determination. The results from one container may be used to determine mass change if mass has flowed from the container. If only one container is used to determine mass change, note it on the report. Use two containers for referee purposes.
- Note 10**—Problems with the asphalt rubber binder flowing from the container during the test have been reported. If this occurs, check the levelness of the circular openings in the carriage and the dimensions of the container. Containers with a small annular ring appear to be particularly susceptible to this problem.
- Note 11**—To improve mass change precision, the containers used for determining mass change should be handled only with clean gloves or tongs. Transfer to the balance should be done with tongs to prevent contamination and temperature changes, which could distort the mass measurement.

8. REPORT

No change

9. PRECISION AND BIAS

- 9.1. The sample as received shall be free of water. Heat the sample in its container with a loosely fitted cover in an oven not to exceed 190°C (374°F) for the minimum time necessary to ensure that the sample is completely fluid. Manually stir the sample but avoid incorporating air bubbles.

APPENDIX

No change

Standard Practice for Accelerated Aging of Asphalt Binder Using a Pressurized Aging Vessel (PAV)

AASHTO Designation: R 28-12 (2016)

DRAFT

AASHTO

**American Association of State Highway and Transportation Officials
444 North Capitol Street N.W., Suite 249
Washington, D.C. 20001**

Standard Practice for Accelerated Aging of Asphalt Binder Using a Pressurized Aging Vessel (PAV)

AASHTO Designation: R 28-12 (2016)



PART B: PROCEDURES FOR ASPHALT RUBBER BINDER

1. SCOPE

- 1.1. This standard practice covers the accelerated aging (oxidation) of asphalt binders by means of pressurized air and elevated temperature. The practice is intended to simulate in-service oxidative aging of asphalt rubber binders and is intended for use with residue from T 240 (RTFOT).
- 1.2. The aging of asphalt rubber binders during service is affected by mixture-associated variables such as the volumetric proportions of the mix, permeability of the mix, properties of the aggregates, and possibly other factors. This practice is intended to provide an evaluation of the relative resistance of different asphalt rubber binders to oxidative aging at selected temperatures and cannot account for mixture variables.
- 1.3. *This standard may involve hazardous materials, operations, and equipment. This standard does not purport to address all of the safety concerns associated with its use. It is the responsibility of the user of this procedure to establish appropriate safety and health practices and to determine the applicability of regulatory limitations prior to use.*

2. REFERENCED DOCUMENTS

No change except:

- T 240, Effect of Heat and Air on a Moving Film of Asphalt Binder (Rolling Thin-Film Oven Test). Part B: Asphalt Rubber Binders

3. TERMINOLOGY

No change

4. SUMMARY OF TEST METHOD

- 4.1. Asphalt rubber binder is first aged using T 240, Part B (RTFOT). A specified thickness of residue, from the RTFOT, is then placed in stainless steel pans and aged at the specified aging temperature for 20 h in a vessel pressurized with air to 2.10 MPa. The aging

temperature is selected according to the grade of the asphalt rubber binder. At the completion of the PAV process, the asphalt rubber binder residue is then vacuum degassed.

5. SIGNIFICANCE AND USE

No change

6. APPARATUS

No change

7. MATERIALS

No change

8. HAZARDS

No change

9. CALIBRATION AND STANDARDIZATION

No change

10. PROCEDURE

10.1. Condition the asphalt rubber binder according to T 240, Part B (RTFOT)

10.2. Preheat the steel pans in an oven at 190°C for 10 minutes.

10.3. After combining the RTFOT residue into a single container and blending as specified in T 240, Part B; (1) pour the hot residue directly into the stainless steel pans, one pan at a time with the remaining preheated pans remaining in the oven until needed for immediate conditioning in the PAV, or (2) pour the residue into the stainless steel pans, cover and set aside for conditioning at a later time (Step 10.2 is still required), or (3) allow the residue to cool in the single container for conditioning at a later time (Step 10.2 is still required). If the residue is allowed to cool in the pans, reheat the pans and residue to the conditioning temperature. If the residue is stored in a single container, heat the residue, stir gently, and pour the heated residue into the pans (Step 10.2 is required).

10.4. Place the pan holder inside the pressure vessel. If an oven is used, place the pressure vessel inside the oven. If an integrated temperature control pressure vessel is used, turn on the heater. Select an aging temperature and preheat the pressure vessel to the aging temperature selected.

Note 4—If conditioning asphalt binders for conformance to M 320, select the appropriate aging temperature from Table 1 of M 320.

Note 5—Preheating the vessel 10 to 15°C above the conditioning temperature can be used to reduce the drop in PAV temperature during the loading process and minimize the time required to stabilize the system, after loading, to attain the required temperature.

Note 6—Aging temperature in the PAV is selected to account for different climatic regions. Temperatures in excess of approximately 115°C can change the chemistry of asphalt binders aged in accelerated tests and should be avoided.

- 10.5. Place the stainless steel pan on a balance and add 63 ± 1 g of asphalt rubber binder to the pan. This amount will yield approximately a 3.2-mm-thick film of asphalt binder.

Note 7— The mass change is not measured as part of this procedure. Mass change is not meaningful because the asphalt rubber binder absorbs air as a result of pressurization. Any gain in mass as a result of oxidation is masked by air absorbed by the asphalt rubber binder as a result of the pressurization.
- 10.6. If the vessel is preheated to other than the desired aging temperature, reset the temperature control on the heating device to the aging temperature.
- 10.7. Place the filled pans in the pan holder. (Pans containing asphalt rubber binders from different sources and grades may be placed in the pressure vessel during a single test.) Place the pan holder with filled pans inside the pressure vessel, and close the pressure vessel.
- 10.8. If an oven is used, place the loaded and closed pressure vessel in the oven.
- 10.9. Connect the temperature transducer line and the air pressure supply line to the loaded pressure vessel's external connections.
- 10.10. Perform the operations described in Sections 10.6 to 10.9 as quickly as possible to avoid cooling of the vessel and pan holder.
- 10.11. Wait until the temperature inside the pressure vessel is within 20°C of the aging temperature, apply an air pressure of 2.1 ± 0.1 MPa, and then start timing the test. If the temperature inside the vessel has not reached the desired temperature for applying pressure within 2 h of loading the pan holders and pans, discontinue the procedure and discard the asphalt samples.

Note 8—Pressures in excess of 2.1 MPa do not substantially increase the rate of aging. Therefore, higher pressures are not warranted.

Note 9—Once pressurized, the temperature inside the pressure vessel will equilibrate rapidly. The time under pressure, not to include any preheating time at ambient pressure, is the aging time. Relatively little aging occurs at ambient pressure during the time that the vessel is being reheated to the test temperature, given that asphalt binder residue under test has been exposed to 190°C in the RTFOT.
- 10.12. Maintain the temperature and air pressure inside the pressure vessel for $20 \text{ h} \pm 10 \text{ min}$.
- 10.13. At the end of the 20-h test period, slowly begin reducing the internal pressure of the PAV, using the air pressure bleed valve. Adjust the bleed valve to an opening that requires 9 ± 1 min to equalize the internal and external pressures on the PAV, thus avoiding excessive bubbling and foaming of the asphalt binder. During this process it may be necessary to adjust the setting of the needle valve as the pressure drops in order to maintain an approximate linear rate of pressure decrease. Do not include the pressure release and equalization time as part of the 20-h aging period.
- 10.14. If the temperature indicated by the temperature-recording device falls above or below the target aging temperature $\pm 0.5^\circ\text{C}$ for more than 60 min during the 20-h aging period, declare the test invalid and discard the material.

- 10.15. Remove the pan holder and pans from the PAV, and place the stainless steel pans in an oven set at a minimum temperature for a minimum time until sufficiently fluid to pour. Stir the residue in the pan gently to assist in the removal of air bubbles. If the binder is conditioned in multiple pans, pour the hot residue into a single container. Scrape residue remaining in the pans into the container, followed by gentle stirring to blend the residue. If the sample must be heated to temperatures greater than 190°C to facilitate pouring, note the temperature and heating time in the report.
- 10.16. *Vacuum Degassing (Optional)*—Preheat the vacuum oven until it stabilizes at 190°C ± 5°C. Follow the instructions in Section 10.15, except select a container of dimensions such that the depth of the residue in the container is between 15 and 40 mm.
- 10.16.1. After the binder has been combined into a single container, immediately transfer the container to the vacuum oven and maintain the temperature in the vacuum oven at 190 ± 5°C for 15 ± 1 min, without a vacuum applied. After the 15 ± 1 min of equilibration, open the vacuum valve as rapidly as possible to reduce the pressure in the oven to 15 ± 2.5 kPa absolute. Maintain the absolute pressure in the oven at 15 ± 2.5 kPa for 30 ± 1 min. At the end of the 30 min, release the vacuum and remove the container. If any bubbles are visible on the surface of the residue, remove them by flashing the surface of the residue with a torch or hot knife.
- 10.17. *Correction to Gauge Reading for Elevation*—A vacuum gauge attached to the vessel indicates the difference between atmospheric pressure and the pressure in the vessel. If the vessel is located above sea level, the gauge reading must be corrected for altitude to indicate the correct absolute pressure within the vessel. This correction is not used if the vessel is fitted with an absolute pressure gauge. Do not correct the reading for temperature or for the barometric pressure reported by a weather station as this pressure is typically already corrected for elevation.
- 10.17.1. Correct the vacuum gauge reading to sea level using a correction factor in accordance with Table 1. If an absolute pressure gauge is used, no correction is needed.
- Note 10**—At sea level, standard atmospheric pressure is 29.92 in.Hg, 760 mmHg, 1.013 kPa, or 14.7 psi.
- Note 11**— If the material foams over the lip of the container during the degassing, reduce the rate at which the vacuum is released until the foaming ceases.

Table 1—Gauge Readings Corrected for Elevation

No change

- 10.17.2. From the residue generated in Sections 10.15 or 10.16, prepare test specimens directly from the residue in the container, pour the residue from the container (Section 10.15) to subdivide into smaller containers for future testing, or set the container aside for future testing.

11. REPORT

No change

12. PRECISION AND BIAS

No change

13. KEYWORDS
No change

DRAFT

Standard Method of Test for

**Standard Method of Test for Determining
the Flexural Creep Stiffness of Asphalt
Binder Using the Bending Beam
Rheometer (BBR)**

AASHTO Designation: T 313-12 (2016)



**American Association of State Highway and Transportation Officials
444 North Capitol Street N.W., Suite 249
Washington, D.C. 20001**

Standard Method of Test for

Standard Method of Test for Determining the Flexural Creep Stiffness of Asphalt Binder Using the Bending Beam Rheometer (BBR)

AASHTO Designation: T 313-12 (2016)



PART B: PROCEDURES FOR ASPHALT RUBBER BINDER

1. SCOPE

- 1.1. This test method covers the determination of the flexural creep stiffness or compliance of asphalt rubber binders by means of a bending beam rheometer. It is applicable to material having a flexural stiffness value from 20 MPa to 1 GPa (creep compliance values in the range of 50 nPa⁻¹ to 1 nPa⁻¹) and can be used with unaged material or with material aged using T 240 (RTFOT) or R 28 (PAV), or both. The test apparatus is designed for testing within the temperature range from -36 to 0°C.
- 1.2. Test results are not valid for beams of asphalt rubber binder that deflect more than 4 mm, or less than 0.08 mm, when tested in accordance with this method.
- 1.3. *This standard may involve hazardous materials, operations, and equipment. This standard does not purport to address all of the safety concerns associated with its use. It is the responsibility of the user of this procedure to establish appropriate safety and health practices and to determine the applicability of regulatory limitations prior to use.*

2. REFERENCED DOCUMENTS

No change

3. TERMINOLOGY

No change

4. SUMMARY OF TEST METHOD

No change

5. SIGNIFICANCE AND USE

No change

6. APPARATUS

- 6.1. *Bending Beam Rheometer (BBR) Test System*—A bending beam rheometer (BBR) test system consisting of (1) a loading frame that permits the test beam, supports, and the lower part of the test frame to be submerged in a constant temperature fluid bath; (2) a controlled-temperature liquid bath that maintains the test beam at the test temperature and provides a buoyant force to counterbalance the force resulting from the mass of the beam; (3) a computer-controlled automated data acquisition component; (4) specimen molds; and (5) items needed to calibrate and/or verify the BBR.
- 6.1.1. *Loading Frame*—A frame consisting of a set of sample supports, a blunt-nosed shaft that applies the load to the midpoint of the test specimen, a load cell mounted on the loading shaft, a means for zeroing the load on the test specimen, a means for applying a constant load to the loading shaft, and a deflection measuring transducer attached to the loading shaft. A schematic of the device is shown in Figure 1.
- 6.1.1.1. *Loading System*—A loading system that is capable of applying a contact load of 35 ± 10 mN to the test specimen and maintaining a test load of 980 ± 50 mN.
- 6.1.1.2. *Loading System Requirements*—The rise time for the test load shall be less than 0.5 s. The rise time is the time required for the load to rise from the 35 ± 10 mN contact load to the 980 ± 50 mN test load. During the rise time, the system shall dampen the test load to 980 ± 50 mN. Between 0.5 and 5.0 s, the test load shall be within ± 50 mN of the average test load, and thereafter shall be within ± 10 mN of the average test load.
- 6.1.1.3. *Sample Supports*—Sample supports with specimen support strips 3.0 ± 0.30 mm in top radius and inclined at an angle of 45 degrees with the horizontal (see Figure 1). The supports, made of stainless steel (or other corrosion-resistant metal), are spaced 102.0 ± 1.0 mm apart. The width of the supporting area of the supporting strips shall be 9.5 ± 0.25 mm. This is required to ensure that the edges of the specimen, resulting from the molding procedure, do not interfere with the mid-span deflection of the specimen measured during testing. The supports shall also include vertical alignment pins 2 to 4 mm in diameter placed at the back of each sample supports at 6.75 ± 0.25 mm from the center of the supports. These pins should be placed on the back side of the support to align the specimen on the center of the supports. See Figure 1 for details.
- 6.1.1.4. *Loading Shaft*—A blunt-nosed loading shaft (with a spherical contact point $6.25 (\pm 0.30)$ mm in radius) continuous with a load cell and a deflection measuring transducer that is capable of applying a contact load of 35 ± 10 mN and maintaining a test load of 980 ± 50 mN. The rise time for the test load shall be less than 0.5 s where the rise time is the time required for the load to rise from the 35 ± 10 mN preload to the 980 ± 50 mN test load. During the rise time, the system shall dampen the test load after the first 5 s to a constant ± 10 mN value.
- 6.1.1.5. *Load Cell*—A load cell with a minimum capacity of 2000 mN, having a minimum resolution of 2.5 mN mounted in line with the loading shaft and above the fluid to measure the contact load and the test load.
- 6.1.1.6. *Linear Variable Differential Transducer (LVDT)*—A linear variable differential transducer or other suitable mounted device mounted axially above the loading shaft capable of resolving a linear movement ≤ 2.5 μ m with a range of at least 6 mm to measure the deflection of the test beam.

- 6.1.1.7. *Controlled-Temperature Fluid Bath*—A controlled-temperature liquid bath capable of maintaining the temperature at all points within the bath between -36 and 0°C within $\pm 0.1^{\circ}\text{C}$. Placing a cold specimen in the bath may cause the bath temperature to fluctuate $\pm 0.2^{\circ}\text{C}$ from the target test temperature; consequently, bath fluctuations of $\pm 0.2^{\circ}\text{C}$ during isothermal conditioning shall be allowed.
- 6.1.2. *Bath Agitator*—A bath agitator for maintaining the required temperature homogeneity with agitator intensity such that the fluid current does not disturb the testing process, and mechanical noise caused by vibrations is less than the resolution specified in Sections 6.1.3 and 6.1.3.1.
- 6.1.2.1. *Circulating Bath (Optional)*—A circulating bath unit separate from the test frame that pumps the bath fluid through the test bath. If used, vibrations from the circulating system shall be isolated from the bath test chamber so that mechanical noise is less than the resolution specified in Sections 6.1.3 and 6.1.3.1.
- 6.1.3. *Data Acquisition System*—A data acquisition system that resolves loads to the nearest 2.5 mN, beam deflection to the nearest 2.5 μm , and bath fluid temperature to the nearest 0.1°C . The system shall sense the point in time when the signal is sent to the solenoid valve(s) to switch from zero load regulator (contact load) to the testing load regulator (test load). This is zero time. Using this time as a reference, the system shall provide a record of load and deflection measurements relative to this time. The system shall record the load and deflection at the loading times of 0.0, 0.5, 8.0, 15.0, 30.0, 60.0, 120.0, and 240.0 s. All readings shall be an average of three or more points within ± 0.2 s from the loading time, e.g., for a loading time of 7.8, 7.9, 8.0, 8.1, and 8.2 s.
- 6.1.3.1. *Signal Filtering*—Digital or analog smoothing of the load and the deflection data may be required to eliminate electronic noise that could otherwise affect the ability of the second-order polynomial to fit the data with sufficient accuracy to provide a reliable estimate of m -value. The load and deflection signals may be filtered with a low-pass analog or digital filter that removes signals of greater than 4Hz frequency. The averaging shall be over a time period less than or equal to ± 0.2 s of the reporting time.
- 6.2. *Temperature Measuring Equipment*—A calibrated temperature transducer capable of measuring the temperature to 0.1°C , over the range of -36 to 0°C mounted within 50 mm of the midpoint of the test specimen supports.
- Note 1**—Required temperature measurement can be accomplished with an appropriately calibrated platinum resistance thermometer (RTD) or a thermistor. Calibrations of an RTD or thermistor can be verified as per Section 6.6. An RTD meeting DIN Standard 43760 (Class A) is recommended for this purpose. The required precision and accuracy cannot be obtained unless each RTD is calibrated as a system with its respective meter or electronic circuitry.
- 6.3. *Test Beam Molds*—Test beam molds of suitable dimensions to yield a demolded test beam 6.35 ± 0.05 mm thick by 12.7 ± 0.05 mm wide by 127 ± 2.0 mm long, fabricated from aluminum flat stock as shown in Figures 2 & 3. To facilitate pouring of the more viscous asphalt rubber binder, it is recommended that a modified mold is used that allows pouring through a 12.7 mm opening instead of the standard 6.35 mm opening.
- Note 2**—Small errors in the thickness of the test specimen can have a large effect on the calculated modulus because the calculated modulus is a function of the thickness, h , raised to the third power.
- 6.4. *Items for Calibration or Verification*—The following items are required to verify and calibrate the BBR.

- 6.4.1. *Stainless Steel (Thick) Beam for Compliance Measurement and Load Cell Calibration*—One stainless steel beam, 6.4 ± 0.1 mm thick by 12.7 ± 0.25 mm wide by 127 ± 5 mm long, for measuring system compliance and calibrating the load cell.
- 6.4.2. *Stainless Steel (Thin) Beam for Overall System Check*—One stainless steel beam, 1.3 ± 0.3 mm thick by 12.7 ± 0.1 mm wide by 127 ± 5 mm long, with an elastic modulus reported to three significant figures by the manufacturer. The manufacturer shall measure and report the thickness of this beam to the nearest 0.01 mm and the width to the nearest 0.05 mm. The dimensions of the beam shall be used to calculate the modulus of the beam during the overall system check. See Section 10.1.2.1.
- 6.5. *Standard Masses*—One or more standard masses are required as follows:
- 6.5.1. *Verification of Load Cell Calibration*—One or more masses totaling 100.0 ± 0.2 g and two masses of 2.0 ± 0.2 g each (see Note 3) for verifying the calibration of the load cell.
Note 3—Any suitable object may be used if the mass is confirmed to be 2.0 ± 0.2 g.
- 6.5.2. *Calibration of Load Cell*—Four masses, each of known mass ± 0.2 g, and equally spaced in mass over the range of the load cell.
- 6.5.3. *Daily Overall System Check*—Two or more masses, each of known mass to 0.2 g, for conducting overall system check as specified by the manufacturer.
- 6.5.4. *Accuracy of Masses*—Accuracy of the masses in Section 6.5 shall be verified at least once every three years.
- 6.6. *Calibrated Thermometers*—Calibrated liquid-in-glass thermometers for verification of the temperature transducer of suitable range with subdivisions of 0.1°C . These thermometers shall be partial immersion thermometers with an ice point and shall be calibrated in accordance with Test Method E77 at least once per year. A suitable thermometer is designated 133C. An electronic thermometer of equal accuracy and resolution may be used.
- 6.7. *Thickness Gauge*—A stepped thickness gauge for verifying the calibrations of displacement transducer as described in Figure 4.

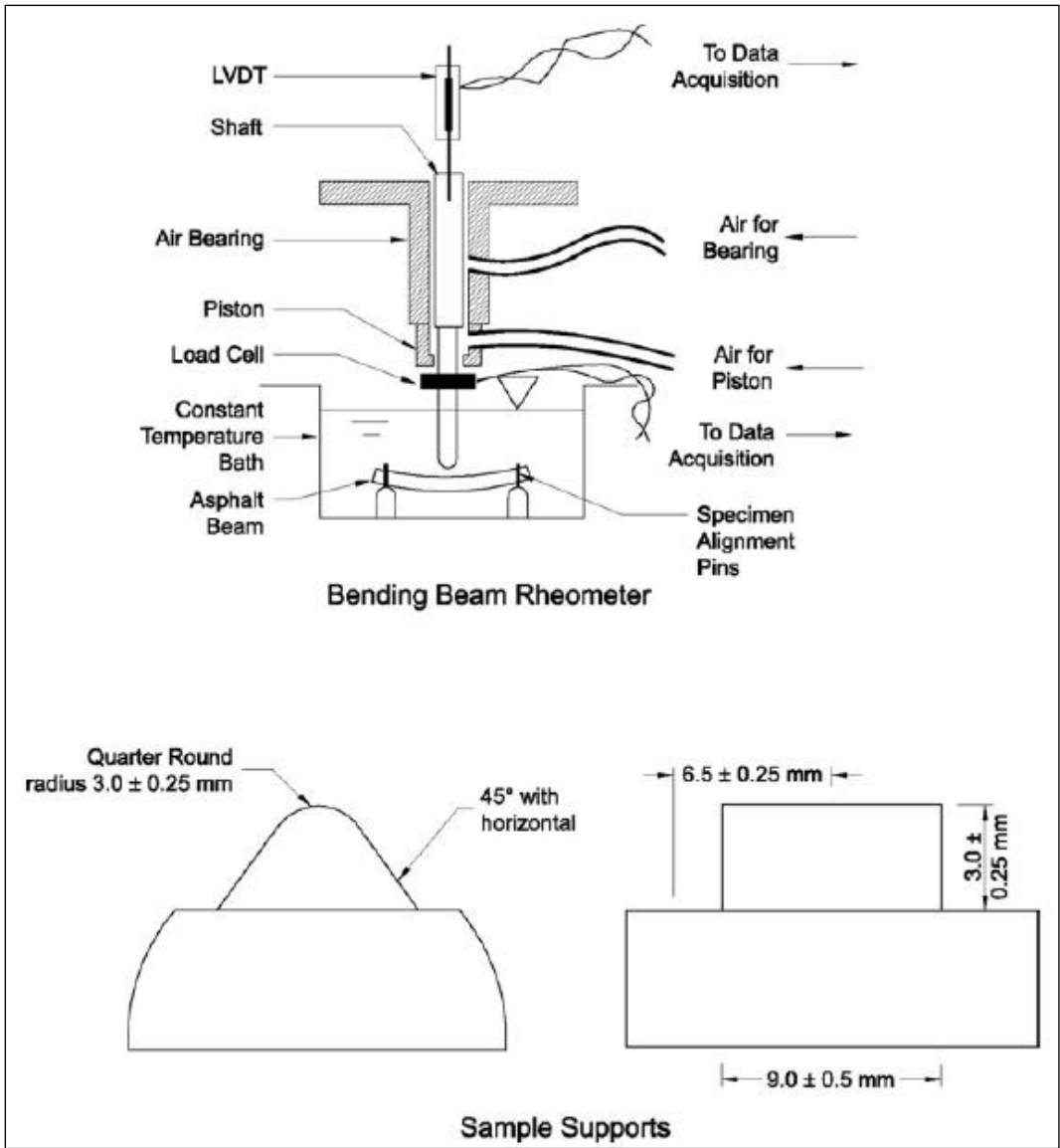


Figure 1—Schematic of the Bending Beam Rheometer.

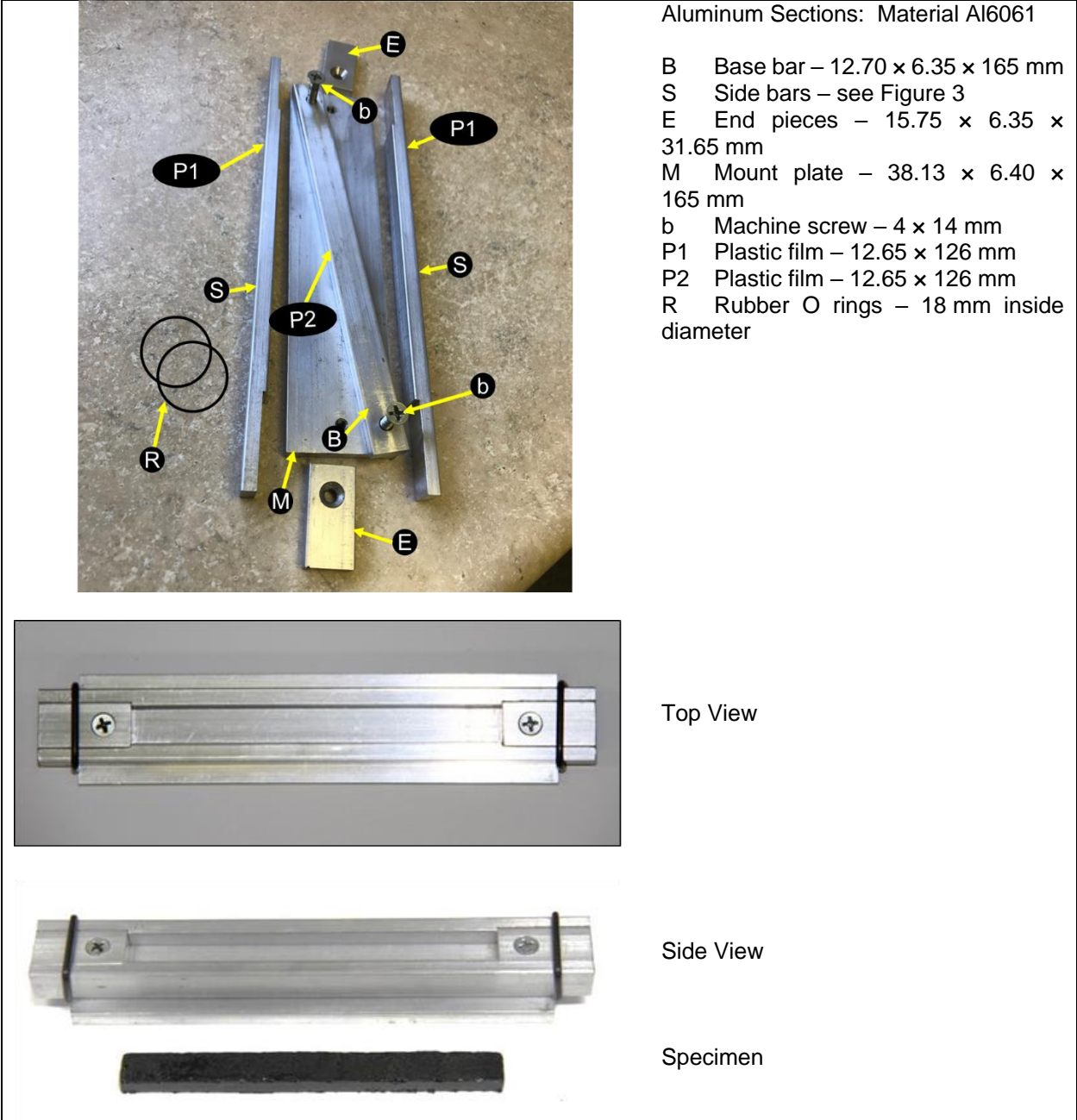


Figure 2— Modified aluminum mold for asphalt rubber binders.

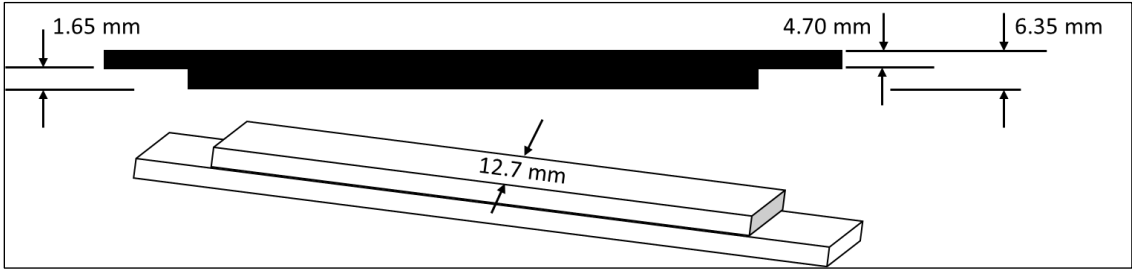


Figure 3— Dimensions and specifications for aluminum side bars.

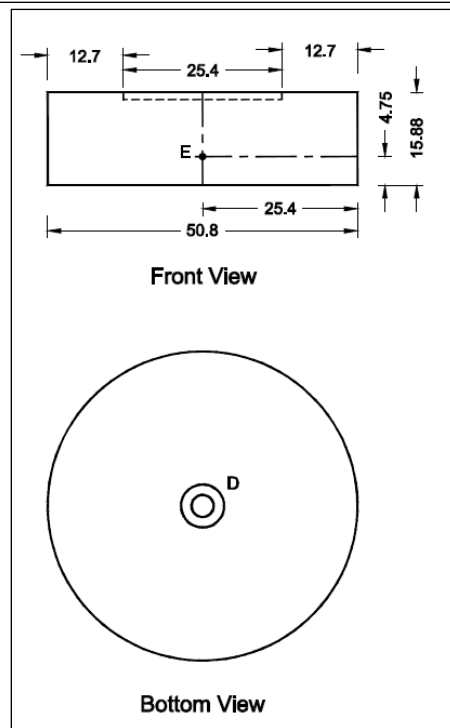
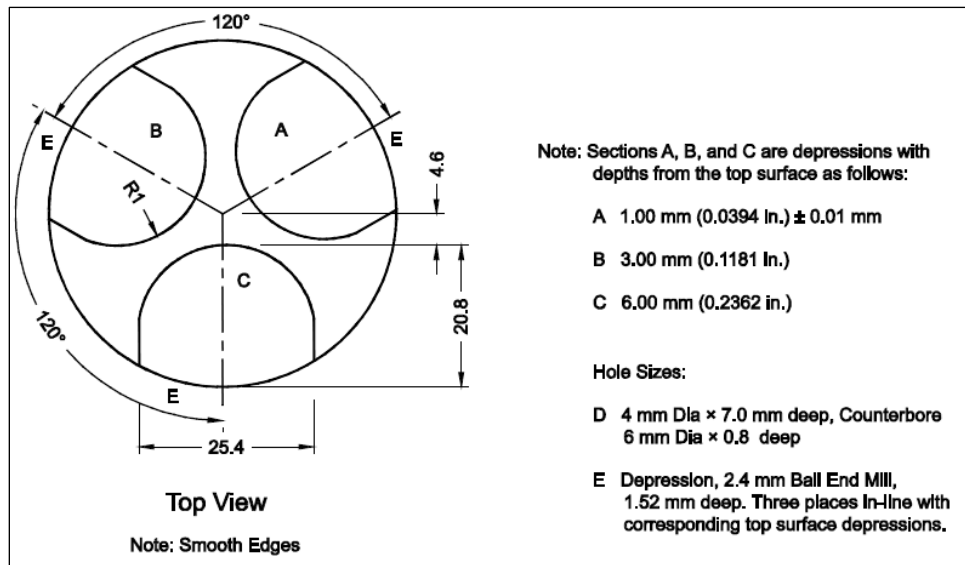


Figure 4— Typical thickness gauge used to calibrate deflection detector

7. MATERIALS

7.1. *Plastic film*—Clear plastic film, 0.12 ± 0.04 mm thick, for lining the interior faces of the aluminum mold sections to prevent asphalt rubber from adhering to them. The film must be resistant to distortion up to temperatures of 200°C.

Note 4—Transparency film for laser printers is suitable.

7.2. *Petroleum jelly (vaseline)*—Used to hold the plastic strips to the interior faces of the aluminum mold sections.

Note 5—Warning: Do not use any silicone-based products.

7.3. *Glycerol talc mixture*—Used to coat the end pieces of the aluminum molds.

Note 6—A mixture of 50 percent by weight USP grade glycerin and 50 percent USP grade talc or kaolin (china clay) is suitable for this purpose.

7.4. *Cooling bath fluid*—A bath fluid that is not absorbed by or does not affect the properties of the asphalt rubber binder tested. The mass density of the bath fluid shall not exceed 1.05 g/cm³ at testing temperatures. The bath fluid shall be optically clear at all testing temperatures. Silicone fluids or mixtures containing silicones shall not be used.

Note 7—Suitable bath fluids include ethanol, methanol, and glycol-methanol mixtures (e.g., 60 percent glycol, 15 percent methanol, 25 percent water).

8. HAZARDS

No change

9. PREPARATION OF APPARATUS

9.1. Clean the supports, loading head, and bath fluid of any particulates and coatings as necessary.

Note 8—Due to the brittleness of asphalt rubber binder at the specified test temperatures, small fragments can be introduced into the bath fluid. If these fragments are present on the supports or the loading head, the measured deflection will be affected. The small fragments will deform under load and add an apparent deflection to the beam. Filtration of the bath fluid will aid in preserving the required cleanliness.

9.2. Select the test temperature and adjust the bath fluid to the selected temperature. Wait until the temperature stabilizes and then allow the bath to equilibrate to the test temperature $\pm 0.1^\circ\text{C}$ prior to conducting a test.

9.3. Activate the data acquisition system and load the software as explained in the manufacturer's manual for the test system.

10. STANDARDIZATION

No change

11. PREPARATION OF MOLDS AND TEST SPECIMENS

11.1. *Mold preparation*—Spread a thin layer of petroleum jelly, sufficient to hold the plastic to the aluminum, on the interior faces of the two aluminum side bars (Figure 2) and one aluminum base bar (Figure 2). Place the plastic strips over the aluminum faces and smooth the plastic with firm finger pressure to force out any air bubbles. Wipe excess jelly from the aluminum. Assemble the mold as shown in Figure 2 using the rubber O-rings to hold the pieces of the mold together. Inspect the assembled mold. If air bubbles remain, disassemble the mold and recoat the aluminum faces with petroleum jelly. Cover the inside faces of the two end pieces with a thin film of glycerol talc. After assembly, keep the mold at room temperature.

Note 9—The thickness of the specimen is controlled by the mold components. The thicknesses of these components should be measured periodically to make sure that they meet the requirements of Section 6.3. The stiffness is proportional to the third power of the thickness.

- 11.2. If unaged asphalt rubber binder is to be tested, obtain test sample according to R 66.
- 11.3. *Degassing prior to testing*—If the asphalt rubber binder is also being tested according to T 314 (DT) and has been conditioned according to T 240 (RTFO) and R 28 (PAV), degas the asphalt rubber binder as described in R 28 prior to testing. Otherwise, degassing of the asphalt rubber binder sample is not required.
- 11.4. Heat the asphalt rubber binder in an oven set at the minimum temperature and for the minimum time necessary for it to be sufficiently fluid to pour.
Note 10—Minimum pouring temperatures that produce a consistency equivalent to that of SAE 10W30 motor oil (readily pours but not overly fluid) at room temperature are recommended. In all cases, heating time should be minimized. These precautions will help avoid oxidative hardening and volatile loss that will further harden the sample. During the heating process, the sample should be covered and stirred occasionally to ensure homogeneity.
- 11.5. *Molding*—Holding the container about 25 mm above the mold, pour the asphalt rubber in a single continuous movement from one end of the mold to the other. The mold should be slightly overfilled after pouring. Allow the mold to cool for 45 to 60 minutes at room temperature. Trim the exposed face of the cooled specimens flush with the top of the mold using a hot knife.
- 11.6. Store all test specimens in their molds at room temperature prior to testing. Schedule testing so that it is completed within 4 hours after specimens were poured.
Note 11—Time-dependent increases in stiffness can occur when asphalt rubber binders are stored at room temperature for even short periods of time. This increase in stiffness is the result of molecular associations and is referred to as steric hardening in the literature.
- 11.7. Just prior to testing, cool the aluminum mold containing the test specimen in a freezer or ice bath at $-5^{\circ}\text{C} \pm 7^{\circ}\text{C}$ for 5 to 10 minutes, just long enough to stiffen the asphalt rubber binder beam so that it can be readily demolded without distortion. Some softer grades may require lower temperatures. Do not cool the molds containing the specimens in the test bath because it may cause temperature fluctuations in the bath to exceed $\pm 0.2^{\circ}\text{C}$.
Note 12—Excessive cooling may cause unwanted hardening of the beam, thereby causing increased variability in the test data.
- 11.8. Disassemble the aluminum mold as soon as it is sufficiently stiff to demold without distortion.
Note 13—If the plastic films do not fully separate from the beam, it can be removed as the beam is being immersed in the test bath. Full contact at the specimen supports is assumed in the analysis. A warped test beam may yield a measured stiffness less than the actual stiffness.

12. PROCEDURE

No change

13. CALCULATION AND INTERPRETATION OF RESULTS

No change

14. REPORT
No change

15. PRECISION AND BIAS
No change

APPENDIX
No change

Blank page

APPENDIX B: PHASE 1 TEST RESULTS

Test results from the different tests are summarized in the following tables:

- Table B.1: Test Results for Binder-Specific Conversion Factor: Operator and Binder Source
- Table B.2: Test Results for Binder-Specific Conversion Factor: Operator and Binder Type
- Table B.3: Test Results for Binder-Specific Conversion Factor: Operator and Binder Source, Type, and Grade
- Table B.4: Test Results for Fixed Conversion Factor
- Table B.5: Rubberized Binder: Comparison of Concentric Cylinder and Parallel Plate
- Table B.6: Test Results for Rubberized Binder: Concentric Cylinder
- Table B.7: Test Results for Rubberized Binder: Parallel Plate
- Table B.8: Test Results for Rubberized Binder: True Performance Grade

Abbreviations in the tables are as follows:

- Binder type
 - + UM = unmodified
 - + PM = polymer-modified
 - + TR = tire rubber-modified
- Aging condition
 - + Unaged
 - + RTFO = Rolling thin film oven-aged
- Grinding method
 - + Amb = ambient
 - + Cryo = Cryogenic
- DSR geometry
 - + CC = concentric cylinder
 - + PP-1 = parallel plate with 1-mm gap
 - + PP-2 = parallel plate with 2-mm gap
- Test parameter
 - + G^* = Shear modulus
 - + δ = Phase angle

Table B.1: Test Results for Binder-Specific Conversion Factor: Operator and Binder Source

Operator	Binder Type	PG	Aging Condition	Binder Source	Geometry	G* (kPa)	δ (Degrees)	G*/sin(δ) (kPa)
1	UM	64-16	Unaged	Ref #1	CC	1.40	87.6	1.41
						1.41	87.7	1.41
						1.43	87.6	1.43
					PP-1	1.46	87.7	1.46
						1.35	87.8	1.35
						1.37	87.8	1.37
				Ref #2	CC	1.12	89.4	1.12
						1.07	89.5	1.07
						1.07	89.4	1.07
					PP-1	1.15	89.4	1.15
						1.09	89.6	1.09
						1.10	89.5	1.10
Ref #3	CC	1.25	87.4	1.25				
		1.22	87.5	1.22				
		1.23	87.5	1.23				
	PP-1	1.24	87.8	1.24				
		1.26	87.7	1.26				
		1.24	87.7	1.24				
2	UM	64-16	Unaged	Ref #1	CC	1.42	87.6	1.42
						1.43	87.6	1.43
						1.41	87.6	1.41
					PP-1	1.38	87.8	1.38
						1.45	87.7	1.45
						1.47	87.7	1.47
				Ref #2	CC	1.08	89.4	1.08
						1.09	89.4	1.09
						1.03	89.5	1.03
					PP-1	1.09	89.5	1.09
						1.09	89.5	1.09
						1.09	89.5	1.09
Ref #3	CC	1.28	87.4	1.28				
		1.28	87.5	1.28				
		1.27	87.5	1.27				
	PP-1	1.29	87.7	1.29				
		1.25	87.7	1.25				
		1.28	87.7	1.28				
3	UM	64-16	Unaged	Ref #1	CC	1.51	87.5	1.51
						1.46	87.6	1.46
						1.49	87.6	1.49
					PP-1	1.42	87.5	1.42
						1.59	87.5	1.59
						1.51	87.6	1.51
				Ref #2	CC	1.17	89.5	1.17
						1.14	89.5	1.14
						1.19	89.4	1.19
					PP-1	1.18	89.4	1.19
						1.12	89.5	1.12
						1.15	89.4	1.15
Ref #3	CC	1.31	87.4	1.31				
		1.30	87.4	1.30				
		1.27	87.5	1.27				
	PP-1	1.30	87.6	1.30				
		1.30	87.6	1.31				
		1.28	87.6	1.28				

Table B.2: Test Results for Binder-Specific Conversion Factor: Operator and Binder Type

Operator	Binder Source	PG	Aging Condition	Binder Type	Geometry	G* (kPa)	δ (Degrees)	G*/sin(δ) (kPa)
1	Ref #1	64-28	Unaged	PM	CC	1.47	70.6	1.56
						1.84	68.8	1.98
						1.81	68.5	1.94
				PM	PP-1	1.69	67.6	1.82
						2.12	66.1	2.32
						1.97	65.8	2.16
TR	CC	2.80	67.1	3.03				
		2.97	66.8	3.23				
		2.22	68.5	2.38				
TR	PP-1	2.78	66.0	3.04				
		2.11	65.6	2.32				
		1.78	66.3	1.95				
2	Ref #1	64-28	Unaged	PM	CC	1.47	70.7	1.55
						1.83	68.7	1.96
						1.89	68.4	2.04
				PM	PP-1	1.55	68.4	1.67
						1.91	66.1	2.09
						1.98	66.3	2.17
TR	CC	2.81	67.0	3.06				
		2.37	68.3	2.55				
		2.38	68.0	2.57				
TR	PP-1	2.25	66.3	2.45				
		2.05	66.0	2.25				
		2.02	65.7	2.22				
3	Ref #1	64-28	Unaged	PM	CC	1.58	67.9	1.71
						1.61	69.6	1.72
						1.59	68.8	1.70
				PM	PP-1	1.65	68.1	1.78
						2.05	65.4	2.25
						2.11	66.2	2.31
TR	CC	2.86	67.0	3.11				
		2.98	66.7	3.24				
		3.00	66.7	3.27				
TR	PP-1	3.06	65.2	3.38				
		2.11	65.6	2.31				
		1.98	67.0	2.16				

Table B.3: Test Results for Binder-Specific Conversion Factor: Operator and Binder Source, Type, and Grade

Operator	Aging Condition	PG	Binder Source	Binder Type	Geometry	G* (kPa)	δ (Degrees)	G*/sin(δ) (kPa)
1	RTFO	64-28	Ref #1	PM	CC	3.77	62.4	4.26
					PP-1	3.75	62.4	4.23
			Ref #1	TR	CC	4.86	64.0	5.40
					PP-1	4.76	63.5	5.32
		64-16	Ref #2	UM	CC	2.69	88.6	2.69
					PP-1	2.34	88.6	2.34
			Ref #3	UM	CC	3.01	83.5	3.03
					PP-1	2.97	84.8	2.99
2	RTFO	64-28	Ref #1	PM	CC	3.56	62.7	4.01
					PP-1	3.88	62.3	4.38
			Ref #1	TR	CC	3.61	64.2	4.01
					PP-1	3.25	63.8	3.62
		64-16	Ref #2	UM	CC	2.76	88.5	2.76
					PP-1	2.28	88.6	2.28
			Ref #3	UM	CC	2.8	84.4	2.81
					PP-1	3.07	84.7	3.09
3	RTFO	64-28	Ref #1	PM	CC	3.74	62.3	4.23
					PP-1	3.82	62.2	4.31
			Ref #1	TR	CC	3.59	64.1	3.99
					PP-1	3.5	63.4	3.92
		64-16	Ref #2	UM	CC	2.71	88.6	2.71
					PP-1	2.4	88.6	2.41
			Ref #3	UM	CC	2.45	84.8	2.46
					PP-1	2.91	84.9	2.92

Table B.4: Test Results for Fixed Conversion Factor

Operator	Binder Source	PG	Test Temp. (°C)	Aging Condition	Geometry	G*	δ	G*/sin(δ)
						(kPa)	(Degrees)	(kPa)
1	Ref #2	64-16	64	Unaged	CC	1.28	89.4	1.28
						1.30	89.4	1.30
						1.27	89.4	1.27
				PP-1	1.20	89.4	1.20	
					1.22	89.4	1.22	
					1.20	89.4	1.20	
		TFO	CC	2.02	88.8	2.02		
				2.17	88.7	2.17		
				2.06	88.8	2.06		
		PP-1	2.07	88.8	2.07			
			2.05	88.8	2.05			
			2.06	88.8	2.06			
	RTFO	CC	2.42	88.5	2.42			
			2.46	88.5	2.46			
			2.43	88.5	2.43			
	PP-1	2.32	88.6	2.32				
		2.31	88.6	2.31				
		2.29	88.6	2.29				
	Ref #3	70-10	70	Unaged	CC	1.40	87.2	1.40
						1.39	87.2	1.39
						1.41	87.1	1.41
				PP-1	1.32	87.3	1.32	
					1.27	87.3	1.27	
					1.32	87.3	1.32	
TFO		CC	2.43	85.2	2.44			
			2.46	85.2	2.47			
			2.56	85.0	2.57			
PP-1		2.53	85.1	2.54				
		2.58	85.1	2.59				
		2.57	85.1	2.58				
RTFO	CC	2.74	85.1	2.75				
		2.73	85.1	2.74				
		2.71	85.1	2.72				
PP-1	2.58	85.3	2.59					
	2.60	85.3	2.61					
	2.61	85.3	2.62					
Ref #3	64-16	64	Unaged	CC	1.28	89.4	1.28	
					1.30	89.4	1.30	
					1.27	89.4	1.27	
			PP-1	1.20	89.4	1.20		
				1.22	89.4	1.22		
				1.20	89.4	1.20		
	TFO	CC	2.02	88.8	2.02			
			2.17	88.7	2.17			
			2.06	88.8	2.06			
	PP-1	2.07	88.8	2.07				
		2.05	88.8	2.05				
		2.06	88.8	2.06				
RTFO	CC	2.42	88.5	2.42				
		2.46	88.5	2.46				
		2.43	88.5	2.43				
PP-1	2.32	88.6	2.32					
	2.31	88.6	2.31					
	2.29	88.6	2.29					

Table B.5: Rubberized Binder: Comparison of Concentric Cylinder and Parallel Plate

Geometry	Particle Size (µm)	Particle Size (# mesh)	Grind Method	Test Temp. (°C)	Binder Type	G* (kPa)	δ (Degrees)	G*/sin(δ) (kPa)	
CC	180-250	60-80	Amb	76	I	1.81	82.7	1.82	
					II	1.93	81.2	1.95	
					82	I	0.96	85.6	0.97
						II	1.05	84.1	1.05
			Cryo	76	I	2.73	78.2	2.69	
					II	2.65	81.1	2.68	
			82	I	1.42	82.3	1.43		
				II	1.39	84.6	1.40		
	250-425	40-60	Amb	76	I	1.81	82.3	1.83	
					II	1.17	84.5	1.17	
					82	I	1.00	84.7	1.00
						II	0.64	86.4	0.64
			Cryo	76	I	3.15	76.7	3.24	
					II	2.39	82.7	2.41	
			82	I	1.66	81.2	1.68		
				II	1.25	85.5	1.25		
	425-850	20-40	Amb	76	I	2.39	77.5	2.45	
					II	1.24	81.9	1.25	
				82	I	1.29	81.3	1.30	
					II	0.69	84.3	0.67	
Cryo			76	I	3.24	75.8	3.34		
				II	1.65	83.3	1.66		
		82	I	1.71	80.6	1.73			
			II	0.88	85.7	0.88			
PP-1	180-250	60-80	Amb	76	I	1.76	83.3	1.77	
					II	1.91	81.8	1.93	
					82	I	0.95	85.9	0.95
						II	1.03	84.6	1.03
			Cryo	76	I	2.73	77.9	2.79	
					II	2.69	81.5	2.72	
		82	I	1.48	82.1	1.49			
			II	1.41	84.8	1.41			
PP-2	250-425	40-60	Amb	76	I	2.27	80.0	2.30	
					II	1.24	84.3	1.24	
					82	I	1.21	83.8	1.21
						II	0.69	85.9	0.69
			Cryo	76	I	2.99	77.8	3.05	
					II	2.35	82.8	2.37	
			82	I	1.67	81.4	1.69		
				II	1.30	84.9	1.30		
	425-850	20-40	Amb	76	I	2.49	77.0	2.56	
					II	1.60	80.5	1.62	
					82	I	1.42	80.0	1.45
						II	0.90	83.2	0.90
Cryo			76	I	3.57	75.2	3.69		
				II	1.38	83.9	1.39		
		82	I	1.96	79.7	2.00			
			II	0.76	85.9	0.76			

Table B.6: Test Results for Rubberized Binder: Concentric Cylinder

Binder Type	Grinding Method	Test Temp. (°C)	Geometry	Particle Sizes (µm)	Particle Sizes (# mesh)	G* (kPa)	δ (Degrees)	G*/sin(δ) (kPa)
I	Amb	76	6 mm CC	425 - 850	20 - 40	2.39	77.5	2.45
				250 - 425	40 - 60	1.81	82.3	1.83
				180 - 250	60 - 80	1.81	82.7	1.82
				150 - 180	80 - 100	2.47	80.1	2.51
				106 - 150	100 - 140	2.45	75.7	2.53
				75 - 106	140 - 200	2.02	72.3	2.12
	82	6 mm CC	425 - 850	20 - 40	1.29	81.3	1.30	
			250 - 425	40 - 60	1.00	84.7	1.00	
			180 - 250	60 - 80	0.96	85.6	0.97	
			150 - 180	80 - 100	1.34	83.1	1.35	
			106 - 150	100 - 140	1.37	76.6	1.40	
			75 - 106	140 - 200	1.19	68.5	1.28	
Cryo	76	6 mm CC	425 - 850	20 - 40	3.24	75.8	3.34	
			250 - 425	40 - 60	3.15	76.7	3.24	
			180 - 250	60 - 80	2.73	78.2	2.69	
			150 - 180	80 - 100	2.25	76.0	2.31	
			106 - 150	100 - 140	2.69	75.4	2.78	
			75 - 106	140 - 200	2.35	75.0	2.43	
82	6 mm CC	425 - 850	20 - 40	1.71	80.6	1.73		
		250 - 425	40 - 60	1.66	81.2	1.68		
		180 - 250	60 - 80	1.42	82.3	1.43		
		150 - 180	80 - 100	1.26	80.3	1.28		
		106 - 150	100 - 140	1.48	79.9	1.50		
		75 - 106	140 - 200	1.33	78.9	1.36		
II	Amb	76	6 mm CC	425 - 850	20 - 40	1.24	81.9	1.25
				250 - 425	40 - 60	1.17	84.5	1.17
				180 - 250	60 - 80	1.93	81.2	1.95
				150 - 180	80 - 100	1.93	80.0	1.96
				106 - 150	100 - 140	1.76	81.8	1.78
				75 - 106	140 - 200	1.45	82.2	1.46
	82	6 mm CC	425 - 850	20 - 40	0.69	84.3	0.70	
			250 - 425	40 - 60	0.64	86.4	0.64	
			180 - 250	60 - 80	1.05	84.1	1.05	
			150 - 180	80 - 100	1.05	83.1	1.06	
			106 - 150	100 - 140	0.95	84.7	0.95	
			75 - 106	140 - 200	0.79	84.8	0.80	
	Cryo	76	6 mm CC	425 - 850	20 - 40	1.65	83.3	1.66
				250 - 425	40 - 60	2.39	82.7	2.41
				180 - 250	60 - 80	2.65	81.1	2.68
				150 - 180	80 - 100	2.57	81.3	2.60
				106 - 150	100 - 140	2.72	79.6	2.77
				75 - 106	140 - 200	2.12	81.6	2.15
82	6 mm CC	425 - 850	20 - 40	0.88	85.7	0.88		
		250 - 425	40 - 60	1.25	85.5	1.25		
		180 - 250	60 - 80	1.39	84.6	1.40		
		150 - 180	80 - 100	1.34	84.7	1.35		
		106 - 150	100 - 140	1.44	83.2	1.45		
		75 - 106	140 - 200	1.14	84.4	1.14		

Table B.7: Test Results for Rubberized Binder: Parallel Plate

Binder Type	Grinding Method	Test Temp. (°C)	Geometry	Particle Sizes (µm)	Particle Sizes (# mesh)	G* (kPa)	δ (Degrees)	G*/sin(δ) (kPa)
I	Amb	76	PP-2	425 - 850	20 - 40	2.49	77.0	2.56
				250 - 425	40 - 60	2.27	80.0	2.31
			PP-1	180 - 250	60 - 80	1.76	83.8	1.46
				150 - 180	80 - 100	2.16	81.2	2.18
		75 - 106	106 - 150	100 - 140	1.98	80.0	2.01	
			140 - 200	140 - 200	1.53	82.0	1.54	
	82	PP-2	425 - 850	20 - 40	1.42	80.0	1.45	
			250 - 425	40 - 60	1.21	83.8	1.21	
	PP-1	180 - 250	60 - 80	0.95	85.6	0.81		
		150 - 180	80 - 100	1.17	83.7	1.18		
	106 - 150	100 - 140	110	82.6	1.10			
		140 - 200	140	84.2	0.85			
Cryo	76	PP-2	425 - 850	20 - 40	3.57	75.2	3.69	
			250 - 425	40 - 60	2.99	77.8	3.05	
		PP-1	180 - 250	60 - 80	2.73	78.4	2.45	
			150 - 180	80 - 100	2.01	76.6	2.06	
	75 - 106	106 - 150	100 - 140	1.38	79.5	1.40		
		140 - 200	140 - 200	1.93	76.8	1.99		
82	PP-2	425 - 850	20 - 40	1.96	79.7	2.00		
		250 - 425	40 - 60	1.67	81.4	1.69		
PP-1	180 - 250	60 - 80	1.48	81.8	1.35			
	150 - 180	80 - 100	1.14	80.3	1.16			
106 - 150	100 - 140	147	82.8	1.48				
	140 - 200	113	79.6	1.15				
II	Amb	76	PP-2	425 - 850	20 - 40	1.60	80.5	1.62
				250 - 425	40 - 60	1.24	84.3	1.24
			PP-1	180 - 250	60 - 80	1.91	81.9	1.68
				150 - 180	80 - 100	1.69	80.5	1.72
		75 - 106	106 - 150	100 - 140	0.81	84.7	0.81	
			140 - 200	140 - 200	1.20	82.9	1.21	
	82	PP-2	425 - 850	20 - 40	0.90	83.2	0.90	
			250 - 425	40 - 60	0.69	85.9	0.69	
	PP-1	180 - 250	60 - 80	1.03	84.0	0.93		
		150 - 180	80 - 100	0.95	82.8	0.96		
	106 - 150	100 - 140	2.20	81.5	2.23			
		140 - 200	0.67	84.7	0.67			
Cryo	76	PP-2	425 - 850	20 - 40	1.38	83.9	1.39	
			250 - 425	40 - 60	2.35	82.8	2.37	
		PP-1	180 - 250	60 - 80	2.69	82.4	2.33	
			150 - 180	80 - 100	2.24	82.3	2.26	
	75 - 106	106 - 150	100 - 140	1.20	84.0	1.21		
		140 - 200	140 - 200	1.74	83.2	1.75		
82	PP-2	425 - 850	20 - 40	0.76	85.9	0.76		
		250 - 425	40 - 60	1.30	84.9	1.30		
PP-1	180 - 250	60 - 80	1.41	84.8	1.28			
	150 - 180	80 - 100	1.22	84.7	1.23			
106 - 150	100 - 140	1.20	84.0	1.21				
	140 - 200	0.95	85.2	0.96				

Table B.8: Test Results for Rubberized Binder: True Performance Grade

Binder Type	Grinding Method	Test Temp. (°C)	Particle Size (µm)	Particle Size (# mesh)	True PG	
					CC	PP
I	Amb	76	425-850	20-40	84.5	86.2
			250-425	40-60	82.0	84.1
			180-250	60-80	81.7	81.5
			150-180	80-100	85.1	83.8
			106-150	100-140	85.8	83.1
			75-106	140-200	85.9	80.4
	82	425-850	20-40	84.5	86.2	
		250-425	40-60	82.0	84.1	
		180-250	60-80	81.7	81.5	
		150-180	80-100	85.1	83.8	
		106-150	100-140	85.8	83.1	
		75-106	140-200	85.9	80.4	
Cryo	76	425-850	20-40	87.0	88.8	
		250-425	40-60	86.7	87.3	
		180-250	60-80	85.4	85.4	
		150-180	80-100	84.7	83.8	
		106-150	100-140	86.4		
		75-106	140-200	85.4	83.7	
82	425-850	20-40	87.0	88.8		
	250-425	40-60	86.7	87.3		
	180-250	60-80	85.4	85.4		
	150-180	80-100	84.7	83.8		
	106-150	100-140	86.4	85.8		
	75-106	140-200	85.4	83.7		
II	Amb	76	425-850	20-40	78.3	81.1
			250-425	40-60	77.5	78.3
			180-250	60-80	82.6	82.3
			150-180	80-100	82.6	81.6
			106-150	100-140	81.5	80.0
			75-106	140-200	79.8	78.0
	82	425-850	20-40	78.3	81.1	
		250-425	40-60	77.5	78.3	
		180-250	60-80	82.6	82.3	
		150-180	80-100	82.6	81.6	
		106-150	100-140	81.5	80.0	
		75-106	140-200	79.8	78.0	
Cryo	76	425-850	20-40	80.8	79.4	
		250-425	40-60	84.1	85.0	
		180-250	60-80	85.1	85.1	
		150-180	80-100	85.1	84.3	
		106-150	100-140	85.9	84.1	
		75-106	140-200	83.4	81.6	
82	425-850	20-40	80.8	79.4		
	250-425	40-60	84.1	85.0		
	180-250	60-80	85.1	85.1		
	150-180	80-100	85.1	84.3		
	106-150	100-140	85.9	84.1		
	75-106	140-200	83.4	81.6		

Blank page

APPENDIX C: PHASE 2 TEST RESULTS

Test results from the different tests conducted during Phase 2 are summarized in the following tables:

- Table C.1: Phase 2a: High-Temperature Test Results for RTFO Preparation Methods
- Table C.2: Phase 2a: Intermediate-Temperature Test Results for PAV Preparation Methods
- Table C.3: Phase 2a: Low-Temperature Test Results for PAV Preparation Methods
- Table C.4: Phase 2b: Low-Temperature Test Results for Modified BBR Mold Tests
- Table C.5: Phase 2c: Intermediate-Temperature Test Results Tested at 25°C
- Table C.6: Phase 2d: Multiple Stress Creep Recovery Test Results
- Table C.7: Phase 2e: High Temperature Test Results (Unaged) for SOL-680
- Table C.8: Phase 2e: High Temperature Test Results (Unaged) for CAL-26
- Table C.9: Phase 2e: High Temperature Test Results (Unaged) for SB-154
- Table C.10: Phase 2e: High Temperature Test Results (RTFO-Aged) for SOL-680
- Table C.11: Phase 2e: High Temperature Test Results (RTFO-Aged) for CAL-26
- Table C.12: Phase 2e: High Temperature Test Results (RTFO-Aged) for SB-154
- Table C.13: Phase 2e: Low-Temperature Test Results
- Table C.14: Phase 2f: Air-Void Contents of Gyratory-Compacted Specimens
- Table C.15: Phase 2f: Air-Void Contents of Rolling Wheel-Compacted Specimens
- Table C.16: Phase 2f: Dynamic Modulus and Phase Angle Test Results
- Table C.17: Phase 2f: Flexural Modulus and Phase Angle Test Results
- Table C.18: Phase 2f: Repeated Load Triaxial Test Results
- Table C.19: Phase 2f: Semicircular Bend Test Results

Table C.1: Phase 2a: High Temperature Test Results for RTFO Preparation Methods

Binder	Test Parameter	Shear Modulus (G*) (kPa)	Phase Angle (δ) (Degrees)	G*\timessin(δ) (kPa)
PG64-16	Unaged	2	86	2
	35g @ 163°C	4	82	4
	45g @ 163°C	3	83	3
	35g @ 190°C	7	77	7
	45g @ 190°C	6	79	6
PG64-16 + Extender Oil	Unaged	1	87	1
	35g @ 163°C	3	83	3
	45g @ 163°C	2	84	2
	35g @ 190°C	5	80	5
	45g @ 190°C	4	81	4
AR Binder with Particles <250 μ m	Unaged	10	70	11
	35g @ 163°C	17	63	19
	45g @ 163°C	17	62	19
	35g @ 190°C	22	56	27
	45g @ 190°C	22	55	27
AR Binder with Particles <250 μ m + Extender Oil	Unaged	7	73	7
	35g @ 163°C	13	65	14
	45g @ 163°C	12	65	13
	35g @ 190°C	15	58	18
	45g @ 190°C	15	58	18
AR Binder with Particles >250 μ m	Unaged	12	66	13
	35g @ 163°C	23	57	27
	45g @ 163°C	23	57	27
	35g @ 190°C	37	51	47
	45g @ 190°C	38	50	49
AR Binder with Particles >250 μ m + Extender Oil	Unaged	10	69	11
	35g @ 163°C	18	59	21
	45g @ 163°C	21	57	25
	35g @ 190°C	31	51	40
	45g @ 190°C	32	50	42

Table C.2: Phase 2a: Intermediate-Temperature Test Results for PAV Preparation Methods

Temp. (°C)	Parameter	Shear Modulus (G*) (kPa)			Phase Angle (δ) (Degrees)			G*×sin(δ) (kPa)		
		PP1/ 64-16AR	PP2/ 64-16AR	PP3/ 64-16AR	PP1/ 64-16AR	PP2/ 64-16AR	PP3/ 64-16AR	PP1/ 64-16AR	PP2/ 64-16AR	PP3/ 64-16AR
Method #1										
25	Rep 1	4,070		8,660	44		32	2,818		4,566
	Rep 2	3,500	Exceeded	9,090	44	Exceeded	32	2,438	Exceeded	4,826
	Rep 3	4,060	Machine	6,020	44	Machine	35	2,800	Machine	3,421
	Mean	3,877	Torque	8,875	44	Torque	32	2,685	Torque	4,696
	Std. Dev.	266	limits	215	0	limits	0	175	limits	130
	Std. Err.	154		152	0		0	101		92
22	Rep 1	5,990		11,700	42		30	3,991		5,869
	Rep 2	5,140	Exceeded	12,300	42	Exceeded	30	3,463	Exceeded	6,215
	Rep 3	5,950	Machine	8,260	42	Machine	33	3,953	Machine	4,496
	Mean	5,693	Torque	12,000	42	Torque	30	3,802	Torque	6,042
	Std. Dev.	392	limits	300	0	limits	0	240	limits	173
	Std. Err.	226		212	0		0	139		122
Method #2										
25	Rep 1	2,340		8,570	49		31	1,755		4,467
	Rep 2	2,640	Exceeded	7,640	51	Exceeded	32	2,043	Exceeded	4,050
	Rep 3	3,660	Machine	6,210	45	Machine	32	2,567	Machine	3,277
	Mean	2,880	Torque	7,473	48	Torque	32	2,122	Torque	3,931
	Std. Dev.	565	limits	971	3	limits	0	336	limits	493
	Std. Err.	326		560	1		0	194		285
22	Rep 1	3,010		11,500	49		30	2,268		5,704
	Rep 2	3,930	Exceeded	10,300	52	Exceeded	30	3,099	Exceeded	5,199
	Rep 3	3,640	Machine	8,350	52	Machine	30	2,869	Machine	4,196
	Mean	3,527	Torque	10,900	51	Torque	30	2,745	Torque	5,452
	Std. Dev.	384	limits	600	1	limits	0	350	limits	253
	Std. Err.	222		424	1		0	202		179

Table C.2: Phase 2a: Intermediate-Temperature Test Results for PAV Preparation Methods (Continued.)

Temp. (°C)	Parameter	Shear Modulus (G*) (kPa)			Phase Angle (δ) (Degrees)			G*×sin(δ) (kPa)		
		PP1/ 64-16AR	PP2/ 64-16AR	PP3/ 64-16AR	PP1/ 64-16AR	PP2/ 64-16AR	PP3/ 64-16AR	PP1/ 64-16AR	PP2/ 64-16AR	PP3/ 64-16AR
Method #5										
25	Rep 1	4,360	Exceeded Machine Torque limits	5,610	44	Exceeded Machine Torque limits	34	3,005	Exceeded Machine Torque limits	3,155
	Rep 2	3,870		5,850	44		34	2,710		3,303
	Rep 3	4,160		44	34		2,909			
	Mean	4,130		5,730	44		34	2,875		3,229
	Std. Dev.	201		120	0		0	123		74
	Std. Err.	116		85	0		0	71		52
22	Rep 1	6,200	Exceeded Machine Torque limits	7,660	42	Exceeded Machine Torque limits	33	4,148	Exceeded Machine Torque limits	4,119
	Rep 2	5,730		7,990	42		33	3,865		4,315
	Rep 3	4,300		51	33		3,348			
	Mean	5,410		7,825	45		33	3,787		4,217
	Std. Dev.	808		165	4		0	331		98
	Std. Err.	466		117	2		0	191		69
Method #6										
25	Rep 1	3,330	Exceeded Machine Torque limits	6,210	47	Exceeded Machine Torque limits	35	2,417	Exceeded Machine Torque limits	3,537
	Rep 2	3,230		5,450	47		35	2,350		3,109
	Rep 3	3,230		6,320	47		34	2,353		3,529
	Mean	3,263		5,993	47		35	2,373		3,392
	Std. Dev.	47		387	0		0	31		200
	Std. Err.	27		223	0		0	18		115
22	Rep 1	637	Exceeded Machine Torque limits	8,550	50	Exceeded Machine Torque limits	33	454	Exceeded Machine Torque limits	4,653
	Rep 2	4,840		7,460	45		33	3,400		4,072
	Rep 3	3,680		8,660	50		32	2,819		4,621
	Mean	3,052		8,223	48		33	2,224		4,449
	Std. Dev.	1,772		542	3		0	1,274		267
	Std. Err.	1,023		313	2		0	735		154

Table C.3: Phase 2a: Low-Temperature Test Results for PAV Preparation Methods

Temp. (°C)	Parameter	Stiffness (MPa)			m-Value		
		PP1/ 64-16AR	PP2/ 64-16AR	PP3/ 64-16AR	PP1/ 64-16AR	PP2/ 64-16AR	PP3/ 64-16AR
Method #1							
-12	Rep 1	66.9	37.1	46.2	0.373	0.327	0.237
	Rep 2	60.6	42.0	57.7	0.356	0.311	0.266
	Rep 3	-	-	45.2	-	-	0.291
	Mean	63.8	39.6	49.7	0.400	0.319	0.265
	Std. Dev.	3.2	2.5	5.7	0.009	0.008	0.022
	Std. Err.	2.2	1.7	3.3	0.006	0.006	0.013
Method #2							
-12	Rep 1	57.3	43.5	60.7	0.359	0.302	0.288
	Rep 2	59.4	42.0	33.9	0.363	0.311	0.284
	Rep 3	64.4	-	34.5	0.361	-	0.288
	Rep 4	-	-	49.8	-	-	0.292
	Mean	60.4	42.8	44.7	0.361	0.307	0.288
	Std. Dev.	3.0	0.8	11.2	0.002	0.005	0.003
Std. Err.	1.7	0.5	5.6	0.001	0.003	0.001	
Method #5							
-12	Rep 1	69.1	52.2	29.2	0.362	0.325	0.304
	Rep 2	77.5	34.1	43.6	0.346	0.320	0.303
	Rep 3	56.0	42.6	48.1	0.357	0.333	0.307
	Mean	67.5	43.0	40.3	0.355	0.326	0.305
	Std. Dev.	8.8	7.4	8.1	0.007	0.005	0.002
	Std. Err.	5.1	4.3	4.7	0.004	0.003	0.001
Method #6							
-12	Rep 1	45.3	57.0	54.3	0.377	0.330	0.291
	Rep 2	58.4	56.0	47.6	0.373	0.303	0.302
	Rep 3	68.9	-	45.1	0.364	-	0.283
	Mean	51.9	56.5	49.0	0.375	0.317	0.292
	Std. Dev.	6.6	0.5	3.9	0.002	0.014	0.008
	Std. Err.	3.8	0.4	2.2	0.001	0.010	0.005

Table C.4: Phase 2b: Low-Temperature Test Results for Modified BBR Mold Tests

Binder Source	Temperature (°C)	Stiffness (MPa)			m-value		
		Rept. 1	Rept. 2	Average	Rept. 1	Rept. 2	Average
Standard Geometry							
R1/64-16	-6	82.9	83.8	83.4	0.333	0.328	0.331
R2/64-16	-6	191.0	190.0	190.5	0.379	0.383	0.381
R3/64-16	-6	94.8	98.2	96.5	0.395	0.403	0.399
R1/64-28PM	-18	167.0	153.0	160.0	0.312	0.320	0.316
R3/64-28PM	-18	49.0	48.4	48.7	0.300	0.324	0.312
R1a/64-28TR	-18	159.0	156.0	157.5	0.339	0.330	0.335
R1b/64-28TR	-18	139.0	142.0	140.5	0.316	0.319	0.318
PP1/64-16AR	-6	Not tested					
PP2/64-16AR	-6						
PP3/64-16AR	-12						
LP1/70-10AR(CS)	-6						
LP1/64-16AR(CS)	-12						
LP1/64-22AR(CS)	-12						
LP1/64-22AR(CS)	-12						
Modified Geometry							
R1/64-16	-6	81.2	84.2	82.7	0.318	0.319	0.319
R2/64-16	-6	167.0	153.0	160.0	0.371	0.370	0.371
R3/64-16	-6	101.0	108.0	104.5	0.390	0.413	0.402
R1/64-28PM	-18	152.0	159.0	155.5	0.314	0.317	0.316
R3/64-28PM	-18	45.7	43.6	44.7	0.325	0.312	0.319
R1a/64-28TR	-18	144.0	148.0	146.0	0.343	0.339	0.341
R1b/64-28TR	-18	140.0	130.0	135.0	0.314	0.324	0.319
PP1/64-16AR	-6	30.5	29.8	30.2	0.376	0.376	0.376
PP2/64-16AR	-6	26.0	25.0	25.5	0.341	0.321	0.331
PP3/64-16AR	-12	33.3	33.5	33.4	0.308	0.296	0.302
LP1/70-10AR(CS)	-6	33.6	37.9	35.8	0.389	0.381	0.385
LP1/64-16AR(CS)	-12	110.0	122.0	116.0	0.353	0.336	0.345
LP1/64-22AR(CS)	-12	73.9	80.0	77.0	0.316	0.313	0.315

Table C.5: Phase 2c: Intermediate-Temperature Test Results Tested at 25°C

Binder Source	Temperature (°C)	Shear Modulus (G*) (kPa)			Phase Angle (δ) (Degrees)			G*×sin(δ) (kPa)		
		Rept. 1	Rept. 2	Average	Rept. 1	Rept. 2	Average	Rept. 1	Rept. 2	Average
Concentric Cylinder Geometry										
R1/64-16	25	9,320	9,480	9,400	37.9	38.1	38.0	5,730	5,850	5,790
R2/64-16		7,590	6,570	7,080	48.9	49.7	49.3	5,720	5,010	5,365
R3/64-16		10,900	9,700	10,300	55.1	55.0	55.1	8,970	7,940	8,455
R1/64-28PM		2,700	2,860	2,780	46.8	46.4	46.6	1,970	2,070	2,020
R3/64-28PM		1,310	1,270	1,290	37.9	38.6	38.3	825	792	809
R1a/64-28TR		1,430	1,560	1,495	52.2	52.2	52.2	1,130	1,240	1,185
R1b/64-28TR		2,030	2,210	2,120	49.4	47.4	48.4	1,540	1,630	1,585
APP1/64-16AR		25	5,090	5,720	5,405	32.4	33.2	32.8	2,730	3,130
APP2/6416AR	4,490		3,980	4,235	46.4	46.5	46.5	3,250	2,890	3,070
APP3/64-16AR	4,830		4,450	4,640	36.1	36.0	36.1	2,850	2,620	2,735
LP1/70-10AR(CS)	3,890		3,660	3,775	42.1	42.3	42.2	2,610	2,470	2,540
LP1/64-16AR(CS)	4,630		4,710	4,670	33.5	34.5	34.0	2,560	2,670	2,615
LP1/64-22AR(CS)	6,740		6,200	6,470	30.9	32.1	31.5	3,458	3,295	3,377
Parallel Plate Geometry										
R1/64-16	25	9,640	8,500	9,070	39.0	39.2	39.1	6,067	5,373	5,720
R2/64-16		7,580	6,360	6,970	49.6	50.2	49.9	5,775	4,885	5,330
R3/64-16		10,355	9,080	9,718	56.0	55.5	55.8	8,622	7,487	8,055
R1/64-28PM		2,590	2,610	2,600	48.1	47.9	48.0	1,926	1,937	1,932
R3/64-28PM		1,020	1,170	1,095	40.8	40.0	40.4	668	752	710
R1a/64-28TR		1,620	1,650	1,635	54.1	54.0	54.1	1,314	1,335	1,325
R1b/64-28TR		2,240	2,170	2,205	48.6	48.3	48.5	1,680	1,623	1,652
APP1/64-16AR		25	5,790	5,200	5,495	34.5	35.6	35.1	3,280	3,030
APP2/6416AR	3,270		2,820	3,045	47.5	47.8	47.7	2,410	2,090	2,250
APP3/64-16AR	3,840		4,990	4,415	38.9	37.4	38.2	2,410	3,040	2,725
LP1/70-10AR(CS)	3,830		4,930	4,380	35.2	35.7	35.5	2,208	2,880	2,544
LP1/64-16AR(CS)	3,310		3,170	3,240	36.8	37.1	37.0	1,982	1,911	1,947
LP1/64-22AR(CS)	5,600		5,460	5,530	34.8	31.9	33.4	3,195	2,887	3,041

Table C.6: Phase 2d: Multiple Stress Creep Recovery Test Results

Geometry	Binder Source	0.1 kPa			3.2 kPa				Percent Difference	
		Rept. 1	Rept. 2	Average	Rept. 1	Rept. 2	Average	Rept. 1	Rept. 2	Average
Average Percent Recovery (Apr)										
Concentric Cylinder	R1/64-28PM	76.0	75.0	75.5	66.0	60.1	63.1	13.2	19.9	16.5
	R3/64-28PM	92.5	92.4	92.4	89.0	89.0	89.0	3.8	3.7	3.7
	R1a/64-28TR	96.5	96.2	96.3	92.9	92.4	92.7	3.7	3.9	3.8
	R1b/64-28TR	72.6	70.3	71.4	57.5	53.6	55.5	20.8	23.8	22.3
	PP1/64-16AR	75.7	75.9	75.8	53.2	53.5	53.3	29.7	29.5	29.6
	PP2/6416AR	93.7	95.2	94.4	89.8	91.8	90.8	4.2	3.5	3.8
	PP3/64-16AR	101.0	100.5	100.8	53.2	57.7	55.5	47.3	42.6	44.9
Parallel Plate	R1/64-28PM	75.9	75.8	75.9	60.6	60.4	60.5	20.2	20.3	20.3
	R3/64-28PM	90.4	90.6	90.5	84.5	84.7	84.6	6.5	6.4	6.4
	R1a/64-28TR	96.4	96.9	96.6	92.2	93.2	92.7	4.4	3.8	4.1
	R1b/64-28TR	68.5	68.4	68.4	47.2	47.7	47.5	31.1	30.2	30.6
	PP1/64-16AR	88.3	91.4	89.8	54.3	58.5	56.4	38.5	35.9	37.2
	PP2/6416AR	103.9	86.3	95.1	92.4	93.8	93.1	11.1	-8.7	1.2
	PP3/64-16AR	90.7	90.0	90.3	81.4	80.0	80.7	10.2	11.0	10.6
Non-Recoverable Creep Compliance (Jnr) (kPa)										
Concentric Cylinder	R1/64-28PM	0.34	0.39	0.37	0.50	0.65	0.58	45.1	65.6	55.3
	R3/64-28PM	0.06	0.06	0.06	0.09	0.08	0.08	36.6	35.7	36.2
	R1a/64-28TR	0.04	0.04	0.04	0.07	0.08	0.07	95.3	96.6	96.0
	R1b/64-28TR	0.47	0.55	0.51	0.75	0.88	0.81	58.3	61.1	59.7
	PP1/64-16AR	0.11	0.11	0.11	0.22	0.22	0.22	101.7	100.4	101.0
	PP2/6416AR	0.00	0.00	0.00	0.01	0.01	0.01	63.7	71.7	67.7
	PP3/64-16AR	No result	No result	No result	0.05	0.04	0.05	N/A	N/A	N/A
Parallel Plate	R1/64-28PM	0.31	0.31	0.31	0.52	0.52	0.52	69.6	69.0	69.3
	R3/64-28PM	0.08	0.08	0.08	0.12	0.12	0.12	49.6	19.7	34.7
	R1a/64-28TR	0.03	0.03	0.03	0.04	0.06	0.05	115.0	111.7	113.4
	R1b/64-28TR	0.54	0.50	0.52	0.93	0.85	0.89	72.1	69.4	70.7
	PP1/64-16AR	0.04	0.03	0.04	0.19	0.15	0.17	353.1	431.2	392.1
	PP2/6416AR	0.00	0.01	0.00	0.00	0.00	0.00	298.3	55.0	176.6
	PP3/64-16AR	0.01	0.01	0.01	0.02	0.02	0.02	106.0	106.3	106.2

Table C.7: Phase 2e: High Temperature Test Results (Unaged) for SOL-680

Test Temp. (°C)	Concentric Cylinder			25-mm Parallel Plate with 3-mm Gap		
	G* (kPa)	Phase Angle (Degrees)	G*/sin(δ) (kPa)	G* (kPa)	Phase Angle (Degrees)	G*/sin(δ) (kPa)
76	2.93	67.20	3.18	3.73	62.20	4.22
	3.19	65.00	3.52	3.87	62.20	4.38
	3.06	64.90	3.38	3.14	64.40	3.48
	-	-	-	3.10	65.80	3.39
Mean	3.06	65.70	3.36	3.46	63.65	3.87
Std. Dev.	0.11	1.06	0.14	0.34	1.53	0.44
Std. Err.	0.06	0.61	0.08	0.17	0.77	0.22
82	1.83	70.80	1.93	2.36	65.40	2.59
	2.01	68.40	2.16	2.48	65.20	2.74
	1.94	68.30	2.09	1.98	67.40	2.15
	-	-	-	1.95	68.90	2.10
	-	-	-	2.14	65.90	2.35
	-	-	-	2.72	60.60	3.12
Mean	1.93	69.17	2.06	2.27	65.57	2.51
Std. Dev.	0.07	1.16	0.10	0.28	2.56	0.35
Std. Err.	0.04	0.67	0.06	0.11	1.05	0.14
88	1.16	73.60	1.21	1.55	67.90	1.67
	1.29	71.10	1.37	1.66	67.50	1.80
	1.25	71.20	1.32	1.26	69.60	1.35
	-	-	-	1.26	71.40	1.33
	-	-	-	1.37	69.40	1.46
	-	-	-	1.84	62.40	2.08
Mean	1.23	71.97	1.30	1.49	68.03	1.62
Std. Dev.	0.05	1.16	0.07	0.21	2.82	0.27
Std. Err.	0.03	0.67	0.04	0.09	1.15	0.11
94	0.76	75.90	0.78	1.03	69.70	1.09
	0.85	73.30	0.89	1.14	69.30	1.22
	0.83	73.50	0.86	0.87	71.00	0.92
	-	-	-	0.84	73.40	0.88
	-	-	-	0.90	71.40	0.95
	-	-	-	1.33	62.30	1.50
Mean	0.81	74.23	0.84	1.02	69.52	1.01
Std. Dev.	0.04	1.18	0.05	0.17	3.49	0.22
Std. Err.	0.02	0.68	0.03	0.07	1.42	0.09
100	-	-	-	0.72	70.80	0.77
	-	-	-	0.81	70.70	0.86
	-	-	-	0.99	62.30	1.11
Mean	-	-	-	0.84	67.93	0.91
Std. Dev.	-	-	-	0.11	3.98	0.15
Std. Err.	-	-	-	0.06	2.30	0.08

Table C.8: Phase 2e: High Temperature Test Results (Unaged) for CAL-26

Test Temp. (°C)	Concentric Cylinder			25-mm Parallel Plate with 3-mm Gap		
	G* (kPa)	Phase Angle (Degrees)	G*/sin(δ) (kPa)	G* (kPa)	Phase Angle (Degrees)	G*/sin(δ) (kPa)
76	4.89	62.40	5.52	5.53	58.10	6.52
	4.75	62.30	5.36	4.88	61.00	5.58
	4.73	63.00	5.30	5.14	59.30	5.97
Mean	4.79	62.57	5.39	5.18	59.47	6.02
Std. Dev.	0.07	0.31	0.09	0.27	1.19	0.39
Std. Err.	0.04	0.18	0.05	0.15	0.69	0.22
82	2.94	67.10	3.19	3.53	63.20	3.95
	2.88	67.00	3.13	2.97	65.80	3.25
	2.79	67.90	3.01	3.21	64.00	3.57
Mean	2.87	67.33	3.11	3.24	64.33	3.59
Std. Dev.	0.06	0.40	0.07	0.23	1.09	0.29
Std. Err.	0.04	0.23	0.04	0.13	0.63	0.17
88	1.77	71.50	1.86	2.21	67.70	2.39
	1.72	71.30	1.82	1.82	69.70	1.94
	1.66	72.10	1.75	2.01	68.00	2.17
Mean	1.72	71.63	1.81	2.01	68.47	2.17
Std. Dev.	0.04	0.34	0.05	0.16	0.88	0.18
Std. Err.	0.03	0.20	0.03	0.09	0.51	0.11
94	1.07	75.20	1.11	1.42	70.80	1.50
	1.05	75.00	1.08	1.15	72.70	1.21
	1.01	75.70	1.04	1.28	71.40	1.35
Mean	1.04	75.30	1.08	1.28	71.63	1.35
Std. Dev.	0.02	0.29	0.03	0.11	0.79	0.12
Std. Err.	0.01	0.17	0.02	0.06	0.46	0.07
100	0.66	78.20	0.68	0.93	73.40	0.97
	0.65	78.00	0.67	0.75	75.00	0.77
	0.63	78.50	0.64	0.84	73.70	0.87
Mean	0.65	78.23	0.66	0.84	74.03	0.87
Std. Dev.	0.01	0.21	0.02	0.07	0.69	0.08
Std. Err.	0.01	0.12	0.01	0.04	0.40	0.05

Table C.9: Phase 2e: High Temperature Test Results (Unaged) for SB-154

Test Temp. (°C)	Concentric Cylinder			25-mm Parallel Plate with 3-mm Gap		
	G* (kPa)	Phase Angle (Degrees)	G*/sin(δ) (kPa)	G* (kPa)	Phase Angle (Degrees)	G*/sin(δ) (kPa)
76	3.80	65.80	4.17	-	-	-
	3.88	66.00	4.25	-	-	-
	3.89	65.10	4.29	-	-	-
Mean	3.86	65.63	4.24	-	-	-
Std. Dev.	0.04	0.39	0.05	-	-	-
Std. Err.	0.02	0.22	0.03	-	-	-
82	2.29	69.70	2.44	3.29	62.20	3.72
	2.35	70.00	2.50	3.20	60.80	3.67
	2.38	68.80	2.55	-	-	-
Mean	2.34	69.50	2.50	3.25	61.50	3.70
Std. Dev.	0.04	0.51	0.04	0.04	0.70	0.03
Std. Err.	0.02	0.29	0.03	0.03	0.49	0.02
88	1.41	72.80	1.48	2.08	65.60	2.29
	1.44	73.30	1.51	2.07	61.60	2.36
	1.47	71.90	1.55	1.96	65.70	2.15
Mean	1.44	72.67	1.51	2.04	64.30	2.27
Std. Dev.	0.02	0.58	0.03	0.05	1.91	0.09
Std. Err.	0.01	0.33	0.02	0.03	1.10	0.05
94	0.76	75.90	0.78	1.36	68.00	1.46
	0.85	73.30	0.89	1.40	60.40	1.61
	0.83	73.50	0.86	1.27	69.30	1.36
Mean	0.81	74.23	0.84	1.34	65.90	1.48
Std. Dev.	0.04	1.18	0.05	0.05	3.93	0.10
Std. Err.	0.02	0.68	0.03	0.03	2.27	0.06
100	-	-	-	0.92	69.90	0.98
	-	-	-	1.00	57.60	1.18
	-	-	-	0.87	70.80	0.92
Mean	-	-	-	0.93	66.10	1.02
Std. Dev.	-	-	-	0.06	6.02	0.11
Std. Err.	-	-	-	0.03	3.48	0.07
106	-	-	-	0.76	53.40	0.95
	-	-	-	-	-	-
	-	-	-	-	-	-
Mean	-	-	-	0.76	53.40	0.95
Std. Dev.	-	-	-	-	-	-
Std. Err.	-	-	-	-	-	-

Table C.10: Phase 2e: High Temperature Test Results (RTFO-Aged) for SOL-680

Test Temp. (°C)	Concentric Cylinder			25-mm Parallel Plate with 3-mm Gap		
	G* (kPa)	Phase Angle (Degrees)	G*/sin(δ) (kPa)	G* (kPa)	Phase Angle (Degrees)	G*/sin(δ) (kPa)
76	6.61	58.20	7.78	-	-	-
	6.80	57.60	8.05	-	-	-
	6.39	59.20	7.44	-	-	-
Mean	6.60	58.33	7.76	-	-	-
Std. Dev.	0.17	0.66	0.25	-	-	-
Std. Err.	0.10	0.38	0.14	-	-	-
82	4.19	61.50	4.77	5.04	57.40	5.98
	4.31	60.80	4.94	4.32	59.30	5.02
	3.96	62.60	4.46	-	-	-
Mean	4.15	61.63	4.72	4.68	58.35	5.50
Std. Dev.	0.15	0.74	0.20	0.36	0.95	0.48
Std. Err.	0.08	0.43	0.11	0.25	0.67	0.34
88	2.63	65.20	2.90	3.25	61.10	3.71
	2.72	64.40	3.02	2.75	63.00	3.09
	-	-	-	-	-	-
Mean	2.68	64.80	2.96	3.00	62.05	3.40
Std. Dev.	0.05	0.40	0.06	0.25	0.95	0.31
Std. Err.	0.03	0.28	0.04	0.18	0.67	0.22
94	1.66	68.80	1.78	2.13	64.30	2.36
	1.73	67.90	1.87	1.78	66.20	1.95
	1.53	70.00	1.63	-	-	-
Mean	1.64	68.90	1.76	1.96	65.25	2.16
Std. Dev.	0.08	0.86	0.10	0.18	0.95	0.21
Std. Err.	0.05	0.50	0.06	0.12	0.67	0.14
100	0.76	75.90	0.78	1.44	66.80	1.57
	0.85	73.30	0.89	-	-	-
	0.83	73.50	0.86	-	-	-
Mean	0.81	74.23	0.84	1.44	66.80	1.57
Std. Dev.	0.04	1.18	0.05	-	-	-
Std. Err.	0.02	0.68	0.03	-	-	-

Table C.11: Phase 2e: High Temperature Test Results (RTFO-Aged) for CAL-26

Test Temp. (°C)	Concentric Cylinder			25-mm Parallel Plate with 3-mm Gap		
	G* (kPa)	Phase Angle (Degrees)	G*/sin(δ) (kPa)	G* (kPa)	Phase Angle (Degrees)	G*/sin(δ) (kPa)
94	6.17	51.10	7.92	5.07	52.70	6.38
	5.92	52.20	7.50	4.46	53.70	5.53
	-	-	-	4.86	54.60	5.96
Mean	6.05	51.65	7.71	4.80	53.67	5.96
Std. Dev.	0.13	0.55	0.21	0.25	0.78	0.35
Std. Err.	0.09	0.39	0.15	0.15	0.45	0.20
100	4.12	54.90	5.03	3.47	56.20	4.17
	4.14	54.90	5.06	3.07	57.60	3.63
	3.93	55.80	4.75	3.29	58.40	3.86
Mean	4.06	55.20	4.95	3.28	57.40	3.89
Std. Dev.	0.09	0.42	0.14	0.16	0.91	0.22
Std. Err.	0.05	0.24	0.08	0.09	0.52	0.13
106	2.75	59.00	3.21	2.37	59.60	2.75
	2.78	58.90	3.24	2.08	61.40	2.37
	2.60	59.60	3.01	2.20	62.10	2.49
Mean	2.71	59.17	3.15	2.22	61.03	2.54
Std. Dev.	0.08	0.31	0.10	0.12	1.05	0.16
Std. Err.	0.05	0.18	0.06	0.07	0.61	0.09
112	1.83	63.00	2.05	1.65	62.50	1.86
	1.86	62.70	2.10	1.43	64.90	1.58
	1.71	63.40	1.92	1.51	65.10	1.67
Mean	1.80	63.03	2.02	1.53	64.17	1.70
Std. Dev.	0.06	0.29	0.08	0.09	1.18	0.12
Std. Err.	0.04	0.17	0.04	0.05	0.68	0.07

Table C.12: Phase 2e: High Temperature Test Results (RTFO-Aged) for SB-154

Test Temp. (°C)	Concentric Cylinder			25-mm Parallel Plate with 3-mm Gap		
	G* (kPa)	Phase Angle (Degrees)	G*/sin(δ) (kPa)	G* (kPa)	Phase Angle (Degrees)	G*/sin(δ) (kPa)
88	5.50	56.90	6.56	5.91	54.60	7.25
	5.10	58.90	5.95	6.26	53.10	7.83
	5.11	58.50	5.99	5.67	56.10	6.82
Mean	5.24	58.10	6.17	5.95	54.60	7.30
Std. Dev.	0.19	0.86	0.28	0.24	1.22	0.41
Std. Err.	0.11	0.50	0.16	0.14	0.71	0.24
94	3.56	60.40	4.09	3.85	58.00	4.54
	3.25	62.70	3.65	4.19	56.30	5.04
	3.26	62.20	3.69	3.72	59.30	4.33
Mean	3.36	61.77	3.81	3.92	57.87	4.64
Std. Dev.	0.14	0.99	0.20	0.20	1.23	0.30
Std. Err.	0.08	0.57	0.11	0.11	0.71	0.17
100	2.30	64.00	2.55	2.52	61.40	2.87
	2.06	66.50	2.24	2.80	59.50	3.25
	2.08	65.70	2.29	2.43	62.50	2.74
Mean	2.15	65.40	2.36	2.58	61.13	2.95
Std. Dev.	0.11	1.04	0.14	0.16	1.24	0.22
Std. Err.	0.06	0.60	0.08	0.09	0.72	0.12
106	1.49	67.30	1.62	1.67	64.40	1.85
	1.31	70.00	1.40	1.87	62.50	2.11
	1.33	69.10	1.43	1.60	65.60	1.76
Mean	1.38	68.80	1.48	1.71	64.17	1.91
Std. Dev.	0.08	1.12	0.10	0.11	1.28	0.15
Std. Err.	0.05	0.65	0.06	0.07	0.74	0.09

Table C.13: Phase 2e: Low-Temperature Test Results (PAV-Aged)

Test Temp. (°C)	SOL-680		CAL-26		SB-154	
	S (MPa)	m-Value	S (MPa)	m-Value	S (MPa)	m-Value
-12	66.90	0.37	37.10	0.33	29.80	0.32
	60.60	0.36	42.00	0.31	30.50	0.33
	-	-	-	-	27.60	0.32
Mean	63.75	0.36	39.55	0.32	29.30	0.32
Std. Dev.	3.15	0.01	2.45	0.01	1.24	0.01
Std. Err.	2.23	0.01	1.73	0.01	0.71	0.00
-18	124.00	0.31	87.00	0.27	46.20	0.24
	109.00	0.31	74.90	0.28	57.70	0.27
	-	-	90.30	0.27	45.20	0.29
Mean	116.50	0.31	84.07	0.27	49.70	0.26
Std. Dev.	7.50	0.00	6.62	0.00	5.67	0.02
Std. Err.	5.30	0.00	3.82	0.00	3.27	0.01
-24	199.00	0.28	132.00	0.25	-	-
	200.00	0.28	198.00	0.25	-	-
	-	-	170.00	0.26	-	-
Mean	199.50	0.28	166.67	0.25	-	-
Std. Dev.	0.50	0.00	27.05	0.00	-	-
Std. Err.	0.35	0.00	15.62	0.00	-	-

Table C.14: Phase 2f: Air-Void Contents of Gyratory-Compacted Specimens

Mix	Specimen Number	Air-Void Content (%)	Average (%)	Standard Deviation
SOL-680	1	7.2	7.1	0.22
	2	7.4		
	3	6.8		
	4	7.0		
	5	7.1		
CAL-26	1	7.0	7.1	0.38
	2	7.1		
	3	7.5		
	4	6.6		
	5	7.5		
SB-154	1	7.7	7.3	0.34
	2	7.0		
	3	7.6		
	4	7.1		
	5	7.0		

Table C.15: Phase 2f: Air-Void Contents of Rolling Wheel-Compacted Specimens

Mix	Specimen Number	Air-Void Content (%)	Average (%)	Standard Deviation
SOL-680	1	7.4	7.1	0.28
	2	7.3		
	3	7.4		
	4	6.7		
	5	6.8		
	6	7.2		
	7	7.3		
	8	7.4		
	9	7.4		
	10	7.2		
	11	6.8		
	12	6.8		
CAL-26	1	6.7	6.7	0.21
	2	6.7		
	3	6.5		
	4	6.6		
	5	6.5		
	6	6.6		
	7	6.6		
	8	7.0		
	9	6.6		
	10	6.6		
	11	6.5		
	12	7.2		
SB-154	1	7.1	7.2	0.27
	2	7.3		
	3	7.0		
	4	6.7		
	5	7.1		
	6	7.5		
	7	7.5		
	8	7.1		

Table C.16: Phase 2f: Dynamic Modulus and Phase Angle

Temperature (°C)	Frequency (Hz)	Dynamic Modulus (E*) (MPa)			Phase Angle (δ) (Degrees)		
		SOL-680	CAL-26	SB-154	SOL-680	CAL-26	SB-154
4	10	11,724	11,125	8,368	8.1	10.8	9.6
	1	9,424	8,272	6,512	10.5	13.3	11.8
	0.1	7,020	5,819	4,819	14.1	16.4	14.7
20	10	6,251	5,152	4,068	16.8	19.1	17.5
	1	3,960	3,158	2,641	22.1	22.6	21.2
	0.1	2,235	1,807	1,579	27.6	26.1	25.3
45	10	1,301	881	1,043	34.0	32.4	31.7
	1	540	390	465	36.0	32.9	34.4
	0.1	207	182	206	36.0	31.7	34.3
	0.01	75	97	92	35.5	29.5	32.3

Table C.17: Phase 2f: Flexural Modulus and Phase Angle

Temperature (°C)	Frequency (Hz)	Flexural Modulus (E*) (MPa)			Phase Angle (δ) (Degrees)		
		SOL-680	CAL-26	SB-154	SOL-680	CAL-26	SB-154
10	15	6,888	5,680	5,815	17.1	19.9	15.7
	10	6,589	5,378	5,602	16.1	19.1	14.3
	5	5,998	4,803	5,183	15.6	18.3	13.7
	2	5,225	4,094	4,611	16.1	18.7	13.9
	1	4,631	3,593	4,189	16.9	19.1	14.1
	0.5	4,079	3,114	3,776	18.1	20.0	14.9
	0.2	3,381	2,547	3,255	20.2	21.7	16.6
	0.1	2,862	2,166	2,750	22.7	22.8	14.4
	0.05	2,416	1,834	2,410	24.3	24.2	16.0
	0.02	1,876	1,458	2,031	26.5	26.1	18.2
	0.01	1,541	1,221	1,764	29.5	27.6	20.4
20	15	4,058	3,112	3,811	25.0	27.0	20.8
	10	3,806	2,878	3,621	25.1	26.2	19.6
	5	3,254	2,447	3,219	25.3	25.5	19.8
	2	2,596	1,959	2,709	26.4	25.8	20.3
	1	2,139	1,628	2,354	27.5	26.4	20.7
	0.5	1,740	1,348	2,022	29.7	27.3	21.8
	0.2	1,283	1,028	1,631	32.3	28.8	23.8
	0.1	1,015	841	1,279	35.0	29.8	22.8
	0.05	787	680	1,071	35.2	32.1	24.1
	0.02	554	509	853	36.4	33.1	26.6
	0.01	422	408	709	36.6	34.0	29.1
30	15	2,066	1,356	2,072	36.2	37.7	29.5
	10	1,856	1,244	1,921	36.0	35.0	28.0
	5	1,489	1,025	1,636	36.0	32.2	28.1
	2	1,081	779	1,281	35.2	31.5	27.9
	1	843	624	1,050	35.7	32.7	28.8
	0.5	660	491	855	36.0	32.0	30.0
	0.2	469	366	652	36.7	34.2	31.6
	0.1	365	291	503	36.9	33.2	30.0
	0.05	288	228	398	37.3	37.6	29.4
	0.02	185	173	316	43.3	38.6	37.2
	0.01	176	129	200	37.2	40.1	37.9

Table C.18: Phase 2f: Repeated Load Triaxial

Mix	Specimen ID	Temperature (°C)	Confining Stress (kPa)	Deviator Stress (kPa)	Flow Number (Cycles)	μstrain at Flow Point	FN @ 1%	FN @ 3%	FN @ 5%
SOL-680	11	52.2	0	599.5	916	23,207	145	1,269	1,814
	12	52.3	0	599.4	307	23,845	34	471	813
	13	52.3	0	599.4	502	17,100	124	1,277	1,875
	14	52.3	0	599.4	447	20,655	84	783	1,187
	15	52.3	0	599.4	304	18,109	77	665	971
CAL-26	1	52.3	0	599.5	913	18,569	132	2,128	3,137
	3	52.3	0	599.5	1,212	20,150	76	1,703	2,663
	8	52.3	0	599.4	793	20,067	161	2,324	3,351
	T1	52.3	0	599.4	2,191	17,423	413	4,958	6,701
	T2	52.3	0	599.5	1,411	23,843	76	2,100	3,298
SB-154	2	52.1	0	599.4	2,130	29,528	88	2,203	4,536
	4	52.1	0	599.4	1,160	33,615	26	878	2,220
	5	52.1	0	599.5	1,384	24,947	71	2,017	3,551
	6	52.1	0	599.4	1,594	31,750	43	1,418	3,070

Table C.19: Phase 2f: Semicircular Bend Test Results

Specimen	Strength (psi)	Slope	Fracture Energy (J/m²)	Flexibility Index
SOL680-4-B1	95.3	-5.5	2,913	5.3
SOL680-4-B2	82.1	-4.8	2,288	4.8
SOL680-5-B1	99.1	-5.7	2,898	5.1
SOL680-5-B2	92.5	-4.6	3,042	6.6
SOL680-5-T1	85.8	-8.2	2,072	2.5
SOL680-5-T2	91.2	-4.6	2,817	6.1
SOL680-6-B1	93.5	-11.5	2,481	2.2
SOL680-6-B2	72.1	-6.0	1,724	2.9
CAL26-13-B1	66.9	-3.2	2,162	6.8
CAL26-13-B2	64.7	-3.7	1,757	4.8
CAL26-13-T1	73.8	-3.9	2,198	5.6
CAL26-13-T2	65.0	-2.8	2,312	8.2
CAL26-14-T1	59.7	-2.6	2,071	8.1
CAL26-14-T2	64.7	-2.8	2,556	9.2
CAL26-15-B1	50.8	-1.9	2,239	11.9
CAL26-15-B2	63.6	-2.8	2,303	8.2
SB154-10-BV	102.5	-6.2	2,597	4.2
SB154-10-B	97.3	-9.7	1,670	1.7
SB154-10-TV	104.3	-7.3	2,344	3.2
SB154-10-T	108.1	-10.9	1,963	1.8
SB154-11-BV	105.1	-15.7	1,644	1.1
SB154-11-B	100.1	-12.9	1,820	1.4
SB154-4-BV	94.3	-6.0	2,145	3.6
SB154-4-B	95.5	-8.9	1,740	2.0
SB154-4-TV	90.7	-8.5	1,666	2.0
SB154-4-T	88.0	-8.9	1,664	1.9
SB154-5-BV	107.2	-7.8	2,331	3.0
SB154-5-B	90.2	-6.8	1,764	2.6
SB154-5-TV	102.9	-5.4	2,481	4.6
SB154-5-T	95.4	-6.6	2,114	3.2
SB154-9-BV	108.8	-8.2	2,356	2.9
SB154-9-B	103.5	-7.1	2,362	3.3
SB154-9-TV	98.3	-7.9	2,027	2.6
SB154-9-T	108.6	-8.5	2,150	2.5

Blank page